UNIVERSITY OF SOUTHAMPTON

INTRACELLULAR CONSEQUENCES OF GLUTAMATE RECEPTOR ACTIVATION IN MOUSE HIPPOCAMPAL NEURONS: AN IMAGING BASED STUDY

Lois Priscilla Margaret Wallach BSc

A thesis submitted for the degree of
Doctor of Philosophy

FACULTY OF SCIENCE
SCHOOL OF BIOLOGICAL SCIENCES

May 2002

UNIVERSITY OF SOUTHAMPTON

ABSTRACT

FACULTY OF SCIENCE
SCHOOL OF BIOLOGICAL SCIENCES

Doctor of Philosophy

INTRACELLULAR CONSEQUENCES OF GLUTAMATE RECEPTOR ACTIVATION IN MOUSE HIPPOCAMPAL NEURONS: AN IMAGING BASED STUDY

By Lois Priscilla Margaret Wallach BSc

Intracellular consequences of glutamate receptor activation were investigated in mouse hippocampal neurons using fluorescent probes for the measurement of Ca^{2+} (Fluo-3 AM; Fluo-5N AM), mitochondrial $\Delta\Psi$ (TMRE) and superoxide (Het) in conjunction with confocal laser scanning microscopy (CLSM). The excessive activation of glutamate receptors is thought to be a common feature of neuronal death in a wide spectrum of neurological disorders. The intracellular events that link toxic glutamate receptor activation to eventual cell death are not well understood, but are likely to involve a loss of Ca^{2+} homeostasis, mitochondrial dysfunction and free radical damage.

Glutamate acts on a large number of ionotropic and metabotropic receptor subtypes. The selective activation of NMDA receptors was particularly damaging, causing neuronal cell death in over 80% of cultured mouse hippocampal neurons 24 hours after drug application. In contrast, agonists at other glutamate receptor subtypes including kainate and ACPD caused only 14% and 7% cell death respectively. Doses of glutamate receptor agonist were selected to elicit equivalent "early" neuronal Ca^{2+} increases as measured by Fluo-3 AM in the first 200 seconds following drug addition. Early neuronal Ca^{2+} increases did not correlate with eventual neuronal death, suggesting that different routes of Ca^{2+} increase could have different pathological consequences for neurons. Experiments were then conducted to investigate intracellular events downstream of glutamate receptor activation that could lead to neuronal death.

The same doses of glutamate receptor agonists had profoundly different effects on mitochondrial $\Delta\Psi$, which correlated to neuronal death. NMDA caused a robust increase in TMRE fluorescence indicative of mitochondrial depolarization, whereas kainate, ACPD, AMPA and quisqualate had no significant effect on mitochondrial $\Delta\Psi$ despite causing equivalent early Ca^{2+} increases. All the glutamate receptor agonists caused increased neuronal superoxide production as measured by increased Het fluorescence. Superoxide production *per se* was not predictive of neuronal death, but the involvement of reactive oxygen species in neurotoxicity was confirmed by assays where antioxidants and L-NAME, an inhibitor of nitric oxide synthase, were highly protective against a 15 minute NMDA insult. EDTA, a metal ion chelator, was also highly protective against NMDA insult, pointing to the involvement of trace metals in neurotoxicity. Large, late neuronal Ca^{2+} responses (after 300 seconds) were measured with the low affinity Ca^{2+} indicator Fluo-5N AM. NMDA caused a delayed Ca^{2+} deregulation that strongly correlated with eventual neuronal death. Kainate did not cause delayed Ca^{2+} deregulation.

Of the measured responses to different glutamate receptor activations, mitochondrial depolarisation and delayed Ca^{2+} deregulation were predictive of neuronal death, whereas early Ca^{2+} elevation and superoxide production alone were not well correlated to neuronal death. However, reactive oxygen species are implicated in neuronal death by the neuroprotection observed with antioxidants, metal chelators and blockade of nitric oxide production.

CONTENTS

LIST OF FIGURES

Chapter 1

Chapter 2

Chapter 3

Chapter 4

Chapter 5

Chapter 6

PREFACE

Neurological disorders represent a major socio-economic burden in the UK, costing the NHS over £800 million each year (Wellcome Trust Report, 2000). The excessive activation of glutamate receptors in the brain is thought to contribute to neuronal damage in acute neurological disorders such as cerebral ischaemia, traumatic brain injury, stroke and epilepsy. Chronic neurodegenerative conditions such as Alzheimer's disease or amyotrophic lateral sclerosis may also involve glutamate-induced neuronal death. Over the past 20 years, much research has focussed on the cellular mechanisms that underlie glutamate-induced neuronal damage. The immediate consequence of toxic glutamate receptor activation is an increase in intracellular calcium levels. This calcium surge is thought to trigger a plethora of damaging cascades, including the generation of free radicals and nitric oxide, the activation of proteases, phospholipases and endonucleases, mitochondrial depolarisation and in some instances, the activation of cellular apoptotic processes. The relative importance of these calcium-triggered cascades in neurotoxicity is uncertain, as is the temporal sequence of neurotoxic events. Glutamate can elevate intracellular calcium by a number of routes, including the activation of calcium-permeable NMDA receptors, the opening of voltage-dependent calcium channels following AMPA receptor-mediated membrane depolarisation, and the activation of metabotropic glutamate receptors coupled to phosphoinositide hydrolysis and calcium release from intracellular stores.

In this study, we have sought to monitor intracellular events including intracellular calcium elevations, changes in mitochondrial membrane potential and free radical production following the activation of different glutamate receptor subtypes in cultured hippocampal neurons, in an attempt to rationalise some of the many factors that may contribute to glutamate neurotoxicity. We have also monitored the ability of glutamate receptor antagonists, antioxidants and metal chelators to protect against glutamate receptor-mediated neurotoxicity.

ACKNOWLEDGEMENTS

Dr John Chad
BBSRC

This thesis is the result of research conducted wholly while in registered postgraduate candidature.

ABBREVIATIONS

(1S, 3R) –ACPD	(1S, 3R)-1-Aminocyclopentane-1,3-dicarboxylic acid
(RS)-AMPA	(RS)-α-Amino-3-hydroxy-5-methyl-4-isoxazolepropionic acid
D-AP5	D(-)-2-Amino-5-phosphonopentanoic acid
4-AP	4-amino pyridine
ATP	adenosine triphosphate
BDNF	brain-derived neurotrophic factor
BHQ	2,5-Di-(*t*-butyl)-1,4-hydroquinone
Ca-A/K channels	Calcium permeable AMPA/kainate receptors
CaMK	Ca^{2+}-calmodulin dependent kinase
CGCs	cerebellar granule cells
CICR	calcium induced calcium release
CNS	central nervous system
CNQX	6-cyano-7-nitroquinoxaline-2,3-dione
CSA	cyclosporin A
DAG	diacyl glycerol
DCD	delayed Ca^{2+} deregulation
DNA	deoxyribose nucleic acid
$\Delta\Psi$	mitochondrial membrane potential (delta psi)
DHP	dihydropyridine
DIV	days in vitro
EAAs	excitatory amino acids
EDTA	ethylenediaminetetraacetic acid
ER	endoplasmic reticulum
ETC	electron transfer chain
FCCP	Carbonyl Cyanide p-Trifluoromethoxyphenylhydrazone
FU	fluorescence unit
L-Glutamic acid	(S)-1-Aminopropane-1,3-dicarboxylic acid
GTP	guanosine triphosphate

HEPES	N-[2-Hydroxyethyl]piperazine-N'-[2-ethanesulfonic acid]
Het	dihydroethidium
HVA	high voltage-activated
IP_3	inositol triphosphate
IP_3R	inositol triphosphate receptor
Kainic acid	[2S-(2α,3β,4β)]-2-Carboxy-4-(1-methylethenyl)-3-pyrrolidineacetic acid
LVA	low voltage-activated
L-NAME	Nω-nitro-L-arginine methyl ester
NMDA	N-methyl-D-aspartic acid
NO	nitric oxide
NOS	nitric oxide synthase
$ONOO^-$	peroxynitrite
PBS	phosphate buffered saline
PFA	paraformaldehyde
PIPES	Piperazine-N,N'-bis[2-ethanesulfonic acid]
PLA_2	phospholipase A_2
PLC	phospholipase C
PTP	permeability transition pore
L-Quisqualic acid	(L)-(+)-α-Amino-3,5-dioxo-1,2,4-oxadiazolidine-2-propanoic acid
RaM	rapid mode
ROI	region of interest
ROS	reactive oxygen species
RyR	ryanodine receptor
SERCA	sarco-endoplasmic reticulum Ca^{2+}-ATPase
SR	sarcoplasmic reticulum
TCA	tricarboxylic acid cycle
TEMPO	5,5-dimethyl-1-pyrroline N-oxide
TMRE	Tetramethylrhodamine ethyl ester
TNFα	tumour necrosis factor α

Trolox	6-hydroxy-2,5,7,8-tetramethylchroman-2-carboxylic acid
VDCC	voltage-dependent calcium channel
X	xanthine
XO	xanthine oxidase

Chapter 1

BACKGROUND

1.1 NEURONAL CALCIUM HOMEOSTASIS

Neurons perform a complex array of communication functions and have developed specialized signalling and regulatory mechanisms to enable them to carry out these tasks. Many of these mechanisms include a central role for calcium, which is the most common signal transduction element in organisms ranging from unicellular bacteria to humans (Racay *et al*, 1996). Fluctuations in neuronal Ca^{2+} concentration are vital for a variety of physiological processes. Calcium is the main trigger for neurotransmitter release and is also involved in the regulation of ion channels, the movement of growth cones in neuronal development, the control of neuronal excitability and synaptic plasticity, and the expression of immediate early genes (Kennedy, 1989). Calcium is also involved in neuronal cell death under several different pathological conditions including traumatic brain injury, ischaemia, seizures, slowly evolving neurodegenerative conditions and programmed cell death (see section **1.2**).

Neuronal calcium homeostasis is very tightly controlled, giving neuronal Ca^{2+} levels of approximately 100nM under resting conditions. In order to act as a signal, $[Ca^{2+}]_i$ must increase several-fold. The complex morphology of neurons allows cellular function and processing to vary considerably between different cellular regions. This necessitates multiple mechanisms for the temporal and spatial distribution of Ca^{2+} transients, so that Ca^{2+} is able to selectively activate diverse processes within the same neuron. This control is provided by the complex interplay between different systems, which allow Ca^{2+} influx across the plasma membrane, Ca^{2+} release into the cytosol from intracellular stores, Ca^{2+} sequestration in intracellular stores, Ca^{2+} buffering in the cytosol and Ca^{2+} extrusion across the plasma membrane.

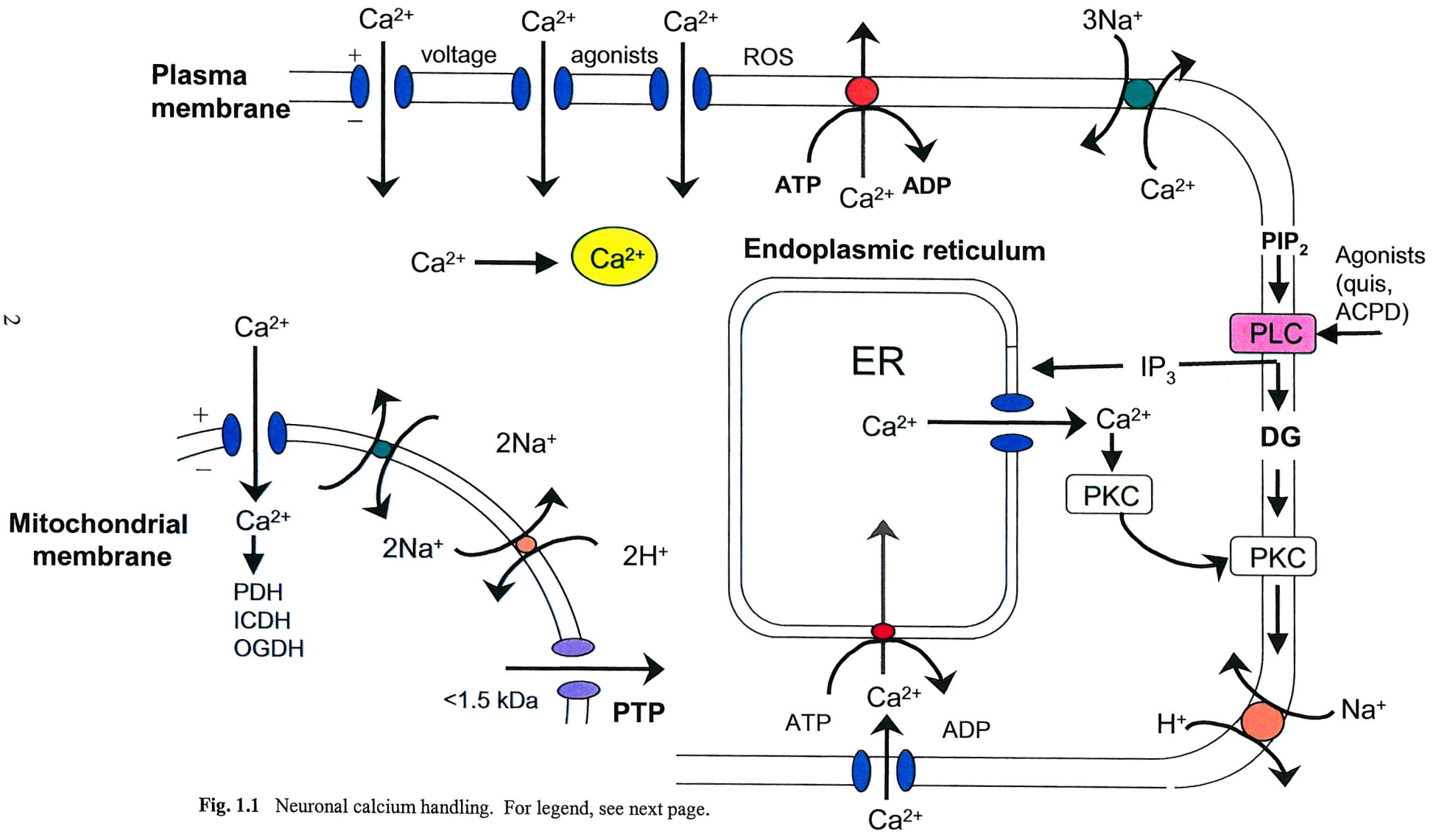

Fig. 1.1 Neuronal calcium handling. For legend, see next page.

1.1.1 PLASMA MEMBRANE CALCIUM TRANSPORT

Voltage-dependent calcium channels

Voltage-dependent calcium channels (VDCCs) are oligomeric transmembrane proteins, which allow the passage of Ca^{2+} into neurons in response to membrane depolarisation. Electrophysiological and pharmacological studies have revealed different Ca^{2+} currents classified as L-, N-, P-, Q-, R-, and T-type. These Ca^{2+} currents have been correlated with cloned Ca^{2+} channel subunits by expression *in vitro* (Catterall, 2000).

Ca^{2+} current types

L-type Ca^{2+} currents have been recorded in neurons (Bean, 1989), and are characterised by high voltage of activation, large single-channel conductance, slow voltage-dependent inactivation, regulation by protein phosphorylation and inhibition by dihydropyridines, phenylalkylamines and benzothiazepines (Reuter, 1983). T-type Ca^{2+} currents were first measured in cerebellar Purkinje neurons (Llinas and Yarom, 1981) and have subsequently been characterised in detail in dorsal root ganglion neurons (Nowycky *et al*, 1985). When compared to L-type Ca^{2+} currents, T-type currents activate at much more negative membrane potentials, so are also designated low-voltage-activated Ca^{2+} currents. They inactivate rapidly, deactivate slowly, have small single-channel conductance and are not blocked by Ca^{2+} antagonists (Catterall, 2000).

Figure 1.1 (previous page): **Neuronal calcium handling.** Ca^{2+} enters the cell through voltage- and agonist-operated channels, and also by non-specific channels such as those operated by ROS. Ca^{2+} is extruded from the cell by the Ca^{2+} -ATPase or by Ca^{2+} -Na^{+} exchange. Cytosolic Ca^{2+} is sequestered by mitochondria and ER at the expense of ATP, and is bound to Ca^{2+} -binding molecules. Ca^{2+} is released from the ER following the activation of receptors coupled to PLC and the formation of IP3 from PIP2. Increased [Ca^{2+}]i can cause the translocation of PKC to membranes where it can be activated by diglycerides (DG). Ca^{2+} accumulation in the mitochondrion may lead to activation of the PTP.

An additional Ca^{2+} current, N-type, was discovered through whole-cell voltage-clamp and single-channel recordings from dissociated dorsal root ganglion neurons (Nowycky *et al*, 1985). The primary method to distinguish N-type Ca^{2+} currents has been their sensitivity to the cone snail peptide ω–conotoxin GVIA (McClesky *et al*, 1987), given that the voltage dependence and kinetics of N-type Ca^{2+} currents varies considerably between different neurons. In initial experiments, N-type Ca^{2+} currents were found to have voltage-dependence and rates of inactivation intermediate to that of L-type and T-type Ca^{2+} currents. Three additional Ca^{2+} current types were distinguished on the basis of their sensitivity to peptide toxins. P-type Ca^{2+} currents were identified by high sensitivity to the spider toxin ω–agatoxin IVA (Mintz et al, 1992). Q-type Ca^{2+} currents were blocked by ω–agatoxin IVA with lower affinity (Randall and Tsien, 1995). In cerebellar granule neurons, R-type Ca^{2+} currents were found to be resistant to both organic and peptide Ca^{2+} channel blockers (Randall and Tsien, 1995). N-type, P-type, Q-type and R-type Ca^{2+} currents are principally found in neurons, and are regulated by many signal transduction pathways. In contrast, L-type and T-type Ca^{2+} currents have been recorded in a multitude of cell types, including smooth, cardiac and skeletal muscle, endocrine cells and starfish eggs (Catterall, 2000).

Subunit structure

The subunit composition of Ca^{2+} channels was elucidated by the solubilization and purification of channel proteins from skeletal muscle, and detailed biochemical analysis, including the examination of hydrophobicity and glycosylation. These studies revealed five Ca^{2+} channel subunits, α_1, α_2, δ, β and γ (Catterall, 2000). The putative arrangement of these 5 subunits is shown in **Figure 1.2** (overleaf). This model incorporates a principal α_1 transmembrane subunit (190 kDa) associated with a disulphide-linked $\alpha_2\delta$ dimer of 170 kDa, an intracellular phosphorylated β subunit (55 kDa) and a transmembrane γ subunit (33 kDa) (Takahashi *et al*, 1987). The subsequent immunoprecipitation of L-type Ca^{2+} channels from neurons showed the presence of α_1, $\alpha_2\delta$ and β subunits, but no γ subunit (Ahlijanian *et al*, 1990).

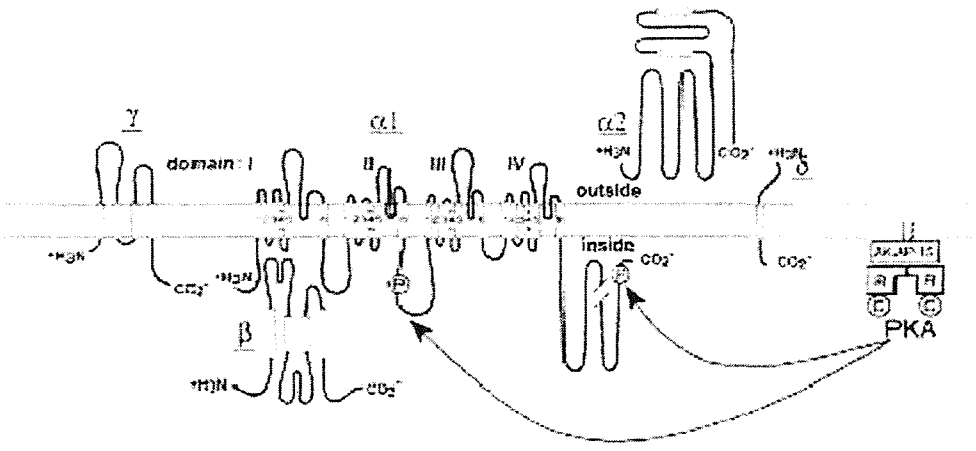

Figure 1.2 Subunit structure and regulation of L-type Ca^{2+} channels purified from skeletal muscle. P, sites of phosphorylation by cAMP-dependent protein kinase that have been demonstrated in intact cells. From Catterall, 2000.

It is likely that the subunit composition of L-type Ca^{2+} channels is similar in cardiac and skeletal muscle and neurons. Similarly, purified N- and P/Q-type Ca^{2+} channels were composed of α_1, $\alpha_2\delta$ and β subunits (McEnery *et al*, 1991; Liu *et al*, 1996; Martin-Moutot *et al*, 1995). The recent discovery of a novel γ subunit which is also the target of the *stargazer* mutation in mice (Letts et al, 1998) has caused much interest. This subunit may associate with Ca^{2+} channels containing α_{1A} subunits in vivo, giving an identical subunit composition to that of Ca^{2+} channels purified from skeletal muscle. In neurons, the β subunit is thought to confer the voltage dependence and gating kinetics of Ca^{2+} channels (Catterall, 2000).

Ca^{2+} channel diversity

The different types of Ca^{2+} current described in the preceding pages are essentially determined by different α_1 subunits. Ten distinct α_1 Ca^{2+} channel subunits are encoded on 10 separate genes. These ten α_1 Ca^{2+} channel subunits have recently been divided into three structurally and functionally related families, Ca_v1, Ca_v2 and Ca_v3 (Ertel *et al*, 2000). The Ca_v1 family of α_1 subunits mediates L-type Ca^{2+} currents, the Ca_v2 family conducts N-type, P/Q-type and R-type Ca^{2+} currents, and T-type currents are carried by the Ca_v3 family of α_1 subunits. Within each family, the amino acid sequence homology of the subunits is greater than 70% whereas between families,

homology can be as low as 25% (between Ca_v3 and the high-voltage-activated Ca^{2+} channels). The presence of multiple β subunits further increases the diversity of Ca^{2+} channel structure and function. Four β subunit genes are known to exist, and each is alternatively spliced to produce extra isoforms.

Receptor operated calcium channels

The opening of receptor operated calcium channels is in direct response to ligand binding to plasma membrane receptors, and is usually independent of membrane potential. Such direct ligand-gating allows a rapid response, as occurs in synaptic transmission. Glutamate is the primary excitatory neurotransmitter in the mammalian CNS, and acts on a number of glutamate receptors, outlined below. Other less well-characterised receptor operated Ca^{2+} channels include the P_{2X} receptor, cyclic nucleotide gated Ca^{2+} channels and channels sensitive to inositol 1,3,4,5 tetrakisphosphate (Racay *et al*, 1996).

Glutamate Receptors

Glutamate receptors are currently divided into two classes: ionotropic (ion channel forming) receptors, further subdivided into AMPA, kainate and NMDA receptor channels, and metabotropic receptors, which are coupled to G-proteins and modulate the production of intracellular messengers. This grouping is similar to other families of neurotransmitter receptors, which either directly gate ion channels (eg $GABA_A$ and $5HT_3$ receptors) or have G-protein links to second messenger systems or ion channels (muscarinic and $GABA_B$ receptors) (Bleakman and Lodge, 1998). Molecular cloning and expression studies of the glutamate receptors have revealed that the diversity of these receptors is much greater than expected from pharmacological studies. Glutamate receptor cDNAs have been successfully identified through expression cloning in *Xenopus* oocytes. Proteins from each class of ionotropic and metabotropic glutamate receptor have been identified, and

homologous genes for each class of receptor subsequently cloned (Michaelis, 1998). So far, 14 cDNAs encoding ionotropic glutamate receptor (iGluR) subunits have been isolated: 4 for AMPA receptor subunits (GluR1-4), 5 for kainate receptor subunits (GluR5-7, KA1 and KA2), and 5 for NMDA receptor subunits (NR1, NR2A-D). A whole family of genes encoding metabotropic glutamate receptor subunits has been identified (mGluR1-8), using the techniques of PCR-mediated amplification and cross-hybridization screening (Ozawa *et al*, 1998). In addition to the large number of genes, the molecular diversity of glutamate receptors is further increased by splice-variants and RNA editing. Figure **1.2** schematically represents the known subtypes of glutamate receptors.

The size of the glutamate receptor proteins represented by their cDNAs ranges from 95 to 163kDa, considerably larger than receptor proteins for other neurotransmitters. The structure of these receptor proteins has been predicted based on known amino acid sequences and hydrophobicity plots. Each ionotropic receptor protein is thought to have a large extracellular amino terminal region, a cytoplasmic carboxy terminal, three transmembrane domains (M1, M3 and M4) and a re-entrant loop (M2). The predicted structure of iGluRs is analogous to the known structure of other ionotropic receptor proteins such as the GABA and nicotinic acetylcholine receptors, each having four transmembrane domains. The metabotropic glutamate receptor proteins are thought to have seven transmembrane domains, similar to other G-protein coupled receptors such as the muscarinic acetylcholine receptors (Michaelis, 1998).

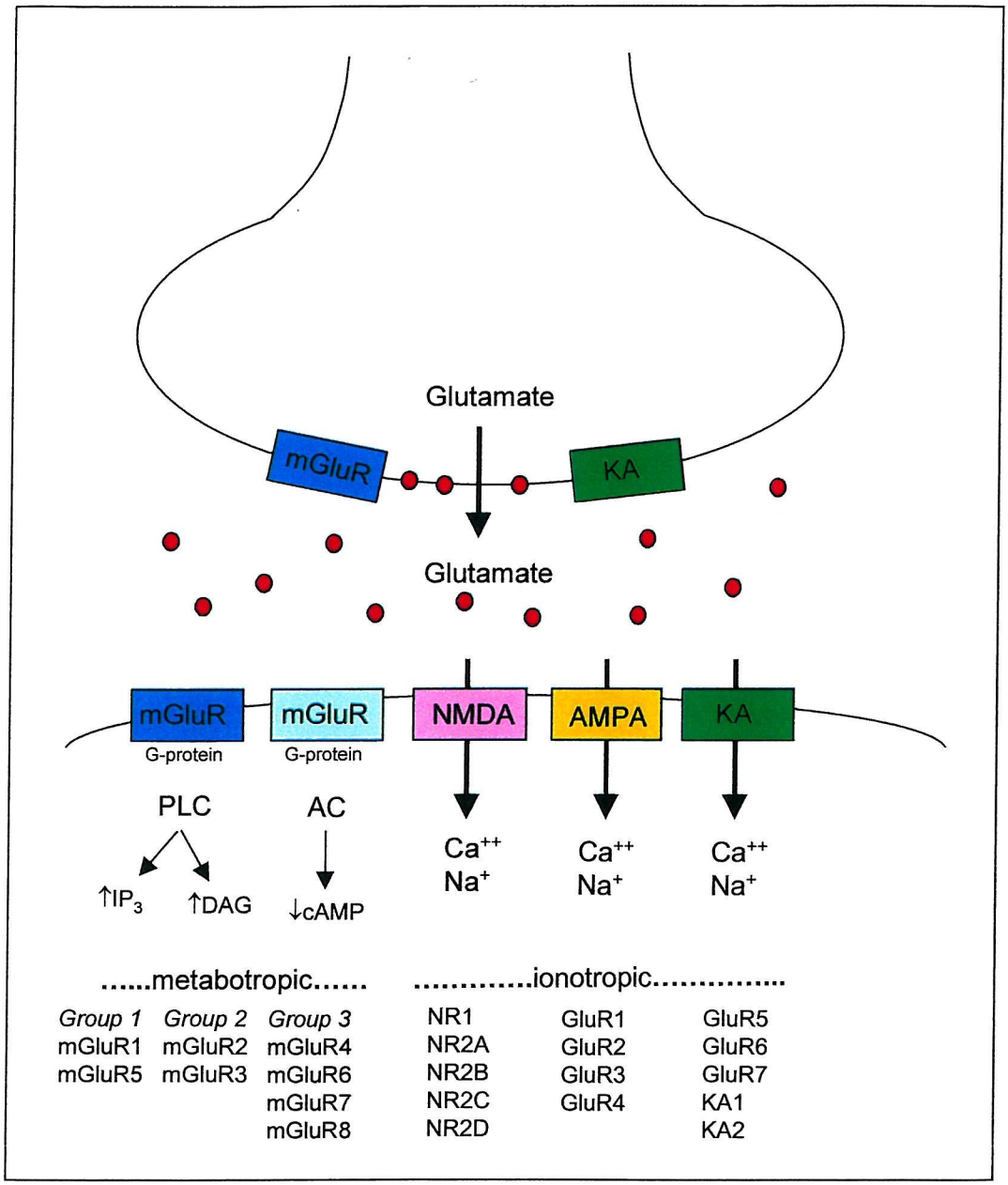

Figure 1.3 Schematic representation of a glutamatergic synapse to show the major receptor subtypes known to play a role in brain function. It is unlikely that all these subunits would be present at any one synapse. Adapted from Bleakman and Lodge, 1998.

AMPA Receptors

At most central synapses, both AMPA and NMDA receptors are activated during synaptic transmission. The rapid kinetics of the AMPA receptor (desensitization time constants of 1-14ms, depending upon subunit composition) facilitate its role in the mediation of fast neurotransmission. The AMPA receptor has a low-affinity binding site for glutamate, and is thought to inactivate rapidly because of the short average boundtime of agonist (Dingledine *et al*, 1999). The neurotransmission mediated by NMDA receptors is much slower but longer-lived, owing to the slower kinetics of the NMDA receptor. The AMPA receptor subunits GluR1-4 have approximately 70% amino acid sequence homology, and are thought to assemble in either homomeric or heteromeric oligomers to form functional AMPA receptors. Recent studies suggest that AMPA receptors form tetrameric structures (Rosemund *et al*, 1998). Each AMPA receptor subunit exists in two splice-variant forms, "flip", which predominates in the embryonic brain, or "flop" which is upregulated postnatally (Ozawa *et al*, 1998). The GluR2 subunit determines Ca^{2+} permeability of AMPA receptors. Electrophysiological studies of recombinant AMPA receptors expressed in Xenopus oocytes showed that AMPA receptors assembled from GluR1, GluR3 or GluR4 alone or in combination are permeable to Ca^{2+}. The expression of GluR2 with other GluR subunits forms Ca^{2+}-impermeable channels (Hollman *et al*, 1991). The GluR2 subunit is able to control the passage of Ca^{2+} and other divalent cations by virtue of the presence of a positively charged arginine (R) in place of a glutamine (Q) residue within the M2 domain. This critical arginine is not encoded by the *gluR2* gene, but is inserted by highly effective (over 99%) RNA editing at the Q/R site (Pellegrini-Giampietro *et al*, 1997). AMPA receptors are found throughout the CNS, but are particularly abundant in the pyramidal cell layer of CA1 in the hippocampus. An immunohistochemical study of GluR1-3 distribution in cultured rat hippocampal neurons has revealed that at an early stage in culture, subunits GluR1, GluR2 and GluR3 were distributed throughout somata, axons and processes. After 4 weeks in culture, the receptor subunits became clustered at postsynaptic sites in the

dendritic spines (Craig *et al*, 1993). Neurons that possess Ca^{2+}-permeable AMPA/kainate (Ca-A/K) receptors can be identified by a histochemical stain based on the kainate-stimulated uptake of Co^{2+} ions (Yin *et al*, 1997). Using this method, Ca-A/K receptors have been identified on GABAergic cortical neurons (Yin *et al*, 1997), on inhibitory interneurons in the hippocampus (Koh *et al*, 1995) and on the dendrites of hippocampal pyramidal neurons (Yin *et al*, 1999).

Kainate Receptors

Kainate receptors are expressed in high numbers in the CA3 region of the hippocampus, and are scattered more sparsely throughout the rest of the CNS. Immunohistochemical studies using antibodies against GluR5-GluR7 have indicated that kainate receptors may be located both presynaptically, in postsynaptic densities and in dendrites (Chittajallu *et al*, 1999). Despite their widespread distribution, the physiological significance of KA receptors is not well understood. Although kainate preferentially activates kainate receptors, it also induces a non-desensitizing response at AMPA receptors, which masks the smaller rapidly desensitizing response of kainate receptors. Traditionally, it has been difficult to distinguish between the functional properties of AMPA and KA receptors due to the lack of specific pharmacological tools. The recent introduction of selective antagonists of the AMPA receptor such as GYKI 52466 has provided evidence for neuronal expression of both types of receptor. This evidence is now fully supported by the identification of separate genes coding for AMPA and KA receptors (Michaelis, 1998). The kainate receptor subunits GluR5-7 share ~75% amino acid homology with each other, and ~ 40% homology with KA1-KA2. It is thought that like AMPA receptors, kainate receptors probably have a role in fast glutamatergic transmission in the CNS (Ozawa *et al*, 1998).

NMDA Receptors

The NMDA receptor responds to glutamate more slowly than AMPA or KA receptors, contributing mainly to the slow component of excitatory postsynaptic currents. This slow response is likely due to tonic inhibition of the receptor by Mg^{2+} present in the extracellular space. NMDA receptors have a higher affinity for glutamate than AMPA receptors, causing some NMDA receptors to be tonically maintained in a partially activated state, "primed" to respond to other excitatory stimuli (McBain and Mayer, 1994). The maximal activation of NMDA receptors requires removal of the voltage-sensitive Mg^{2+} block. When glutamate is released into the synaptic cleft, the rapid activation of AMPA/KA receptors causes depolarization of the postsynaptic membrane, which relieves the Mg^{2+} block of NMDA receptors and leads to their activation. The co-localization of AMPA and NMDA receptors in synapses means this is a common event in neural transmission (Cotman *et al*, 1987). NMDA receptor ion channels desensitize slowly, and have high permeability to Ca^{2+}. The entry of Ca^{2+} through the NMDA receptor may trigger a variety of Ca^{2+}-dependent intracellular cascades and induce the expression of immediate early genes. The voltage-dependent Mg^{2+} block of the NMDA receptor is unique, and provides the basis for the involvement of this receptor in processes of synaptic plasticity and pathological conditions such as excitotoxicity and neurodegeneration.

It would appear that the neuronal NMDA receptors have a pentameric structure (Michaelis, 1998). Of the four NMDA receptor subunits, NR1 is thought to serve as a fundamental subunit to form a current-conducting heteromeric NMDA receptor, whereas the NR2 subunits are better regarded as modulatory subunits which do not form functional NMDA receptor channels by themselves. The NR2 subunits show little homology with NR1 (~18% amino acid sequence identity), but possess similar structural characteristics (Yamakura and Shimoji, 1999). The highest levels of NMDA receptors are found in the CA1 region of the hippocampus, an area of the brain intensively studied by researchers interested in synaptic plasticity. The

expression of NMDA receptor subunits is developmentally regulated, and it is probable that the spatial and temporal expression of the NR2 genes allows precise regulation of the functional properties of NMDA receptor channels (Ozawa *et al*, 1998).

Metabotropic Glutamate Receptors

The discovery of G-protein coupled glutamate receptors in the late 1980s (Sugiyama *et al*, 1987) revolutionised conventional thinking about glutamatergic neurotransmission, since mGluRs provide a mechanism by which glutamate can precisely modulate synaptic activity whilst simultaneously causing rapid synaptic responses. The eight subtypes of mGluR (mGluR1-8) are closely related in primary structure, showing more than 40% amino acid sequence homology (Conn and Pinn, 1997). However, the mGluR family shows no sequence homology with other G-protein coupled receptors, and has a uniquely large extracellular domain, thought to contain glutamate-binding sites. The intracellular C-terminal domain may determine agonist potency. In terms of pharmacology, glutamate, quisqualate and ibotenate are known to activate mGluRs as well as iGluRs, whereas the glutamate analogue 1S, 3R-ACPD is specific for mGluRs.

The eight mGluRs can be divided into groups I – III based on their amino acid sequence identity (see **Fig. 1.2**). mGluRs of the same group show 70% sequence homology, whereas between groups this percentage drops to ~45%. This grouping is upheld by the transduction mechanisms of the different mGluR subtypes. Activation of group I receptors stimulates PLC and the concurrent release of Ca^{2+} from intracellular stores, via IP_3 formation. In addition, mGluR1 may be coupled to cAMP formation. The remaining mGluRs of groups II and III are linked to the inhibition of adenylate cyclase, and are strongly inhibited by PTX, suggesting that the G-proteins involved are of the G_i family (Ozawa *et al*, 1998). The physiological functions of mGluRs are varied, and are thought to include the regulation of neuronal

excitability, and an involvement in presynaptic inhibition and synaptic plasticity (Ozawa *et al*, 1998).

Plasma membrane Ca^{2+}-ATPase

The large Ca^{2+} concentration gradient and electrical driving force which exist across the plasma membrane of neurons promote the net gain of Ca^{2+} at rest, and necessitate the expenditure of ATP to extrude Ca^{2+} and retain neuronal Ca^{2+} homeostasis. Neurons have two parallel, independent mechanisms for Ca^{2+} extrusion: The Ca^{2+} -ATPase and the Na^{+} /Ca^{2+} exchanger. The Ca^{2+} -ATPase is a high affinity, low capacity pump, transporting approximately 0.5nmoles Ca^{2+} per mg of membrane proteins per sec. The ATPase is stimulated by calmodulin, via a direct interaction mechanism (Carafoli, 1987).

Na^{+}/Ca^{2+} exchanger

The Na^{+}/Ca^{2+} exchanger is particularly active in excitable plasma membranes and is regulated both by intracellular $Ca^{2+}$and by phosphorylation. The phosphorylation of the exchanger in rat brain synaptosomes by protein kinase C has been observed to increase its maximum velocity by 50% (Blaustein, 1996). The Na^{+}/Ca^{2+} exchanger has a low affinity for Ca^{2+}, but its capacity for Ca^{2+} extrusion is ten times greater than the Ca^{2+}-ATPase. Ca^{2+} is exchanged for Na^{+} (in the ratio 3 Na^{+}: 1 Ca^{2+}) out of the cytoplasm into the extracellular space when Ca^{2+} levels increase over normal resting levels. In contrast, when the plasma membrane is depolarised, the driving force favours Ca^{2+} entry through the Na^{+}/Ca^{2+} exchanger (Blaustein, 1988). The high density of Na^{+}/Ca^{2+} exchanger in presynaptic terminals suggests a direct role in the control of intracellular Ca^{2+} and synaptic vesicle recycling. The exchanger may be colocalized with underlying ER in many brain areas, implying an indirect role in the regulation of intracellular Ca^{2+} stores (Racay *et al*, 1996).

Store operated calcium entry

The idea that Ca^{2+} influx across the plasma membrane might occur through a capacitative mechanism has been in existence for over a decade. The suggested hypothesis was that Ca^{2+} influx was stimulated by the depletion of intracellular stores. This capacitative Ca^{2+} entry can be induced by a variety of agonists which release intracellular Ca^{2+}, and is thought to be present in both excitable and non-excitable cells (Berridge, 1995). The depletion of Ca^{2+} stores is thought to cause the release of a second messenger which initiates Ca^{2+} entry from the extracellular space through a putative Ca^{2+} channel located on the plasma membrane (Racay *et al*, 1996). The best characterised store-operated Ca^{2+} current to date is I_{CRAC} (Ca^{2+} release-activated Ca^{2+} current), which was first identified in mast cells (Hoth and Penner, 1992).

Two factors are required to link the Ca^{2+} content of cellular stores to CRAC channel activity in the plasma membrane: firstly a sensor of the store Ca^{2+} content, and secondly an activating signal. The molecular nature of the sensor is not known, but the IP3 receptor and the Ca^{2+} binding protein calreticulin have been proposed as possible candidates, on the basis of their sensitivity to Ca^{2+}. The nature of the activating signal has still not been elucidated, but several different models have been proposed. CIF (calcium influx factor) is a second messenger which could act as a ligand to open Ca^{2+} channels or even insert channels into the plasma membrane. CIF is thought to be stored in the ER awaiting store depletion for its release (Berridge, 1995). Alternatively, direct coupling mechanisms could be involved, which assume a physical interaction between proteins in the organelle and surface membrane (for full review, see Parekh, 1997).
Although its role is not completely understood in neurons, I_{CRAC} is thought to fulfil many physiological functions including the replenishment of intracellular stores, the generation of Ca^{2+} oscillations, and stimulation of exocytosis in non-excitable cells (Parekh, 1997).

1.1.2 CALCIUM TRANSPORT MECHANISMS OF THE ENDOPLASMIC RETICULUM

Neurons have a complex endoplasmic reticulum (ER) which extends throughout all compartments including the soma, dendrites and synaptic terminals. The ER plays an essential role in the folding and processing of newly synthesised proteins and must therefore maintain a high Ca^{2+} activity to support these Ca^{2+} dependent processes. Similar to the extracellular space, ER calcium levels lie in the millimolar range (Paschen, 1996). The ER has been considered as a neuron-within-a-neuron, given its continuous network throughout the cell and its integrative and regenerative properties, which are vital for neuronal signalling (Berridge, 1998).

The ER is able to function both as a calcium source and a calcium sink. Calcium stored within the ER is a significant source of signal Ca^{2+} which can be released by the activation of either the RyRs or the IP_3Rs. In addition, the ER is able to rapidly accumulate Ca^{2+} through its SERCA pumps.

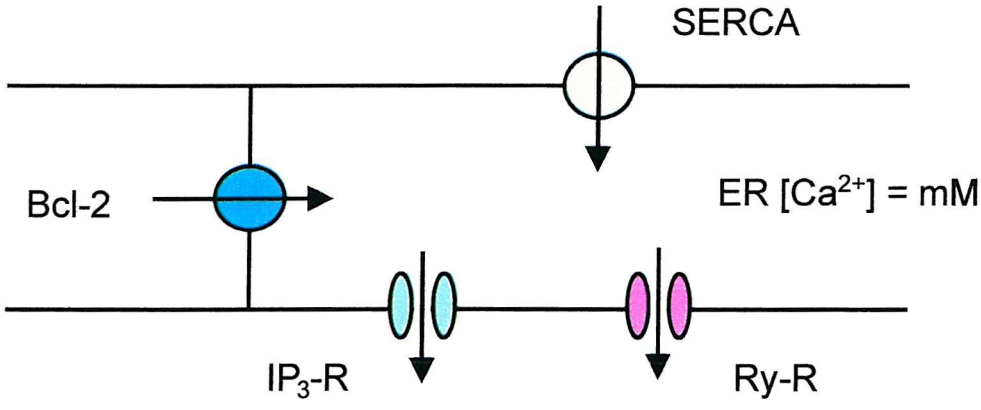

Figure 1.4: Control of ER calcium homeostasis. The ER intraluminal Ca^{2+} activity is in the millimolar range, essential for the Ca^{2+} -dependent reactions of protein folding. Calcium homeostasis is controlled the IP3R and the RyR, which upon activation release Ca^{2+} from the ER, and by the SERCA, which pumps Ca^{2+} ions back in against a steep concentration gradient. SERCA activity may be controlled by growth factors. Ca^{2+} transfer between ER subcompartments may be facilitated by bcl-2 (Paschen, 1998).

The ER as a calcium source

Immunohistochemical studies of the location of RyRs and IP_3Rs throughout the brain have revealed interesting differences in the distribution of these receptors. In the hippocampus, IP_3Rs are concentrated in CA1 pyramidal cells, with considerably fewer in CA3 and moderate levels in dentate gyrus granule cells (Sharp *et al*, 1993). The RyRs show a reverse pattern with highest levels in the dentate gyrus and CA3. Of the RyR subtypes, RyR2 has a widespread distribution throughout the brain whereas RyR3 predominates in hippocampal CA1. RyRs are predominantly located in neuronal soma, but in hippocampal dendritic spines, RyRs outnumber IP_3Rs (Fagni, 2000).

There is considerable controversy over the site of Ca^{2+} release in neurons: whether it originates from functionally common or two distinct IP_3- and ryanodine-sensitive Ca^{2+} pools. In cultured hippocampal neurons, Ca^{2+} release caused by IP_3 has been observed to occur independently of that caused by the RyR agonist caffeine, an observation consistent with the existence of two distinct Ca^{2+} pools (Murphy and Miller, 1989). This is further supported by the discovery of two Ca^{2+}ATPases in cerebellar granule cells, which show different pharmacological sensitvity to BHQ (Simpson *et al* 1996). In PC12 cells, three pharmacologically distinct Ca^{2+} pools have been identified, with very little apparent transfer of Ca^{2+} between the pools (Fasolato *et al*, 1991). The ER is therefore not homgeneous with respect to Ca^{2+}, and calcium fluxes between different subcompartments are probably facilitated by Bcl-2 (Paschen and Doutheil, 1998, He *et al*, 1997). However, regardless of the existence of separate Ca^{2+} pools in neurons, IP_3 mediated Ca^{2+} release seems to be dependent on the integrity of RyRs. IP_3 and ryanodine receptors are capable of regenerative Ca^{2+} release, allowing the amplification of external Ca^{2+} signals and the generation of Ca^{2+} waves via CICR. Calcium entering the cell via the plasma membrane provides the trigger Ca^{2+} to stimulate Ca^{2+} release from internal stores. The ER therefore plays a major role in neuronal Ca^{2+} signalling by virtue of its capacity to produce repetitive Ca^{2+} spikes and far-reaching Ca^{2+} waves. It should be emphasised that much of this evidence for IP_3-mediated Ca^{2+} waves has been

gleaned from non-excitable cells. There is very little evidence for IP_3 mediated calcium waves in neurons.

The ER as a calcium sink

The ER is able to rapidly take up Ca^{2+} through its SERCA pumps, representing a major sink for Ca^{2+} signals. Neuronal recovery from depolarisation induced Ca^{2+} increase is greatly hindered by thapsigargin, an inhibitor of the SERCA pumps (Markram *et al*, 1995). The amount of Ca^{2+} stored in the ER is highly variable. In central neurons, the ER store may be only partially filled under resting conditions. The ER can act as a Ca^{2+} sink for a large number of spikes, but the increasing luminal calcium load primes the intracellular channels, increasing the likelihood of CICR. The ER is therefore well able to function as a "memory" of neuronal activity. The ER can buffer Ca^{2+} spikes associated with action potentials and then signal this information to the nucleus through repeated bursts of Ca^{2+}. Such signalling may be important in the initiation of gene transcription. New evidence (Blaustein and Golovina, 2001).suggests that in neurons, sub-plasmalemmal components of the ER are functionally coupled to overlying plasmalemmal microdomains in units called PlasmERosomes. These might be important in the regulation of membrane potential via sub-plasmalemmal ER Ca^{2+} release through ryanodine-sensitive channels and activation of local Ca^{2+}-dependent K+ channels. PlasmERosomes may also provide a mechanism for the movement of Ca^{2+} between the ER and the extracellular fluid without altering bulk $[Ca^{2+}]_i$ (Blaustein and Golovina, 2001). Release of Ca^{2+} from the ER lumen contributes to slow after-hyperpolarisations which modify neuronal activity by suppressing firing patterns (Berridge, 1998).

A hypothesis has recently been put forward suggesting that disturbances of the functioning of the ER may be a common denominator of neuronal injury in both acute and chronic brain pathologies (Paschen, 1996). The "ER hypothesis" was put forward because high ER calcium activity is a prerequisite for normal cellular functioning, and the response of neurons to a transient depletion of ER Ca^{2+} stores is virtually identical to their response to

transient metabolic stress, implying similar underlying mechanisms. Calcium handling by the ER therefore acquires a new significance in the life and death of neurons.

1.1.3 CALCIUM TRANSPORT MECHANISMS OF MITOCHONDRIA

Mitochondria are the organelles primarily responsible for ATP production in all eukaryotic cells. As such, they have been dubbed the "powerhouse of the cell", producing, via oxidative phosphorylation, more than 95% of the ATP essential for the maintenance of cellular activities.

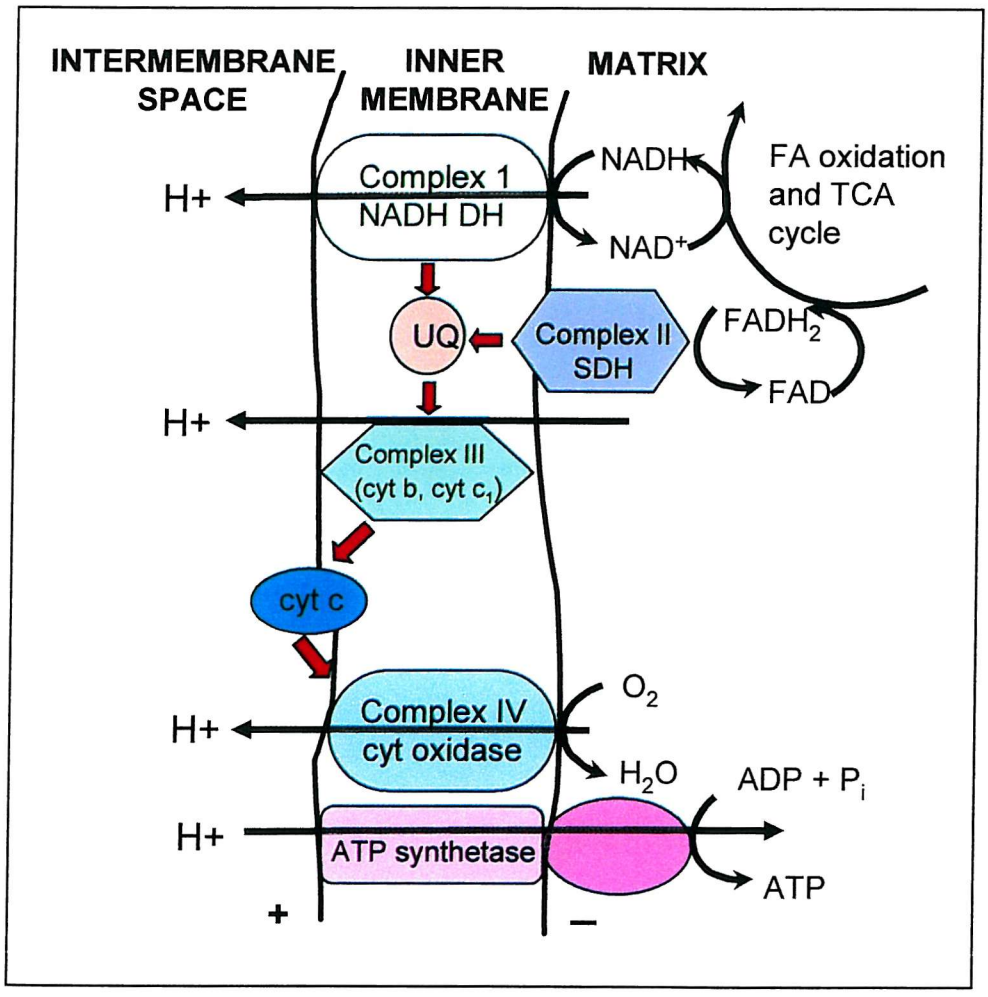

Figure 1.5 Mitochondrial electron transport, the electrochemical gradient of protons, and oxidative phosphorylation. DH, dehydrogenase; UQ, ubiquinone. Adapted from Murphy *et al*, 1999.

The outer mitochondrial membrane contains mitochondrial porin (VDAC) which forms an open β-barrel structure similar to that of the bacterial porins (Berg *et al*, 2002). These non-specific pores allow the free diffusion of molecules up to 10 kD, i.e. most ions and metabolites (Nicholls and Ferguson, 2002). The inner mitochondrial membrane is relatively impermeable to solutes, and contains the enzyme complexes of the electron transport chain (ETC). The TCA cycle occurs in the mitochondrial matrix. NADH and $FADH_2$ are generated from the TCA cycle and act as electron donors to the ETC. As electrons pass through the ETC, protons are pumped across the inner membrane which results in an electrochemical gradient, $\Delta\Psi$, a store of potential energy. The return flow of protons down their concentration gradient through the ATP synthase results in the production of ATP. Oxidative phosphorylation is the mechanism that couples the transfer of electrons to oxygen with the synthesis of ATP.

It is becoming increasingly clear that mitochondria are not simply generators of ATP, but participate in a multitude of cellular responses as diverse as the regulation of neurotransmitter release (David *et al*, 1998), modulation of Ca^{2+} signalling (Ichas *et al*, 1997), Ca^{2+} buffering in the case of extreme cytosolic Ca^{2+} overload (Miller, 1991) synaptic plasticity (Tang and Zucker, 1997) and thermogenesis in areas sparsely supplied with brown adipose tissue (Gunter and Pfeiffer, 1990). The fundamental importance of mitochondria is underscored by the suggestion that mitochondrial health is a major determinant of the human lifespan (Kalous and Drahota, 1996; Harman, 1994).

Mitochondria comprise an important part of the Ca^{2+} buffering capacity of the cell cytoplasm and employ a variety of mechanisms to facilitate the transport of Ca^{2+} across the mitochondrial inner membrane. Three of the mechanisms use channel kinetics while the fourth may involve a generalised change in membrane permeability (Gunter and Pfeiffer, 1990). Mitochondrial Ca^{2+} transport was discovered in the early 1960s and was originally thought to consist of active Ca^{2+} uptake and passive release. More recent experimental evidence would suggest that uptake of Ca^{2+} into the mitochondrial matrix

occurs via a Ca^{2+} permeable uniporter or channel located on the inner mitochondrial membrane.

Calcium influx

During normal physiological respiration, protons are pumped out of the mitochondrial matrix into the intermembrane space, making a potential known as $\Delta\Psi$ of -150 to -200mV across the inner membrane. The normal function of this electrochemical gradient is to provide a proton motive force, causing protons to flow back into the matrix. ATP is generated when protons flow back to the matrix through the ATP synthase, an enzyme complex located on the inner mitochondrial membrane. In this way, the mitochondrial membrane potential serves to couple oxidation and phosphorylation (Stryer, 1991). The steep electrochemical gradient ($\Delta\Psi$) also functions in the calcium buffering capacity of the mitochondrion, since when calcium levels increase in the cytoplasm, Ca^{2+} enters the matrix down the inner membrane potential, via the Ca^{2+} uniporter (Gunter *et al*, 1994). This process is energetically downhill, and is not coupled to the transport of any other ion. The uniporter is known to be a rapid, high capacity, low affinity transport mechanism, but the exact molecular nature of the uniporter still awaits elucidation. Some data suggest that the uniporter may act like a very fast gated channel or pore, opening with increased probability once local levels of Ca^{2+} increase (Gunter and Pfeiffer, 1990). Indeed, studies of mitochondrial Ca^{2+} transport velocity vs Ca^{2+} have indicated positive cooperativity. The uniporter may possess a separate activation site located on the cytoplasmic side of the inner mitochondrial membrane which, when bound by Ca^{2+}, increases the affinity for binding of Ca^{2+} at the transport site (Gunter and Pfeiffer, 1990). The uniporter is inhibited by magnesium, barium, manganese, the polyamines spermine and spermidine, and ruthenium red, which is commonly used experimentally to inhibit the uniporter, despite inhibiting Ca^{2+} flux through a number of different channels (Duchen, 2000). The activity of the uniporter decreases sharply as pH falls (Gunter and Pfeiffer, 1990). In a suspension of mitochondria at 1mg/ml, the uniporter can deplete free Ca^{2+} in a suspension of 10-50μM in seconds (Gunter and Gunter, 1994). Mitochondria in situ in

synaptosomes have been observed to carry out the net accumulation of Ca^{2+} from the cytosol when $[Ca^{2+}]_c$ exceeds 100nM (Martinez-Serrano and Satrustegui, 1992). Earlier work has shown the calcium content of mitochondria to be low in resting neurons, and considerably increased following pulsed neuronal depolarisation (Thayer and Miller, 1990).

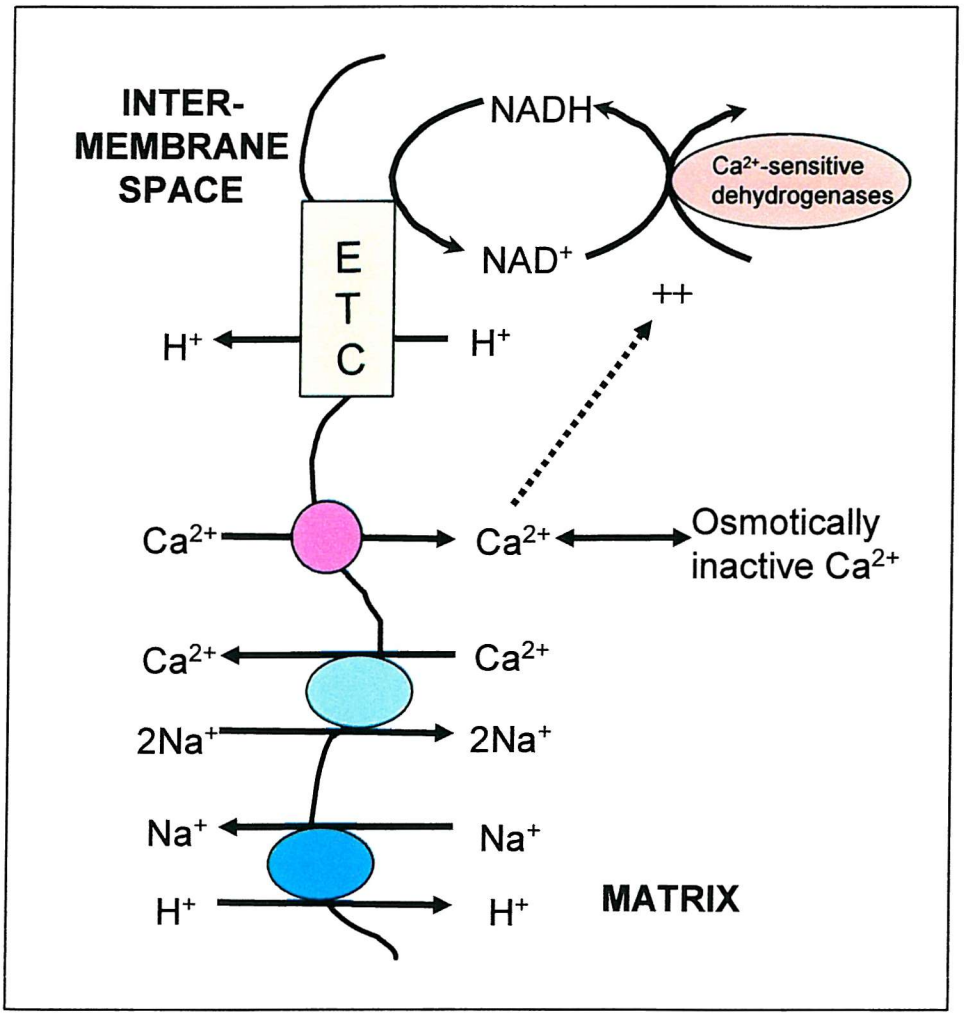

Figure 1.6 Calcium transport mechanisms of mitochondria The Ca^{2+} efflux mechanism shown is believed to be that which operates in neurons. The Na+/H+ exchanger that is driven by pH influences efflux through the Na+/Ca^{2+} exchanger. Adapted from Murphy ***et al***, 1999.

The recent discovery of a new mechanism of mitochondrial Ca^{2+} sequestration, the RaM (rapid mode) is of great interest since it would appear to be adapted for the uptake of Ca^{2+} from physiological transients, showing a

greater Ca^{2+} conductivity at the onset of a Ca^{2+} pulse than that of the uniporter (Gunter *et al*, 1998). Studies on isolated liver mitochondria have suggested that Ca^{2+} uptake via the RaM is additive between Ca^{2+} pulses, meaning that $[Ca^{2+}]_m$ increases more rapidly following a series of separate Ca^{2+} pulses than following longer exposure to a constant concentration of Ca^{2+}. The RaM is apparently "reset" by the fall in $[Ca^{2+}]$ between pulses. Evidence is accumulating for an external Ca^{2+} binding site, which closes the RaM. It has been postulated that the RaM and the uniporter could be the same transporter functioning in different modes. This is unlikely, however, given the pharmacological evidence that ten times more ruthenium red is required to completely inhibit the RaM as to completely inhibit the uniporter. In addition, 1mM spermine causes a two-fold increase in uniporter rate, whilst causing a six-fold increase in uptake via the RaM. These findings underscore the importance of the RaM as a means of Ca^{2+} uptake from physiological type Ca^{2+} transients (Gunter *et al*, 1998).

Calcium efflux

There are at least two separate Ca^{2+} efflux mechanisms located in the mitochondrial inner membrane - Na^+-dependent and Na^+-independent mechanisms, both of which show carrier like kinetics and are thought to function as selective carriers or gated pores. Na^+ is well suited for involvement in the control of $[Ca^{2+}]$, since its concentration in the cell cytosol (5-10mM) is much lower than in the extracellular fluid (Gunter *et al*, 1994). The outward transport of Ca^{2+} from the mitochondrial matrix requires energy which may be provided by the electrochemical gradient of a cotransported or exchanged ion e.g. by the pH component of the mitochondrial proton electrical gradient, by chemical energy from ATP/GTP hydrolysis or by conformational energy (Gunter *et al*, 1994). The Na^+-dependent Ca^{2+} efflux mechanism involves the outward transport of Ca^{2+} across the mitochondrial inner membrane in exchange for two or more Na^+. This is the primary Ca^{2+} efflux mechanism of mitochondria from heart, brain, parotid gland, skeletal muscle, adrenal cortex, brown fat and most tumour tissue. The greater velocity of this mechanism in heart and brain mitochondria allows these

tissues to rapidly change their metabolism in response to altered workload. The main efflux mechanism of liver, lung, kidney and smooth muscle is Na^+ independent (Wingrove and Gunter, 1986; Gunter *et al*, 1994). Several different mechanisms have been put forward to explain the Na^+ independent mode of transport including passive $Ca^{2+}/2H^+$ exchange, cotransport of Ca^{2+} and P_i or ATP and an active mechanism in which energy for Ca^{2+} efflux comes from the electron transport chain (ETC) or from ATP hydrolysis. Na^+-dependent and Na^+-independent transport are not thought to be mediated by the same mechanism working in the presence or absence of Na^+ since the two mechanisms are affected differently by activators and inhibitors (Gunter *et al*, 1994).

It has been postulated that the existence of *two* specific mechanisms of calcium efflux in the mitochondrial inner membrane may reflect the elaborate systems required to fully integrate mitochondrial calcium metabolism with the many ion transport systems vital for the control of different cellular activities. Alternatively, the Na^+-independent mechanism may be a less specific cation efflux mechanism used to rid mitochondria of Ca^{2+}, Mn^{2+} and other ions before elimination from the cell (Gunter and Pfeiffer, 1990).

Permeability transition

Mitochondrial permeability transition is characterized by a sudden increase in the permeability of the inner mitochondrial membrane to small ions and molecules. The transition is mediated by a proteinaceous pore, the permeability transition pore (PTP). The PTP, located in the inner mitochondrial membrane, is a nuclear encoded, voltage-gated ion channel. Its opening is favoured by depolarisation, intramatrix Ca^{2+} and oxidising agents, and precluded by protons, adenine nucleotides and cyclosporin A (CSA) (Miller, 1998).

The PTP provides a novel route for calcium release from mitochondria and its recent discovery has generated much interest. The PTP is thought to function in both high and low conductance modes. Recent work has shown that activity of the channel in its low conductance mode may play a role in

normal mitochondrial function, and that under such conditions, PTP opening is both transient and reversible (Ichas *et al*, 1997). Operation of the PTP in its high conductance mode has been connected with cell damage. Under these conditions, pore opening is irreversible and the pore becomes permeable to larger molecules (MW up to 1.5kDa) and even matrix proteins, leading to complete collapse of the membrane potential and colloid-osmotic swelling of the mitochondrial matrix.

Transient opening or "flicker" of the PTP appears to be part of its normal mode of behaviour. The frequency of such transient openings is determined by matrix free [Ca^{2+}] (Crompton, 1999). At low flicker frequencies, only a small proportion of mitochondria has open pores at any given moment, and mitochondrial $\Delta\Psi$ of the overall population of cells is maintained. PT pore flicker has been elegantly studied in single mitochondria immobilized on cover slips and stained with TMRE (Huser *et al*, 1998). Transient depolarisations reflecting pore flicker were observed to last from a few seconds to over one minute, showing variation in pore opening duration. Single PT flicker has also been measured in electrophysiological studies of the inner mitochondrial membrane (Crompton, 1999).

1.1.4 PHYSIOLOGICAL SIGNIFICANCE OF MITOCHONDRIAL CALCIUM TRANSPORT

Given that mitochondria possess four distinct mechanisms for the transport of Ca^{2+} and the well established importance of Ca^{2+} as a second messenger within the cytosol, questions arise as to the physiological significance of mitochondrial Ca^{2+} transport in an organelle dedicated to metabolic energy transduction. It has been suggested that mitochondria transport Ca^{2+}

- To regulate cytosolic Ca^{2+}
- To buffer cells against excess Ca^{2+} levels

- To control metabolism by the regulation of mitochondrial matrix Ca^{2+} $[Ca^{2+}]_m$

- To provide a releasable source of activator Ca^{2+} (reviewed in Gunter and Pfeiffer, 1990)

Initially, it was thought that the predominant role for mitochondrial Ca^{2+} transport was in the protection of cells against Ca^{2+} overload and in the control of metabolism. This followed the finding that mitochondria contained little stored Ca^{2+} under normal resting cellular conditions, precluding a role in the regulation of cytosolic calcium or as a source for activator Ca^{2+}. However, the recent discovery of the rapid mode (RaM) of Ca^{2+} uptake points to a mechanism ideally suited to uptake from physiological Ca^{2+} transients. The efficiency of Ca^{2+} uptake via the RaM reduces the risk of accidental activation of the PTP, whilst accurately relaying cytoplasmic Ca^{2+} fluctuations into the mitochondrial matrix. The amount of Ca^{2+} uptake depends more on the number of Ca^{2+} pulses than on $[Ca^{2+}]$, permitting the system to function in a frequency modulated mode (Gunter *et al*, 1998).

Mitochondrial calcium buffering

Cytosolic Ca^{2+} is buffered by mitochondria and other Ca^{2+} sequestering organelles (ER and SR) as well as by cytosolic P_i and other Ca^{2+} binding species. Under appropriate conditions, mitochondria can be shown to accumulate large quantities of Ca^{2+} (Miller, 1991), and the calcium transport properties of isolated mitochondria are well suited to a role in limiting any increase in calcium which might otherwise damage cell integrity (Nicholls, 1985). It is probable that the accumulation of calcium causes a decrease in the mitochondrial membrane potential, $\Delta\Psi$. The large capacity of mitochondria for Ca^{2+} transport has been well documented, and a putative role for the mitochondrion in the protection of cells against Ca^{2+} overload was first proposed over a decade ago (Nicholls, 1985). The large potential, $\Delta\Psi$, which exists across the inner mitochondrial membrane provides the driving force for Ca^{2+} accumulation. The Ca^{2+} content of mitochondria

within resting cells is believed to be low, yet isolated mitochondria can accumulate large quantities of Ca^{2+} when it is provided to them (Gunter and Pfeiffer, 1990) and inhibitors of mitochondrial Ca^{2+} uptake have been seen to severly compromise clearance of cytoplasmic Ca^{2+} after an imposed Ca^{2+} load (White and Reynolds, 1996). This indicates that Ca^{2+} accumulation by mitochondria is important for cellular Ca^{2+} homeostasis, and indeed has been observed to account for as much as 70% of cytosolic Ca^{2+} buffered during the initial rapid phase of recovery from imposed Ca^{2+} loads in chromaffin cells (Herrington *et al*, 1996).

Control of metabolism

There is considerable experimental evidence to endorse a role of the intramitochondrial Ca^{2+} concentration as a mediator of metabolism. Mitochondrial Ca^{2+} uptake in response to limited cytoplasmic Ca^{2+} elevations has been described in several preparations (Simpson and Russell, 1998) and may relay cytoplasmic fluctuations in Ca^{2+} into the mitochondrial matrix. Cytoplasmic Ca^{2+} oscillations are "decoded" by mitochondria and result in the maintained activation of mitochondrial dehydrogenases. This provides an efficient mechanism to allow the coupling of ATP production with cellular activity (White and Reynolds, 1996). There are many steps in the production of ATP that may be regulated by Ca^{2+}. Intramitochondrial dehydrogenases including pyruvate dehydrogenase, isocitrate dehydrogenase and 2-oxoglutarate dehydrogenase are activated by Ca^{2+} in the concentration range expected in the matrix following the sequestration of Ca^{2+} pulses in the cytoplasm. Other steps include the stimulation of electron transport through a Ca^{2+}-induced increase in matrix volume, a Ca^{2+}-induced decrease in inhibition of the ATPase via a Ca^{2+}-sensitive inhibitor protein and also activation of the adenine nucleotide translocase, increasing the availability of substrate nucleotides (Gunter *et al*, 1994). Interestingly, a sustained elevation of intramitochondrial Ca^{2+} results in a different mitochondrial response than Ca^{2+} spikes. A monophasic $[Ca^{2+}]_m$ elevation causes only a transient activation of mitochondrial enzymes. In addition, $[Ca^{2+}]_c$ oscillations are

transmitted into mitochondria much more efficiently than "plateau" Ca^{2+} elevations (Hajnoczky *et al*, 1995).

It is clear that mitochondria exhibit a rapid Ca^{2+} uptake mechanism, which enables mitochondria to sequester Ca^{2+} in the early phase of cytoplasmic Ca^{2+} spikes, and to rapidly reset in normal Ca^{2+}. Such a mechanism is ideal for sequestering Ca^{2+} during cellular Ca^{2+} oscillations and waves, and allows mitochondria to interact quickly and sensitively with Ca^{2+} in its local microenvironment (Simpson and Russell, 1998).

Synaptic plasticity

It would appear from new evidence that mitochondria are not simply passive "sponges" on the receiving end of cytoplasmic calcium signals, but also have the capacity to actively participate in them. Having buffered calcium, for example during the intense cellular activity following stimulation, mitochondria are in a position to release their accumulated calcium. Traditionally, the major route of calcium egress from the matrix has been thought to be a Na^{+}/Ca^{2+}exchanger in the inner mitochondrial membrane. Calcium release by this means provides a way of increasing the duration of the cytoplasmic calcium signal far beyond that of the original stimulus. In this way. the mitochondria behaves as a calcium signalling memory storage device (Miller, 1998). The importance of this in processes of synaptic plasticity has recently been highlighted in a study on post-tetanic potentiation (Tang and Zucker, 1997). It was observed that post-tetanic potentiation was specifically blocked by different inhibitors of mitochondrial Ca^{2+} transport. This suggests that post-tetanic potentiation could be due to presynaptic mitochondrial sequestration of the elevated cytoplasmic Ca^{2+} found during a tetanic stimulus, and the slow release of this Ca^{2+} into the cytoplasm in the post-tetanic phase.

Calcium signalling

The recent discovery of the mitochondrial permeability transition pore (PTP) as an additional route of calcium release has caused much interest, since it

permits mitochondrion to behave as an excitable organelle. When exposed to high extracellular levels of calcium, mitochondria rapidly accumulate calcium until a certain degree of loading is reached. Further addition of calcium at this point leads to large-scale calcium release, followed by reaccumulation. This is a similar phenomenon to the calcium induced calcium release (CICR) observed at ryanodine receptors. Mitochondrial CICR has the potential to allow calcium waves to propagate between mitochondria in cellular or even transcellular networks, and may integrate with and amplify IP3 dependent calcium waves, emitted primarily from the endoplasmic reticulum (Miller, 1998). The activity of the mitochondrial PTP is believed to be critical to the ability of mitochondria to participate in cellular signalling.

It would appear that mitochondria in some cellular populations are anchored to specific locations within the cell. This spatial arrangement may be important for the discrete local regulation of Ca^{2+} signals and other cellular functions (Simpson and Russell, 1998). It has been hypothesised that during the release of IP_3 in cell signalling, microdomains of high $[Ca^{2+}]_i$ may be generated close to IP_3 gated channels and detected by local mitochondria. This could provide an efficient way of maximising mitochondrial activity upon cell stimulation (Rizzuto *et al*, 1993). This local uptake of Ca^{2+} by mitochondria may also alter channel opening and activity, as the activation and inactivation kinetics of IP_3 receptors are highly dependent on local $[Ca^{2+}]$ (Simpson and Russell, 1998). Mitochondrial uptake of cytosolic Ca^{2+} could therefore raise the threshold for IP_3 receptor activation, decreasing asynchronous IP_3 receptor channel openings and amplifying IP_3-dependent Ca^{2+} waves and oscillations. Analysis of the spatial relation between mitochondria and ER with the imaging of targeted GFPs has shown numerous close contacts between the organelles and also showed that mitochondria exist as an interconnected, dynamic network (Rizzuto *et al*, 1998). This spatial organization would potentially allow mitochondria to be exposed to a higher concentration of Ca^{2+} than the bulk cytosol upon opening of IP_3 receptors, providing a strong structure function relationship and

showing the importance of cell architecture in the regulation of Ca^{2+} signalling.

Physiological role of permeability transition

PTP opening in its low conductance mode may have numerous roles in normal cell physiology since opening in this mode does not threaten mitochondrial integrity. Transient opening of the PTP may have a role in protein turnover, given the slow release of matrix proteins upon PTP opening. *In vivo*, permeability transition may function as an independent protein release mechanism, but little is known about the release or degradation mechanisms required to complete a turnover cycle (Gunter and Pfeiffer, 1990).

Secondly, opening of the PTP may be used to divert the energy of substrate oxidation from ATP synthesis to the production of heat. In mammals, brown adipose tissue is known to be an important source of heat for the maintenance of body temperature. The mitochondria in brown fat are rich in uncoupling protein (UCP). In cold-adapted animals, UCP constitutes 15% of the mitochondrial inner membrane (Voet and Voet, 1995). UCP or thermogenin is a dimer of 33kd subunits that is located in the mitochondrial intermembrane space and is structurally similar to the mitochondrial anion transporter. UCP forms a channel that allows the flow of protons from the cytosol to the mitochondrial matrix without the synthesis of ATP, thereby uncoupling oxidative phosphorylation and generating heat (Berg *et al*, 2002). UCP is thought to be activated by free fatty acids (Voet and Voet, 1998). In some animals, however, there is insufficient adipose tissue to account for thermogenic capacity, and other organs including liver are thought to participate in non-shivering thermogenesis. Mitochondria which have undergone permeability transition could produce heat via the oxidation of NADH (Gunter and Pfeiffer, 1990).

Thirdly, permeability transition may be an energetically cheap way to rid mitochondria of a Ca^{2+} overload following mitochondrial buffering of excess cytosolic Ca^{2+} (in conditions of low $[Ca^{2+}]_i$), but there is scant evidence for

PTP opening as a protective mechanism. It has been argued that if the main function of mitochondrial Ca^{2+} is to control the TCA cycle and mitochondrial ATP production, then mitochondrial Ca^{2+} is unlikely to be regulated by PTP opening, a mechanism which allows ATP hydrolysis and the loss of TCA cycle components from the matrix (Crompton, 1999). PTP opening is therefore thought to be a critical event in cell death following Ca^{2+} overload, rather than a Ca^{2+} homeostatic mechanism in viable cells.

Finally, PT pores may be important in establishing contact between mitochondria in the formation of mitochondrial networks. Tight intermitochondrial junctions could allow connected mitochondria to function as a single bioenergetic entity, allowing efficient energy transfer between different cellular compartments (Crompton, 1999). These mitochondrial junctions may form reversibly according to cellular energy requirements, which would agree with the three-dimensional reconstruction and observed plasticity of the mitochondrial space (Rizutto *et al*, 1998).

1.1.5. OTHER CALCIUM STORES

Calciosomes

Another organelle involved in Ca^{2+} storage has recently been descibed. The calciosome is present in a variety of cell types, and contains calsequestrin, a protein found in the Ca^{2+}-binding organelles of skeletal muscle (Miller, 1988). There are probably many more Ca^{2+} storage organelles awaiting discovery, given the recent report of a novel calcium containing organelle (CCO) in rat hippocampal neurons (Korkotian and Segal, 1997). CCOs were not colocalised with the ER or with mitochondria, and showed a unique response to stimulation with caffeine, whilst being insensitive to ryanodine. These organelles may therefore regulate the release of Ca^{2+} from ryanodine-insensitive stores.

The nuclear envelope

There is considerable controversy over whether or not Ca^{2+} gradients can exist across the nuclear membrane. The existence of large, non-specific nuclear pores, which allow the passage of molecules up to 75kDa, would make the existence of any Ca^{2+} gradients across the nuclear membrane very unlikely. However, Ca^{2+} gradients may exist in the sub-second timescale, and under certain conditions, nuclear pores may be blocked by an internal "plug", facilitating the generation of ionic gradients (Rutter *et al*, 1998). Ryanodine and IP_3 receptors have been identified on the nuclear membrane, as has a nuclear Ca^{2+} ATPase, suggesting that the nuclear envelope serves as a Ca^{2+} pool (Malviya and Rogue, 1998). IP_3 may provoke the release of Ca^{2+} from this store, producing isolated changes in Ca^{2+} in the vicinity of the nucleus. Invaginations in the nuclear membrane have been identified in HeLa cells, which may well be the site of generation of such Ca^{2+} microdomains (Lui *et al*, 1998). Changes in nucleoplasmic Ca^{2+} levels are likely to be involved in the control of gene expression, and may coordinate the location of key transcription factors (Rutter *et al*, 1998).

Calcium binding proteins

Neurons contain a variety of calcium-binding proteins, including calmodulin, calbindin and parvalbumin. The affinity constants of the Ca^{2+} binding sites on these proteins are in an appropriate range for them to contribute to Ca^{2+} buffering (0.1-10μM) (McBurney and Neering, 1987). Calmodulin is a 15kDa Ca^{2+} -binding regulatory protein of the E-F hand family of proteins, and is present in brain cytosol at approximately 50μM. Little Ca^{2+} is bound to calmodulin at resting Ca^{2+} levels, but at micromolar levels of Ca^{2+}, its four Ca^{2+} binding sites become successively occupied. Activated CaM is able to mediate the activity of various proteins including CaM kinase II, adenylate cyclase, cylcic nucleotide phosphodiesterase and calcineurin, which in turn mediate a multitude of downstream signalling events (Kennedy, 1989). Interestingly, the distribution of Ca^{2+} binding proteins is thought to vary considerably between different neurons, allowing heterogeneity in the local regulation of Ca^{2+}. Parvalbumin, for example, is present in high

concentrations in GABAergic neurons that fire at high frequency, but not in those which fire at lower frequencies. Parvalbumin is able to maintain the excitability of the high frequency neurons, by rapidly buffering intracellular Ca^{2+} and thereby preventing the activation of Ca^{2+}-dependent K^+ conductances (Blaustein, 1988). The high concentration of calbindin in cerebellar Purkinje cells (150μM) would suggest that calbindin constitutes the main early component of Ca^{2+} buffering in these neurons. Even the intraneuronal distribution of Ca^{2+} buffering proteins can vary: calmodulin is located in the cell bodies and dendrites of most CNS neurons, but not in axons or presynaptic terminals (McBurney and Neering, 1997). Ca^{2+} binding proteins are able to buffer cytosolic Ca^{2+} rapidly, but may quickly saturate in neurons that fire at high frequencies. Intracellular organelles are then required to sequester Ca^{2+} until the extra Ca^{2+} burden can be extruded across the plasma membrane.

Synaptic vesicles

Synaptic vesicles sequester Ca^{2+} by an ATP driven mechanism, and have a high Ca^{2+} content, but a significant contribution to the regulation of $[Ca^{2+}]i$ is unlikely given their low affinity for Ca^{2+} (Blaustein, 1988). The large vesicular pool of Ca^{2+} is surprisingly undynamic, given the probable presence of IP_3 receptors on the synaptic vesicle membrane (Rutter *et al*, 1998). However, a recent report on the transient accumulation of Ca^{2+} by vesicles following synaptic stimulation suggests that synaptic vesicles may contribute to the shape of Ca^{2+} microdomains in synaptic terminals (Israel and Dunant, 1998).

1.2 CALCIUM AND NEURONAL DEATH

Research conducted over the past decade has brought to light two major components of neuronal cell death: firstly, a loss of calcium homeostasis, and secondly, mitochondrial dysfunction, which will be discussed in the following sections.

The central role of calcium in normal neuronal function and neuronal calcium homeostatic mechanisms has been discussed (**Section 1.1**). Viable neurons maintain a Ca^{2+} concentration gradient across the plasma membrane of more than four orders of magnitude. $[Ca^{2+}]_i$ can increase transiently and generate cellular responses following physiological stimuli. Under pathological conditions, however, Ca^{2+} increases are generally greater and more prolonged, triggering damaging processes that ultimately lead to neuronal death.

Calcium was proposed to be the final common denominator of toxic cell death more than twenty years ago, when cell death following exposure to a variety of toxins was observed to be highly Ca^{2+}dependent. It was suggested that "attempts to specifically interrupt Ca^{2+} fluxes could have significant theraputic consequences" (Schanne *et al*, 1979). Since the early 1980's, the role of Ca^{2+} in cell death has been the focus of intensive research, and it has become apparent that disruption of the mechanisms that regulate intracellular calcium homeostasis is often seen early in the development of irreversible cell injury. Cellular calcium overload is thought to involve multiple intra- and extracellular routes that are normally used in physiological signalling (Leist and Nicotera, 1998; Nicotera *et al*, 1992; Orrenius and Nicotera, 1994).

1.2.1 TOXIC MECHANISMS TRIGGERED BY ELEVATED Ca^{2+}

The toxicity caused by elevated Ca^{2+} is probably not an intrinsic property of the Ca^{2+} ion itself; but rather the consequence of downstream processes triggered by transient or continuous exposure to Ca^{2+}.

Nitric Oxide Synthase

Several different classes of nitric oxide synthases (NOS) exist in the brain. A constitutive form of nitric oxide synthase, nNOS, is expressed in neurons, and is activated by Ca^{2+}/calmodulin following an increase in $[Ca^{2+}]_i$. Other inducible isoforms, iNOS, are present in astrocytes and glia, and function at basal Ca^{2+} concentrations, being inducible by stimuli such as cytokines. NOS is a cytochrome P450-related enzyme which converts arginine to nitric oxide and citrulline (Leist and Nicotera, 1998). NOS are known to be anchored to intracellular protein scaffolding such as PSD95, associated with the inner portion of NMDA receptors (Sattler *et al*, 1999), and are therefore well placed to interact with Ca^{2+} entering the neuron through this receptor. The role of nitric oxide within neurons is controversial. It has been implicated in processes of synaptic plasticity (Malen and Chapman, 1997) and is also thought to be involved in cytotoxicity (Dawson *et al*, 1991). NO *per se* may not be toxic, but may combine with superoxide to form the highly damaging reactive oxygen species peroxynitrite ($ONOO^-$).

Activation of hydrolytic enzymes

Ca^{2+} activates several enzymes involved in the breakdown of proteins, lipids and nucleic acids. Sustained increase in $[Ca^{2+}]_i$ is therefore likely to cause the unregulated breakdown of vital intracellular components. The following enzymes have been implicated in Ca^{2+} -mediated toxicity:

- Calpains are Ca^{2+} -dependent proteases which are thought to be involved in excitotoxic neuronal death (Brorson *et al*, 1994). The selective calpain inhibitor leupeptin has been seen to reduce the extent of proteolysis and cell killing, strongly implicating a proteolytic system in the overall toxic

process (Lee *et al*, 1991). Calpains are thought to degrade cytoskeletal and cytoskeletal anchoring-integral proteins (Nicotera *et al*, 1992).

- Ca^{2+} -dependent DNAases are responsible for the DNA "laddering" (cleavage into fragments of approximately 200 base-pairs) that is frequently observed in apoptosis. BT-20 cells exposed to TNF-α have been observed to undergo apoptosis following a selective increase in intranuclear Ca^{2+}, suggesting that a compartmentalized increase in Ca^{2+} may be sufficient to trigger DNA damage (Nicotera *et al*, 1992). DNA single strand breaks can be generated through a Ca^{2+} -dependent process in cells exposed to oxidative stress (Dypbukt *et al*, 1990), although the specific mechanism is still not known. Clearly, Ca^{2+} overload may trigger a variety of enzymatic processes culminating in lethal DNA damage.

- A number of phospholipases are Ca^{2+}-dependent and play important physiological roles as second messengers. The sustained activation of PLA_2 can result in the generation of toxic metabolites, such as ROS, which cause membrane damage, and lysophosphatids, known to alter membrane structure so as to facilitate Ca^{2+} influx and Ca^{2+} release from internal stores (Leist and Nicotera, 1998).

Xanthine Oxidase

The persistent elevation of $[Ca^{2+}]_i$ can promote the conversion of xanthine dehydrogenase to xanthine oxidase, which disrupts normal handling of electrons in the TCA cycle and can lead to the massive generation of ROS. This activation of xanthine oxidase is thought to play a role in ischaemic neuronal death *in vivo* (Coyle and Puttfarcken, 1993).

Protein Phosphorylation and Gene Regulation

Transient elevations in $[Ca^{2+}]_i$ may trigger long lasting cellular effects by altering processes of gene transcription and protein phosphorylation. Calcium activates type II and IV CaMK, involved in transcriptional regulation, calcium-sensitive adenylate cyclases, and a variety of protein

kinase C isozymes. These enzymes may modify neuronal calcium entry through action on cell surface receptors. Calcineurin is a calcium-activated phosphatase that regulates numerous cellular components involved in neurotoxicity. For example, calcineurin may limit Ca^{2+} influx into the neuron by dephosphorylating the NMDA receptor, and may increase the activity of NOS by dephosphorylation of the enzyme (Leist and Nicotera, 1998). Calcineurin thus has a multitude of effects in neurons, including the recent discovery of its involvement in the nuclear import of NF-AT transcription factors from the cytoplasm (Timmerman *et al*, 1996).

Gene transcription is regulated by calcium via a number of signalling cascades including protein kinase A, MAP kinases and CaMK. The route of calcium entry is apparently deterministic of downstream events, for example, BDNF is induced in cortical neurons by Ca^{2+} entry through VDCCs, but not through the NMDA receptor (Leist and Nicotera, 1998).

Cytoskeletal modifications

Ca^{2+} directly controls the organization of the neuronal cytoskeleton, either through direct effects on cytoskeletal proteins, or by changing their polymerization rates. Raised Ca^{2+} may cause the cleavage of cytoskeletal elements through the activation of proteases, and may trigger the depolymerization of microtubules, microfilaments and nuclear laminins (Leist and Nicotera, 1998). An early event in toxic cell injury is the appearance of "blebs" (multiple surface protrusions), thought to result from Ca^{2+}-induced disruption of cytoskeletal interactions with the plasma membrane (Nicotera *et al*, 1992). The modification of cytoskeletal components can have further effects on cell surface receptors and channels, since receptor desensitization is often dependent upon microfilament interactions. For example, stabilization of F-actin with phalloidin prevents desensitization of the NMDA receptor (Rosenmund *et al*, 1993).

1.2.2 GLUTAMATE EXCITOTOXICITY

Glutamate and Ca^{2+} influx

In 1977, it was observed that in cerebellar tissues, anoxia triggers the rapid movement of Ca^{2+} into cells from the extracellular space (Nicholson *et al*, 1977). This, with further findings, led to the theory of calcium-mediated neuronal death under conditions of hypoxia, ischaemia and hypoglycaemia. A speculative link between hypoxia and glutamate was made by Van Harreveld in 1959, who saw that cortical spreading depression could be induced in rabbits by the addition of glutamate, and had many of the characteristics of neuronal hypoxia. An important advance was the finding that glutamate could trigger neuronal cell death in cultured neurons (Rothman, 1984) and in brain slices (Garthwaite and Garthwaite, 1986). This damage was originally assumed to be osmolytic, but further research showed that although the early cell swelling was usually reversible, cells exposed to glutamate showed a Ca^{2+}-mediated delayed cell death (Choi, 1987).

Glutamate is the major excitatory neurotransmitter in the CNS, acting at approximately 40% of synapses, but has the potential to become lethally toxic to neurons when extracellular levels of this neurotransmitter rise dramatically. Typical conditions leading to increased extracellular levels of glutamate include neuronal depolarization, energy depletion following hypoxia or hypoglycaemia, or defects in glutamate re-uptake systems (Leist and Nicotera, 1998). An increase in glutamate concentration from its normal synaptic level of 1μM to pathological levels of 100μM or greater, results in the overstimulation of both voltage-dependent and receptor operated Ca^{2+} channels, resulting in an unregulated excessive Ca^{2+} influx into the neuron (Abe *et al*, 1995). Calcium buffering mechanisms are overwhelmed, and the unchecked rise in Ca^{2+} can set in motion a number of damaging cascades leading ultimately to neuronal death.

The neurotoxicity of glutamate is thought to be triggered by Ca^{2+} influx through NMDA receptor channels (Tymianski *et al*, 1993) and the selective

antagonism of NMDA receptors blocks the late neuronal degeneration induced by exposure to glutamate (Choi, 1988). Ca^{2+} influx through NMDA receptors is much more effective than other routes in mediating cell death. This suggests the compartmentalization of Ca^{2+}-dependent neurotoxic processes within neurons, perhaps with a preferential localization in the submembrane space adjacent to NMDA receptors (Beal, 1995). The NMDA receptor could therefore provide a major route for the toxic calcium influx which accompanies excessive exposure to glutamate, but other means of calcium entry are still important here, namely voltage-dependent calcium channels, Ca^{2+}-permeable AMPA/kainate receptors, the Na^{+}/Ca^{2+} exchanger, and nonspecific membrane leakage. Neuroprotection by a selective N-type voltage dependent calcium channel blocker, MVIIA, has been reported in an experimental stroke model (Pringle *et al*, 1996). Calcium may also be released from intracellular stores following the activation of metabotropic glutamate receptors. Depending on the subtype of receptor, mGluR stimulation may be neuroprotective (Pizzi *et al*, 1996; Sagara and Schubert, 1998) or may exacerbate neurotoxicity, as in the case of mGluR1 (Mukhin *et al*, 1996).

Excitotoxicity and raised $[Ca^{2+}]_i$

Several lines of evidence support the key role of Ca^{2+} in excitotoxicity. Firstly, there is a well documented increase in $[Ca^{2+}]_i$ in *in vivo* and *in vitro* models of excitotoxic cell death. Excitatory amino acid-induced neuronal Ca^{2+} uptake has been shown directly in cultured neurons by measurement of $^{45}Ca^{2+}$ uptake (Eimerl and Schramm, 1994; Hartley *et al*, 1993; Manev *et al*, 1989) and by Ca^{2+} microfluorimetry (Brorson *et al*, 1994; Ogura *et al*, 1988). Increased neuronal Ca^{2+} activity following glutamate receptor stimulation has repeatedly been demonstrated using fluorescent probes (Hyrc *et al*, 1997; Perez Velazquez, 1997; Khodorov *et al*, 1993; Tymianski *et al*, 1993b; Randall and Thayer, 1992; Segal and Manor, 1992; Dubinsky and Rothman, 1991; Michaels and Rothman, 1990). Secondly, prevention of Ca^{2+} entry into the cell by removal of extracellular Ca^{2+} (Manev *et al*, 1989; Choi, 1987) or by the use of glutamate receptor antagonists (Pringle *et al*, 1997; Brorson *et*

al, 1994; Manev *et al*, 1989; Hartley *et al*, 1993; Michaels and Rothman, 1990) attenuates neuronal death in many paradigms of excitotoxicity. Thirdly, a causal role for Ca^{2+} in excitotoxicity is strongly suggested by studies where neurotoxicity is prevented by the inhibition of downstream effects of Ca^{2+} overload. Excitotoxic neuronal damage can be prevented with intracellular Ca^{2+} chelators (Tymianski *et al*, 1994, Abdel-Hamid and Tymianski, 1997). In addition, inhibitors of calcineurin, an effector of Ca^{2+} toxicity, protect neurons from EAA induced toxicity (Dawson *et al*, 1993).

Delayed Ca^{2+} overload in neurotoxicity

Neurons challenged with an excitotoxic stimulus typically show three phases of Ca^{2+} increase. An initial Ca^{2+} spike is followed by semi-recovery to an elevated plateau. This recovery may reflect desensitisation of NMDA receptors and VDCCs, and Ca^{2+} clearance by mitochondrial sequestration. Finally, an uncontrolled failure of Ca^{2+} homeostasis is seen, termed delayed Ca^{2+} deregulation (DCD), which reliably predicts cell lysis (Nicholls and Budd, 2000), and may reflect total cellular ATP depletion. In CGCs continuously exposed to glutamate, DCD occurred after approximately 60 minutes of glutamate exposure (Nicholls and Budd, 2000). The second and third phases can proceed after the removal of extracellular glutamate (Randall and Thayer, 1992; Tymianski *et al*, 1993; Wang and Thayer, 1996). The sustained Ca^{2+} plateau, which persists even after glutamate removal, was originally attributed to an increase in Ca^{2+} permeability of the neuronal membrane. Further investigations have suggested that the origin of the sustained elevation of Ca^{2+} is an impairment of Ca^{2+} extrusion systems, in particular the transmembrane Na^{+}/Ca^{2+} antiporter (Khodorov *et al*, 1993).

It is known that excitotoxic insults result in a loss of neuronal Ca^{2+} homeostasis, but the Ca^{2+} mediated changes in cellular function that initiate an irreversible progression towards cell death need further elucidation.

1.2.3 EXCITOTOXICITY CAUSED BY OTHER EAAS

There is much evidence to implicate disturbances in Ca^{2+} homeostasis in the neurotoxicity caused by EAAs apart from glutamate. The glutamate-induced increase in $[Ca^{2+}]_i$ is mediated by the activation of both NMDA and non-NMDA receptors, although most studies report that the activation of NMDA receptors may be quantitatively more important, given that the selective NMDA antagonist D-AP5 blocks the majority of the excitotoxic glutamate response in cerebral cortical neurons (Frandsen and Schousboe, 1992). The NMDA-induced Ca^{2+} response is thought to originate in the most part from Ca^{2+} entry through the NMDA receptor (Savidge and Bristow, 1997) with a considerable dantrolene-sensitive contribution from intracellular Ca^{2+} pools (Mody and MacDonald, 1995; Segal and Manor, 1992; Frandsen and Schousboe, 1992). AMPA and kainate-induced toxicity in cortical neurons is greatly attenuated by the omission of extracellular Ca^{2+}, but is unaffected by dantrolene (Frandsen and Schousboe, 1993, Camins *et al*, 1998), suggesting that Ca^{2+} influx is highly significant in the actions of AMPA and kainate. However, only a minor component of the calcium elevation caused by AMPA and kainate may be accounted for by influx of Ca^{2+} through VDCCs (Frandsen and Schousboe, 1992). A recent study has provided evidence for the presence of Ca^{2+}-permeable AMPA/kainate channels on the dendrites of hippocampal neurons (Yin *et al*, 1999), which could provide a route for Ca^{2+} entry following stimulation with AMPA or kainate. The calcium increase induced by quisqualate is mainly but not exclusively mediated by IP_3-sensitive intracellular Ca^{2+} pools, being insensitive to the removal of extracellular Ca^{2+} (Garthwaite and Garthwaite, 1989), but showing a degree of attenuation upon treatment with verapamil, a VDCC blocker (Frandsen and Schousboe, 1992). ACPD is known to activate mGluRs, causing the release of IP_3 and the elevation of $[Ca^{2+}]_i$ through release from intracellular Ca^{2+} stores. The ability of VDCC blockers to reduce neurotoxicity in *in vivo* models of ischaemia (Jacewicz *et al*, 1990) has been taken as evidence that the Ca^{2+} influx through voltage-gated channels may follow exposure to high levels of glutamate, but this may not necessarily be true. The neuroprotective effect of calcium channel blockers may be based on their ability to increase

cerebral blood flow or to prevent Ca^{2+} release from intracellular stores rather than their action in reducing Ca^{2+} influx (Frandsen and Schousboe, 1993). The complexity of intact brain models can be overcome by the use of simpler cell culture systems in the study of the mechanisms lying behind calcium increases caused by EAAs, but even so, the mechanisms of EAA disruption of Ca^{2+} homeostasis may vary considerably depending upon the neuronal subtype. For example, the VDCC blocker nitrendipine is considerably more protective against glutamate neurotoxicity in hippocampal neurons than in cortical neurons (Kudo *et al*, 1990; Weiss *et al*, 1990).

1.2.4 ROLE OF CALCIUM IN BRAIN AGING

There is compelling evidence for the role of aberrant neuronal calcium homeostasis in acute neurological disorders such as hypoxia/ischaemia. It is of interest, therefore, that changes in Ca^{2+} homeostasis are also likely to be involved in the pathogenesis of chronic, neurodegenerative conditions, and in the alterations in neuronal function characteristic of brain aging. Brain aging is characterised by general neuronal loss, compensated for by the extension of dendritic ramifications of remaining neurons. These changes are much greater in degenerative diseases like Alzheimer's disease. Studies have shown a decrease in the calcium content of cerebrospinal fluid from geriatric patients. Changes in calcium homeostasis that occur during aging include an upregulation of L-type VDCCs and therefore increased Ca^{2+} voltage-dependent conductance, a reduction in the density of NMDA receptors, decreased Ca^{2+} sequestering capacity of intracellular organelles such as mitochondria and ER, and decreased Ca^{2+} extrusion from cells by cell surface ATPases and exchangers (Gareri *et al*, 1995). Overall, intracellular Ca^{2+} levels appear to be increased, which could be an important mechanism for the neuronal death associated with aging and Alzheimer's disease.

1.3 MITOCHONDRIAL DYSFUNCTION AND NEURONAL DEATH

The brain is uniquely dependent on blood-borne glucose for its normal functioning, being unable to store energy supplies. In the absence of energy provision from cellular stores, mitochondria therefore acquire a new significance as the major providers of energy for the brain. Recent research has shown that subtle changes in the functioning of mitochondria can lead to both immediate and long term pathological changes in neurons (Cassarino and Bennett, 1999; Abe *et al*, 1995; Zamzami *et al*, 1997; Beal *et al*, 1993). Several distinct lines of research have converged on the mitochondrion and its role in neuronal pathology, including excitotoxicity, mitochondrial permeability transition, free radicals and nitric oxide, mitochondrial DNA damage, and apoptosis. These themes will be discussed in the following section.

1.3.1 MITOCHONDRIA AND EXCITOTOXICITY

Mitochondria have been implicated in the excitotoxic cascade, given the considerable metabolic requirements of the brain and large Ca^{2+} buffering capacity of these organelles. Excessive Ca^{2+} accumulation in mitochondria uncouples electron transfer from ATP synthesis and this impairment of energy metabolism causes the generation of free radicals (Luetjens *et al*, 2000). Mitochondria therefore emerge as a plausible link between the elevation of Ca^{2+} and glutamate neurotoxicity.

Mitochondrial Ca^{2+} buffering

There have been a number of studies examining the role of mitochondrial Ca^{2+} buffering during excessive or excitotoxic Ca^{2+} loading of the cytoplasm. It has been shown in cultured rat hippocampal cells that glutamate induced Ca^{2+} loads are sequestered by mitochondria (Wang and Thayer, 1996).

Similarly, in cultured striatal neurons, confocal imaging of the Ca^{2+} probe rhod-2 has shown mitochondrial Ca^{2+} accumulation after treatment with NMDA (Peng *et al*, 1998). The total mitochondrial uptake of $^{45}Ca^{2+}$ in cultured cerebellar granule cells exposed to glutamate can approach 20mM (Eimerl and Schramm, 1994) suggesting a protective role for mitochondria against neuronal Ca^{2+} overload (Nicholls, 1985). Indeed, suppression of mitochondrial Ca^{2+} uptake by antimycin or NaCN has revealed an important role for mitochondria in protection against a delayed Ca^{2+} overload following the treatment of cerebellar granule cells with glutamate (Khodorov *et al*, 1996). However, once the Ca^{2+} buffering capacity of mitochondria is exceeded, further Ca^{2+} uptake by mitochondria can be highly damaging to neurons.

Mitochondrial depolarisation follows toxic NMDA receptor activation

A large number of studies have proposed that mitochondria may be an early target of injury in the events following intense NMDA receptor stimulation. Confocal imaging of the mitochondrial membrane potential using JC-1, a ratiometric indicator of $\Delta\Psi$, has shown that in cultured forebrain neurons, mitochondria accumulate Ca^{2+} following toxic glutamate stimulation, and that this Ca^{2+} accumulation is accompanied by the dissipation of $\Delta\Psi$. The sudden mitochondrial depolarisation was attenuated by the NMDA receptor antagonist MK801, and was CsA sensitive, suggesting a possible involvement of the mPTP. Furthermore, using a specific inhibitor of the mitochondrial Na^+/Ca^{2+} exchanger, it was demonstrated that Ca^{2+} efflux from mitochondria contributes to the prolonged $[Ca^{2+}]$ elevation after glutamate removal (White and Reynolds, 1996). The critical role of the mitochondrion in excitotoxicity has further been consolidated by the finding that the dysfunction of mitochondria is a primary event in the excitotoxic death triggered by glutamate (Schinder *et al*, 1996). Confocal imaging of Ca^{2+} and mitochondrial membrane potential in cultured rat hippocampal neurons showed that the toxic activation of NMDA receptors caused an irreversible Ca^{2+} overload and the persistent depolarisation of mitochondria, events which closely paralleled neuronal death. Mitochondrial depolarisation was

prevented by pretreatment with CsA. In another study, [Ca^{2+}] and mitochondrial membrane potential were simultaneously measured in cultured cerebellar granule cells following glutamate exposure (Khodorov *et al*, 1996). This study revealed a close correlation between the extent of mitochondrial depolarisation and the failure of the neuron to restore Ca^{2+} homeostasis. The de-energisation of mitochondria may therefore underlie the neuronal Ca^{2+} overload that follows prolonged exposure to glutamate. Similarly, it has been shown in cultured cerebellar granule cells that neurotoxic glutamate treatment causes both structural and functional damage to mitochondria, causing mitochondrial swelling and inducing non-specific permeability of the inner mitochondrial membrane, indicated by a loss of ability of the mitochondria to sequester Rh123 (Isaev *et al*, 1996). Recent work has further corroborated the theory of mitochondrial involvement in processes of neurotoxicity. The stimulation of cultured rat hippocampal cells with glutamate was observed to cause an increase in Rh123 fluorescence, reflecting mitochondrial depolarisation (Vergun *et al*, 1999). In mature cultures (>11 DIV), glutamate caused a profound mitochondrial depolarisation and failure of neurons to recover from the Ca^{2+} load. In contrast, a similar glutamate treatment of young (6-8 DIV) cultures caused only a transient mitochondrial depolarisation, and neurons went on to recover [Ca^{2+}]$_i$ after glutamate washout. These differences may reflect changes in the expression of NMDA receptors over time in cultured neurons, or altered NOS expression over time.

How much depolarisation for how long?

There are well-documented differences in the degree of mitochondrial depolarisation that follows NMDA receptor activation. Unsurprisingly, the ability of mitochondria to repolarise is closely related to the severity (concentration of excitotoxin and/ or duration of exposure) of the initial neurotoxic insult. Therefore, exposure of cultured hippocampal neurons to 200μM NMDA for 0.5 min caused only a transient mitochondrial depolarisation, whereas this depolarisation was persistent when exposure to NMDA was increased to 50 min (Schinder *et al*, 1996). In cultured hippocampal neurons at 11-17 DIV, a 10-minute treatment with 100μM

glutamate caused a near-complete mitochondrial depolarisation which could not be further increased with FCCP (Vergun *et al*, 1999). Presumably, in these cells where complete mitochondrial "shutdown" has occurred, death will occur as soon as ATP stores are depleted. In cultured forebrain neurons, the fraction of neurons with permanently depolarised mitochondria was greater following treatment with 500μM glutamate than when neurons were treated with 100μM glutamate (White and Reynold, 1996), but in both cases, a significant proportion of mitochondria were able to repolarize following glutamate wash off. The general consensus would appear to be that mitochondria remain partially depolarised in the presence of glutamate (Ankarcrona *et al*, 1995; Isaev *et al*, 1996; Khodorov *et al*, 1996). The mitochondria in CGCs have been observed to remain bioenergetically competent and to generate ATP throughout conditions of glutamate-induced Ca^{2+} overload, even though these cells ultimately show delayed Ca^{2+} deregulation and die (Nicholls *et al*, 1999). A transient mitochondrial depolarisation may therefore be sufficient to trigger eventual cell death. It is thought that the mode of neuronal death following toxic insult is determined by mitochondrial function (Ankarcrona *et al*, 1995). Cerebellar neurons treated with glutamate which underwent a complete collapse of $\Delta\Psi$ were seen to die through necrosis, whereas neurons which survived the necrotic phase and recovered their mitochondrial membrane potential and ATP levels, went on to die through apoptosis at a later time point.

Mitochondrial Ca^{2+} uptake: a critical event in neurotoxicity

It would appear that the uptake of Ca^{2+} by mitochondria is a critical event in the cell damage which follows toxic NMDA receptor activation. The prevention of mitochondrial Ca^{2+} uptake with the use of the protonophore FCCP or with rotenone (an ETC inhibitor) in conjunction with oligomycin (the ATP-synthase inhibitor) has been observed to greatly reduce glutamate-induced cell death in cultured rat forebrain neurons (Stout *et al*, 1998), and in cultured cerebellar granule cells (Budd and Nicholls, 1996). The finding that the complete depolarization of mitochondria before glutamate exposure is neuroprotective implies that polarized mitochondria, in response to excessive

Ca^{2+} loading, create a condition triggering subsequent cell death. The nature of this condition, however, remains unclear, but could include altered cytoplasmic Ca^{2+} dynamics due to mitochondrial depolarisation, ATP depletion, production of ROS, or mitochondrial permeability transition.

There are differing reports as to the effect of prior mitochondrial depolarisation on the cytoplasmic Ca^{2+} increase caused by glutamate. In general, the blockade of mitochondrial Ca^{2+} uptake by mitochondrial inhibitors is reported to significantly potentiate glutamate-stimulated increases in $[Ca^{2+}]$ (Stout *et al*, 1998, Khodorov *et al*, 1999). In contrast, the depolarization of granule cell mitochondria has been seen, counterintuitively, to result in lower cytoplasmic Ca^{2+} responses to glutamate (Budd and Nicholls, 1996, Castilho *et al*, 1998). In the absence of mitochondrial Ca^{2+} accumulation, this was proposed to reflect either an enhanced efflux from the cell, or decreased Ca^{2+} uptake via VDCCs and the NMDA receptor. It was proposed that with no mitochondrial Ca^{2+} uptake, Ca^{2+} would accumulate in submembrane microdomains, causing the inactivation of NMDA receptors and VDCCS, thus reducing the glutamate Ca^{2+} response. These findings have been put forward by one research group only, and have not been substantiated by other groups using identical experimental models, so should be interpreted with care.

ATP depletion is an inevitable consequence of excessive Ca^{2+} buffering by mitochondria, since profound mitochondrial depolarisation reverses the mitochondrial ATP synthase which both suppresses mitochondrial ATP production and promotes ATP hydrolysis, in an attempt to retain $\Delta\Psi$. ATP is required for the extrusion of Ca^{2+} from neurons through the Na^{+}/Ca^{2+} exchanger and the Ca^{2+}-ATPase, so it is conceivable that ATP depletion could account for impaired Ca^{2+} recovery following glutamate exposure. Available data do not strongly support this hypothesis: a 60 min treatment of cerebellar granule cells decreased the population ATP/ADP ratio by only 35% (Budd and Nicholls, 1996) but this could reflect a population of dying ATP-depleted cells diluted by surviving cells with high energy levels (Nicholls and Ward, 2000). It is possible that a persistent mitochondrial

depolarisation following glutamate exposure could effectively prevent a neuron from replenishing its ATP stores. The neuron could then re-establish Ca^{2+} homeostasis to a certain extent, drawing upon glycolysis and cellular ATP stores; delayed Ca^{2+} deregulation and death would then occur when the neuron eventually becomes completely depleted of ATP. The extent of glutamate-induced Ca^{2+} deregulation in cerebellar granule cells has been shown to be unaffected by inhibition of the mitochondrial ATP synthase (Castilho *et al*, 1998), but these cells are known to have a high glycolytic capacity which may not hold true for other neuronal cell types.

The depolarisation of mitochondria by excessive Ca^{2+} buffering causes the uncoupling of oxidative phosphorylation and accelerated production of ROS, natural by products of the ETC (Wang and Thayer, 1996). ROS may well contribute to post-glutamate Ca^{2+} deregulation and neuronal damage, given the knowledge that oxidative stress favours opening of the PTP. Ca^{2+} extrusion from neurons may also be hindered by ROS, since the plasma membrane Ca^{2+}-ATPase is highly susceptible to oxidative stress (Vergun, 1999; Nicholls and Ward, 2000). The role of free radicals and mitochondrial permeability transition in neuronal pathology will be discussed fully in later sections.

Recent research would therefore appear to bear out the theory that the mitochondrion is the cellular sensor that converts the intracellular elevation of Ca^{2+} from a physiological modulator into a trigger for cell death. However, it is difficult to conclude from the available data which processes in particular define the correlation between glutamate-induced mitochondrial depolarisation and the deregulation of neuronal Ca^{2+} homeostasis. Processes such as altered Ca^{2+} buffering by mitochondria, ATP depletion and free radical generation all contribute, but the relative importance of each mechanism is likely to vary between different neuronal systems, and requires further investigation.

1.3.2 MITOCHONDRIA AND APOPTOSIS

There is considerable experimental evidence to implicate the mitochondrion as a major player in apoptosis. Apoptosis is a rigorously controlled process responsible for the removal of damaged, aged or superfluous cells. It is important in the formation of the vertebrate CNS where 50% of embryonic neurons are eliminated to facilitate correct synapse formation (Raff *et al*, 1993). An abnormal cellular resistance to apoptosis can lead to malformations, autoimmune disease or cancer since superfluous cells are not dealt with. Excessive apoptosis, in contrast, is involved in both acute diseases such as septic shock and anoxia, and chronic pathologies such as neurodegeneration, neuromuscular diseases and AIDS (Zamzami *et al*, 1997).

In apoptosis, the cell actively contributes to its own removal, and undergoes several stereotyped biochemical and ultrastructural alterations. Each cell contains a set of proteins, caspases, which comprise the "death machinery" capable of killing the cell from within (Barinaga, 1998). These can be activated by a multitude of different factors, including anoxia, viral infections, second messengers such as *fas* and cytochrome c, and a lack of growth factors. The activation of caspases sets in motion the gradual dismantling of the cell into small fragments ready for disposal, avoiding the pro-inflammatory release of intracellular factors into the interstitium. Stages of apoptosis include chromatin condensation, nuclear displacement, DNA laddering into 180bp fragments via calcium dependent endonucleases, cleavage of cytoskeletal elements, loss of plasma membrane asymmetry and cell shrinkage. This highly orchestrated process requires the presence of ATP (Bär, 1996).

1.3.2.1 Evidence for the involvement of mitochondria in apoptosis

Evidence for the central role of mitochondria in apoptosis is compelling. In more than fifty different models of apoptosis, it has been observed that a characteristic collapse of $\Delta\Psi m$ precedes the laddering of DNA and plasma membrane blebbing (Zamzami *et al*, 1997; Wadia *et al*, 1998; Tenneti *et al*, 1998; Ankarcrona *et al*, 1995; Zamzami *et al*, 1996; Kroemer *et al*, 1995; Hirsch *et al*, 1997). The bulk of current experimental data supports the theory that the dissipation of $\Delta\Psi$ constitutes an early and irreversible stage of the apoptotic process, preceeding caspase activation, and probably marking the point of convergence of different apoptosis induction pathways. The disruption of $\Delta\Psi$ could be due to (a) non-specific damage of the inner mitochondrial membrane, (b) opening of the PTP, or (c) could result from inhibition of the respiratory chain, possibilities considered later in this report. The collapse of $\Delta\Psi$ is associated with a loss of mitochondrial membrane integrity, given the cytosolic leakage of cytochrome c, a protein normally confined to the intermembrane space, yet capable of triggering caspase activation (Liu *et al*, 1996). Mitochondria may therefore be seen to undergo considerable structural and functional changes early during the apoptotic process.

Cell-free systems combining purified mitochondria and nuclei have provided strong causal evidence for altered mitochondrial function in apoptosis, revealing the requirement for mitochondria or mitochondrial products in the induction of nuclear apoptosis (Liu *et al*, 1996; Zamzami *et al*, 1996). This requirement can be circumvented by the addition of substances that induce the mitochondrial permeability transition pore (Ellerby *et al*, 1997, Kroemer *et al*, 1998).

Pharmacological evidence shows that the induction of PT may account for the collapse of $\Delta\Psi$ which in turn could trigger cell death. Agents which specifically act on mitochondria to induce PT can trigger cell death, whilst nuclear apoptosis is impeded by pharmacological agents such as bongkrekic acid, cyclosporin A and *N*-methyl-4-Val-cyclosporin A which prevent PT

(Miller, 1998; Susin *et al*, 1998). Prevention of PT would appear to block the manifestation of all signs of apoptosis. Opening of the PTP may therefore be a critical coordinating event of apoptosis (Hirsch *et al*, 1997). This is further corroborated by evidence that the oncoprotein bcl-2 is an endogenous inhibitor of apoptosis, through its stabilising effect on mitochondria (Davies, 1995; Reed *et al*, 1998; Motyl, 1999). Bcl-2 proteins are discussed in more detail in section **1.3.2.3** below.

The data outlined above fit neatly into a three-stage mechanism of apoptosis proposed by the research group of Guido Kroemer (see Susin *et al*, 1998). The first pre-mitochondrial induction phase consists of the activation of damage pathways or signal transduction cascades, which converge on the mitochondrion. The second mitochondrial effector phase is then triggered, during which mitochondrial membrane integrity is compromised, and an irreversible "death decision" is made. The post-mitochondrial degradation phase entails the release of mitochondrial proteins, which activate specific apoptogenic proteases, culminating in the systematic degradation of the cell. Each phase of this general mechanism of apoptosis has special features, discussed below.

1.3.2.2 The pre-mitochondrial induction phase of apoptosis

The induction phase of apoptosis is concerned with the mechanisms whereby the mitochondrion senses cell damage and integrates pro-apoptotic signals. The structure, location and regulation of the PTP complex make it an ideal candidate for a metabolic integrator, which is able to sense stress within the cell and, if necessary, trigger apoptotic processes by compromising mitochondrial membrane integrity.

Structure and function of the PTP

The PTP is a non-specific, voltage sensitive pore located at contact sites between the inner and outer mitochondrial membranes. When open, the PTP allows solutes of less than 1.5Kd to equilibrate across the membrane. The conductance of the megachannel is such that opening of a single PT pore is estimated to be sufficient to cause mitochondrial depolarization and swelling (Zoratti and Szabo, 1995). Analogies have been drawn between the PTP and the NMDA receptor channel. Both channels are regulated by similar systems and may have structural similarities, suggesting that the PTP may be a member of the ligand gated ion channel family (Bernardi *et al*, 1994).

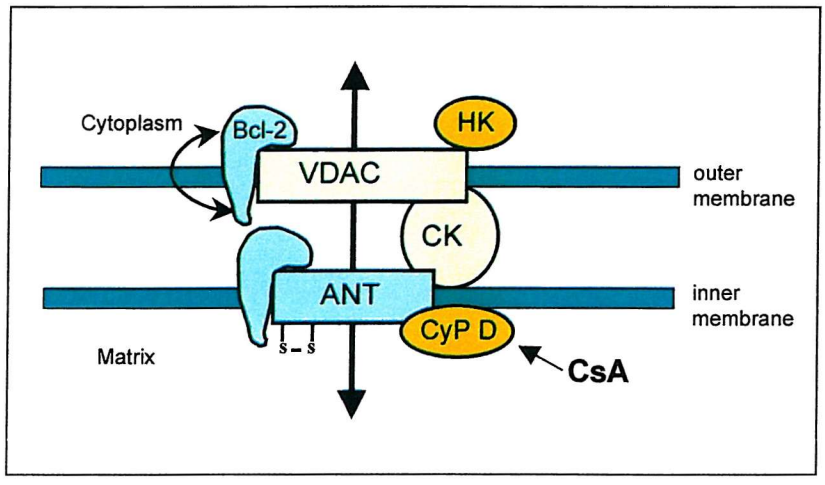

Figure 1.7 Proposed functional components of the mitochondrial permeability transition pore. Adapted from Vander Heiden and Thompson, 1999.

The PTP is composed of a complex of proteins, including the voltage-dependent anion channel (VDAC), the adenine nucleotide translocase (ANT) and cyclophilin-D (CyP D). Mitochondrial creatine kinase (CK) is located in the intermembrane space where it interacts with VDAC-ANT complexes. The VDAC-ANT complex is known to attract other proteins such as hexokinase (see Figure **1.6**). This arrangement is thought to provide a conduit for ATP, produced by oxidative phosphorylation, to be channelled directly to kinases (Crompton, 1999). Bcl-2 proteins are thought to interact directly with pore components in the regulation of PTP opening (see section **1.3.2.3**). The

experiments that led to the discovery of the different pore components are outlined in several recent reviews (Halestrap, 1999; Bernadi *et al*, 1998; Crompton, 2000; Crompton *et al*, 2000). Opening of the mitochondrial PTP is induced when mitochondria are exposed to high Ca^{2+} concentrations, especially when this is associated with adenine nucleotide depletion, acidification of the mitochondrial matrix, membrane depolarization and oxidative stress. These are exactly the conditions that accompany many cellular insults that lead to cell death.

How then are these cellular perturbations translated into opening of the PTP? One model proposes that calcium triggers a conformational change in the ANT, converting it into a non-specific channel. This process is greatly facilitated by the binding of cyclophilin-D, which is enhanced when thiol groups on the ANT are modified by oxidative stress. CyP-D is an isomerase, ideally suited for causing the conformational change in a membrane protein that would be required to induce formation of a pore. ATP and ADP competitively inhibit the Ca^{2+} trigger site by binding to the ANT. A high mitochondrial membrane potential enhances this binding, which is why the PTP opens more readily in de-energized mitochondria. There is experimental evidence that reversible PTP closure occurs upon the protonation of certain histidyl residues (Fontaine and Bernadi, 1999). Ca^{2+} binding is also inhibited by protons, which accounts for the progressive inhibition of PTP opening at pH values below 7.0 (Halestrap, 1999). There is much evidence in favour of this model involving the conformational change of ANT as a mechanism of PTP opening. PTP inducers such as atractylate stabilize the ANT in the C conformation (cytosol-facing), while PTP inhibitors such as bongkrekic acid stabilizt the ANT in the M conformation (matrix-facing). Furthermore, ADP is known to stabilize the ANT in the M conformation (Fontaine and Bernadi, 1999). However, in a novel approach, anti-porin (VDAC) antibodies were observed to reduce ischaemia-induced cell death in organotypic hippocampal slices (Perez Velazquez *et al*, 1999). Evidently, the identity of the pore-forming component of the PTP is still not resolved, but is likely to be either VDAC or ANT. The existence of more than one permeability pathway remains a possibility.

The PTP has the characteristics of a mechanism that is well suited to mediate neuronal injury, but evidence for the activation of the PTP in neurons is ambiguous. Most studies that have examined PTP in neurons have relied upon (i) measurements of mitochondrial membrane potential and/or changes in mitochondrial morphology, or (ii) pharmacological approaches, to infer the activation of the PTP. There are several drawbacks in each method, which should be considered.

Firstly, several groups have observed an NMDA receptor-mediated, Ca^{2+} dependent mitochondrial depolarization using potentiometric indicators of $\Delta\Psi$ (White and Reynolds, 1996; Schinder *et al*, 1996; Nieminen *et al*, 1996). In addition, there is evidence that the mitochondrial depolarization triggered by exposure to calcium ionophore is accompanied by mitochondrial swelling, consistent with PTP opening (Dubinsky and Levi, 1998). In each of these paradigms, mitochondrial depolarization was CsA sensitive, further supporting the PTP hypothesis (see below). However, mitochondrial depolarization and/or swelling are not associated exclusively with PTP opening, so do not provide definitive proof of this process.

Secondly, CsA is a very potent inhibitor of PTP opening. Several mechanisms have been proposed for this inhibition, including:

1. Blockade of the PTP by CsA preventing the association of ANT with CyP-D;

2. Steric blockade of solute flux by CsA binding close to the pore entrance;

3. Induction of inhibitory conformational changes by CsA binding to CyP-D (Crompton, 1999).

Many researchers have reported that CsA is protective in various paradigms of neurotoxicity, including rat models of transient focal ischaemia and hypoglycaemia (Uchino *et al*, 1995; Friberg *et al*, 1998), rat organotypic hippocampal slices subjected to hypoxia-hypoglycaemia (Perez Velazquez *et al*, 1999), cultured rat cortical neurons and cerebellar granule cells challenged with NMDA and glutamate (Nieminen *et al*, 1996; Ankarkrona *et al*, 1996),

and rodent models of traumatic brain injury (Scheff and Sullivan, 1999; Sullivan *et al*, 1999). However, the measure of protection afforded by CsA in *in vitro* models is variable, ranging from no effect (Isaev *et al*, 1996) to a delay in the manifestations of neurotoxicity (Nieminen *et al*, 1996; Schinder *et al*, 1996; White and Reynolds, 1996) and partial protection (Dubinsky *et al*, 1999) to very considerable protection (Ankarkrona *et al*, 1996; Keelan *et al*, 1999).

However, in addition to inhibiting the PTP, CsA also inhibits calcineurin, a factor that could account for its neuroprotective qualities. The inhibition of calcineurin downregulates nitric oxide synthase, thereby reducing the free radical component of neurotoxicity (Murphy *et al*, 1999). In support of this argument, protection against glutamate neurotoxicity is also imparted by FK-506, a drug that inhibits calcineurin (Ankarcrona *et al*, 1996; Keelan *et al*, 1999). Furthermore, a series of agents that inhibit PTP, including trifluoperazine, tamoxifen and ubiquinone analogues, are not neuroprotective against excitotoxic stimuli (Reynolds, 1999). The CsA analogue methyl valine cyclosporin (mvCs) does not inhibit calcineurin and has greater specificity for the PTP. Studies have shown that mvCs is neuroprotective against glutamate neurotoxicity in cultured hippocampal neurons (Duchen, 2000) and in a rat model of cerebral ischaemia (Matsumoto *et al*, 1999), but is not neuroprotective in cerebellar granule cells (Castilho *et al*, 1998). Evidently, whilst the involvement of mitochondria in neurotoxicity is clearly important, more unequivocal evidence for PTP activation is required. A new approach has been pioneered to directly visualise onset of the PTP in intact cells. This technique involves imaging the movement of calcein, a mitochondrially impermeant probe, from the cytosol into the mitochondrial matrix (Lemasters *et al*, 1998; Lemasters *et al,* 1999). This approach is a powerful tool to observe PTP opening in intact cells, but has not yet been applied to neurons.

Pro-apoptotic signals

Apoptosis can be induced by a divergent array of stimuli, which, through a myriad of signaling pathways, converge on mitochondria and trigger apoptotic processes, likely through activation of the PTP.

Reactive Oxygen Species

The mitochondrial megachannel contains several redox-sensitive sites, and may therefore be activated by changes in the cellular redox potential i.e. enhanced generation of ROS or depletion of cellular antioxidant defences (reduced glutathione or $NAD(P)H_2$). Increased production of ROS may result from cellular damage, overexpression of p53 or exposure to ceramide (Susin *et al*, 1998). Other components of the apoptotic pathway that are redox-sensitive include apoptosis signaling kinase (ASK-1), and the Fas receptor/Fas ligand system (Cai and Jones, 1999). These systems may be upregulated by ROS, thereby enhancing cellular susceptibility to the activation of apoptosis. There is plentiful evidence that apoptosis can be induced by ROS (Luetjens *et al*, 2000) and prevented by antioxidants (Keller *et al*, 1998). However, there is unlikely to be an absolute requirement for redox signalling in apoptosis, since apoptosis has been observed in cells grown under nearly anaerobic conditions (Jacobsen and Raff, 1995).

Energy metabolism

The depletion of ATP favours opening of the PTP since ATP is a physiological ligand of the ANT, and functions as an endogenous inhibitor of the pore (Simbula *et al*, 1997). The PTP can also be triggered by inhibition of the respiratory chain, which reduces $\Delta\Psi$, and by inhibition of the F_1ATPase, which leads to matrix alkalinization (Bernadi and Petronilli, 1996).

Cytosolic calcium

Elevation of the intracellular Ca^{2+} level represents a common trigger for apoptosis in diverse cell types. Agents which increase $[Ca^{2+}]_i$ such as Ca^{2+} ionophores or thapsigargin are known to induce apoptosis (Takei and Endo,

1994, Korge and Weiss, 1999). Conversely, a reduction in $[Ca^{2+}]_i$ by the use of Ca^{2+} chelators or over-expression of Ca^{2+} binding proteins is protective against apoptosis (Prehn *et al*, 1997). Experimental evidence suggests that mitochondrial Ca^{2+} overload is an early and critical event in apoptosis (Kruman and Mattson, 1999). Ca^{2+} ions are very efficient inducers of the PTP, causing PTP opening at doses greater than 10μM, and facilitating PTP induction by other stimuli at lower doses (Ankacrona *et al*, 1995). IP_3 receptor-mediated Ca^{2+} spikes have been identified as a potent signal for the induction of apoptosis in cells exposed to pro-apoptotic stimuli such as ceramide (Szalai *et al*, 1999). Since Ca^{2+} spikes are also closely involved in the physiological control of mitochondrial metabolism (see section **1.1.4**), it would appear that the coincident detection of proapoptotic stimuli and Ca^{2+} signals is required to switch cells from the life program to the death program. There are several stages in the induction phase of apoptosis which are indirectly controlled by Ca^{2+}, including (1) the activation of gene expression, where transcription factors such as CREB are themselves regulated by Ca^{2+} dependent protein kinases, and (2) the production of ROS. NO metabolism, for example, has a crucial Ca^{2+} dependent step (Toescu, 1998).

Caspases

Apoptotic cell death can be potently triggered by the ligation of cell surface "death receptors". Death signalling from these receptors involves the activation of caspases, a family of proteases activated via specific proteolytic cleavage. The best-characterised death receptor is the Fas receptor, which oligomerizes in response to binding of its ligand, and facilitates the formation of the multiprotein death-inducing signaling complex (DISC). Caspase 8 is recruited to this complex and activated. Cell-free experiments have shown that purified caspase 8 is incapable of inducing apoptosis in the absence of mitochondria and cytosolic factors (Thress *et al*, 1999). Subsequent work has indicated that caspase 8 cleaves Bid, a pro-apoptotic member of the bcl-2 family. The C-terminal part of Bid then translocates to mitochondria and triggers the release of apoptogenic factors (Luo *et al*, 1998).

1.3.2.3 The mitochondrial effector phase of apoptosis

The effector phase of apoptosis is concerned with the release of pro-apoptotic factors from mitochondria, following the integration of pro-apoptotic stimuli and the loss of mitochondrial membrane integrity. There is ample evidence for the involvement of cytochrome c (cyt c) and apoptosis-inducing factor (AIF) in the onset of apoptosis. These proteins normally reside in the mitochondrial intermembrane space. Experimental evidence shows they are released from mitochondria during apoptosis (Richter and Ghafourifar, 2000; Pérez-Pinzón *et al*, 1999), precede the appearance of apoptotic changes, and initiate the caspase cascade and nuclear apoptosis in cell-free systems (Liu *et al*, 1996; Susin *et al*, 1996). The release of mitochondrial cyt c and AIF would therefore appear to be a key step in the route to cell suicide.

Cytochrome c normally functions as a component of the electron transport chain to accept electrons from Complex III and shuttle them to Complex IV, and is therefore critical in the cellular energy transduction pathway (Murphy *et al*, 1999). Cytochrome c may have become a major trigger to cell death because its presence in the cytosol indicates that mitochondria are damaged, energetic function is compromised, and that a bioenergetic and redox catastrophe is imminent (Duchen, 1999).

Which exit route for apoptogens?

There is much controversy as to how cyt c and AIF escape from mitochondria. Exit through the mitochondrial PTP would be a convenient hypothesis, since numerous pro-apoptotic stimuli are known to trigger PTP opening. However, there is no evidence that the pore is of sufficient size or orientation to allow the direct efflux of cyt c (Murphy *et al*, 1999). Nonetheless, PTP opening induces a non-specific increase in permeability of the inner mitochondrial membrane. This can lead to osmotic swelling.of the matrix and ultimately rupture of the outer membrane, given the greater surface area of the invaginated inner membrane. Such a loss of outer membrane integrity would provide an alternative mechanism for the release of cyt c and other intermembrane proteins through PTP opening (Petit *et al*,

1998). Recent experimental evidence suggests that cultured cortical neurons release cyt c into the cytosol 30 minutes after glutamate exposure by a process involving activation of the PTP, mitochondrial swelling and rupture of the outer membrane (Brustovetsky *et al*, 2002).

There are two conflicts associated with the theory that the PTP is responsible for apoptogen release. Firstly, mitochondrial swelling should be a common morphologic change that accompanies apoptosis, but traditionally, a general characteristic of apoptosis is the *lack* of change in mitochondrial ultrastructure (Brenner *et al*, 1998). Secondly, activation of the PTP always causes a loss of $\Delta\Psi$ (Zoratti and Szabo, 1995), but several studies argue that there is no measureable drop in $\Delta\Psi$ before cyt c release (Vander Heiden and Thompson, 1997; Andreyev *et al*, 1998; Finucane *et al*, 1999; Krohn *et al*, 1999). These studies raise the possibility that any change in $\Delta\Psi$ may depend on (i) the specific apoptogenic stimulus and (ii) the cell type being studied. For example, stimuli that involve significant mitochondrial Ca^{2+} loading or oxidative stress may well induce cyt c release through PTP activation, whereas the signaling process to mitochondria through death receptors could involve novel pathways without PTP activation. Also, the execution of apoptotic processes is likely to vary between neuronal and non-neuronal cell types. Experimental evidence shows that brain mitochondria are more resistant to triggering of the PTP than liver mitochondria (Berman *et al*, 2000), so the cell type used in experiments should be carefully considered. Technically, several issues should be examined. Many studies employ potentiometric dyes in the measurement of mitochondrial $\Delta\Psi$. It is possible that a loss of $\Delta\Psi$ in a small subpopulation of mitochondria may be sufficient to propagate the apoptotic signal, but may escape experimental detection. As a subpopulation of mitochondria depolarizes, others with normal $\Delta\Psi$ may sequester the excess dye, giving little detectable change in fluorescence (Murphy *et al*, 1999). Permeability transition is a reversible process (Minimikawa *et al*, 1999), so it is highly probable that cells could undergo PTP opening, release cyt c, and then recover $m\Delta\Psi$ before undergoing apoptosis.

It is certain that other mechanisms (besides PTP activation) must exist for the translocation of apoptogens across the outer mitochondrial membrane. Theoretically, the opening of specific pores in the outer mitochondrial membrane would allow the release of cyt c in the absence of permeability transition or loss of $\Delta\Psi$. The ion channel forming ability of members of the bcl-2 family is well documented (Schendel *et al*, 1998). Recent evidence suggests that Bax can functionally and physically associate with the adenine nucleotide translocator (ANT) component of the PTP to cause channel formation in artificial membranes (Thress *et al*, 1999), and may be able to induce cyt c release from isolated mitochondria (Jurgensmeier *et al*, 1998). There is also evidence to show that Bax and Bak accelerate the opening of VDAC (porin), a protein abundant in the outer membrane of mitochondria, and allow cyt c to pass through VDAC out of liposomes (Shimizu *et al*, 1999). However, these channels may not be large enough to transport the 15kd cyt c or the 50kd AIF, since VDAC is only known to accommodate 8kd proteins. Cyt c may be able to escape through VDAC if cyt c was partially unfolded.

Other strategies for the release of cyt c include reversal of the protein import process (Murphy *et al*, 1999) or permeabilisation of the outer mitochondrial membrane by proteolysis (Susin *et al*, 1997). Finally, K^+ is the major determinant of mitochondrial matrix volume, so altered activity of K^+ transporters on the inner mitochondrial membrane could initiate swelling and rupture of the outer mitochondrial membrane and the release of apoptogens (Reed, 1997).

On balance, it is reasonable to propose that the permeability transition is responsible for apoptogen release in many pathological conditions that involve apoptotic death. It is highly probable that the PTP is activated in only a subpopulation of mitochondria within the cell, which would allow the remaining mitochondria to meet the ATP requirements of apoptosis.

The Bcl-2 protein family: controlling the life/death switch

The Bcl-2 proteins are the principal regulatory molecules acting at the effector stage of apoptosis. These proteins are either anti-apoptotic (Bcl-2, Bcl-X_L, Bcl-w, Mcl-1, A1) or pro-apoptotic (Bax, Bak, Bok, Bcl-X_S, Bad, Bid, Bik, Bim, Krk, Mtd) (Antonsson and Martinou, 2000). The common feature shared by Bcl-2 family members is the presence of four Bcl-2 homology regions, which determine the capacity of these proteins to interact with each other and other molecules. Many Bcl-2 proteins have a carboxy-terminal transmembrane tail that functions to target them to intracellular membranes: the outer mitochondrial membrane, endoplasmic reticulum and nuclear envelope (Motyl, 1999). It would appear that the association of some Bcl-2 proteins with mitochondrial membranes is inducible. Proteins which normally reside in the cytosol insert into mitochondrial membranes upon delivery of an apoptotic signal (Reed *et al*, 1998). The relative ratio of anti-apoptotic and pro-apoptotic Bcl-2 proteins expressed in a cell is pivotal in determining the cellular response to the numerous stimuli and insults that may induce apoptosis.

Experimental evidence shows that over-expression of anti-apoptotic members of the Bcl-2 family is protective in paradigms of apoptosis, reducing the likelihood of PTP opening and AIF release (Marchetti *et al*, 1996, Susin *et al*, 1996). Conversely, over-expression of the pro-apoptotic protein Bax induces mitochondrial depolarization and the release of cytochrome c (Jurgensmeier *et al*, 1998). It is not clear how Bcl-2 proteins regulate cellular life/death decisions, but it is likely that these proteins are multifunctional. The mechanisms that they employ to modulate cell death are thought to include (i) ion channel activity; (ii) dimerization with other Bcl-2 proteins; and (iii) binding to non-homologous proteins.

Ion channel formation

The three-dimensional structure of Bcl-X_L is strikingly similar to the pore forming domains of bacterial toxins such as diptheria toxin. As predicted by their structure, many Bcl-2 proteins are known to form ion channels in

synthetic membranes. It has consequently been theorized that Bax forms novel channels in the outer mitochondrial membrane, which liberate cytochrome c (Reed *et al*, 1998). Bcl-2 can regulate mitochondrial proton flux, thereby stabilizing mitochondrial membrane potential in the face of death-inducing stimuli (Shimizu *et al*, 1998). This action is likely mediated through the formation of an H^+ ion channel by Bcl-2. Bcl-2 also regulates the flux of Ca^{2+} across membranes of the mitochondria, endoplasmic reticulum and nucleus, thereby maintaining cellular Ca^{2+} homeostasis and preventing the Ca^{2+} signalling of apoptosis. This may be due to the pore forming action of bcl-2, or possibly via a direct effect on Ca^{2+} channels (Paschen and Doutheil, 1998; Zhu *et al*, 1999). Bcl-2 enhances the ability of neural cell mitochondria to buffer large Ca^{2+} loads without undergoing respiratory inhibition (Murphy *et al*, 1996). Bcl-X_L is known to inhibit the mitochondrial depolarization and swelling that follows an apoptotic insult. This ability to modulate the osmotic and electrical homeostasis of mitochondria may again be a direct result of the pore-forming properties of Bcl-X_L (Vander Heiden and Thompson, 1997).

Dimerization

A major site of anti-apoptotic Bcl-2 action is at the outer mitochondrial membrane, where it forms heterodimers with Bax, thereby preventing the incorporation of Bax into the PTP formed at contact sites between the inner and outer mitochondrial membranes (Motyl, 1998). Bax must form homodimers to exert its pro-apoptotic effect (Vander Heiden and Thompson, 1999). The overexpression of Bcl-2 will therefore be protective by increasing the likelihood of Bax forming innocuous heterodimers. The expression of Bcl-2 reduces oxidative damage, not by scavenging ROS, but by blocking mitochondrial superoxide production through the inhibition of cytochrome c release. This loss of cyt c is prevented by the formation of heterodimers between Bcl-2 and Bax (Cai and Jones, 1999).

Binding of non-homologous proteins

Bcl-2 may be able to suppress apoptosis by binding to and effectively inactivating Apaf-1, a vital component of the caspase activating machinery (Reed *et al*, 1998). Opening of the PTP is thought to be regulated by the binding of Bcl-2 proteins to the VDAC component of the megachannel. Bcl-XL is thought to maintain the VDAC in a cytochrome c-impermeant configuration, while Bax induces a larger open state for the VDAC that allows cytochrome c release and triggers PTP opening (Shimizu *et al*, 1999). Bcl-2 may also protect against apoptosis by less well-defined mechanisms, including the regulation of ATP exchange between mitochondria and cytosol (Vander Heiden and Thompson, 1999) and by snagging the apoptosis-inducing protein p53 during translocation into the nucleus through nuclear pores (Reed *et al*, 1998). Bcl-2 transfection into hippocampal neurons has been observed to be protective against ischemia-induced necrosis (Antonawich *et al*, 1999), suggesting a wider role for Bcl-2 proteins in the regulation of cell physiology.

1.3.2.4 The post-mitochondrial degradation phase of apoptosis

The degradation phase of apoptosis is concerned with how PTP opening and /or release of apoptogens from mitochondria causes cell killing. Firstly, opening of the PTP has immediate damaging metabolic consequences. Uncoupling of the respiratory chain leads to the rundown of ATP synthesis and excess production of superoxide. This leads to the oxidation of mitochondrial components and depletion of cellular antioxidant defences. Oxidative damage leads to a secondary disruption of Ca^{2+} homeostasis. Permeability transition also causes acidification of the cytosol (Kroemer and Reed, 2000). PTP activation therefore inflicts lethal damage on the cell.

Secondly, the release of apoptogens has a multitude of damaging downstream effects. Once released, cytochrome c forms a complex with Apaf-1, ATP and caspase 9, and activates caspase 3. In turn, caspase 3 cleaves and activates

DNA fragmentation factor, which, together with the endonucleases activated by AIF and other DNases, starts the process of DNA laddering. Pro-caspases 2 and 9 are released from the intermembrane space upon PTP opening, and become proteolytically activated once released. Once caspases are activated, they cleave a variety of specific cellular proteins, including proteins of the nucleus, nuclear lamina, cytoskeleton, endoplasmic reticulum and cytosol (Mignotte and Vayssiere, 1998). In addition, recombinant caspases have been observed to increase mitochondrial membrane permeability, dissipating $\Delta\Psi$ and causing the release of cytochrome c and AIF. This suggests that mitochondria and caspases can engage in a self-amplifying loop thereby accelerating the apoptotic process (Marzo *et al*, 1998). Several lines of evidence suggest that caspases are important mediators of cell death in neurons. The caspase inhibitor Z-D-DCB was seen to block the cellular manifestations of apoptosis in neurons exposed to excitotoxins and hypoxia (Nath *et al*, 1998). In another neuronal model, caspase inhibitors were protective against NMDA-induced apoptosis. The caspase inhibitors prevented ROS formation and lipid peroxidation, but did not prevent the NMDA-induced Ca^{2+} influx or loss of $\Delta\Psi$. These results suggest that Ca^{2+} influx and mitochondrial depolarization occur upstream of caspase activation, whereas ROS formation and lipid peroxidation may be downstream events in neuronal apoptosis (Tenneti *et al*, 1998).

Ca^{2+} plays an important role in the degradation phase of apoptosis, regulating a series of enzymatic systems involved in the execution of apoptosis. Many of the proteases and endonucleases involved in cellular dismantling are Ca^{2+} dependent, as is transglutaminase, which functions to stabilize the cytoplasm and prevent leakage of intracellular contents via the formation of cross-links (McConkey and Orrenius, 1997; Toescu, 1998).

Mitochondrial redox signalling is another critical factor in the execution phase of apoptosis. The release of mitochondrial cytochrome c triggers the generation of ROS. This produces a sustained oxidation in apoptotic cells, especially when combined with the loss of cellular antioxidants such as GSH, another feature of apoptosis. This redox pathway is separate from, but

parallel to, the caspase cascade. Its function may be to amplify the apoptotic process by PTP activation, to assist in the rapid elimination of apoptotic cells, and to terminate proteolytic activity after phagocytosis (Cai and Jones, 1999).

1.3.2.5 The apoptosis/necrosis debate

Apoptosis and necrosis are traditionally held as two distinct forms of cell death with profoundly different implications for the surrounding tissue. It has recently become clear that that distinction between the two modes of cell death may not be so clear cut as originally thought. Several necrosis inducing agents can induce apoptosis if applied at a subnecrotic dose (Ankarcrona *et al*, 1995). The apoptosis suppressor gene bcl-2 can prevent death from necrosis in several models (Clark *et al*, 1997) which suggests that necrosis and apoptosis may involve similar rate limiting steps. Activation of the mitochondrial PTP is thought to be a common step of both modes of cell death (Nicotera and Lipton, 1999). Cells that undergo apoptosis will eventually undergo secondary necrosis (Utoh, 1995). Oxidative stress in neuronal cells has been reported to induce a form of PCD with characteristics of both apoptosis and necrosis (Tan *et al*, 1998). The apoptosis/necrosis antithesis may therefore be better regarded as a continuum with the intensity of the pathogenic stimulus and/or cellular ATP levels determining the final mode of cell death. The level of intracellular ATP has been put forwards as a determinant in the decision between apoptosis and necrosis, with apoptosis having an absolute requirement for ATP (Tsujimoto, 1997; Leist *et al*, 1997). This is not surprising, as apoptosis involves many active processes, namely cytoskeletal proteolysis, DNA condensation and fragmentation, and the alteration of surface antigens (Roy and Sapolsky, 1999). Cells induced to undergo apoptosis may die from necrosis if appropriate proteases fail to come into action. Following PT induction by a large, rapid acting pathological stimulus compromising ATP pools, necrosis may occur before apoptotic proteases are activated to act on nuclear and cytoplasmic targets. In contrast, PT induction in a slower manner would allow specific proteases to be activated and take action before ATP depletion and ROS production could

cause cell death (Lemasters *et al*, 1999). This model would be compatible with the finding that many drugs induce necrosis at high doses and apoptosis at lower doses (Zamzami *et al*, 1997). In many paradigms of neurotoxicity, neurons show features of both apoptosis and necrosis (Ankarcrona, 1998). It is thought that this heterogeneous profile of cellular changes occurs because of the complex nature of neurons. Depending upon energy availability, neurons will initiate apoptosis, but may revert to necrosis when ATP runs out. The transition to Ca^{2+}-dependent degeneration will vary spatially within each neuron, given the unequal distribution of Ca^{2+} influx and Ca^{2+}-dependent enzymes. Also, given the structure of neurons, with far-reaching processes, the activation of apoptotic cascades may have different effects depending on the subcellular localization of the activated caspases (Roy and Sapolsky, 1999).

It is widely accepted that apoptosis should confer a compensatory advantage, being an energy expensive process (Abe *et al*, 1995). This is evident during postnatal brain development, when the elimination of certain neurons allows the formation of synapses essential for information processing. The question arises, however, as to the purpose of PCD in adult neurons which, as terminally differentiated cells, cannot be regenerated. Perhaps sufficient advantage is conferred by the prevention of any inflammatory response, which would follow damaged cells undergoing the alternative mode of cell death, necrosis.

1.3.3 MITOCHONDRIA AND NITRIC OXIDE

Nitric oxide (NO) is an inorganic free-radical gaseous molecule that has many roles in the CNS as a messenger molecule. It is synthesised by various isoforms of NO synthase (NOS), which catalyse the conversion of arginine into citrulline with the release of NO. NMDA receptor activation generates nitric oxide via the Ca^{2+}-dependent activation of neuronal NO synthase (Aizenman *et al*, 1998). Nitric oxide is very different to other signalling molecules in the CNS. It is extremely diffusible in both lipid and aqueous environments, which allows it to move rapidly through cell cytoplasm and membranes alike. NO is not stored in synaptic vesicles, but is synthesized on demand. NO mediates its biological actions by chemically reacting with intracellular components, rather than by binding discretely located receptor proteins. Being a free radical, NO is unstable, with a half-life of a few seconds. (Dawson and Dawson, 1996; Knowles, 1997). The mode of action of NO is totally different to that of conventional neurotransmitters, and has changed long-held ideas about processes of neuronal communication.

Roles for NO in the CNS include:

- modification of the electrical activity of neurons through modulation of their firing pattern or modulation of ion channels;
- modification of neurotransmitter release and uptake;
- down-regulation of the NMDA receptor by nitrosylation of critical thiol groups;
- regulation of hormone release in the hypothalamo-pituitary axis;
- control of synaptic plasticity, by acting as a retrograde messenger in LTP and some forms of LTD (Garthwaite and Boulton, 1995)
- Direct effects on the ETC, thereby regulating metabolism.

1.3.3.1 Evidence for the involvement of NO in neurotoxicity

Despite these many roles in neuronal physiology, NO is thought to mediate neurotoxicity when produced in excess (Dawson *et al*, 1991). There is considerable experimental evidence to support the involvement of NO in neurotoxicity. Firstly, inhibitors of nitric oxide synthase are protective in many models of neuronal death, including glutamate toxicity in cultured rat cortical neurons (Almeida *et al*, 1999), NMDA toxicity in retinal neurons (Kashii *et al*, 1999), NMDA toxicity in hippocampal slices (Izumi *et al*, 1992), animal models of Parkinson's disease and Huntingdon's disease (Schulz *et al*, 1997), and cerebral ischaemia (Buisson *et al*, 1993).

Secondly, NO donors are known to cause toxicity in cultured hippocampal neurons (Brorson *et al*, 1999). Indeed, the release of caged NO caused neurotoxicity in young hippocampal neurons exposed to glutamate. These neurons are normally resistant to a glutamate challenge alone (Keelan *et al*, 1999).

Thirdly, there is evidence that the production of NO increases during cerebral ischemia in rats (Kader *et al*, 1993). Elevated concentrations of NO metabolites have been observed in CSF from human subjects with acute ischemic stroke (Castillo *et al*, 2000), and from patients with multiple sclerosis (Heales *et al*, 1997). In the stroke patients, the concentration of NO metabolites in CSF strongly correlated with poor prognosis (Castillo *et al*, 2000).

Finally, the development of transgenic mice deficient in NOS has revealed the role of different NOS isoforms in neurotoxic processes. Neuronal cultures made from neuronal NOS (nNOS) knockout mice show complete resistance to NMDA toxicity (Dawson and Dawson, 1996), while mice lacking inducible NOS (iNOS) showed reduced susceptibility to cerebral ischemia (Iadecola *et al*, 1997). The role of endothelial NOS (eNOS) is thought to differ from the other isoforms. The inhibition of eNOS in animal models of stroke is detrimental, since the resultant decrease in cerebral blood flow worsens ischemic damage (Dawson and Dawson, 1996). There is new

evidence for a mitochondrially located NOS (Ghafourifar *et al*, 1999). Mitochondrial NOS would be ideally placed for stimulation by Ca^{2+}, given that mitochondria buffer the Ca^{2+} load that follows NMDA receptor activation. The NO produced intramitochondrially would be well placed to exert its inhibitory effects on mitochondrial components and to react with superoxide generated by the respiratory chain.

Models suggest that NO could diffuse up to 300μm from its point of origin, an area encompassing nearly 2 million synapses in the brain (Wood and Garthwaite, 1994). It is not certain, therefore, what determines whether NO acts as a neuronal messenger or as a neurotoxin. There could be a critical concentration at which NO becomes toxic, or neurotoxicity could result from the joint overproduction of NO and superoxide (O_2^-), which combine to produce peroxynitrite, ONOO-, a potent oxidant. This is highly probable, given the evidence that superoxide dismutase blocks the toxicity of NO (Radi *et al*, 1991). The extent of damage caused by NO is highly dependent on the redox state of the cellular environment since oxidising conditions, as expected, favour the formation of peroxynitrite whereas reducing conditions support S-nitrosylation of the NMDA receptor thiol, which down regulates the receptor and confers protection against neurotoxicity (Coyle and Puttfarcken, 1993).

1.3.3.2 Cellular Targets of Nitric Oxide

By virtue of its unpaired electron, the main biological targets of NO include oxygen, transition metals, iron-sulphur containing proteins and haem-containing proteins. Many of the neurotoxic actions of NO centre on the mitochondrion and the inhibition of neuronal energetics. NO inhibits several components vital for oxidative phosphorylation, namely NADH-ubiquinone oxide reductase and NADH-succinate oxide reductase, by removal of iron from iron-sulphur centres, and cytochrome oxidase, by competing with O_2 (Bolanos *et al*, 1997). In addition to impairing respiration, NO inhibits *cis*-aconitase, thereby inhibiting glycolysis. NO also inhibits creatinine kinase through nitrosothiol modification, which reduces the availability of ATP to the cell. Nitric oxide causes DNA fragmentation and the activation of PARS,

an enzyme that rapidly consumes ATP (Samdani *et al*, 1997; Brown and Borutaite, 1999). Evidently, NO may severely deplete cellular ATP stores, simultaneously inhibiting ATP production and accelerating its consumption.

The application of NO donors causes mitochondrial depolarisation in cultured neurons (Brorson *et al*, 1999; Almeida *et al*, 1999), a phenomenon which could be linked to the inhibition of oxidative phosphorylation, or to opening of the PTP via peroxynitrite formation (Packer *et al*, 1997).

NO neurotoxicity is associated with a loss of neuronal Ca^{2+} homeostasis. The exposure of cultured hippocampal neurons to a NO donor, SNOC, caused a persistent elevation in Ca^{2+}_i that was blocked by haemoglobin, a NO scavenger (Brorson and Zhang, 1997). This could be attributed to reduced Ca^{2+} extrusion through the plasma membrane Ca^{2+}ATPase, resulting from neuronal ATP depletion. Nitric oxide and/or peroxynitrite may cause oxidative damage to SERCAs (Davis *et al*, 2001), perturbing neuronal Ca^{2+} levels. Finally, NO may trigger Ca^{2+} release from mitochondria, flooding the cytoplasm with Ca^{2+} (Richter *et al*, 1997). Interestingly, NO reduces the opening frequency of the NMDA receptor-associated ion channel, so should serve as negative feedback for excessive NMDA receptor channel activity (Choi *et al*, 2000).

Nitric oxide is thought to increase oxidative stress in neurons as well as being a free radical itself. NO may stimulate the production of $O_2^{\cdot}$ by the respiratory chain (through the inhibition of cytochrome oxidase) (Knowles, 1997) and may reduce neuronal antioxidant defences by binding the haem group of catalase, thereby inhibiting the breakdown of H_2O_2 (Brown and Borutaite, 1999). In addition, the inactivation of Mn-SOD by $ONOO^{\cdot}$ could further worsen the vicious cycle of oxidative damage (Samdani *et al*, 1997).

It should be mentioned that several research groups have failed to observe a NO component to neurotoxicity (Garthwaite and Garthwaite, 1994; Lernernatoli *et al*, 1992; Pauwels and Leysen, 1992). It is possible that in these experimental models, NOS was not expressed at sufficient levels (Dawson and Dawson, 1996). However, the requirement for NO in

neurotoxicity is unlikely to be absolute; it is more probable that NO is involved in only some instances of neuronal death, where it acts in synergy with other elements of neurotoxicity such as ROS and Ca^{2+} elevations.

1.3.4 MITOCHONDRIA AND REACTIVE OXYGEN SPECIES

Reactive oxygen species are radical derivatives of molecular oxygen, and include superoxide ($O^{\bullet}_2^-$), hydroperoxyl radical ($HO^{\bullet}_2$) and hydroxyl radical (•OH) as well as hydrogen peroxide (H_2O_2). In addition, nitric oxide (NO) and peroxynitrite ($ONOO^-$) are derived from the interaction of nitrogen-based radicals with O_2 (Maher and Schubert, 2000). With the exception of H_2O_2, these species contain an orbital with an unpaired electron, so are highly reactive and capable of extracting an electron from neighbouring molecules in order to fill the gap in their orbital (Olanow, 1993).

There are numerous cellular sources of ROS. Firstly, mitochondria consume about 90% of inhaled oxygen, and are a powerful source of ROS, given the inefficiency of the respiratory chain. It is calculated that under physiological conditions, 1-4% of the oxygen consumed during respiration reacts with electrons leaked from the upstream components of the respiratory chain to produce superoxide. The dismutation of superoxide then produces hydrogen peroxide. In the presence of iron, hydrogen peroxide can be converted to the highly destructive hydroxyl radical in the Fenton reaction:

$$Fe(II) + H_2O_2 \rightarrow Fe(III) + OH^- + \bullet OH.$$

Uncoupling of the respiratory chain enhances oxygen consumption, thereby decreasing mitochondrial ROS production (Lenaz, 1998). Under conditions of excess ATP, electron transfer through mitochondria is reversed, greatly increasing $O^{\bullet}_2^-$ production. A high ADP/ATP ratio due to energy consumption may minimize ROS production by mitochondria, which could explain why the life span of some animals can be extended by calorie restriction (Maher and Schubert, 2000). There are two major regions on the respiratory chain where ROS are produced, firstly NADH coenzyme Q reductase (complex I) and secondly ubiquinol cytochrome c reductase (complex III) (Lenaz, 1998).

Additionally, cosmic and terrestrial radiation can ionize water and generate a variety of radical products, which can themselves generate additional ROS:

$H_2O \rightarrow \rightarrow \rightarrow e^-, \bullet OH, \bullet H, H_3O^+, H_2, H_2O_2$

Other sources of ROS in the CNS include the NADPH oxidase of macrophages and microglia, and the large number of oxidases found within peroxisomes, endoplasmic reticulum and cytoplasm (lipoxygenases, cyclooxygenases, cytochrome P450 oxidases, monoamine oxidases and nitric oxide synthase) (Maher and Schubert, 2000). The activation of NMDA receptors sets in motion a variety of pathways that may cause oxidative stress. The stimulation of PLA_2 and subsequent release of arachidonic acid (AA) generate ROS. AA and ROS then promote a vicious cycle by enhancing the release of glutamate and inhibiting its uptake, via the oxidation of glutamate transporters on astrocytes.

The brain is particularly vulnerable to oxidative damage for several reasons. Neuronal cell membranes are enriched in polyunsaturated fatty acids which are particularly vulnerable to free radical attack, because the double bonds within membranes allow for easy lipid peroxidation (Coyle and Puttfarcken, 1993). The brain has a very high metabolic rate to meet the energy requirement of synaptic communication. The brain uses 20% of the body's total O_2 intake despite accounting for only 2% of the total body weight, meaning its respiratory rate is 10 times greater than that of average tissue. Specific brain regions are rich in the transition metals iron and copper, which support Fenton chemistry to generate hydroxyl radicals. These factors necessitate elaborate cellular mechanisms for protection against ROS. However, the human CNS is relatively deficient in oxidative defences, another factor rendering it more susceptible to ROS damage (Cassarino and Bennett, 1999).

A variety of naturally occurring antioxidant defence mechanisms normally minimize ROS production and limit oxidative tissue damage. **Figure 1.7** outlines the pathways involved in ROS generation and disposal.

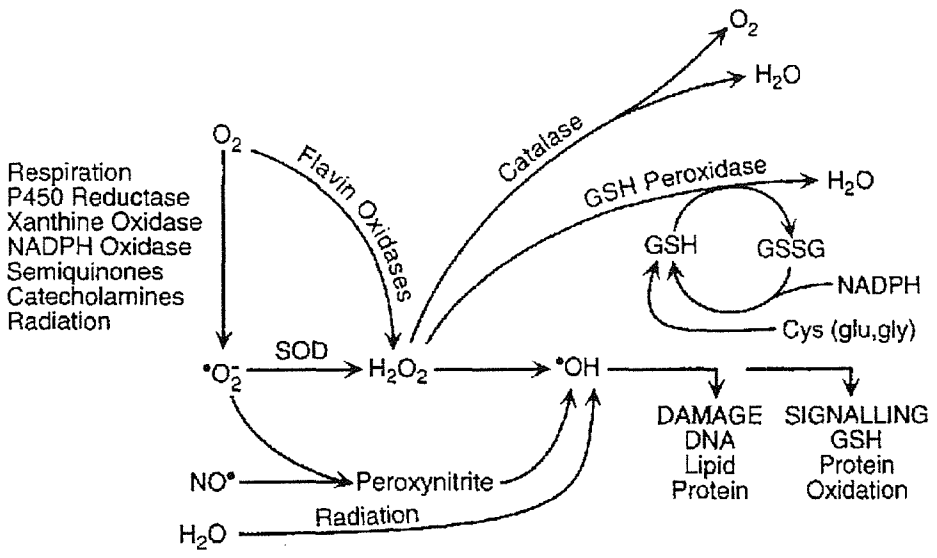

Figure 1.7 Sources of ROS and mechanisms for their removal from cells. SOD, superoxide dismutase; GSH, glutathione. Adapted from Maher and Schubert, 2000

Oxidative phosphorylation is spatially restricted to the inner mitochondrial membrane where ROS are tightly bound and can be safely disposed of by several intramitochondrial antioxidant enzymes. Superoxide is reduced by superoxide dismutase (Mn form) to H_2O_2 which is then broken down to water by catalase or glutathione peroxidase (Melov, 1999). Glutathione peroxidase is more abundant than catalase in CNS mitochondria, and has a higher turnover rate. Vitamin E and ascorbate are chain-breaking free radical scavengers that directly inactivate ROS. Superoxide dismutase may be regarded as a "double edged sword" because it converts the less harmful radical $O^{\bullet}{}_2^-$ to H_2O_2, which is readily degraded to the highly reactive •OH via the Fenton reaction. Fenton chemistry requires multivalent transition metals such as iron or copper to facilitate electron transfer. Proteins such as transferrin or ferritin that sequester iron should therefore be regarded as an anti-oxidant defense mechanism. Finally, glutathione (GSH) is a tripeptide with considerable reducing potential found intracellularly at concentrations between 2 and 10 mM, of which 99% is usually in the reduced state (Maher and Schubert, 2000).

Although ROS have the potential to damage intracellular macromolecules such as proteins, lipids and DNA, under physiological conditions, the majority of the effects of ROS on cells are mediated by the induction of signalling pathways. These effects mainly comprise the reversible modification of intracellular protein components such as sulfhydryl groups. ROS are known to increase the activity of protein tyrosine kinases and serine/threonine kinases, probably via the inhibition of specific phosphatases. A number of transcription factors are activated by ROS, including NF- κB, STATs, Jun and Fos. ROS may act directly on the transcription factors to cause activation, or may mediate regulatory binding partners or upstream signalling pathways such as JNK and ERK (Maher and Schubert, 2000).

Recent evidence would suggest that peroxynitrite is able to cause the influx of Ca^{2+} into neurons by depolarizing the neuronal plasma membrane. In cultured cortical neurons, $OONO^-$ induced the influx of $_{45}Ca^{2+}$ through P/Q and L-type VDCCs, but interestingly, inhibited Ca^{2+} influx through N-type channels (Ohkuma *et al*, 2001).This neuronal Ca^{2+} influx could then have a multitude on knock on effects, including the neuronal release of neurotransmitters.

Oxidative stress has been implicated in virtually every area of human pathology, including acute neurotoxicity, chronic neurodegeneration, and ageing. Oxidative stress may arise when ROS production is excessive, due to perturbed metabolism or pathological release of catalysts such as transition metals, or when cellular defences are lowered by the depletion of antioxidants (Lenaz, 1998). The damage inflicted on intracellular macromolecules by ROS can lethally disrupt cellular functions and integrity.

1.3.4.1 Evidence for the involvement of ROS in acute neurotoxicity

Several different experimental approaches have revealed the involvement of ROS in processes of acute neurotoxicity.

Antioxidants are protective in models of acute neuronal damage

Antioxidants have been observed to reduce neuronal injury in many paradigms of brain damage. The peroxynitrite scavenger uric acid and the antioxidants propyl gallate and glutathione prevented apoptosis in an *in vivo* mouse model of ischaemia (Keller *et al*, 1998). Similarly, the free radical scavenger PBN was neuroprotective in brain slices subjected to hypoxia and reoxygenation (Murata *et al*, 2000), and the addition of cell-permeant superoxide dismutase reduced neuronal death following hypoxia in both cultured hippocampal neurons (Rosenbaum *et al*, 1994) and cultured forebrain neurons (Cazevieille *et al*, 1993).

The striatal production of •OH caused by glutamate infusion in an *in vivo* rat model was significantly reduced by Ensaculin, a drug that has direct ROS scavenging effects in addition to blocking NMDA receptors (Teismann and Ferger, 2000). In this model, MK-801 was not as effective as Ensaculin at reducing •OH production, despite having a 1000-fold greater affinity for the NMDA receptor. Glutamate excitotoxicity in cultured cerebellar granule cells was significantly reduced by Vitamin E, and by the inhibition of PLA_2 (Ciani *et al*, 1996), although these protective effects were not additive. Neuronal death caused by the exposure of cultured rat hippocampal neurons to NMDA was reduced by the SOD mimetic MnTBAP, and by α–tocopherol (Vitamin E) (Luetjens *et al*, 2000). Similarly, the failure of protein synthesis observed in rat hippocampal slices exposed to NMDA was attenuated by α–tocopherol (Monje *et al*, 2000).

Peroxynitrite scavengers were effective in the acute treatment of traumatic brain injury (Hall *et al*, 1999). Neuronal oxidative stress may also be modelled by the direct addition of ROS to cultured neurons. Pyruvate can

scavenge H_2O_2, and was strongly neuroprotective against H_2O_2-induced injury in cultured striatal neurons (Desagher *et al*, 1997). The induction of the endogenous antioxidant GSH by dimethyl fumarate strongly attenuated the toxicity of dopamine and H_2O_2 in a neuroblastoma cell line (Duffy *et al*, 1998).

Transgenic mice overexpressing antioxidants are neuroprotected

Transgenic technology has been used to alter the levels of antioxidants and oxidant-related enzymes or proteins expressed by animals. These animals are very useful to study the role of a particular antioxidant in ischaemic brain injury. In studies using transgenic mice overexpressing *SOD-1* (CuZn superoxide dismutase), it has been observed that the total infarct volume following focal cerebral ischaemia was reduced by 36% compared with wild-type mice. This points to the protective role of CuZn-SOD against neuronal injury. Transgenic mice in which neurons overexpress *BCL-2* were also protected against cerebral ischaemia (Chan, 1996). A more recent study has shown that transgenic mice that overexpress *MnSOD* (Mn superoxide dismutase) show a marked reduction in nitrated proteins, membrane lipid peroxidation and neuronal death after focal cerebral ischaemia (Keller *et al*, 1998).

Ischaemia or excitotoxins increase the neuronal generation of ROS

Recent technological advances have allowed the detection of intracellularly generated ROS with oxidation-sensitive fluorescent dyes or electron paramagnetic resonance. The neuronal production of ROS has thus been measured in a large number of experimental models involving the exposure of cultured neurons to excitotoxins (Dugan *et al*, 1995; Bindokas *et al*, 1996; Patel *et al*, 1996; Prehn *et al*, 1998; Carriedo *et al*, 2000; Ceccon *et al*, 2000; Luetjens *et al*, 2000; Vergun *et al*, 2001). Increased ROS production has also been observed in organotypic hippocampal slices subjected to ischaemia (Perez Velazquez , 1997). These experimental findings will be explored further in **Chapter 5**.

1.3.4.2 Evidence for the involvement of ROS in ageing and chronic neurodegeneration

Oxidative damage to mitochondria may be involved in the longer term pathological changes associated with neurodegenerative diseases such as amyotropic lateral sclerosis (ALS) Alzheimer's disease (AD), Huntingdon's disease (HD) and Parkinson's disease (PD). The most reliable risk factor for such diseases is normal aging, and there is substantial evidence that mitochondrial function declines with age. It has been suggested that an age related reduction in physical activity could be an important contribution to this decline, since the decline in respiratory chain function is greater than that anticipated from mtDNA mutations (Brierly *et al*, 1996). The endogenous production of ROS due to normal physiological processes is thought to limit the lifespan of animals, since transgenic mice deficient in *SOD-2* die within the first week of life, and the overexpression of superoxide dismutase significantly extends the lifespan of *Drosophila* (Melov, 1999).

Mitochondrial membranes are one of the primary sources of free radicals and may suffer considerable damage at the hands of such species. Damage by ROS to mitochondrial components includes lipid peroxidation, protein oxidation and mitochondrial DNA mutations. Lipid peroxidation is thought to be particularly harmful in mitochondria, since cardiolipin, a major component of the inner mitochondrial membrane, is required for the activity of cytochrome oxidase and other mitochondrial proteins. Disorder of the mitochondrial membrane could negatively affect the function of membrane linked enzymes which are sensitive to the structural integrity of their microenvironment. Protein oxidation may cause damage to respiratory chain enzymes, ANT (which may trigger opening of the PTP) and the ATPase. The structure of mitochondrial DNA, with its close proximity to the respiratory chain, limited repair mechanisms, paucity of non-coding sequences (introns) and absence of protective packaging with histones renders it particularly susceptible to oxidative damage. After an oxidative stress to cultured cells, the damage to mtDNA is higher and persists longer than that to nuclear DNA (Lenaz, 1998).

Several mitochondrial DNA mutations occur spontaneously with aging. In brain tissue, studies have identified age dependent increases in a 4,977 base pair deletion which are of the highest magnitude in the striatum and substantia nigra, possibly due to free radicals produced by the breakdown of dopamine by mitochondrial monoamine oxidase (Soong *et al*, 1992). The largest numbers of mitochondrial deletions accumulate in brain, heart and muscle tissue, which are post-mitotic tissues in which DNA damage is likely to accumulate over time. Mitochondrial oxygen radical production appears to increase with age in parallel with levels of mutated mtDNA. In a study conducted on human brain DNA there was seen to be a 10 fold increase in the levels of oxidatively damaged bases in mtDNA compared to nuclear DNA (Mecocci *et al*, 1993). These data show a progressive and preferential age related accumulation of oxidative damage in mtDNA in human brain. Such damage may well be linked with age-dependent increases in the incidence of neurodegenerative diseases.

Free radicals are known to cause damage to the ETC in mitochondria, both directly, and by causing mtDNA mutations. Structural genes located on mtDNA encode for 13 polypeptide chains that comprise the protein complexes and ATPase of the respiratory chain. It is therefore highly likely that mitochondrial DNA mutations will be manifested as defects in mitochondrial oxidative phosphorylation. The "redox theory of ageing" suggests that defective oxidative phosphorylation arises from the accumulation of somatic mutations of mtDNA, as described above. Respiratory chain defects may lead to increased generation of ROS, precipitating a vicious circle of oxidative stress and mtDNA damage (Wallace, 1999).

A decline in oxidative phosphorylation with normal ageing may combine with subclinical genetic defects to produce delayed onset neurodegeneration. There is much evidence for impaired neuronal energetics and oxidative damage in neurodegenerative diseases. Mitochondrial function is thought to be impaired in amyotrophic lateral sclerosis (ALS) (Beal, 2000). Markers of protein oxidation were observed to be elevated by 85% in patients with ALS

as compared to controls (Coyle and Puttfarcken, 1993), and point mutations in CuZnSOD have been associated with familial ALS (Beal, 1995). In idiopathic Parkinson's disease (PD), a 40% reduction in mitochondrial complex I activity was noted in the substantia nigra (Schapira, 1998), and a several fold increase in brain lipid peroxides was identified (Coyle and Puttfarcken, 1993). Studies have shown a threefold increase in oxidative damage to mtDNA in postmortem tissue from patients with Alzheimer's disease (AD) compared with age-matched controls (Beal, 2000). In patients with Huntingdon's disease (HD), severe defects in the mitochondrial respiratory chain have been identified, specifically a 55% deficiency in complex II and III (Schapira, 1998). In concert with subclinical genetic defects, the underlying bioenergetic crisis in neurodegenerative diseases eventually triggers neuronal death, but the precise mechanism of neuronal loss may vary.

Slow or weak excitotoxicity is thought to underlie some types of slowly evolving neurodegenerative diseases and may occur as a result of defects in energy metabolism. Reduced cellular ATP levels may lead to the partial depolarisation of neurons that would then become persistently activated by ambient glutamate levels due to the relief of the voltage-dependent Mg^{2+} block of the NMDA receptor. Low cellular energy levels could also interfere with Ca^{2+} buffering, with increased $[Ca^{2+}]_i$ initiating damaging processes including the activation of nitric oxide synthase and free radical generation (Beal, 1995). Apoptotic processes are also likely to be involved in many neurodegenerative conditions. Defective energy transduction could lead to the collapse of the mitochondrial membrane potential, with concurrent opening of the PTP and release of pro-apoptotic factors into the cytoplasm causing eventual tissue atrophy (Ozawa, 1999). Apoptosis has been described in a variety of human neurodegenerative disorders, based on the identification of neuronal nuclei with DNA cleavage in postmortem tissue. Such nuclei have been reported in brains or spinal cords of patients with AD, PD, HD and ALS (Tatton and Olanow, 1999).

Oxidative stress and excitotoxic processes have long been implicated in neuropathology, and these mechanisms may converge to represent sequential as well as interacting processes providing a final route for neuronal vulnerability to insult (Coyle and Puttfarcken, 1993).

1.3.5 TRACE METALS

Zinc is the second most abundant trace metal in the body. The brain has the highest Zn^{2+} content of all organs, with an overall content of 150μM. This Zn^{2+} is not uniformly distributed, with the highest concentration occuring in the hippocampus, amygdala and cortex. Neuronal levels of Zn^{2+} are kept at subnanomolar levels by a family of zinc transporter proteins and intracellular metallothionins (peptides with multiple binding sites for Zn^{2+}). Up to 15% of brain zinc is contained in presynaptic terminals of glutamatergic neurons, where it occurs at millimolar levels. Strong activation of Zn^{2+}-containing presynaptic terminals may result in transient local Zn^{2+} concentrations of up to 300μM (Weiss *et al*, 2000). Zinc is an essential cofactor for many neuronal enzymes such as Cu-Zn SOD, and has the potential to alter the behaviour of multiple membrane channels and receptors. Synaptic Zn^{2+} release from hippocampal mossy fibres is thought to be important for the tonic inhibition of NMDA receptors on CA3 pyramidal neurons (Vogt, 2000), and may foster LTP induction in CA1 neurons by preventing "untimely" NMDA receptor activation (Choi and Koh, 1998).

1.3.5.1 Involvement of trace metals in acute brain injury

Zinc is relatively non-toxic compared to other transition metals since it lacks redox activity. Excessive human zinc consumption (12 grams over 2 days) was reported to produce only reversible lethargy (Choi and Koh, 1998). However, Zn^{2+} is potently toxic to neurons in culture (Kim *et al*, 1999; Sheline *et al*, 2000). The translocation of Zn^{2+} from pre- to postsynaptic neurons contributes to the selective nerve injury seen in traumatic brain injury, epilepsy and cerebral ischaemia (Frederickson, 1989; Koh, 1996; Suh, 2000). In each of these conditions, there was a strong correlation between those neurons which accumulated Zn^{2+} and those that were lethally damaged. Furthermore, the intraventricular injection of the metal chelator EDTA reduced both the postsynaptic Zn^{2+} accumulation, and subsequent neuronal death (Suh, 2000). However, it is likely that Zn^{2+} has a contributory rather than causative role in brain damage, since epileptic neuronal injury can occur in the absence of vesicular Zn^{2+} (Cole, 2000).

Zn^{2+} is co-released with glutamate at excitatory synapses, and is thought to gain entry to postsynaptic neurons predominantly through Ca^{2+} permeable AMPA/kainate receptors (Ca-A/K channels), with some residual entry through NMDA receptors and VDCCs (Carriedo *et al*, 1998; Sensi *et al*, 1999). In agreement with this, the hilar interneurons that are selectively damaged in ischaemia and epilepsy express high numbers of Ca-A/K channels (Weiss and Sensi, 2000). Furthermore, the toxicity of Zn^{2+} to cortical cultures was exacerbated by the inclusion of AMPA or KA (Kim *et al*, 1999), and zinc has been shown to potentiate the toxicity of AMPA and kainate in cultured cortical neurons (Yin and Weiss, 1995). In contrast, metal chelators could not reduce the neuronal loss caused by the intra-amygdaloid injection of kainate in an *in vivo* situation (Lees *et al*, 1998).

Intracellular Zn^{2+} is thought to promote cell death through a number of mechanisms, including metabolic inhibition and the generation of ROS. The exposure of cortical cultures to Zn^{2+} caused lipid peroxidation and neuronal necrosis, which could be attenuated by the antioxidant Trolox (Kim *et al*, 1999). Zinc may generally reduce neuronal antioxidant capacity by interfering with reduced sulfhydryl groups and by inhibiting enzymes such as glutathione reductase and peroxidase. Microfluorimetric studies have shown that the exposure of cortical cultures to Zn^{2+} causes a steep increase in the intracellular concentration of Zn^{2+}, concurrent with prolonged mitochondrial depolarisation and ROS generation of mitochondrial origin (Sensi *et al*, 1999), probably resulting from Zn^{2+} uptake into mitochondria. Prolonged exposure of cultured neurons to lower concentrations of Zn^{2+} (up to 50μM) is thought to activate apoptotic mechanisms, causing DNA fragmentation and other morphological features specific to apoptosis (Kim *et al*, 1999). Oxidative stress likely also contributes to these more slowly evolving forms of Zn^{2+}-neurotoxicity. The Zn^{2+} -induced depletion of NAD+ and inhibition of glycolysis may also be a critical factor in neuronal injury (Sheline *et al*, 2000).

1.3.5.2 Involvement of trace metals in neurodegenerative diseases

In the brain, the presence of small quantities of copper and iron are required in addition to Zn^{2+} for the proper functioning of enzymes. The disruption of copper metabolism has been implicated in prion diseases, ALS and AD. Uncomplexed iron ions are thought to exert neurotoxicity in PD and AD. ALS is characterized by the selective degeneration of spinal motor neurons, whereas in AD, hippocampal pyramidal neurons are among those neuronal groups adversely affected (Armstrong *et al*, 2001). These neuronal populations are thought to express Ca-A/K channels, providing a route for rapid and direct Zn^{2+} entry. Similarly to ischaemia, the downregulation of GluR2 in AD could contribute to the progressive neuronal loss by increasing Ca-A/K channels and facilitating Zn^{2+} entry. Repeated exposures to Zn^{2+} could contribute to the oxidative damage and mitochondrial dysfunction seen in AD and ALS. Zn^{2+} could also promote the aggregation of amyloid deposits in AD (Weiss and Sensi, 2000). The interaction of amyloid protein with copper has been shown to increase oxidative damage and cell death in a neuronal culture model of AD (White *et al*, 1999). The intrahippocampal injection of cupric sulphate, ferric citrate or zinc chloride caused extensive neurological deficits and eventual neuronal loss in rats, which could be fully prevented by the co-administration of EDTA (Armstrong *et al*, 2001).

Chapter 2

MATERIALS AND METHODS

2.1. Chemicals and reagents

All buffer components were purchased from Sigma (UK) and were used as recommended by the manufacturers. Enzymes for neuronal dissociation and enzyme inhibitors were also purchased from Sigma (UK). Media and supplements for cell culture were supplied by Life Technologies (UK) and cell culture plastics obtained from Helena Biosciences (UK). Dyes used for fluorescent imaging were purchased from Molecular Probes (Europe, BV). All drugs used were analytical grade or better, and were supplied by the following companies: FCCP, glutamate, kainate, NMDA, 4-AP, $CdCl_2$, xanthine, xanthine oxidase, EDTA and L-NAME from Sigma (UK), BHQ from Calbiochem (UK), thapsigargin from Alomone (Israel) and ACPD, AMPA, quisqualate, CNQX, D-AP5 and dantrolene from Tocris (UK).

2.2. Preparation of acutely dissociated hippocampal neurons

Dissociated neurons were prepared from hippocampal slices from both neonatal mice aged 5-8 days and adult mice aged 18-21 days using a method adapted from Chad et al (1991).

2.2.1. Dissociated hippocampal neurons from neonatal (5-8 day) mice

The hippocampi of neonatal mice were dissected out into chilled PIPES buffer (composition: NaCl 120mM; KCl 5mM; $MgCl_2$ 1mM; PIPES 20 mM; sucrose 5mM; glucose 25mM and pH 7.4 with NaOH). 300μm slices were then prepared on a McIlwain tissue chopper and incubated at 30°C with approximately 0.25 mg/ml pronase E (Sigma type XIV) and 0.25 mg/ml thermolysin (Sigma type X) for 60 minutes in continuously oxygenated PIPES buffer. The hippocampal slices were then rinsed in PIPES buffer supplemented with 1mM $CaCl_2$ and triturated by passing the slices through a series of flame polished pasteur pipette tips of decreasing diameter. This process yielded a mixture of isolated neurons and neuronal clumps in solution.

2.2.2. Dissociated hippocampal neurons from adult (18-21 day) mice

Mice were decapitated and the brain rapidly removed to iced oxygenated (95% O_2, 5% CO_2) ACSF (NaCl 118mM; $NaHCO_3$ 26 mM; KCl 3mM; KH_2PO_4 1.25mM; $MgSO_4$ 1mM; $CaCl_2$ 2.5mM and glucose 10mM). Hippocampi were then removed using blunt dissection techniques and 400µm slices prepared as above. The hippocampal slices were maintained for at least 60 minutes at room temperature in an interface chamber then incubated with proteases in continuously oxygenated PIPES buffer as above for approximately 90 minutes, then rinsed and triturated.

2.3 Culture of dissociated mouse hippocampal cells

Dissociated mouse hippocampal cells were maintained in culture using a method modified from Mynlieff et al (1997). Care was taken to maintain sterile technique whenever possible. All solutions were autoclaved and only opened in a sterile laminar flow hood. All instruments and glassware were sterilised with ethanol.

2.3.1. Poly-L-Lysine coated cover slips

Poly-L-Lysine solution (1 mg/ml of 38 500 to 60 000 molecular weight poly-L-lysine in 0.15 M boric acid, pH 8.4 with NaOH) was pipetted onto 25 mm diameter circular cover slips and allowed to stand overnight in the laminar flow hood. Each cover slip was rinsed twice with sterile distilled water, then covered with sterile HEPES buffer (146 mM NaCl, 5 mM KCl, 2mM $CaCl_2$, 1 mM $MgCl_2$, 10 mM HEPES, pH 7.4) for 30 min. The cover slips were again rinsed in sterile distilled water and allowed to dry before being placed in 6-well plates.

2.3.2 Dissociation of neurons

5-7 day old mice were sacrificed by decapitation and the hippocampi dissected into chilled growth medium (Neurobasal medium with B27 supplement, 0.5 mM L-glutamine, 0.02mg/ml gentamicin, Gibco BRL, Life Technologies, UK). Hippocampi were placed on Melinex film and sliced at a thickness of 400μm. Slices were then transferred to 0.5mg/ml trypsin XI (Sigma) in continuously oxygenated PIPES buffer (120 mM NaCl, 5 mM KCl, 1 mM $CaCl_2$, 1 mM $MgCl_2$, 25mM glucose, 20 mM PIPES, pH 7.0) for 30 min at room temperature, followed by incubation for 60 min at 35°C. The tissue was rinsed in HEPES buffer with glucose (11 mM) containing 1mg/ml BSA and 1mg/ml trypsin inhibitor type II-O (Sigma, UK) and rinsed again in 1 ml of growth media. Slices were triturated in fresh media using flame polished Pasteur pipettes of decreasing diameter, and 0.5 ml plated onto each poly-L-lysine coated cover slip. Each hippocampus was triturated in approximately 1 ml of growth medium. After 5 minutes, allowing time for the neurons to adhere to the cover slips, 1.5-ml growth media was added to each well to bring the volume up to 2 ml per well. Neurons were then maintained at 37°C in a 5% CO_2 incubator for up to 20 days.

2.4 Neuronal loading with fluorescent probes

2.4.1. Acutely dissociated neurons

Neurons were incubated with 5μM TMRE in PIPES buffer (for composition see section **2.2.1**.) for 10 min at room temperature with minimal light exposure, then rinsed in fresh PIPES buffer. For calcium imaging, neurons were incubated with 10μM Fluo-3 AM (Molecular Probes) for 30 minutes at room temperature also with minimal light exposure. Neurons were then rinsed and plated out onto poly-L-lysine (0.01%) coated modified coverslips for imaging.

2.4.2 Cultured dissociated neurons

TMRE loading

Neurons were incubated in 5μM TMRE in Neurobasal medium for 5-10 min at 37°C. Neurons on cover slips were then removed from this TMRE solution, mounted in a Peltier chamber for imaging, and covered with fresh PIPES buffer (see section **2.3.2**. for composition).

Fluo-3 AM/ Fluo-5N AM loading

Neurons were incubated with 10 μM Fluo-3 AM/ Fluo-5N AM in PIPES buffer for a minimum of 120 minutes at 37°C. Neurons were then removed from this dye solution, fixed in a Peltier chamber for imaging, and covered with fresh PIPES buffer at room temperature.

Dihydroethidium (Het) loading

Neurons were incubated with 10μM dihydroethidium in PIPES buffer for 30 minutes at 37°C. Neurons were then removed from this dye solution, fixed in a Peltier chamber for imaging, and covered with fresh PIPES buffer at room temperature.

MitoTracker Green loading

Neurons were incubated in 5nM Mitotracker Green FM in PIPES buffer for 10 minutes at 37°C, then rinsed and imaged.

2.5. Confocal Imaging techniques

Cellular fluorescence was imaged using a confocal laser scanning microscope (Biorad MRC 600) with a krypton-argon laser coupled to an inverted microscope (Nikon) fitted with a x40 objective. The optical configuration of the CLSM used the dual excitation (488 and 568 nm) lines of a krypton-argon laser to excite Fluo-3, Fluo-5N, dihydroethidium, TMRE and MitoTracker Green near to peak efficiency. Photomultiplier tubes detected fluorescence emissions at <560 nm (Fluo-3, Fluo-5N, and MitoTracker Green) or >560 nm (TMRE and Het). Laser exposure was limited to 25 scans per sample to avoid photo-oxidation of the dye. For drug application, 100μl

of drug at X10 concentration was applied by pipette directly to the imaging chamber (volume 1 ml) to give the correct final concentration of drug. Drugs were applied at room temperature. Images were collected at fixed intervals and stored on computer hard drive for subsequent analysis. Properties of the fluorescent probes used in this study are summarised in **Table 2.1** (below).

Fluorescent Probe	Abs (nm)	Em (nm)	Structure	Spectra
Fluo-3 AM	506	526	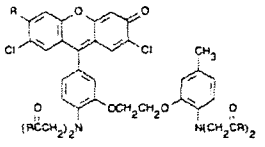	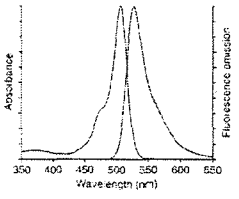
Fluo-5N AM	494	516	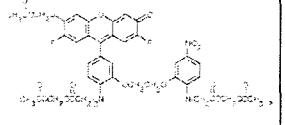	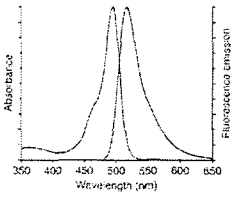
Dihydro-ethidium (Het)	518	605	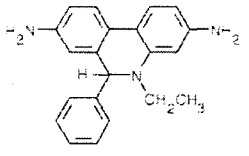	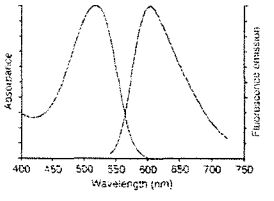
Tetra-methyl-rhodamine ethyl ester	549	574	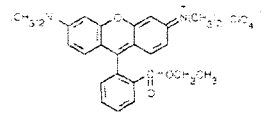	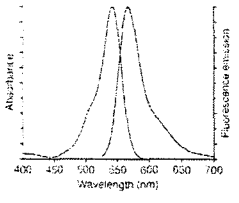
Mito-Tracker Green AM	490	516	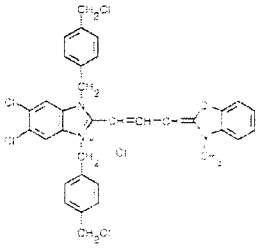	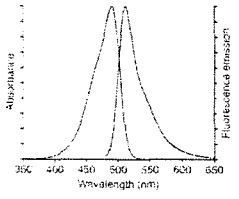

Table 2.1 Summary of the properties of fluorescent probes used in this study. Data from Haugland, 1999.

2.6 Immunocytochemistry techniques

2.6.1 Fixation of neurons

Cultured dissociated hippocampal neurons were fixed in 4% paraformaldehyde (PFA) for 24 hours. PFA was prepared by adding 10mls phosphate buffered saline (PBS) (5.17g KH_2PO_4 and 58g $Na_2HPO_4.12H_2O$ in 1000 ml distilled water) to 4g PFA and heating the mixture to 70°C. 5M NaOH was added drop by drop until the solution became clear, then a further 90 mls PBS were added and the solution adjusted to pH 7.2-7.4. Following this fixation period, neurons were rinsed in 0.05M Tris buffered saline (TBS) (8.75g NaCl and 6.05g Tris in 1000 ml distilled water, pH 7.4) and maintained in TBS for up to 2 weeks.

2.6.2 Staining with MOM monoclonal NeuN antibody (Vector Labs Inc)

Neurons were exposed to 10% H_2O_2 in TBS with 25% EtOH for 10 minutes to abolish endogenous peroxidase activity. Neurons were rinsed in TBS and permeabilised by exposure to 0.3% Triton-X for 10 minutes, then rinsed again. Neurons were incubated with blocking antibody for 1 hour, rinsed twice in TBS, and incubated with MOM protein concentrate (diluent) for 10 minutes in order to prevent non-specific antibody binding. Cells were then incubated with the primary NeuN antibody (anti-mouse IgG) diluted to 1:1000 in diluent for 45 minutes, and rinsed twice in TBS. A second incubation was then carried out with the secondary antibody (biotinylated anti-mouse IgG reagent) diluted to 4:1000, for 20 minutes. Following 2 rinses in TBS, cells were incubated for 10 minutes with an avidin-biotin complex in TBS, rinsed again, and stained with DAB (3,3'-diaminobenzidine) until brown cell colouration was evident, rinsed, and kept in TBS.

2.7 Validation of TMRE as a potentiometric probe to measure changes in mitochondrial membrane potential

Mitochondrial membrane potential can be measured at the single cell level by using lipophilic cationic probes such as TMRE, TMRM and rhodamine 123 (R123) in conjunction with microscopy. These probes accumulate in the mitochondrial matrix because of their charge and solubility in both the inner mitochondrial membrane and matrix space. Each probe contains a positively charged quaternary nitrogen and an extensive π–orbital system that delocalises the positive charge, thereby greatly increasing the membrane permeability of the probe (Nicholls and Ward, 2000). Upon mitochondrial sequestration, these probes undergo quenching of their fluorescence if loaded at a sufficiently high concentration. Subsequent changes in whole cell fluorescence are indicative of changes in mitochondrial $\Delta\Psi$ (Bernardi *et al*, 1999). For example, mitochondrial depolarisation results in the redistribution of probe from the mitochondrial matrix to the cytoplasm (dequenching) with a concurrent change in cellular fluorescence.

In the literature, the loading concentration of potentiometric probes ranges from 0.1μM TMRE (Schinder *et al*, 1996) to 2-200nM TMRE (Kiedrowski, 1998) to 1μM R123 (Castilho *et al*, 1998, Vergun *et al*, 2001) depending whether the probe is intended to be quenched in mitochondria or not. The interpretation of cellular changes in the fluorescence of these probes is therefore related to the loading concentration of probe. If the loading concentration of the probe is high enough to cause mitochondrial quenching of the probe, then an *increase* in the cellular fluorescence of the probe is indicative of a decrease in $\Delta\Psi_m$ (mitochondrial depolarisation) (Khodorov *et al*, 1996; Brorson *et al*, 1999; Almeida *et al*, 1999; Vergun , 2001). However, other groups minimize the quenching of the dye in mitochondria by using a low loading concentration of probe, in which case the collapse of $\Delta\Psi_m$ is manifested as a *decrease* in fluorescence intensity (Schinder *et al*, 1996; Bernardi *et al*, 1999; Kiedrowski, 1998; Tenneti *et al*, 1998).

Potentiometric probes are invaluable in the measurement of in situ mitochondrial function, but there are several problems and potential sources of artifacts associated with their use. Firstly, these potentiometric probes may inhibit mitochondrial respiration, possibly through inhibition of the mitochondrial F_0F_1-ATPase (Scaduto and Grotyohann, 1999). Secondly, the probes are able to bind to mitochondrial and other cellular membranes independently of $\Delta\Psi_m$.which could adversely affect the response of cell fluorescence to $\Delta\Psi_m$ (Bernardi *et al*, 1999). Thirdly, phototoxic effects are likely to be caused by fluorescent molecules particularly upon radiation by confocal laser beams, through the production of oxyradicals (Bernardi *et al*, 1999). Thus, the fluorescent probes could themselves alter rather than simply measure the changes of $\Delta\Psi_m$. It would then be difficult to ascertain whether a change in cellular fluorescence was caused by a decrease in $\Delta\Psi_m$ or rather on the bleaching caused by oxyradicals. Indeed, upon photoirradiation, the MitoTracker dyes are reported to cause mitochondrial depolarisation, through induction of the PTP (Scorrano *et al*, 1999; Minimikawa *et al*, 1999).

The distribution of fluorescent cationic probe across the inner mitochondrial membrane is determined by the Nernst equation:

$$[C^+]_{matrix} = [C^+]_{cytoplasm} \times 10^{(\Delta\Psi m/61.5)}$$

where $[C^+]_{matrix}$ and $[C^+]_{cytoplasm}$ represent the concentrations of probe in the relevant cellular compartments. However, given that the probe is freely permeant across lipid bilayers, and must cross the neuronal plasma membrane in order to load into the mitochondrial matrix, the accumulation of the probe into the neuronal cytoplasm and into the mitochondrial matrix will each be governed by the plasma membrane potential, $\Delta\Psi_p$.

$$[C^+]_{cytoplasm} = [C^+]_{out} \times 10^{(\Delta\Psi p/61.5)}$$

$$[C^+]_{matrix} = [C^+]_{out} \times 10^{[(\Delta\Psi m - \Delta\Psi p)/61.5]}$$

(Nicholls and Ward, 2000). It follows that owing to the driving forces of $\Delta\Psi_m$ and $\Delta\Psi_p$, probes are accumulated within the mitochondrial matrix at a concentration four orders of magnitude greater than that of the extracellular milieu (Bernardi et al, 1999). However, it also follows that any redistribution of cationic probe in response to an experimental agent (e.g. NMDA) cannot

be safely attributed to the depolarisation of $\Delta\Psi_m$ if that experimental agent also depolarizes $\Delta\Psi_p$.

If potentiometric probes are considered to be present in one of 3 compartments (mitochondrial matrix, cytoplasm or extracellular space) dependent on $\Delta\Psi_p$ and $\Delta\Psi_m$, it is possible to predict cellular fluorescence changes following the addition of agents that alter either $\Delta\Psi_p$ or $\Delta\Psi_m$ or both. Following the addition of any agent that depolarises both $\Delta\Psi_m$ and $\Delta\Psi_p$, the probe that is quenched in mitochondria would be expected to redistribute to the cytoplasm very rapidly due to the high membrane permeability of the probe and the high surface-to-volume ratio of the inner membrane matrix, to increase the cytoplasmic signal and cause an increase in overall cellular fluorescence.. Consequent to the depolarisation of $\Delta\Psi_p$, the probe would then be expected to slowly efflux across the plasma membrane, causing further depletion of the matrix pool and causing the slow fade of cellular fluorescence (Nicholls and Ward, 2000). The re-equilibration of probe across the plasma membrane is dependent on the size of the cell being studied. For example, cerebellar granule cells (CGCs) are relatively small cells, so have a large surface area to volume ratio. The repartitioning of TMRM from the cytoplasm of CGCs to the extracellular milieu following the addition of glutamate is particularly rapid. In terms of neuronal fluorescence changes, this is observed as a small initial fluorescence increase upon mitochondrial depolarisation, followed by a pronounced decrease as probe is quickly lost to the extracellular space after dequenching (Nicholls and Ward, 2000).

In choosing a loading concentration of TMRE for our experiments, we were mindful that TMRE carries a positive charge, so an excessively high loading concentration could theoretically cause mitochondrial depolarisation ahead of any neurotoxic experimental intervention (Nicholls, personal communication).To find an experimentally workable loading concentration of TMRE for our experiments, cultured hippocampal neurons were loaded with increasing concentrations of TMRE, and the mitochondria

experimentally depolarised with 1μM FCCP. The resulting fluorescence changes are shown in Figures **2.1** and **2.2**.

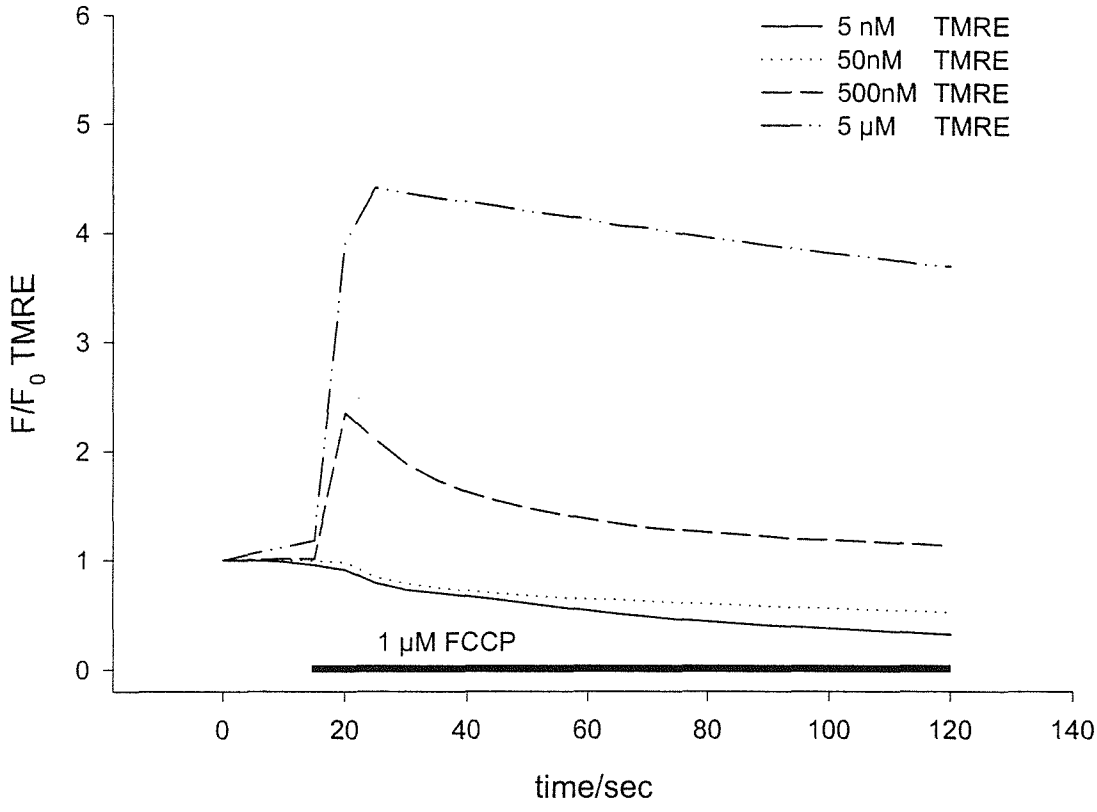

Figure 2.1 Change in neuronal fluorescence elicited by the addition of 1μM FCCP to cultured hippocampal neurons loaded with different concentrations of TMRE. It is evident that the neuronal fluorescence change following FCCP induced mitochondrial depolarisation is highly dependent upon the concentration of TMRE used to load the cells.

Neurons at each loading concentration changed their *pattern* of TMRE fluorescence upon the addition of FCCP, from punctate staining to diffuse fluorescence, reflecting the release of TMRE from mitochondria (see Fig. **2.2**). However, this dye redistribution only caused *increased overall neuronal fluorescence* at loading concentrations of 500nM or greater. This suggests that mitochondrial quenching of TMRE only occurred at loading concentrations of 500nM or greater. All subsequent TMRE experiments were therefore carried out at a loading concentration of 5μM TMRE, to ensure the greatest possible fluorescence change upon mitochondrial depolarization and

dequenching of dye. During confocal imaging, laser exposure was limited to 25 scans per neuronal sample to minimise photodamage.

2.8 Image analysis and statistical analysis

Images were analysed using NIH Image, an image analysis program written by NIH researchers and modified for PCs by Scion Ltd. A customised macro allowed Biorad files to be imported and manipulated. Regions of interest (ROI) within image frames were identified, and the total pixel value of a particular ROI was calculated for a stack of images, allowing fluorescence changes in specific neurons to be followed over time. Pixel values ranged from 0 (black) to 255 (white) on a grey scale. Pixel data was exported from Scion Image directly into the graphical package Sigma Plot, where timecourses of fluorescence changes could be plotted.

All colour images represent raw fluorescence data and have not been ratioed.

Data are given as means ± SEM. For statistical comparison, the student's *t*-test was used. *P* values smaller than 0.05 were considered to be statistically significant.

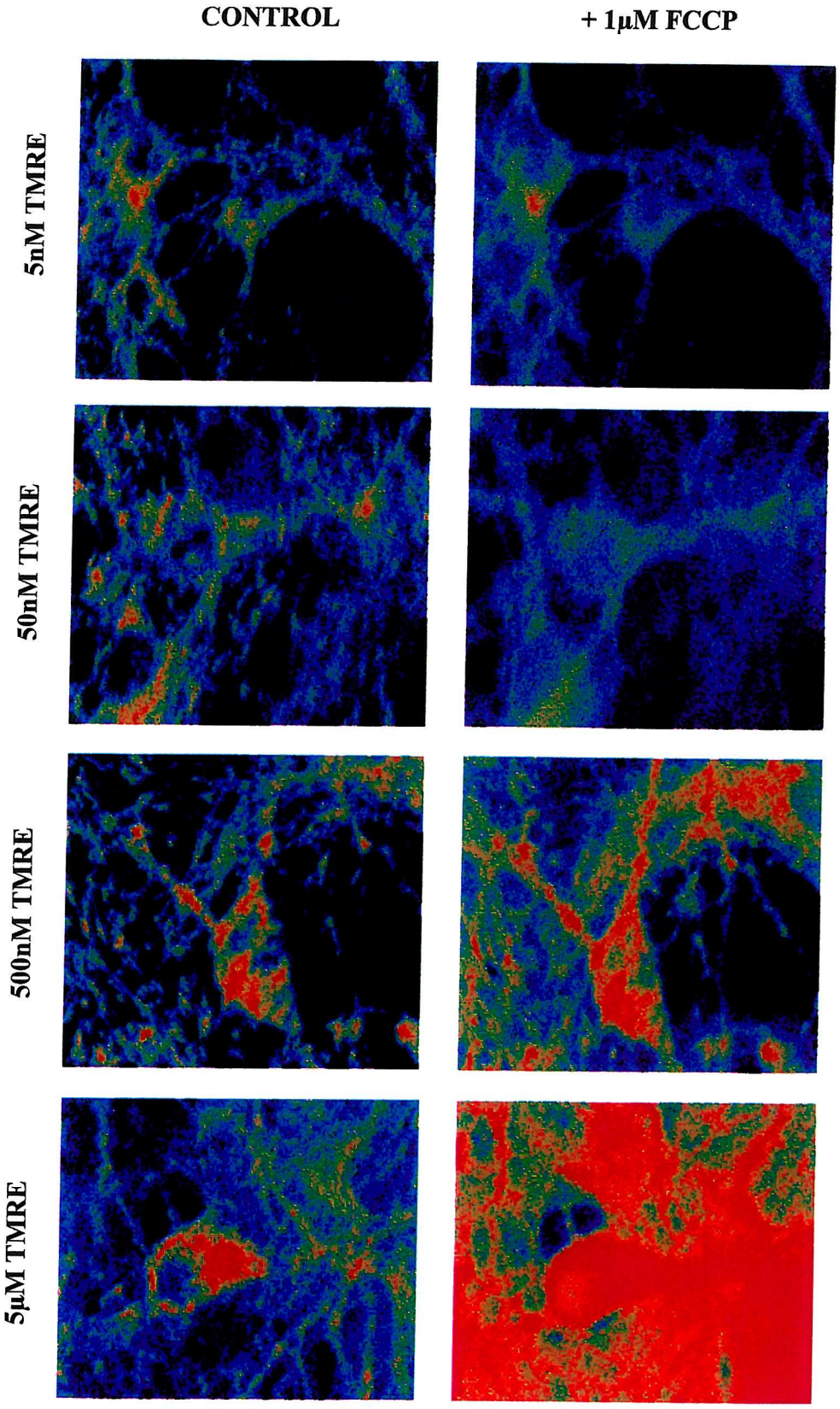

Figure 2.2 Confocal images showing fluorescence in cultured hippocampal neurons loaded with 5nM, 50nM, 500nM and 5μM TMRE, before (LHS) and following (RHS) the addition of 1μM FCCP.

Chapter 3

NEUROTOXICITY OF EAAS IN MOUSE HIPPOCAMPAL NEURONS

CHAPTER 3 NEUROTOXICITY OF EAAS IN HIPPOCAMPAL NEURONS

3.1 Introduction

The neurotoxicity of glutamate and related endogenous excitatory amino acids (EAAs) is thought to play an important role in the pathogenesis of hypoxic/ischemic and traumatic brain injury. The onset of hypoxia is followed by a run-down in neuronal ATP levels and neuronal depolarization. This causes the release of glutamate from presynaptic terminals, whilst cellular EAA uptake mechanisms are inactivated by energy depletion (Choi, 1988). This combination of synaptic release and impaired uptake leads to a massive build up of glutamate in the extracellular space. The primary lesions of traumatic brain injury (TBI) are, by definition, physical, but an increase in glutamate release has been observed in experimental TBI (Faden *et al*, 1989). The mechanisms by which exposure to glutamate and other EAAs can produce neuronal cell injury are not fully understood, but extracellular Ca^{2+} and Na^{+} have been implicated by numerous studies. More than 20 years ago, it was postulated that the toxicity of glutamate was a direct consequence of its interaction with the receptors that mediated its excitatory effect on neurons, and this phenomenon was christened "excitotoxicity" (Olney, 1978). In excitotoxicity, elevated levels of extracellular glutamate cause persistent depolarisation of the neuron and trigger a cascade of events leading to neuronal death. Ischemic damage can be modelled *in vitro* by the addition of toxic doses of glutamate or other EAAs to cultured neurons. Cultured hippocampal neurons showed irreversible toxic swelling upon 30 minute exposure to EAAs, which was blocked by the replacement of extracellular sodium with an impermeant cation (Rothman, 1985). Similarly, the removal of Ca^{2+} from the extracellular milieu prevented the neurotoxicity of glutamate (Choi, 1985). The excitotoxic cascade is now known to include events depending on sodium influx and events depending on Ca^{2+} influx. Elevated levels of glutamate cause prolonged neuronal depolarisation primarily by

activation of AMPA receptors and subsequently by the activation of voltage-dependent sodium channels. The entry of Na^+ ions is followed by a passive entry of Cl^- to maintain ionic equilibrium, then by entry of water following the osmotic gradient. Sustained osmotic swelling can lead ultimately to neuronal lysis. It is therefore probable that sodium is responsible for early necrotic events in excitotoxicity (Doble, 1999). Ca^{2+} entry into neurons is thought to be vital for delayed neurodegeneration. Glutamate could produce a toxic Ca^{2+} influx into neurons by four routes: first, through the Ca^{2+} - permeable NMDA receptor; second, through voltage-dependent Ca^{2+} channels, activated by the glutamate-induced membrane depolarization; third, via the membrane Na^+/Ca^{2+} exchanger which may operate in reverse when cytosolic Na^+ levels are elevated; and finally, via non-specific membrane leak associated with osmotic swelling (Choi, 1988). Unregulated Ca^{2+} entry can trigger a number of highly damaging intracellular cascades (section **1.2.1**). Further studies of excitotoxicity using cell culture models have implicated the NMDA receptor as a critical component of excitotoxic damage. In most cell culture models, antagonists of the NMDA receptor can block the excitotoxic effects of glutamate (Olney, 1987). However, it is unlikely that all the damage inflicted by glutamate is mediated by the NMDA receptor, since protection against glutamate neurotoxicity by AMPA/kainate receptor antagonists has been described in a number of systems (Prehn *et al*, 1995). It is highly unlikely that the same mechanism of neurotoxicity operates in all instances of excitotoxic and/or traumatic brain injury, especially given the complex structure of the brain and the variety of circumstances under which episodes of brain injury may occur. This is further complicated by the number of different tissue systems and conditions used to model brain injury. However, the mechanisms of neuronal death following TBI have several key features in common with the mechanisms known to occur in excitotoxic neuronal injury. For example, TBI is followed by neuronal Ca^{2+} elevations, which could occur due to the neuronal membrane becoming leaky or by ion channels becoming activated when exposed to physical shear stress (McIntosh *et al*, 1998). Furthermore, elevations in extracellular glutamate have been observed after TBI (Palmer, 1994). Therefore, similar neuronal

mechanisms could be in operation in both excitotoxic and traumatic brain injury.

In this study, mechanisms of excitotoxicity were investigated in acutely dissociated hippocampal neurons, and in cultured hippocampal neurons. Acutely dissociated hippocampal neurons provide a good model of neuronal trauma, given the considerable enzymatic and mechanical stress imposed by the dissociation procedure. Ionic and pharmacological manipulations during the isolation process can give an insight into possible routes of neuronal damage. Specifically, we sought to investigate whether the following factors would increase the yield of dissociated hippocampal neurons:

- reduction in neuronal excitability, by use of a reduced Na^+ buffer
- non-selective blockade of VDCCs with Cd^{2+}
- selective blockade of L-type Ca^{2+} channels with nimodipine
- non-competitive antagonism of NMDA receptors with MK801

Hippocampal neurons in culture allow a more direct examination of the long-term effects of glutamate receptor agonists on healthy, viable cells. We sought to distinguish which of the glutamate receptor subtypes are primarily involved in mediating neurotoxicity by exposing cultured hippocampal neurons to different glutamate receptor agonists (NMDA, kainate, AMPA and ACPD). We also examined the effect of mitochondrial disruption on neuronal viability, by exposing cultured neurons to different doses of the mitochondrial uncoupler FCCP. In addition, neurons were exposed to NMDA for increasing time periods to examine the time profile of NMDA toxicity. Finally, we investigated the putative neuroprotection afforded by MK801 against NMDA toxicity in cultured hippocampal neurons.

3.2 Methods

Acutely dissociated hippocampal neurons

Neurons were acutely isolated from the hippocampi of adult (18-21 day) MF1 mice as previously described (section **2.2**). A 1ml aliquot of dissociated neurons in suspension was placed in a perspex chamber on the stage of an inverted Nikon microscope fitted with a x10 objective. The number of viable neurons (phase bright neurons with well-defined, rounded somata and dendrites) in a defined field of view was counted, and the average of 5 randomly-selected fields of view taken per chamber. Each experimental treatment was repeated in at least 5 separate animals.

Cultured hippocampal neurons

Cultured hippocampal neurons were prepared as previously described (section **2.3**). All experiments were conducted at room temperature. Cultured cells were positively identified as neurons by staining with NeuN antibody, which is reactive against neuronal nuclear protein (section **2.6**). In the neurotoxicity experiments, neurons were exposed to EAAs for controlled time periods, then allowed a 24-hour recovery time in fresh culture medium. Neuronal viability was assessed by counting the number of viable neurons (defined as being phase bright with dendrites) in a defined field of view at x40 magnification, using an inverted Nikon microscope. The average of 5 randomly selected fields of view was taken for each coverslip of neurons. . Each treatment was repeated in at least 3 separate cultures. Each treatment group was compared to age-matched controls (untreated) in which cell counts were taken as 100%. In the neuroprotection experiments, neurons were exposed to the protective agent for at least 30 minutes prior to insult, then left for a 24-hour recovery period post-insult in fresh culture medium supplemented with the protective agent. Each treatment was repeated in at least 3 separate cultures. In the imaging experiments, neurons were loaded with 10μM Fluo-3 AM then imaged using CLSM, as previously described

(sections **2.3.2** and **2.5**). For drug application in the imaging experiments, 100µl of drug at x10 concentration was applied by pipette directly to the imaging chamber (volume 1 ml) to give the correct final concentration of drug.

3.3 Results

3.3.1 Effect of altered ionic and pharmacological conditions on yield of acutely dissociated hippocampal neurons

To examine potential routes of neuronal damage during the dissociation of hippocampal neurons, the composition of ACSF used in the isolation process was altered, and the effect on cell yield examined. ACSF was modified in four different ways, firstly, with NaCl substitued by equimolar sucrose; secondly with 100μM Cd^{2+}, a non-selective blocker of VDCCs; thirdly with 100μM nimodipine, a selective antagonist of L-type Ca^{2+} channels; and finally with 100μM MK801, a potent non-competitive antagonist at NMDA receptors. Figure **3.1** shows that the yield of hippocampal neurons was very highly significantly increased by each experimental manipulation, compared to control yields in experiments using standard ACSF. Figures **3.2** shows the typical appearance of acutely dissociated hippocampal neurons, including both viable and non-viable neurons.

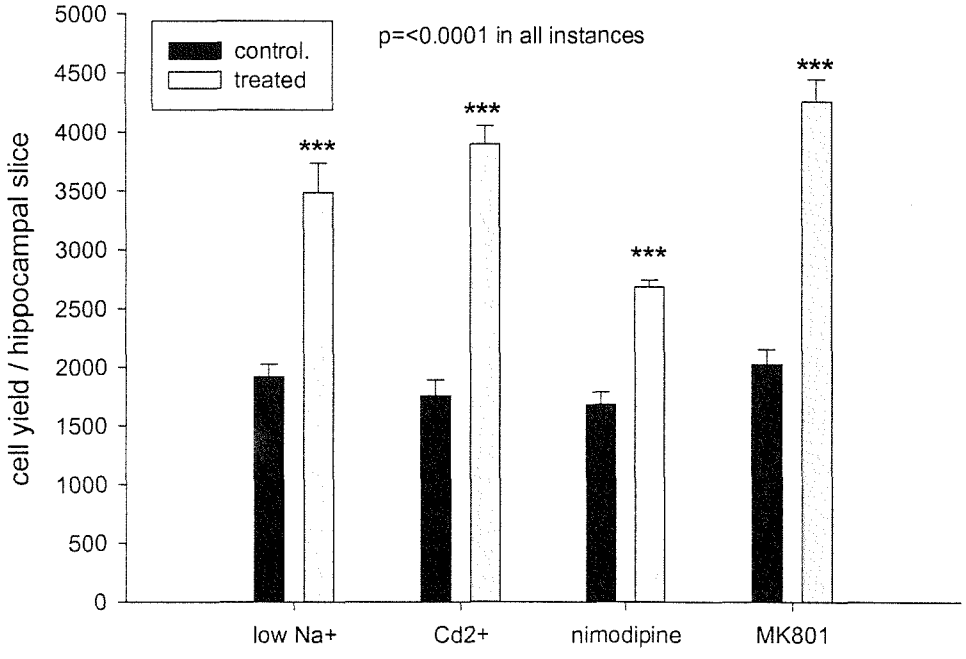

Figure 3.1 Yield of hippocampal neurons with altered ACSF composition. Cell yield was very significantly increased by the removal of NaCl, and by the addition of 100μM Cd^{2+}, 100μM nimodipine or 100μM MK801, compared to control yields with standard ACSF. All experiments were repeated at least 5 times in a minimum of 3 separate animals.

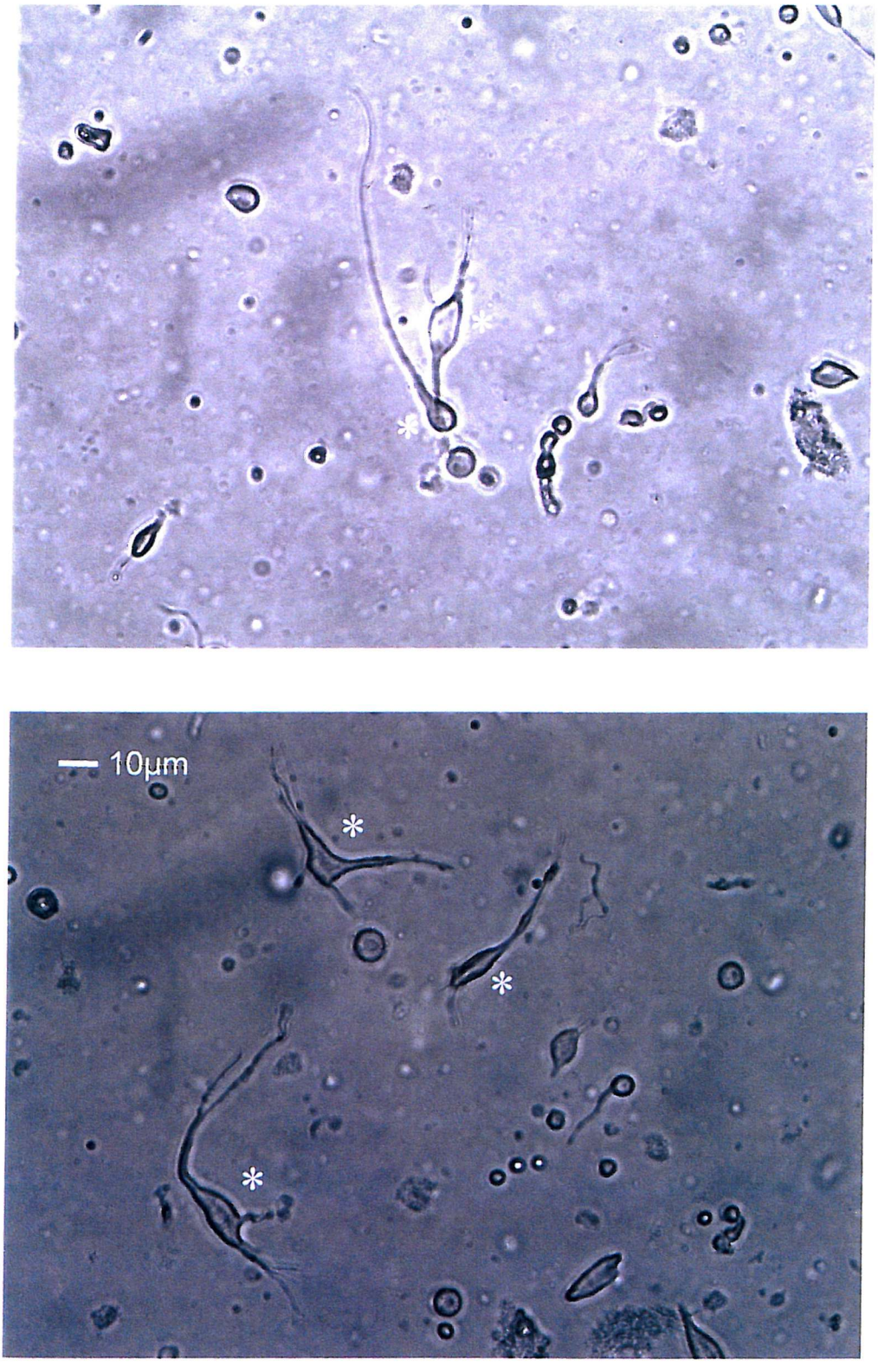

Figure 3.2 Acutely dissociated hippocampal neurons from adult (18-21 day) MF1 mice. Included in the field of view are neurons with well-defined somata and dendrites that were counted as viable (indicated by white asterisks). Neurons that were rounded or had no visible dendrites were not counted as viable.

3.3.2 NeuN staining in cultured hippocampal neurons

Cultured hippocampal cells were validated for experimental use by staining with NeuN antibody, which is reactive against neuronal nuclear protein. **Fig. 3.3** shows the pattern of NeuN staining in cultured hippocampal cells. Many of the cells that have characteristic neuronal morphology are also labelled with NeuN (dark staining), confirming the identity of these cells as neurons. The cultures are prepared from whole slices of hippocampus, so a mixed cell population is inevitable. However, this staining procedure confirmed that the types of cells monitored experimentally are indeed neurons, rather than glia or other non-neuronal cell types.

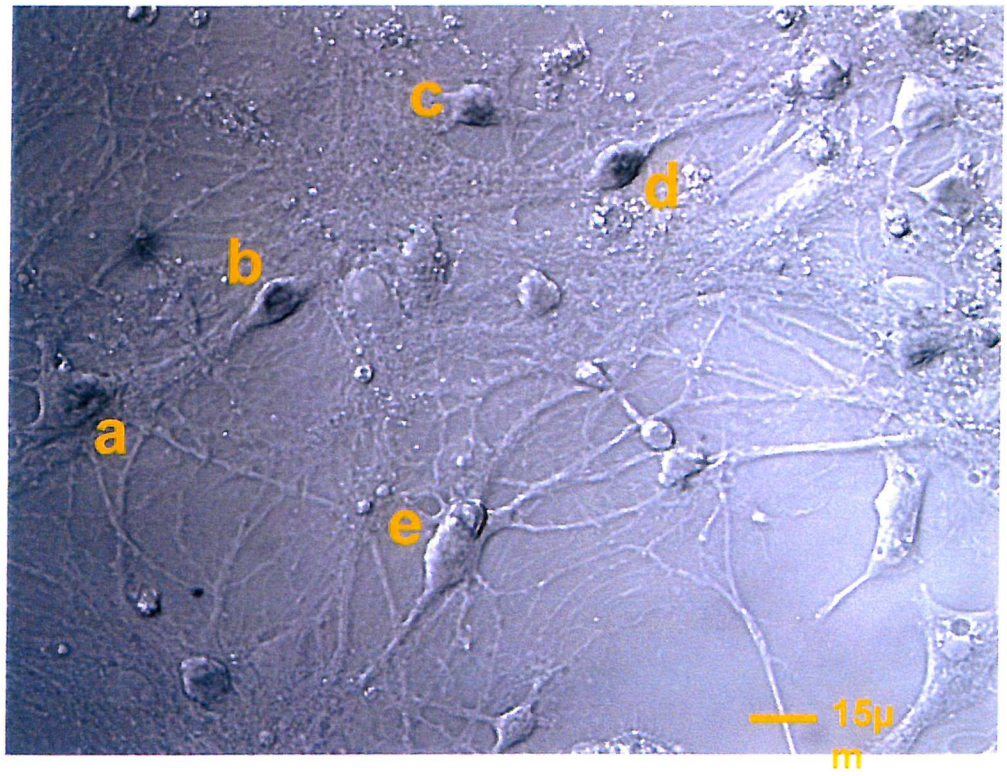

Fig. 3.3 Light transmission image of NeuN antibody staining in cultured hippocampal neurons (dark staining). Neurons (a), (b), (c), and (d) are strongly labelled with NeuN. Cell (e), however, is not stained whilst having typical neuronal morphology.

3.3.3 Viability of cultured hippocampal neurons following exposure to EAAs and FCCP

Doses of EAAs were chosen to elicit an equivalent initial increase in neuronal $[Ca^{2+}]_i$ as monitored by Fluo-3 AM (initial increase being the peak fluorescence increase within 20 seconds of drug addition, see Figure **4.49**. Equivalent initial increases in neuronal Fluo-3 fluorescence were not significantly different when compared with the students t-test). To assess the impact of EAAs on neuronal viability, the number of healthy neurons (phase bright with dendrites) in a defined field of view was counted in both control and treated cultures. The viability of neurons was confirmed by neuronal loading with Fluo-3 AM (Figure **3.4**), a process that requires the activity of intracellular esterases. Figures **3.5** and **3.6** show striking morphological differences between healthy, untreated cultured hippocampal neurons, and neurons following 24 hour exposure to 500μm NMDA. The viability of cultured hippocampal neurons was very highly significantly reduced by 24-hour exposure to 500μM NMDA, which killed over 80% of neurons (Figure **3.7**). 100μM AMPA reduced neuronal viability by over 70%, and 10μM FCCP reduced neuronal viability by over 90%. In contrast, 24 hour exposure to 1μM FCCP reduced neuronal viability by only 35%. 10μM kainate and 100μM ACPD were found to be less neurotoxic, reducing neuronal viability by 14% and 7% respectively (Figure **3.7**).

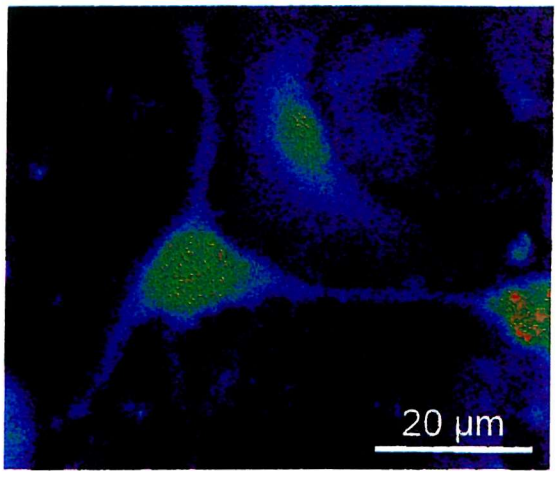

Figure 3.4 Confocal image of pyramidal neuron loaded with Fluo-3 AM, following 24 hour exposure to 500μM NMDA.

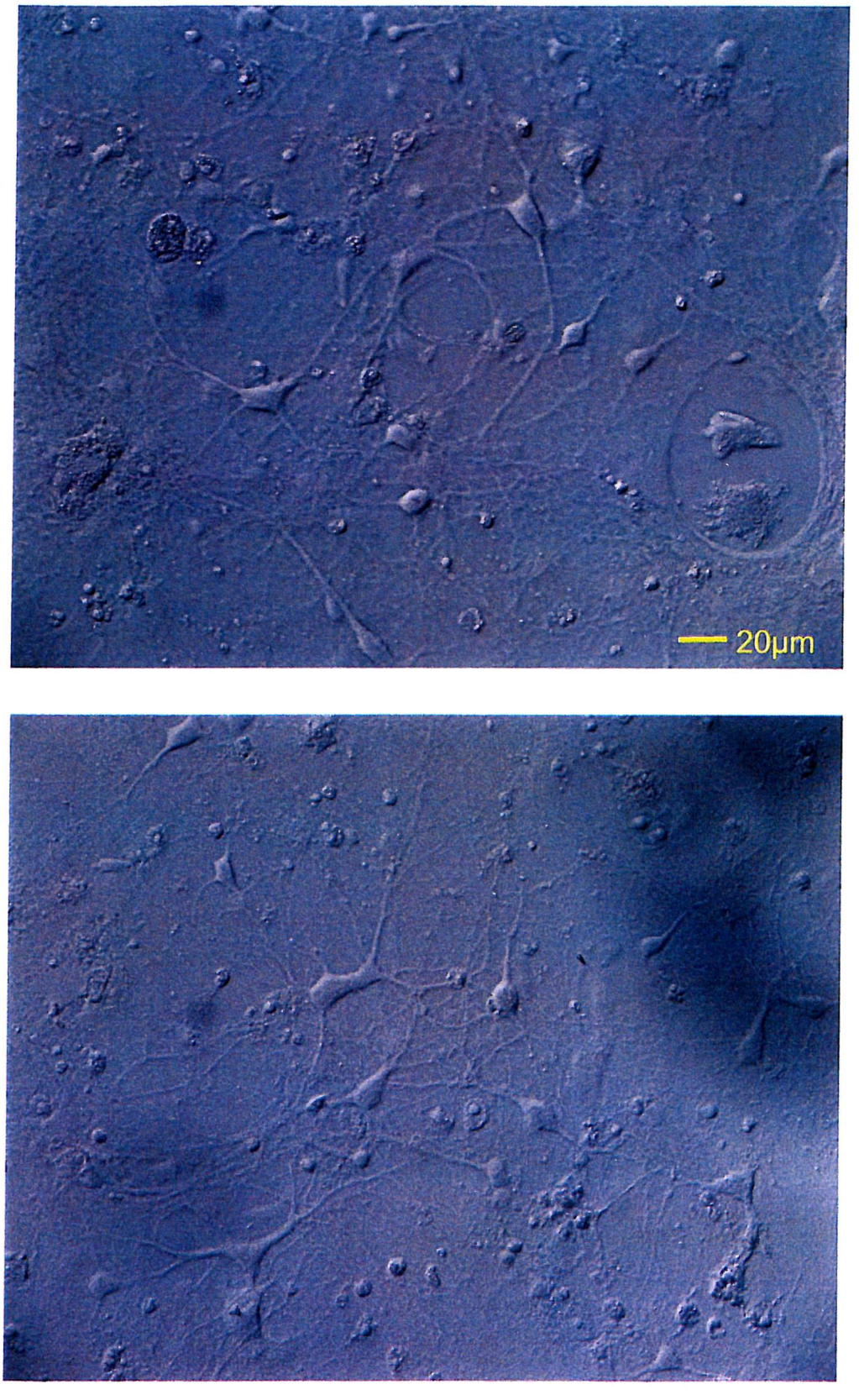

Figure 3.5 Gallery of light transmission images showing untreated cultured hippocampal neurons. Note the well rounded, phase-bright appearance of the neurons, with smooth somata and extensive processes. Magnification: x20.

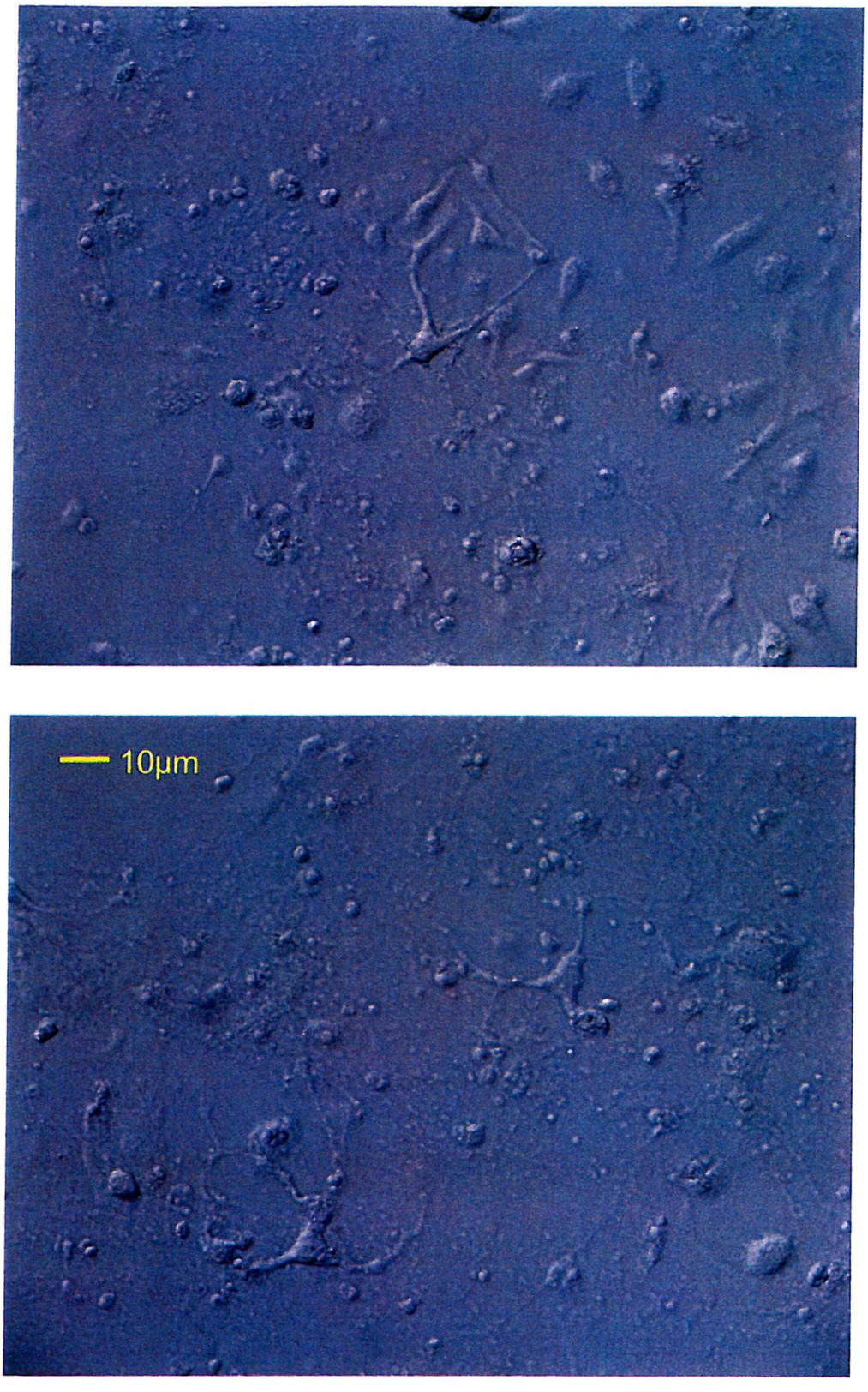

Figure 3.6 Light transmission images showing cultured hippocampal neurons, following 24 hour treatment with 500µM NMDA. Note the extensive cellular debris and markedly reduced cell number. Remaining neurons are granular, shrunken and ragged in appearance. Magnification x20.

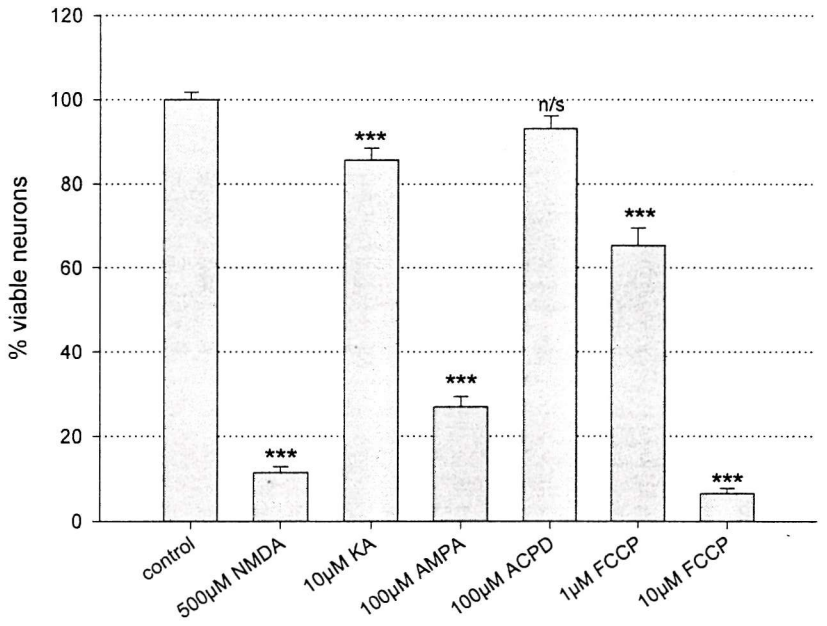

Figure 3.7 Percentage viability of cultured hippocampal neurons in control cultures and in cultures treated for 24 hours with EAAs or FCCP, after a 24-hour recovery period. Each bar represents the average of at least 3 culture plates from each treatment group. Each treatment group was compared to age-matched controls (untreated) in which cell counts were taken as 100%.

3.3.4 Timecourse of NMDA toxicity

Hippocampal neurons were exposed to 500μM NMDA for 15 minutes, 1 hour or 24 hours, and neuronal viability determined for each length of insult. Neuronal viability was very similar regardless of the length of NMDA exposure (Figure **3.8,** overleaf). Preincubation of neurons with 100μM MK801, a potent antagonist of the NMDA receptor, reduced neuronal death very highly significantly, by 35% following a 15-minute NMDA insult (Figure **3.9**). The neuroprotective action of MK801 would indicate that a significant proportion of the toxicity of NMDA is exerted through the activation of NMDA receptors.

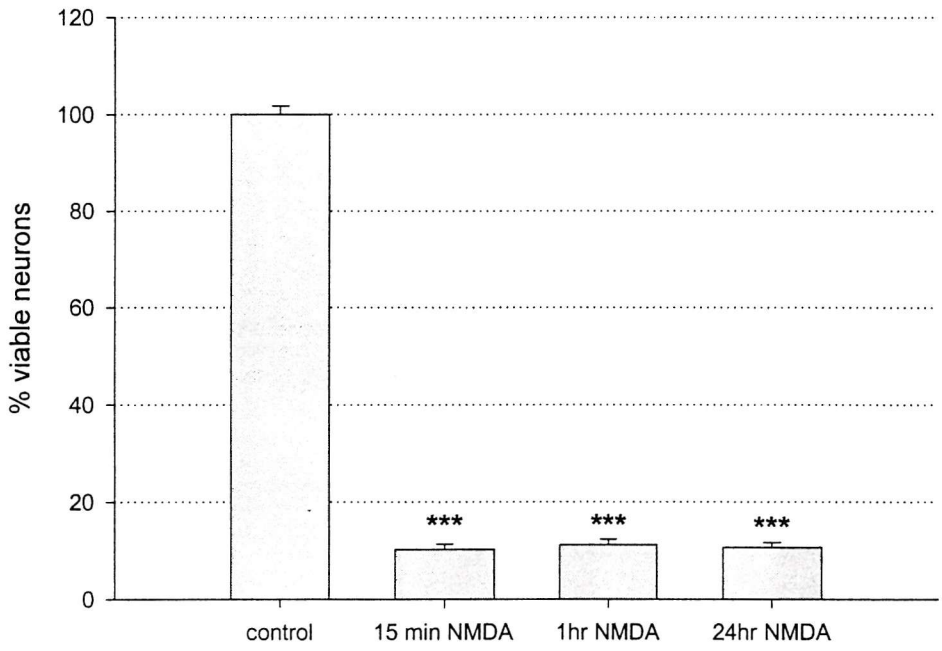

Figure 3.8 Percentage viability of neurons in untreated cultures, and in cultures following exposure to 500μM NMDA for increasing periods of time. Each bar represents the average of at least 3 culture plates from each treatment group.

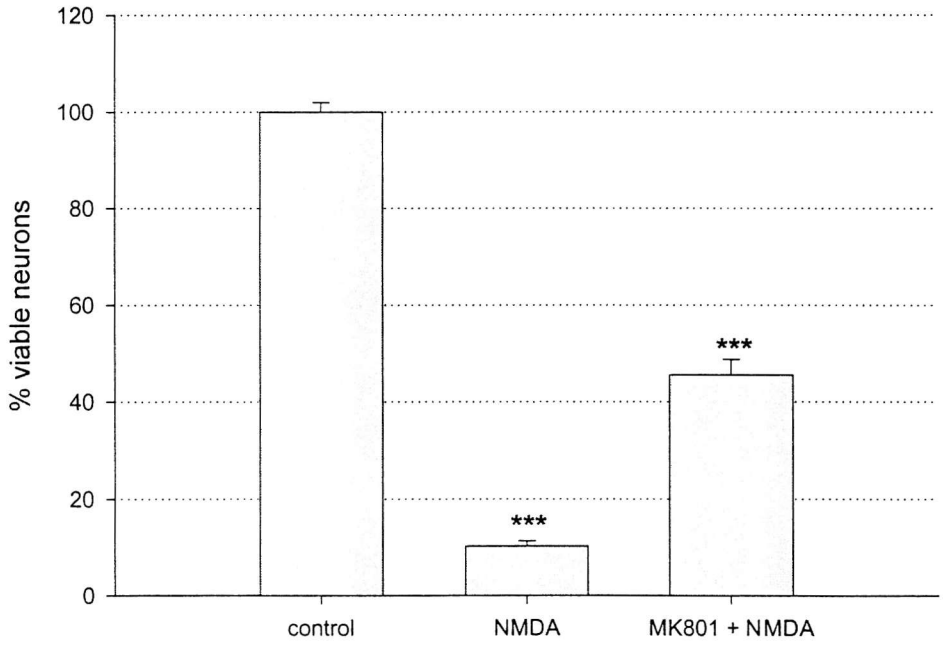

Figure 3.9 Percentage viability of hippocampal neurons in untreated cultures, cultures treated with 500μM NMDA for 15 minutes, and in cultures pretreated with 100μM MK801 and then exposed to NMDA for 15 minutes. Each bar represents the average of at least 3 culture plates from each treatment group.

3.4 Discussion

3.4.1 Effect of altered ionic and pharmacological conditions on yield of acutely dissociated hippocampal neurons

In the first part of the study, we investigated how manipulating the composition of ACSF used in the dissociation procedure may increase the yield of acutely dissociated hippocampal neurons. This gave insights into probable routes of neuronal damage following neuronal trauma. Neurons that are ruptured during the dissociation process are likely to release glutamate into the extracellular milieu, causing the activation of glutamate receptors on the remaining viable neurons. Voltage dependent Ca^{2+}- and Na^{+} channels may also become activated following neuronal depolarisation by glutamate or ATP depletion. The omission of NaCl from ACSF significantly increased cell yield, probably by reducing cell death through osmotic swelling. The excessive entry of sodium and chloride into neurons draws water across the plasma membrane, leading eventually to cell lysis. The damaging effect of sodium in excitotoxicity was demonstrated in a recent study where the use of low sodium buffer greatly reduced the dendritic damage caused by NMDA exposure in cortical cultures (Hasbani *et al*, 1998). The addition of 100μM Cd^{2+}, a non-specific antagonist of VDCCs, and 100μM nimodipine, an antagonist of L-type Ca^{2+} channels, increased neuronal yield very highly significantly (Figure **3.1**). Following neuronal trauma, Ca^{2+} entry through VDCCs may therefore be an important cause of neuronal death. Nimodipine has also been shown to be neuroprotective in a number of models of cerebral ischaemia, both *in vivo* (Bogaert *et al*, 2001; Korenkov *et al*, 2000) and *in vitro* (Greiner *et al*, 2000). In models of traumatic brain injury, calpain antagonists were reported to be protective against post-traumatic cognitive and motor deficits (Saatman et al, 1996), but there is little evidence for protection by Ca^{2+} channel blockers (McIntosh *et al*, 1998).

The addition of 100μM MK801 caused the largest increase in cell yield, suggesting that NMDA receptor activation may be particularly damaging in processes of neurotoxicity. It has been observed that the quantity of $_{45}Ca^{2+}$

taken up through NMDA receptors strongly correlates with the extent of acute cell death in cultured cerebellar granule cells exposed to NMDA (Eimerl and Schramm, 1994). There is long-standing interest in the use of MK801 as a neuroprotective agent. In a model of traumatic brain injury, MK801 significantly attenuated neurological deficits after injury, when administered post-injury and when administered prophylactically (McIntosh *et al*, 1998). MK801 has been observed to significantly reduce neuronal damage in the organotypic hippocampal slice model of cerebral ischaemia (Newell *et al*, 1995; Pringle *et al*, 1997). However, its use in clinical trials as a possible therapy for stroke patients was discontinued because of unacceptable side effects (De Keyser *et al*, 1999). It is likely therefore that MK801 was neuroprotective in our model due to its ability to protect against both excitotoxic and mechanically inflicted damage, possibly by blocking Ca^{2+} influx through the pathologically activated NMDA receptor.

The use of acutely dissociated hippocampal neurons can therefore give some insight into the processes occurring in excitotoxicity and traumatic injury, but the method is rather indirect because so many variables are involved (mechanical trauma, enzymatic damage, glutamate toxicity etc.) We therefore took a more direct approach by adding EAAs to healthy, viable hippocampal neurons in culture.

3.4.2 Viability of cultured hippocampal neurons following exposure to EAAs

The viability of cultured hippocampal neurons was measured, following 24-hour treatment with a range of different glutamate receptor agonists. The doses of glutamate receptor agonist used were identical to those used in Chapter 4. Doses of glutamate receptor agonist were chosen to elicit a similar initial increase in neuronal $[Ca^{2+}]_i$ as monitored by Fluo-3 AM (initial increase being the peak fluorescence increase within 20 seconds of drug addition, see Figure **4.49**). Despite causing "equivalent" initial increases in neuronal $[Ca^{2+}]_i$ (initial increases in neuronal Fluo-3 fluorescence caused by each drug were not significantly different when compared with the students t-

test) each EAA had a profoundly different effect on neuronal survival, with the order of neurotoxicity being NMDA>AMPA>KA>ACPD (Figure **3.7**). This suggests that the initial neuronal elevation of $[Ca^{2+}]_i$ is not predictive of neuronal death, and points to the activation of NMDA receptors being particularly damaging to neurons. The toxicity of the glutamate receptor agonists used in this study has been observed in a multitude of different neuronal models (Brorson *et al*, 1994; Iihara *et al*, 2001; Ambrosio *et al*, 2000; Frandsen *et al*, 1989; Blaabjerg *et al*, 2001; Schoepp *et al*, 1995). In cultured cortical neurons, NMDA was found to be considerably more neurotoxic than AMPA (Hyrc *et al*, 1997). 24-hour exposure to 1μM FCCP reduced neuronal viability to 65%, meaning that the uncoupling of mitochondrial oxidative phosphorylation was not particularly toxic to cultured hippocampal neurons over a 24-hour period. Viability was reduced to 7% with an increased dose of FCCP (10μM). A 1μM dose of FCCP caused profound mitochondrial depolarisation as measured with TMRE (see **Figs 4.33** and **4.44**), but may not have necessarily depolarised the *entire* neuronal population of mitochondria, such that toxicity was only evident at higher doses of FCCP.

In order to investigate the temporal aspect of NMDA toxicity, neurons were exposed to NMDA for increasing periods of time, and neuronal viability examined after a 24-hour recovery period. The extent of neuronal death was very similar with 15 minute, 1 hour or 24 hour exposure to NMDA (Fig. **3.8**), suggesting that neurotoxic processes were triggered within 15 minutes of NMDA receptor activation. Pretreatment with MK801 was neuroprotective against a 15 minute NMDA insult (Fig. **3.9**), very highly significantly increasing neuronal survival from 10.2% to 45.5% ($p<0.001$). These data confirm that NMDA exerts much of its neurotoxic effect through the activation of NMDA receptors. MK801 is neuroprotective in many paradigms of excitotoxicity, including the exposure of chick retina to NMDA (Olney *et al*, 1987) and the addition of glutamate to rat hippocampal neurons (Michaels and Rothman, 1990).

In summary, two major factors associated with neuronal death were identified:

1. Activation of VDCCs, suggesting that under certain circumstances, neuronal Ca^{2+} influx through voltage-gated Ca^{2+} channelsmay be neurotoxic.
2. Activation of the NMDA receptor. We found that a 15-minute exposure to NMDA was as toxic as a 24-hour exposure. It is therefore likely that neurotoxic processes are triggered within the first 15 minutes of NMDA receptor activation.

Experiments were then conducted to investigate intracellular events downstream of glutamate receptor activation, including neuronal $[Ca^{2+}]_i$ elevations and changes in mitochondrial function that could account for the particular toxicity of NMDA receptor activation.

Chapter 4

INVOLVEMENT OF CHANGES IN $[Ca^{2+}]_I$ AND $\Delta\Psi_M$ IN EAA TOXICITY IN HIPPOCAMPAL NEURONS

CHAPTER 4 INVOLVEMENT OF CHANGES IN $[Ca^{2+}]_I$ AND $\Delta\Psi_M$ IN EAA TOXICITY IN CULTURED HIPPOCAMPAL NEURONS

4.1 Introduction

Many neurodegenerative conditions have been linked with excessive neuronal levels of Ca^{2+}, thought to be the trigger for damaging processes such as protease activation and the production of reactive oxygen species. The exact relationship between Ca^{2+} overload and neurotoxicity remains controversial, and the specific mechanism of Ca^{2+} toxicity is not fully understood. There is convincing evidence that many forms of neurodegeneration are Ca^{2+}-dependent (Choi, 1987). Ca^{2+} influx has been associated with both early neuronal damage, which rapidly follows exposure to EAAs (Randall and Thayer, 1992) and delayed neurotoxicity which occurs many hours after the initial insult (Weiss *et al*, 1990). It has been suggested that toxicity is a direct function of the quantity of Ca^{2+} that enters a cell (Eimerl and Schramm, 1994; Lu *et al*, 1996), following the observation that the quantity of $^{45}Ca^{2+}$ accumulated by cultured neurons following excitotoxic exposure to EAAs can be directly correlated with subsequent neuronal death (Hartley *et al*, 1993). A similar correlation has been made with the use of low affinity Ca^{2+} indicators, showing a strong relationship between the Ca^{2+} load imposed by different EAAs and the extent of neuronal death 24 hours later (Hyrc *et al*, 1997).

Contrary to this, several reports have failed to establish a clear link between Ca^{2+} load and the likelihood of neuronal death after potentially lethal insults (Michaels and Rothman, 1990; Dubinsky and Rothman, 1991). Recent reports have suggested that the main determinant of Ca^{2+} toxicity is not the degree of neuronal Ca^{2+} loading, but rather the route through which Ca^{2+} ions gain access to the neuronal cytoplasm. Neuronal Ca^{2+} increases may be elicited by different routes including the activation of plasma membrane ligand- or voltage-dependent Ca^{2+} channels, or by Ca^{2+} release from intracellular stores (see section 1.1). Tymianski *et al* (1993) conducted a study to address the question of whether an equal rise in $[Ca^{2+}]_i$ mediated

through different receptor pathways would cause equal neurotoxicity. To this end, equivalent measureable Ca^{2+} elevations were elicited in spinal neurons by the addition of high-K^+, kainate, and glutamate. Significantly more neurons died after glutamate treatment, a finding thought to reflect a difference in the mechanism by which Ca^{2+} triggers neurotoxicity, depending on the route of entry. In a further study, the relationship between neuronal $[Ca^{2+}]_i$ elevation and total $^{45}Ca^{2+}$ accumulation following different stimuli was investigated (Sattler *et al*, 1998) This relationship was found to depend on the route of Ca^{2+} entry. In particular, NMDA produced a higher average $[Ca^{2+}]_i$ increase for a given total $^{45}Ca^{2+}$ load as compared with high-K^+, suggesting that Ca^{2+} entering through different pathways is handled by different subcellular compartments.

Calcium entry through the NMDA receptor is thought to be particularly detrimental in processes of neurotoxicity, given the finding that NMDA receptor blockade prevents glutamate toxicity, whilst allowing a Ca^{2+} transient of similar amplitude to be elicited by glutamate in spinal neurons (Tymianski *et al*, 1993). This toxicity is not due to the ability of NMDA receptors to trigger greater initial $[Ca^{2+}]_i$ increases than other pathways, but is linked with some other attribute specifically associated with NMDA-mediated Ca^{2+} influx. This could include a physical colocalization of damaging Ca^{2+} -dependent phenomena with NMDA receptors. It has been suggested that Ca^{2+} influx through NMDA receptors has "privileged" access to mitochondria (Peng and Greenamyre, 1998). The simultaneous measurement of cytosolic and mitochondrial $[Ca^{2+}]$ in striatal neurons challenged with various agonists showed a faster mitochondrial Ca^{2+} uptake in response to an increase in cytosolic Ca^{2+} during NMDA receptor activation than during non-NMDA receptor or voltage-dependent Ca^{2+} channel activation. This fast mitochondrial Ca^{2+} uptake could explain the particular toxicity of Ca^{2+} entry through the NMDA receptor. Mitochondrial Ca^{2+} uptake is known to play a prominent role in buffering the large Ca^{2+} load induced by intense glutamate receptor stimulation (Wang and Thayer, 1996; Peng and Greenamyre, 1998). Mitochondrial Ca^{2+} overload may cause the sustained mitochondrial depolarisation which follows intense NMDA receptor stimulation and closely parallels the incidence of neuronal death

(Schinder *et al*, 1996). Toxic doses of glutamate and kainate have been observed to kill cultured cerebellar granule cells by different mechanisms: glutamate by irreversible mitochondrial depolarisation, and kainate by excessive neuronal swelling leading to rupture of the plasma membrane (Kiedrowski, 1998). It is clear, therefore, that different routes of Ca^{2+} increase may have different toxic consequences for neurons. The temporal profile of neuronal Ca^{2+} increases is another important consideration in processes of neurotoxicity. Neurons challenged with glutamate or NMDA typically show an initial Ca^{2+} spike followed by semi-recovery to an elevated plateau, and an eventual delayed Ca^{2+} deregulation, which invariably predicts cell death (Alano *et al*, 2002; Keelan *et al*, 1999; Nicholls *et al*, 1999; Manev *et al*, 1989; Randall and Thayer, 1992; Tymianski *et al*, 1993).

Given these findings, we sought to investigate changes in cytosolic Ca^{2+} and mitochondrial $\Delta\Psi$ evoked by different glutamate receptor agonists (not solely glutamate or NMDA, which appear to be the focus of much of the literature) in hippocampal neurons, using CLSM. Specifically, we wanted to examine:

1. Neuronal Ca^{2+} handling and mitochondrial energetics in dissociated hippocampal neurons prior to being placed in culture
2. Time profiles of Ca^{2+} changes in cultured hippocampal neurons exposed to agonists of different glutamate receptor subtypes
3. Dose-Ca^{2+} response relationships of cultured hippocampal neurons exposed to agonists of different glutamate receptor subtypes
4. Changes in mitochondrial $\Delta\Psi$ following neuronal exposure to different glutamate receptor agonists
5. A possible correlation between increases in neuronal $[Ca^{2+}]_i$ and changes in neuronal mitochondrial $\Delta\Psi$
6. The mechanism of the kainate-induced increase in $[Ca^{2+}]_i$
7. Putative large, delayed neuronal Ca^{2+} responses to glutamate receptor agonists, measured with a low-affinity Ca^{2+} indicator

4.2 Methods

Acutely dissociated hippocampal neurons

Neurons were acutely isolated from the hippocampi of adult (18-21 day) and neonatal (5-8 day) MF1 mice as previously described (section **2.2**). Neurons were loaded with either Fluo-3 AM or TMRE as described in section **2.4.1**, and imaged as described in section **2.5**.

Cultured hippocampal neurons

Cultured neurons were prepared as described in section **2.3**, loaded with either Fluo-3 AM, TMRE, MitoTracker Green or Fluo-5N AM as described in section **2.4.2** and imaged as described in section **2.5**.

Plotting of fluorescence timecourses

Plots were normalized to baseline, and are shown as F/F_0, where F is the emitted fluorescence at any time and F_0 is the baseline fluorescence of the cell under resting conditions. All average data represent the mean ± standard error.

Confocal Images

Confocal images showing neuronal fluorescence are displayed in psuedocolour using an optimized spectrum (Clarke and Leonard, 1989) to aid visual perception of the magnitude of fluorescence changes. The pseudocolour display has been standardized to show the full fluorescence range from zero pixel values (black), through blue, green, yellow and red to maximum pixel values of 255 (white); see colour bars in Figures **4.2** and **4.6**. From ratiometric experiments, it is known that fluorescence in the blue range corresponds a pixel value of approximately 50, and to resting neuronal Ca^{2+} levels of approximately 100nM.

4.3 Results

4.3.1 Calcium responses and mitochondrial membrane potential measured in acutely dissociated hippocampal neurons, prior to being placed in culture

Calcium responses were examined in dissociated hippocampal neurons prepared from mice aged 18-21 days and loaded with the fluorescent calcium indicator Fluo-3 AM. Fluo-3 is essentially non-fluorescent unless bound to Ca^{2+}, and undergoes an increase in fluorescence of at least 100-fold upon binding Ca^{2+}. Between normal resting cytosolic free Ca^{2+} concentrations and dye saturation, the increase is normally between 5 and 10 fold, making Fluo-3 useful in the measurement of neuronal Ca^{2+} transients (Haugland, 1996).

The addition of 40mM K^+ caused a reversible increase in the Fluo-3 signal in both isolated neurons (**Fig. 4.1**) and neuronal clumps (**Fig. 4.3**). A false colour display is used to aid perception of the magnitude of these changes, as shown in **Figs. 4.2** and **4.4.** The use of Fluo-3 does not allow the measurement of $[Ca^{2+}]$ *per se*, since the dye does not undergo significant shifts in emission or excitation wavelength upon binding to Ca^{2+}, which precludes ratiometric measurements. Comparisons of changes in the relative $[Ca^{2+}]$ can be made, however, as all changes in fluorescence are normalised to resting fluorescence levels prior to drug addition. Neuronal fluorescence was imaged at set time intervals, allowing a time course of neuronal fluorescence change to be constructed (**Figures 4.1** and **4.3**).

The elevation of extracellular K^+ causes the depolarisation of the neuronal plasma membrane, and the activation of voltage-dependent ion channels. The increase in Fluo-3 signal, reflecting increased neuronal $[Ca^{2+}]$, likely corresponds to the influx of calcium through VDCCs. In isolated hippocampal neurons, this Ca^{2+} elevation was particularly marked in the vicinity of the nucleus (**Fig. 4.2**).

In the same preparation, no reproducible changes in Fluo-3 signal were observed following the addition of 1mM glutamate, 100μM kainate or

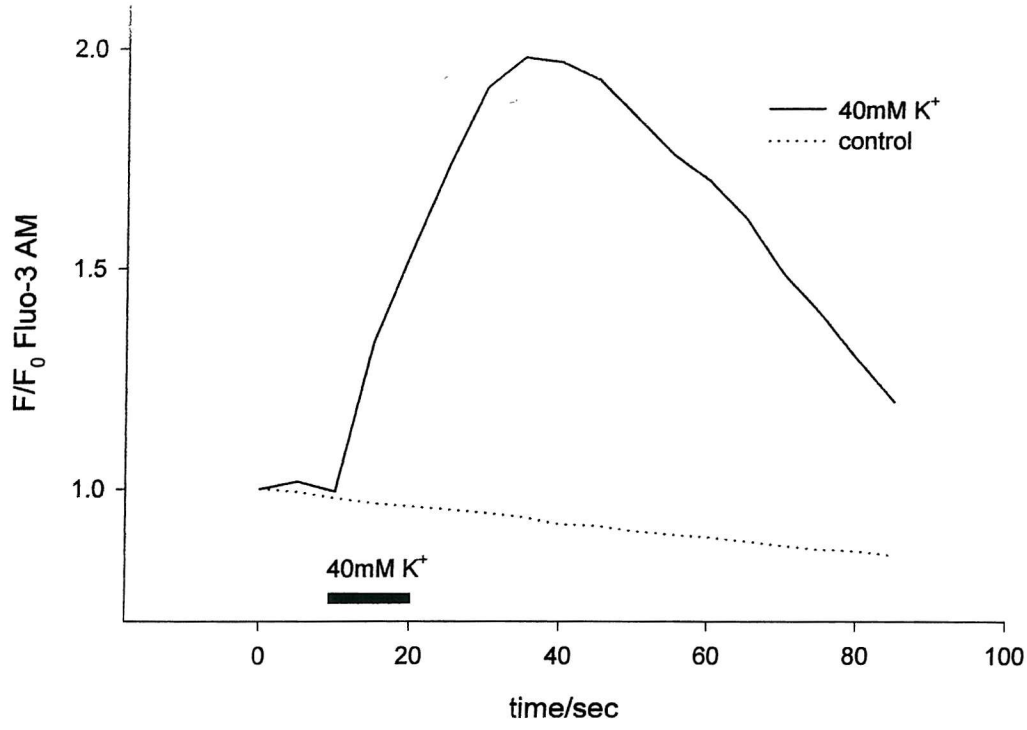

Fig. 4.1. Typical change in neuronal Fluo-3 fluorescence in response to 40mM K^+. The trace shows the reversible calcium response of a single neuron to elevated extracellular K^+. Horizontal bar indicates time and duration of exposure to K^+.

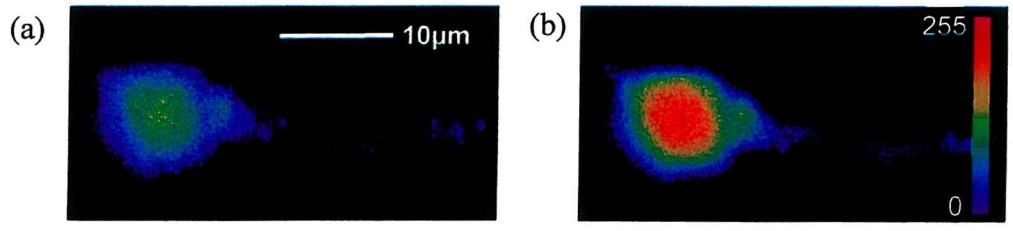

Fig. 4.2 Images selected from a series of confocal images showing Fluo-3 fluorescence in a single neuron acutely isolated from the mouse hippocampus before (a) and after (b) exposure to 40mM K^+. The increase in fluorescence is particularly marked in the vicinity of the nucleus, and reflects increased neuronal calcium levels following the activation of voltage dependent calcium channels by elevated extracellular K^+.

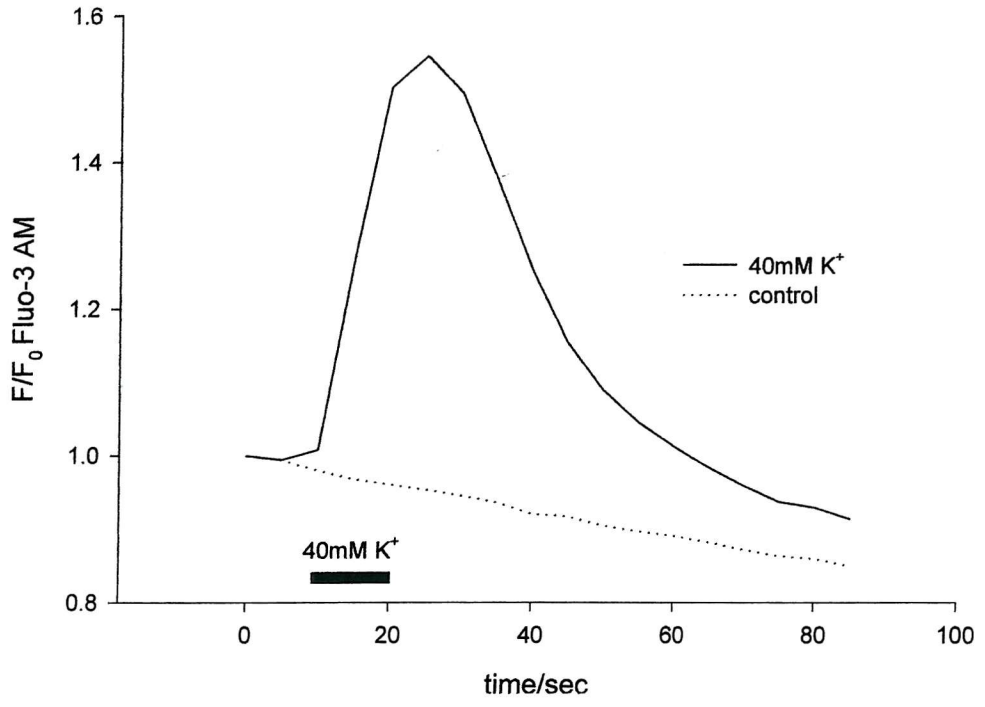

Fig. 4.3 Typical increase in neuronal Fluo-3 fluorescence in response to 40mM K^+. The trace shows the response of an acutely dissociated neuronal clump, and is representative of eleven separate experiments. Horizontal bar indicates time and duration of exposure to K^+.

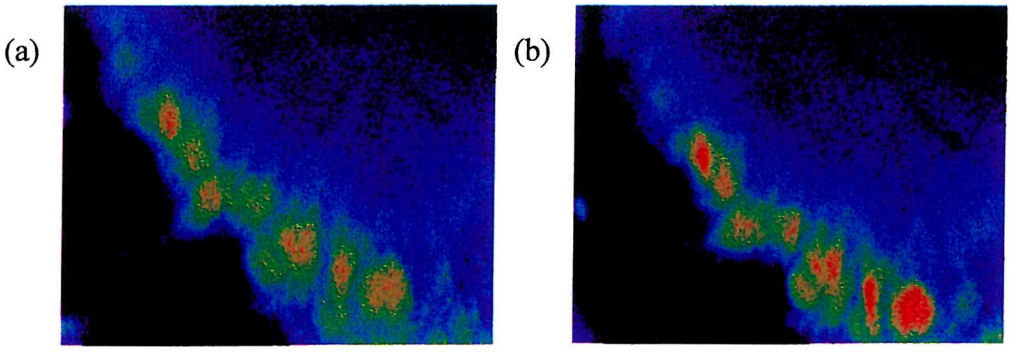

Fig. 4.4 Images selected from a time series of confocal images showing Fluo-3 fluorescence in a neuronal clump acutely isolated from the hippocampus before (a) and after (b) the addition of 40mM K^+. The increase in fluorescence indicates increased $[Ca^{2+}]_i$, likely resulting from calcium influx through voltage dependent calcium channels. Elevated extracellular K^+ depolarises the plasma membrane, causing the activation of VDCCs.

100μM ACPD, glutamate receptor agonists that are reported to increase neuronal calcium levels. It is possible that in the process of dissociation, hippocampal neurons undergo substantial damage to their cell surface receptors as a consequence of exposure to proteases and mechanical damage during the process of trituration. This could render the neurons unable to respond to certain agonists. Additionally, the process of trituration causes the shearing off of the majority of neuronal dendrites. This could therefore limit the investigation of neuronal responses, since a significant proportion of the cell surface receptors are located on the distal parts of the neuron. However, a period of culture allows neurons to re-establish dendrites and to re-insert their usual complement of receptors to the plasma membrane (Mynlieff, 1997; Brewer *et al*, 1993).

In order to ascertain whether neurons had sustained lethal damage during the dissociation procedure, mitochondrial energetics were examined in both neonatal (5-7 day) and adult (18-21 day) dissociated hippocampal neurons. Neurons were loaded with 5μM TMRE, a positively charged derivative of the dye rhodamine. TMRE accumulates in healthy mitochondria as a function of mitochondrial $\Delta\Psi$. When imaged, this is seen as a punctate pattern of neuronal staining (**Fig. 4.6a**). Following mitochondrial depolarisation, the driving force for mitochondrial accumulation of TMRE is lost, and the dye is redistributed into the cytoplasm. Mitochondrial depolarisation can therefore be measured as an increase in the neuronal TMRE signal. Mitochondria were depolarised experimentally by the addition of 1μM FCCP, a protonophore that uncouples oxidative phosphorylation and dissipates mitochondrial $\Delta\Psi$.

The addition of 1μM FCCP caused an increase in TMRE fluorescence in isolated neurons and neuronal clumps prepared from both neonatal and adult mice (**Figs 4.6** and **4.8**). Time courses of increased neuronal TMRE signal following exposure to FCCP are shown in **Fig. 4.5** and **4.7.** These increases in neuronal TMRE fluorescence reflect mitochondrial depolarisation, suggesting that dissociated hippocampal neurons are energetically healthy, with polarised mitochondria. The large "tail-off" in TMRE fluorescence seen in **Figure 4.7** probably represents the repartitioning of TMRE to the

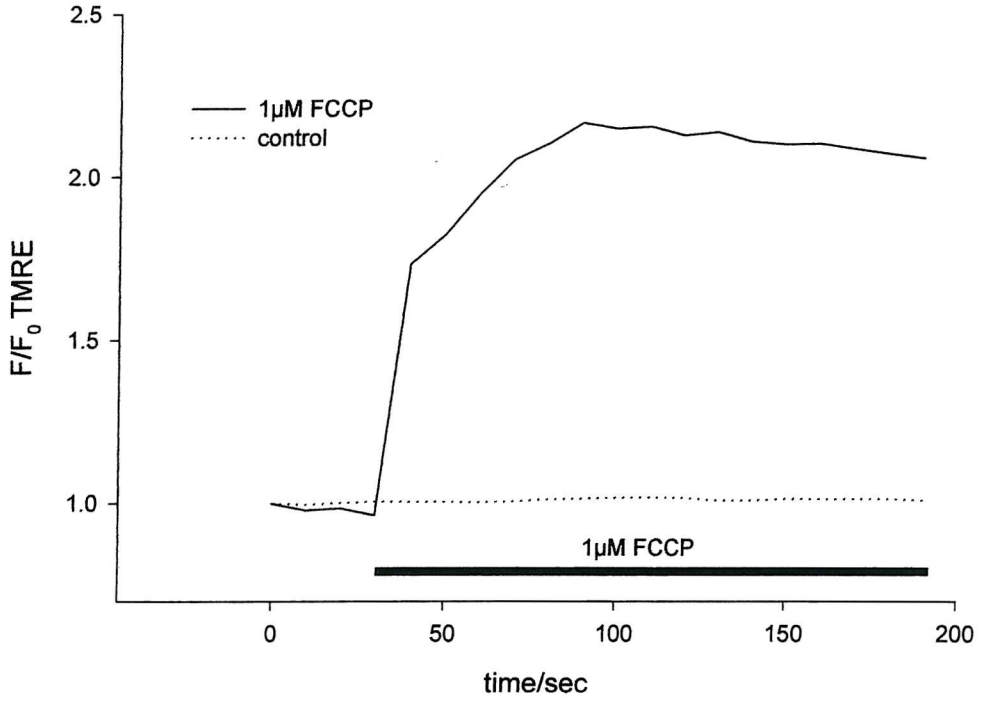

Fig. 4.5 Typical change in neuronal TMRE fluorescence in response to 1μM FCCP. The trace shows the response of a single neuron acutely isolated from the adult (18-21 day) mouse hippocampus. The change in TMRE fluorescence is representative of seven cells monitored in four separate experiments.

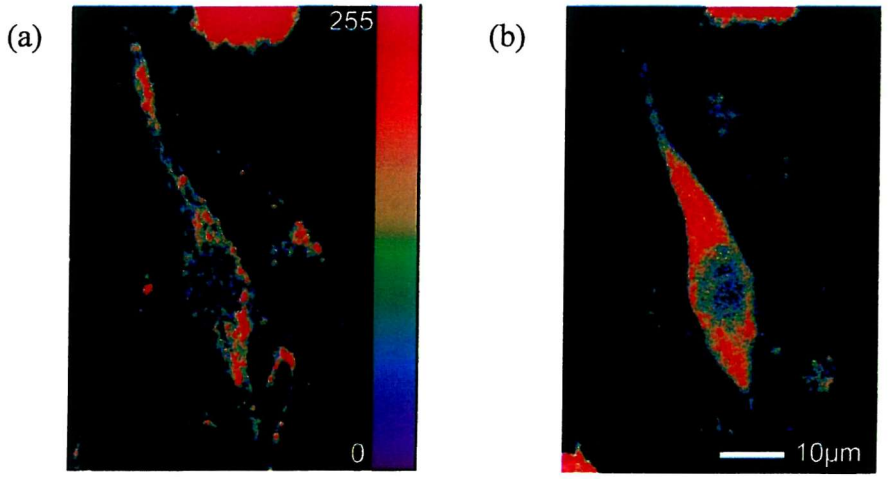

Fig. 4.6 Images selected from a series of confocal images showing TMRE fluorescence in an adult (18-21 day) hippocampal neuron before (a) and after (b) the addition of FCCP. TMRE is sequestered in healthy mitochondria as a function of mitochondrial $\Delta\Psi$, visible as a punctate pattern of staining in the cytosol. FCCP reduces $\Delta\Psi$, causing the redistribution of TMRE into the cytoplasm and a concurrent increase in neuronal fluorescence.

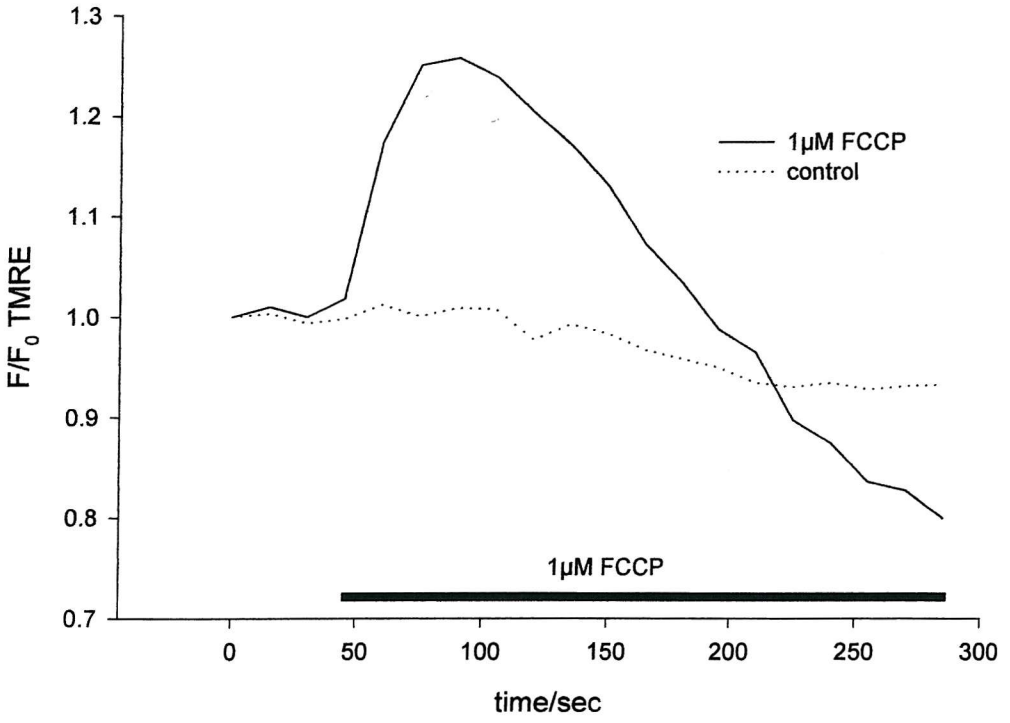

Fig. 4.7 Typical change in neuronal TMRE fluorescence in response to 1μM FCCP. The trace shows the response of a neuronal clump acutely isolated from the neonatal (5-7 day) mouse hippocampus. The increase in TMRE fluorescence is representative of 4 separate experiments. The downwards shift in fluorescence is an experimental artifact, and reflects TMRE leaking out of the neurons.

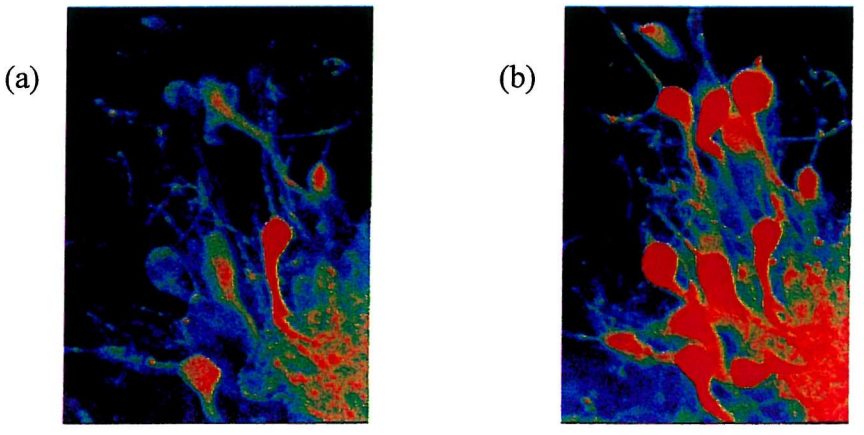

Fig. 4.8 Images selected from a series of confocal images showing TMRE fluorescence in neonatal (5-7 day) mouse hippocampal neurons before (a) and after (b) the addition of FCCP. The sequestration of TMRE in mitochondria is driven by mitochondrial $\Delta\Psi$. FCCP is a protonophore which depolarises mitochondria, causing the redistribution of TMRE from the mitochondrial matrix to the cytoplasm.

extracellular solution following its release to the cytoplasm caused by mitochondrial depolarisation. The maximum neuronal TMRE fluorescence changes elicited by the addition of FCCP are summarised in **Fig. 4.9**.

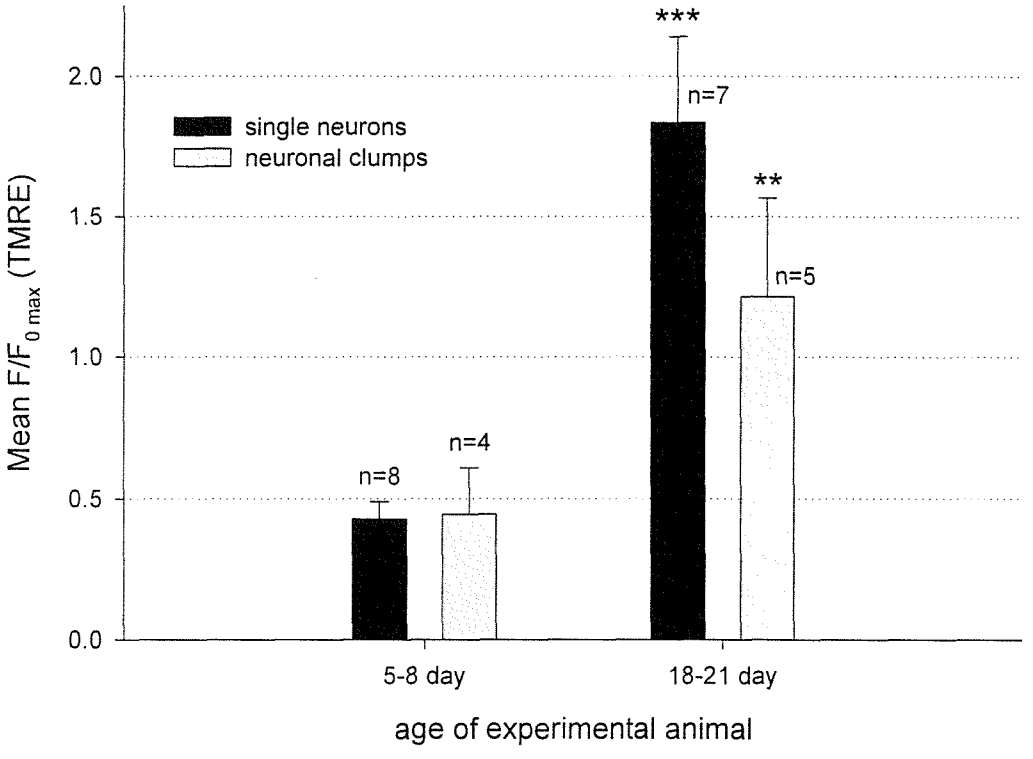

Figure 4.9 Maximal increases in neuronal TMRE fluorescence elicited by the addition of 1μM FCCP to acutely dissociated mouse hippocampal neurons. The increase in TMRE fluorescence was significantly greater in both single neurons and neuronal clumps isolated from the adult (18-21 day) mouse hippocampus, compared to changes in neonatal (5-7 day) mouse neurons (p=0.0003 and 0.017 respectively, determined by the students t-test, significance level set at p=0.05).

There are significant differences in maximal TMRE fluorescence changes between the two different age groups of mice. This could either reflect a resistance of neonatal hippocampal neurons to the toxic effect of FCCP, which is unlikely, or a larger mitochondrial volume in the older neurons, which could sequester and then release a greater amount of TMRE, giving a larger fluorescence shift. Alternatively, there could be age-related differences in the basal level of mitochondrial polarisation.

4.3.2 Dose-dependent calcium responses to excitatory amino acids and plasma membrane depolarisation measured in cultured hippocampal neurons

Initial neuronal calcium responses to different glutamate receptor agonists were measured in cultured hippocampal neurons loaded with the calcium sensitive dye Fluo-3, using CLSM (initial response being the peak fluorescence increase within 20 seconds of drug addition). Calcium responses were measured for no longer than 200 seconds following drug addition. The dose dependency of these responses was examined. Responses to FCCP and 4-AP were also measured as a positive control to show the neuronal response to the experimental alteration of $\Delta\Psi$ and $[Ca^{2+}]_i$ respectively. Exposure of neurons to 4-AP caused a concentration-dependent initial increase in Fluo-3 fluorescence across the range of concentrations investigated (100μM – 2mM) (Fig **4.10**).

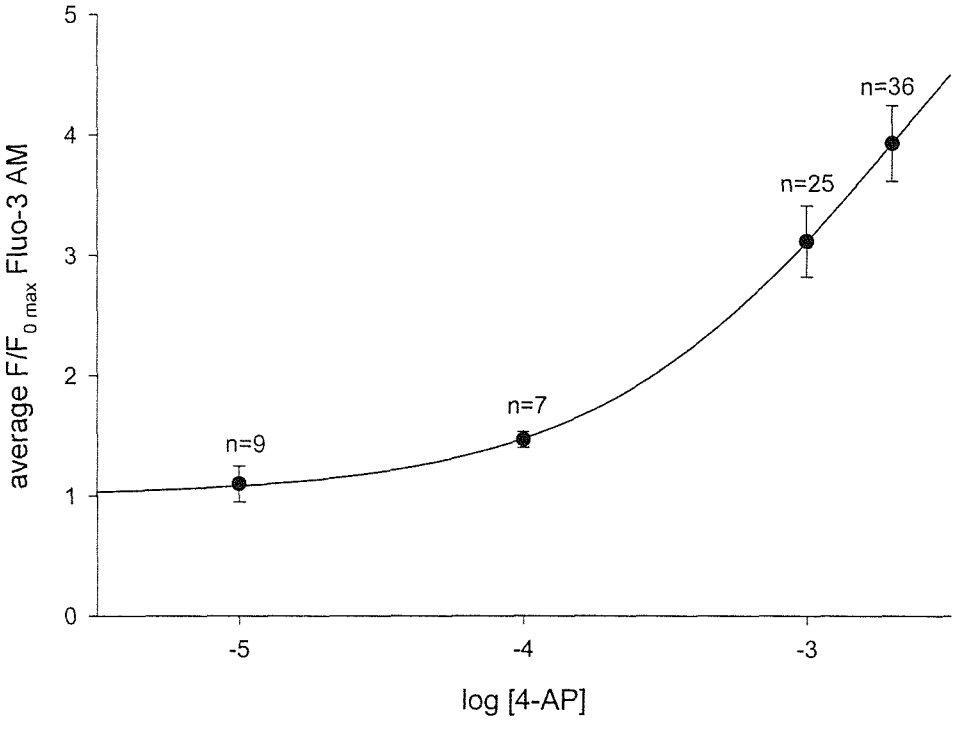

Fig. 4.10 Concentration-response relationship for 4-AP. The neuronal Fluo-3 fluorescent signal is plotted against the concentration of 4-AP to which neurons were exposed for 5 minutes. Data is presented as averages for the fluorescent signal from neuronal soma ± s.e.m. and n values are given for each data point. All experiments were repeated in a minimum of three separate cultures.

Figs. 4.11 and **4.12** show a typical time course of neuronal Fluo-3 fluorescence following exposure to 4-AP, and confocal images of neuronal fluorescence changes.

The addition of 1μM FCCP caused an initial increase in Fluo-3 fluorescence of 2.41 ± 0.46 fluorescence units (FU) (increases normalised to resting fluorescence levels ± SEM). This increase in Fluo-3 signal is indicative of elevated cytoplasmic Ca^{2+}, and may relect Ca^{2+} dumping from depolarised mitochondria (see **Fig 4.13** and **4.14**).

The addition of 1mM glutamate caused a maximal initial increase in neuronal Fluo-3 fluorescence of 1.32 ± 0.18 FU, from 1 to 2.32 FU (see **Figs 4.15** and **4.16**).

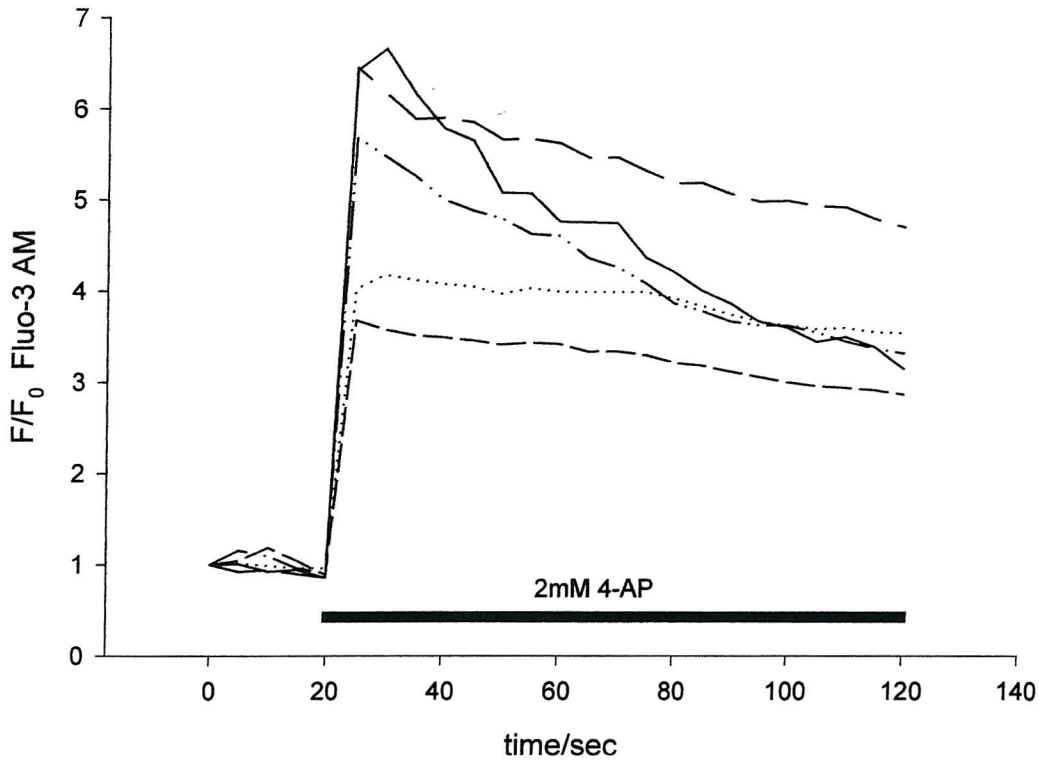

Fig. 4.11 Typical increase in neuronal Fluo-3 fluorescence in response to 2mM 4-AP. The trace shows the response of five neurons in a single coverslip, and is representative of the response of thirty-six cells monitored in eight separate experiments. Horizontal bar indicates time and duration of exposure to 4-AP.

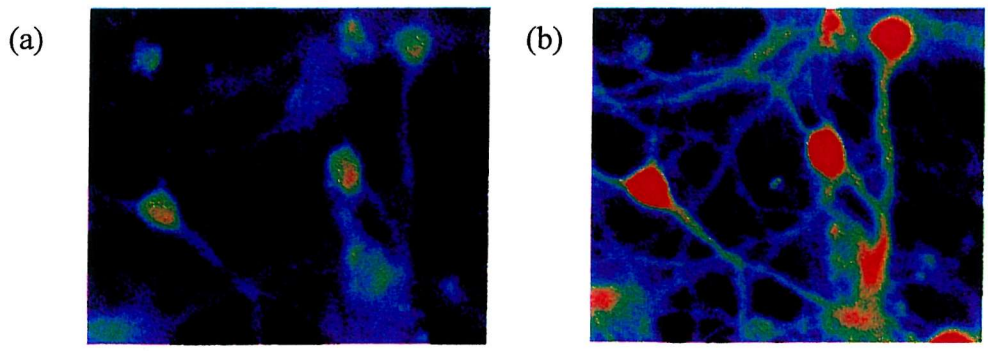

Fig. 4.12 Images selected from a time series of confocal images showing Fluo-3 fluorescence in hippocampal neurons before (a) and after (b) the addition of 4-AP. The increase in fluorescence is indicative of elevated $[Ca^{2+}]_c$ and probably arises from Ca^{2+} influx through VDCCs following the persistent depolarisation of the plasma membrane by 4-AP.

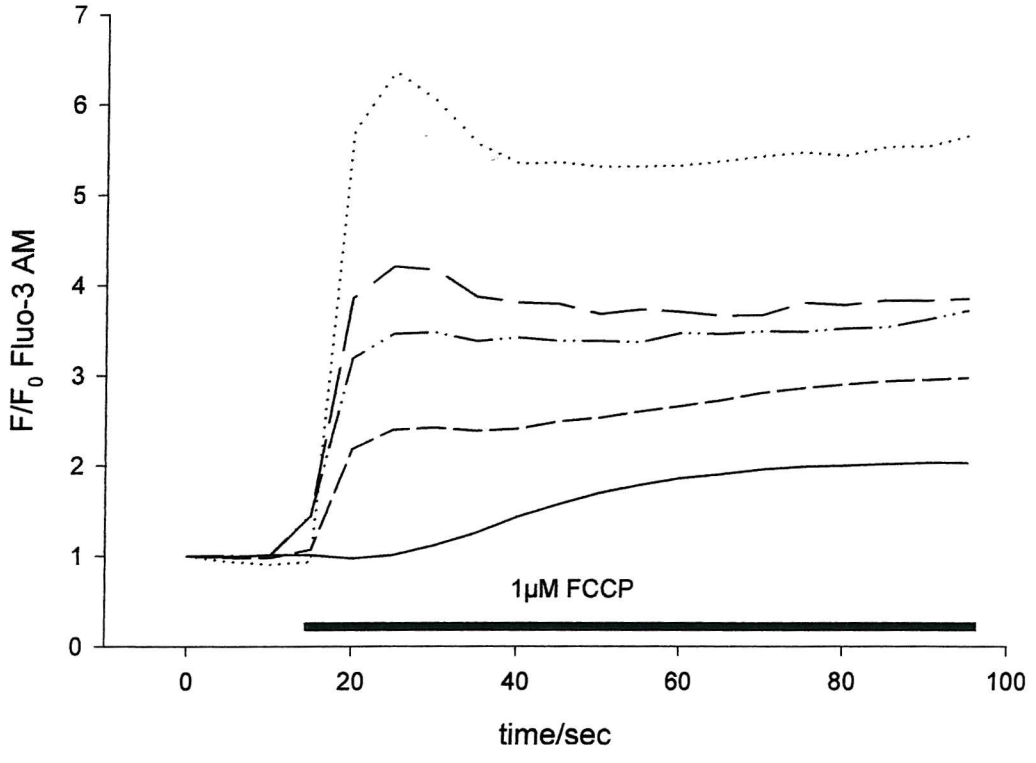

Fig. 4.13 Typical increase in neuronal Fluo-3 AM fluorescence in response to 1μM FCCP. The trace shows the heterogeneity of response of five neurons in a single cover slip, and is representative of 5 other separate experiments carried out on different cultures. Horizontal bar indicates time and duration of exposure to FCCP.

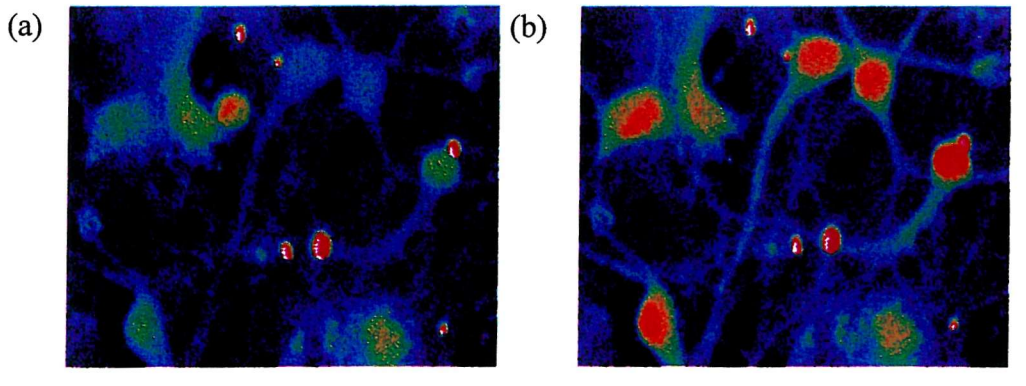

Fig. 4.14 Images selected from a time series of confocal images showing Fluo-3 fluorescence in hippocampal neurons before (a) and after (b) the addition of FCCP. The increase in fluorescence signal indicates increased $[Ca^{2+}]_c$ suggesting that in cultured hippocampal neurons, mitochondria represent a significant source of releasable calcium.

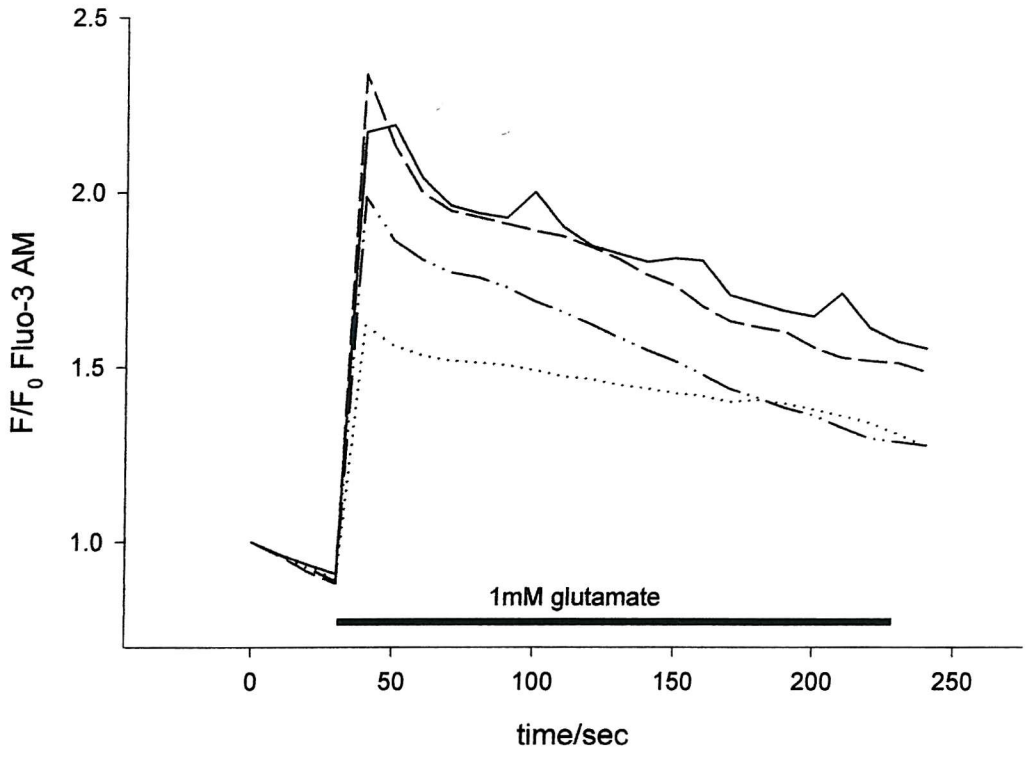

Fig. 4.15 Typical increase in neuronal Fluo-3 fluorescence in response to 1mM glutamate. The trace shows the response of four neurons in a single coverslip, and is representative of the response of eight cells monitored in three separate experiments. Horizontal bar indicates time and duration of exposure to glutamate.

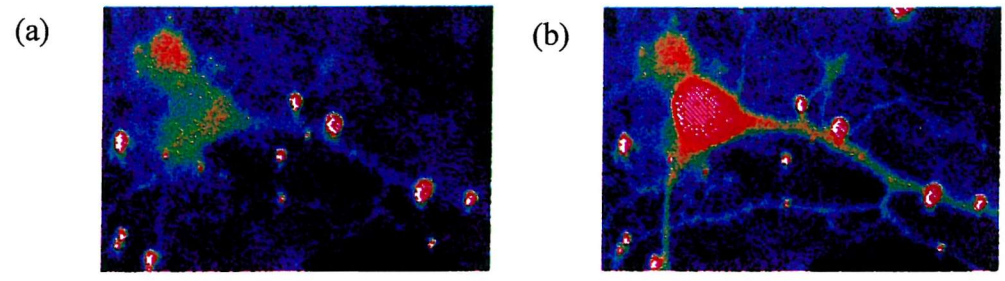

Fig. 4.16 Images selected from a time series of confocal images showing Fluo-3 fluorescence in a single hippocampal neuron before (a) and after (b) the addition of glutamate. The increase in fluorescence is a reflection of elevated $[Ca^{2+}]_c$, and probably arises from both Ca2+ influx through the NMDA receptor and intracellular release of stored Ca^{2+}.

Neuronal calcium responses to agonists of specific glutamate receptor subtypes were then examined. Kainate caused a concentration-dependent initial increase in Fluo-3 fluorescence (see **Fig. 4.17**).

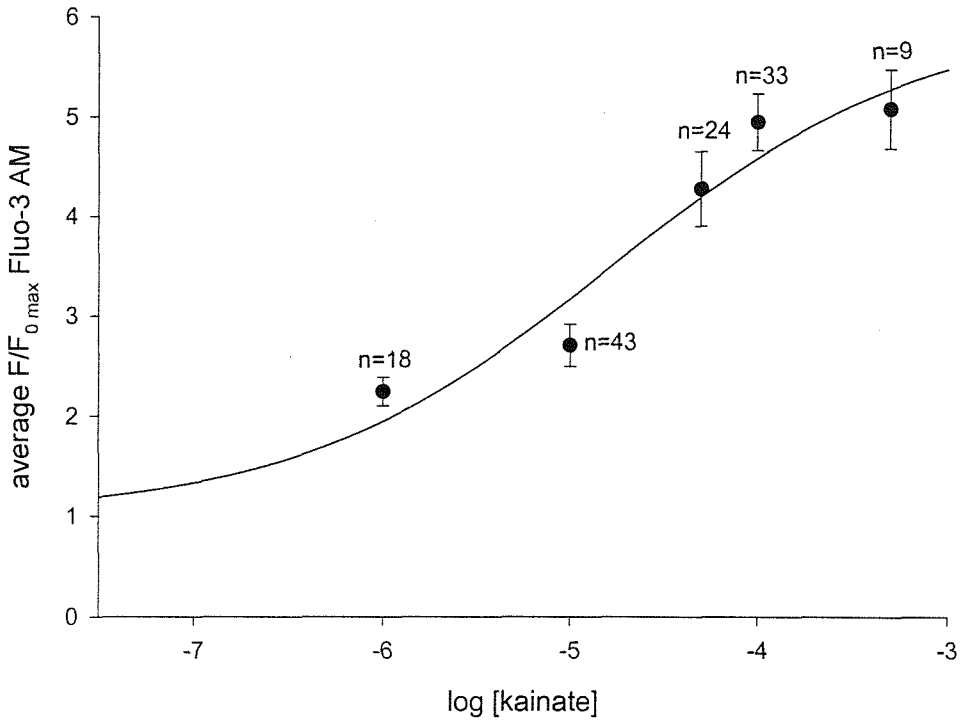

Fig 4.17 Concentration-response relationship for kainate. The neuronal Fluo-3 fluorescent signal is plotted against the concentration of kainate to which neurons were exposed for 5 minutes. Data is presented as averages for the fluorescent signal from neuronal soma ± s.e.m., and n values are given for each data point. All experiments are repeated in a minimum of three separate cultures.

The initial neuronal Ca^{2+} response to kainate was half maximal at 20μM and appeared to be approaching plateau at 500μM, the highest concentration used. A typical fluorescence timecourse and confocal images of neuronal fluorescence changes following the addition of 10μM kainate are shown in Figs **4.18** and **4.19**.

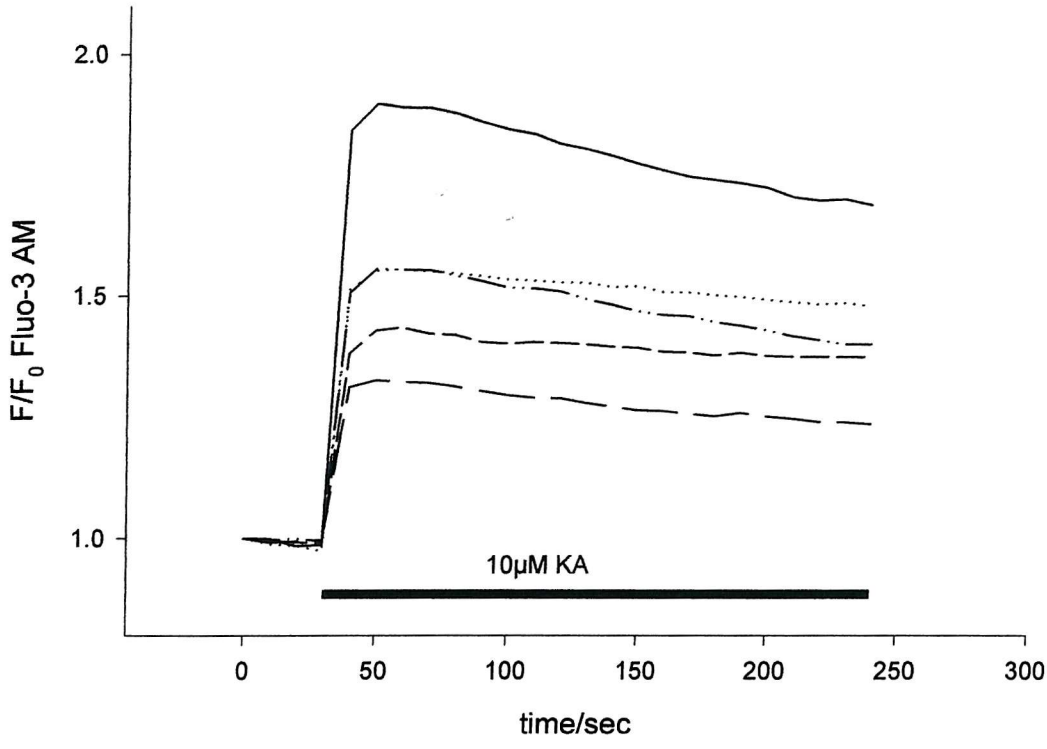

Fig. 4.18 Typical increase in neuronal Fluo-3 fluorescence in response to 10μM kainate. The trace shows the response of five neurons on the same coverslip, and is representative of nineteen cells monitored in three separate experiments. Horizontal bar indicates time and duration of exposure to kainate.

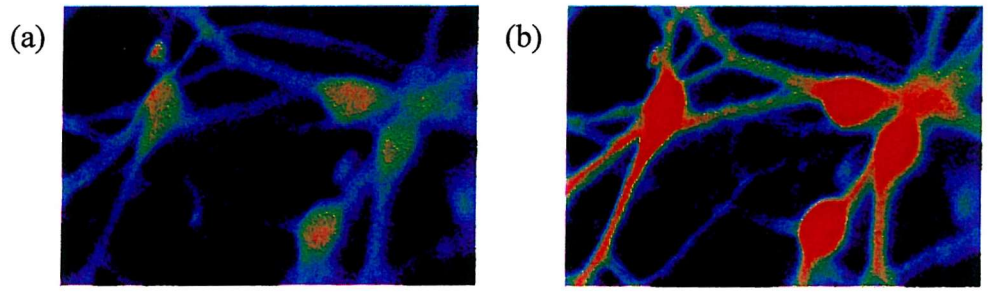

Fig. 4.19 Images selected from a time series of confocal images showing Fluo-3 fluorescence in hippocampal neurons before (a) and after (b) the addition of kainate. The increase in fluorescence is indicative of elevated $[Ca^{2+}]_c$ and probably arises from both calcium influx through Ca^{2+} permeable kainate receptors and release from intracellular Ca^{2+} stores.

1S, 3R-ACPD, an agonist at metabotropic glutamate receptors, caused a concentration-dependent initial increase in neuronal Fluo-3 fluorescence (see Figure **4.20**). The initial neuronal response to ACPD was half maximal at approximately 100μM, and increased steadily over the range of concentrations used (1-500μM). A typical fluorescence timecourse and confocal images of neuronal fluorescence changes are shown in Figs **4.21** and **4.22**.

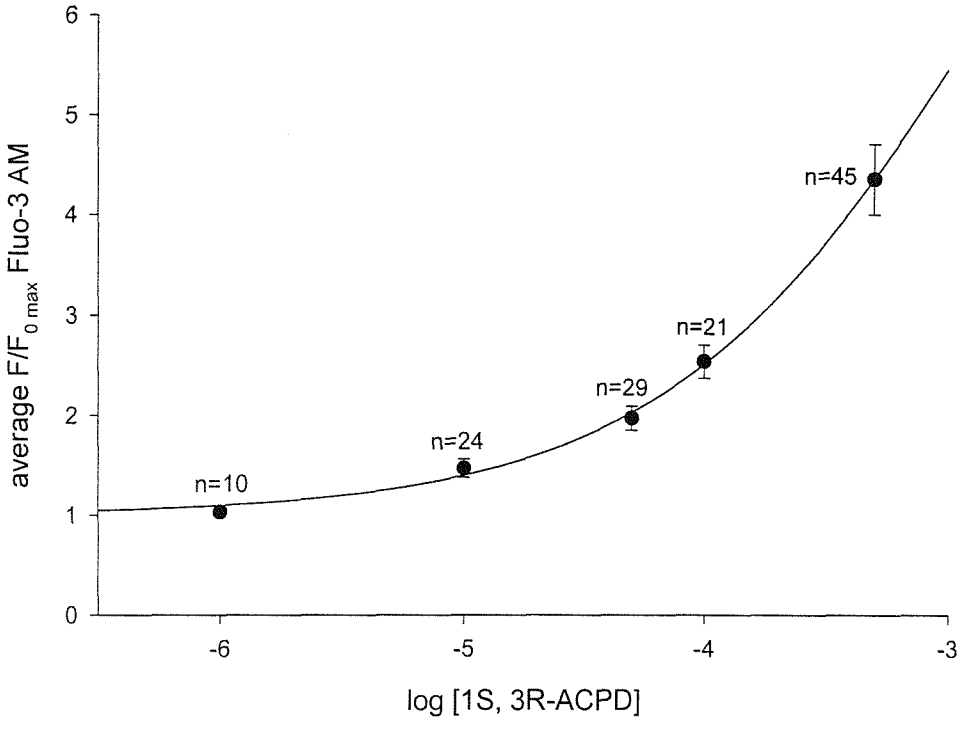

Figure 4.20 Concentration-response relationship for 1S,3R-ACPD. The neuronal Fluo-3 fluorescent signal is plotted against the concentration of ACPD to which neurons were exposed for 5 minutes. Data is presented as averages for the fluorescent signal from neuronal soma ± s.e.m., and n values are given for each data point. All experiments are repeated in a minimum of three separate cultures.

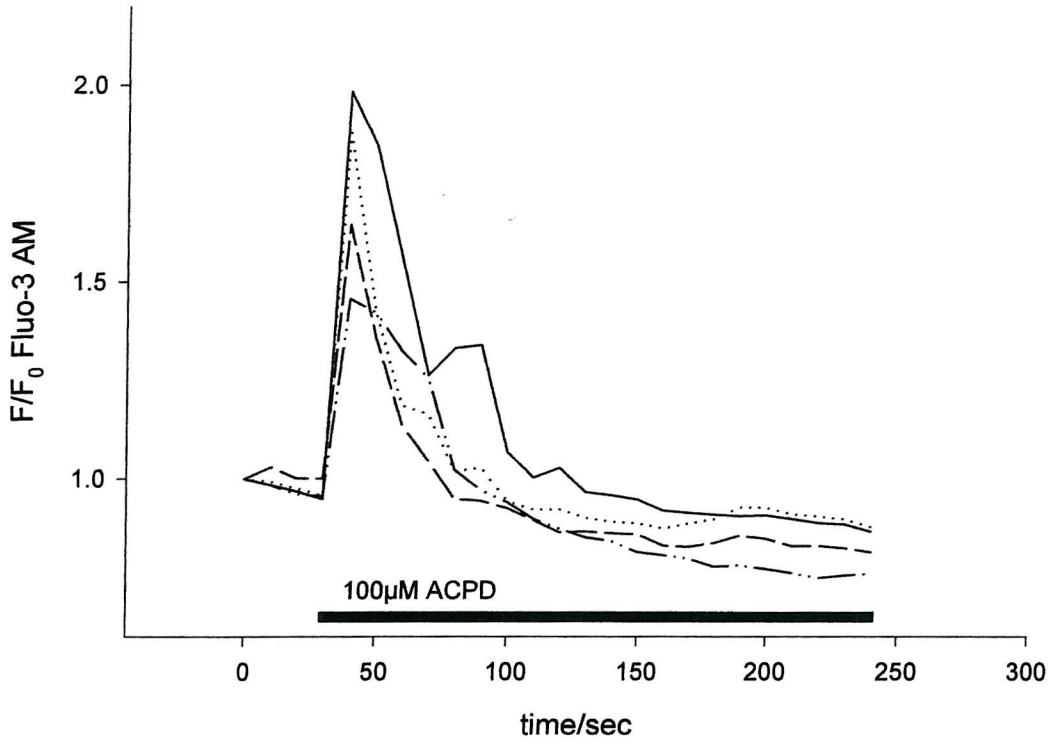

Fig. 4.21 Typical change in neuronal Fluo-3 fluorescence in response to 100μM 1S,3R-ACPD. The trace shows the heterogeneity of response of four neurons in a single cover slip, and is representative of twenty nine cells monitored in four separate experiments. Horizontal bar indicates time and duration of exposure to 1S,3R-ACPD.

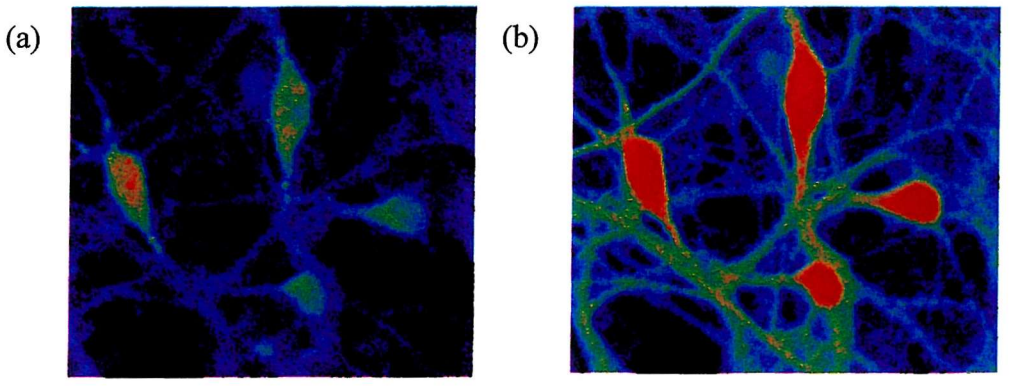

Fig. 4.22 Images selected from a time series of confocal images showing Fluo-3 fluorescence in hippocampal neurons before (a) and after (b) the addition of 1S,3R-ACPD. The increase in fluorescence reflects elevated $[Ca^{2+}]_c$ likely arising from Ca^{2+} release from intracelluar stores. 1S,3R-ACPD binds to mGluRs, causing the release of IP_3, which in turn causes the release of Ca^{2+} by binding to IP_3 receptors on intracellular Ca^{2+} stores.

The addition of NMDA caused an initial increase in neuronal Fluo-3 fluorescence (see **Fig 4.24** and **4.25**, overleaf) which was concentration-dependent, giving a sigmoidal dose-neuronal calcium response curve (see **Fig. 4.23**, below) which was half maximal at approximately 3μM and plateaued at 100μM.

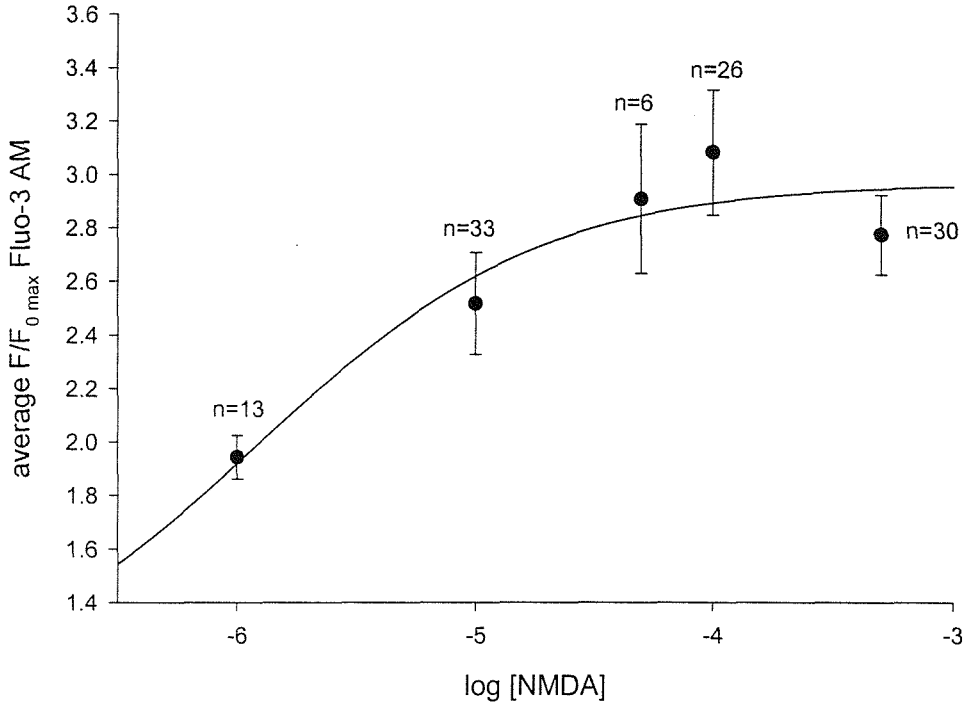

Fig. 4.23 Concentration-response relationship for NMDA. The neuronal Fluo-3 fluorescent signal is plotted against the concentration of NMDA to which neurons were exposed for five minutes. Data is presented as averages for the fluorescent signal from neuronal soma ± s.e.m., and n values are given for each data point. All experiments were repeated in a minimum of three separate cultures.

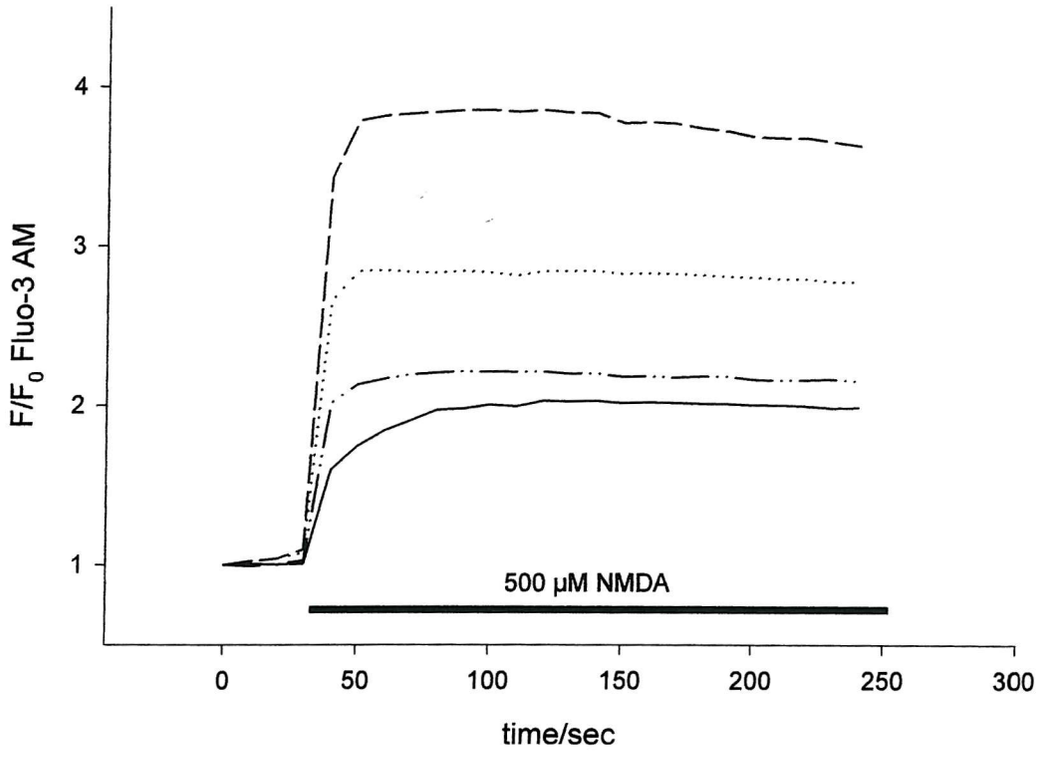

Fig. 4.24 Typical change in neuronal Fluo-3 fluorescence in response to 500µM NMDA. The trace shows the response of four neurons in the same field of view, and is representative of thirty-nine cells monitored in six separate experiments. Horizontal bar indicates time and duration of exposure to NMDA.

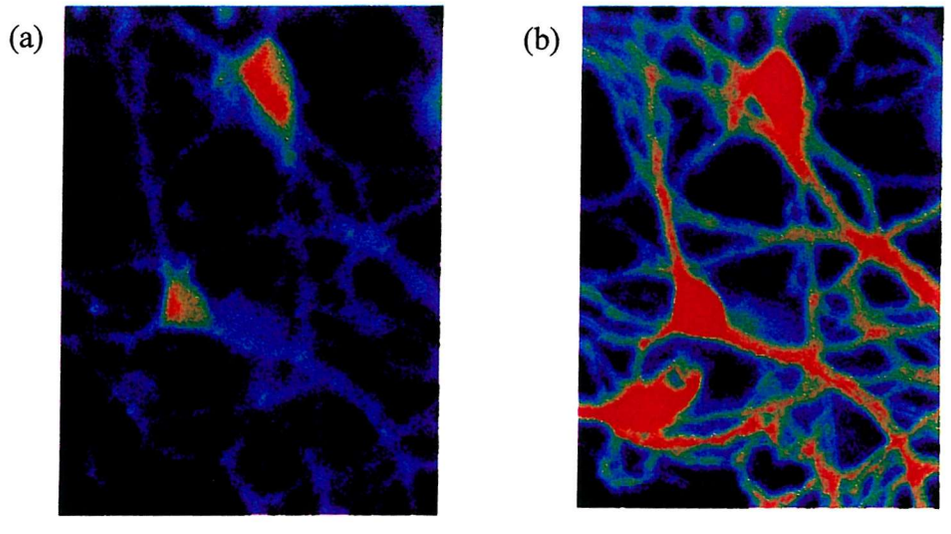

Fig. 4.25 Images selected from a time series of confocal images showing Fluo-3 fluorescence in hippocampal neurons before (a) and after (b) the addition of NMDA. The increase in fluorescence is indicative of elevated $[Ca^{2+}]_c$ and probably arises from both calcium influx through Ca^{2+} permeable NMDA receptors and release from intracellular Ca^{2+} stores.

AMPA caused an initial increase in neuronal Ca^{2+} activity, as shown in **Figs 4.27** and **4.28** (overleaf). Apparently, this neuronal Ca^{2+} response was not concentration dependent (see **Fig. 4.26**, below), showing a maximal response at approximately 25μM. This may reflect the rapid inactivation kinetics of the AMPA receptor, and the high affinity of this receptor for its ligand.

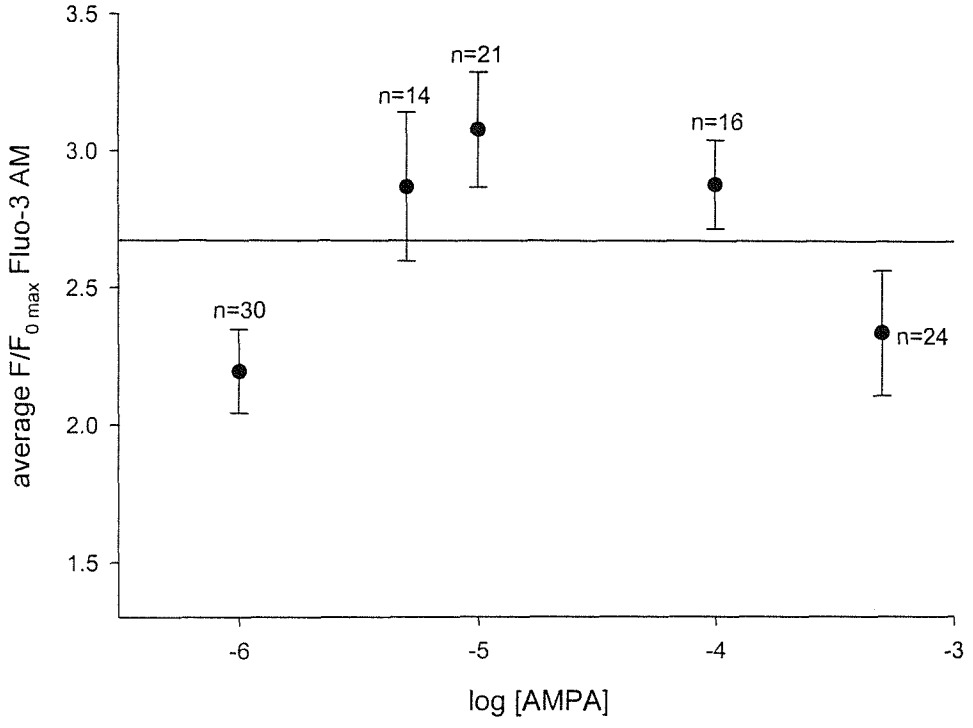

Fig. 4.26 Concentration-response relationship for AMPA. The neuronal Fluo-3 fluorescent signal is plotted against the concentration of AMPA to which neurons were exposed for five minutes. Data is presented as averages for the fluorescent signal from neuronal soma ± s.e.m., and n values are given for each data point. All experiments were repeated in a minimum of three separate cultures.

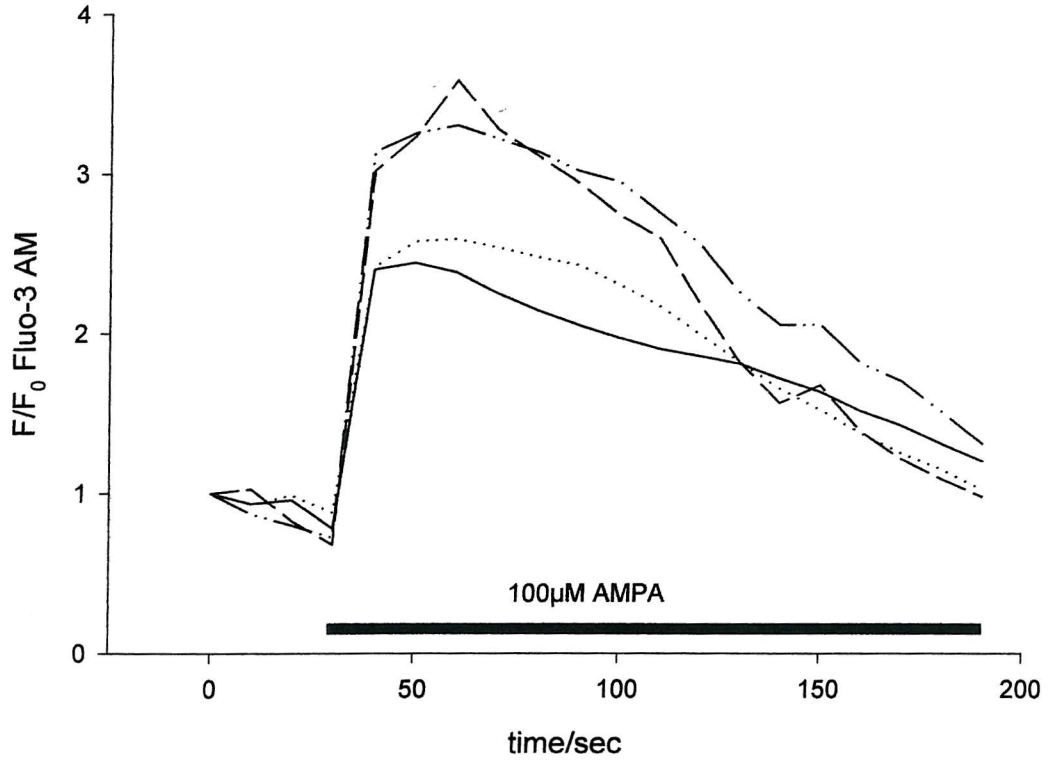

Fig. 4.27 Typical increase in neuronal Fluo-3 fluorescence in response to 100μM AMPA. The trace shows the response of four neurons in the same cover slip, and is representative of sixteen neurons monitored in four separate experiments. Horizontal bar indicates time and duration of exposure to AMPA.

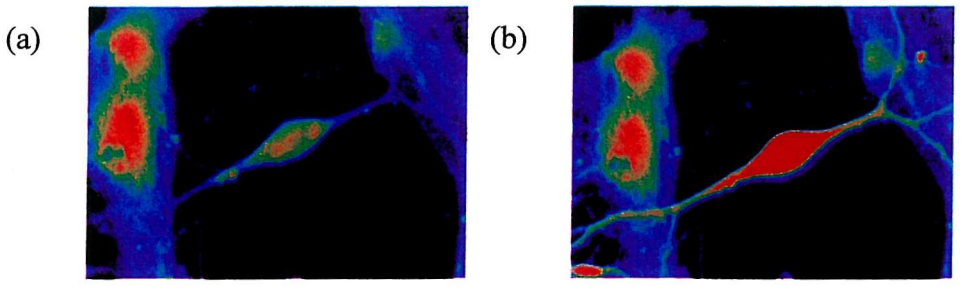

Fig. 4.28 Images selected from a time series of confocal images showing Fluo-3 fluorescence in hippocampal neurons before (a) and after (b) the addition of 100μM AMPA. The increase in fluorescence indicates an increase in $[Ca^{2+}]_c$, probably arising from a mixture of Ca^{2+} influx through calcium-permeable AMPA receptors and influx through VDCCs.

Exposure to quisqualate caused a dose-dependent initial increase in neuronal Fluo-3 fluorescence (**Fig. 4.29**). Figs **4.30** and **4.31** show confocal images of neurons loaded with Fluo-3 and a typical timecourse of neuronal Fluo-3 fluorescence following the addition of quisqualate.

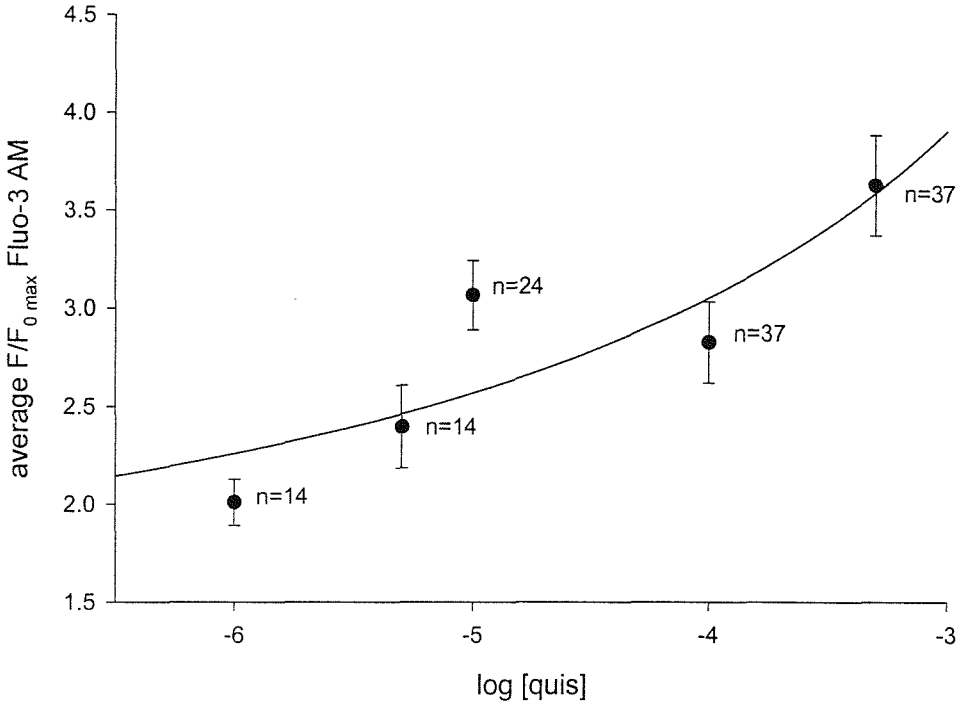

Fig. 4.29 Concentration-response relationship for quisqualate. The neuronal Fluo-3 fluorescent signal is plotted against the concentration of quisqualate to which neurons were exposed for five minutes. Data is presented as averages for the fluorescent signal from neuronal soma ± s.e.m., and n values are given for each data point. All experiments were repeated in a minimum of three separate cultures.

The timecourses of neuronal Fluo-3 fluorescence illustrate the effect of specific doses of glutamate receptor agonist, chosen to elicit maximal initial neuronal Ca^{2+} increases of a similar magnitude (**Figs 4.11, 4.13, 4.15, 4.18, 4.21, 4.24, 4.27 and 4.30**). Each glutamate receptor agonist caused an initial increase in neuronal $[Ca^{2+}]_i$, which peaked within the first 20 seconds of drug exposure. Since we wished to investigate only the *initial* neuronal Ca^{2+} changes following glutamate receptor activation, neuronal calcium responses were monitored for a maximum of 200 seconds following drug addition.

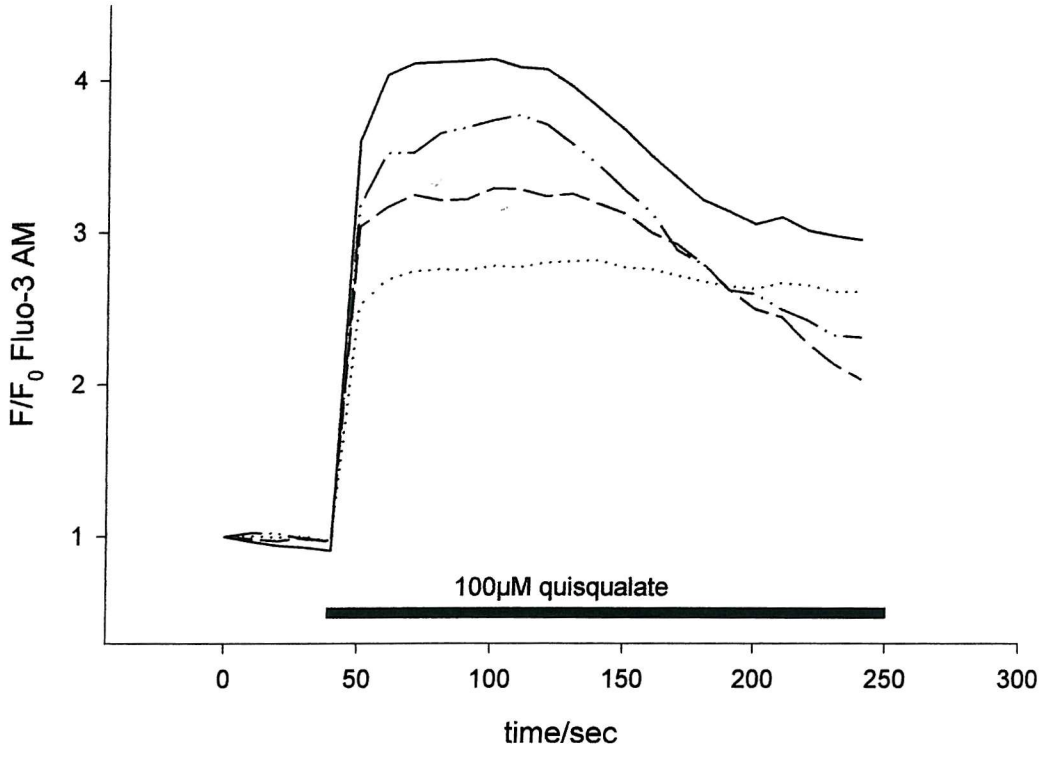

Fig. 4.30 Typical increase in neuronal Fluo-3 fluorescence in response to 100μM quisqualate. The trace shows the response of four neurons in a single coverslip, and is representative of twenty-six cells monitored in five separate experiments. Horizontal bar indicates time and duration of exposure to quisqualate.

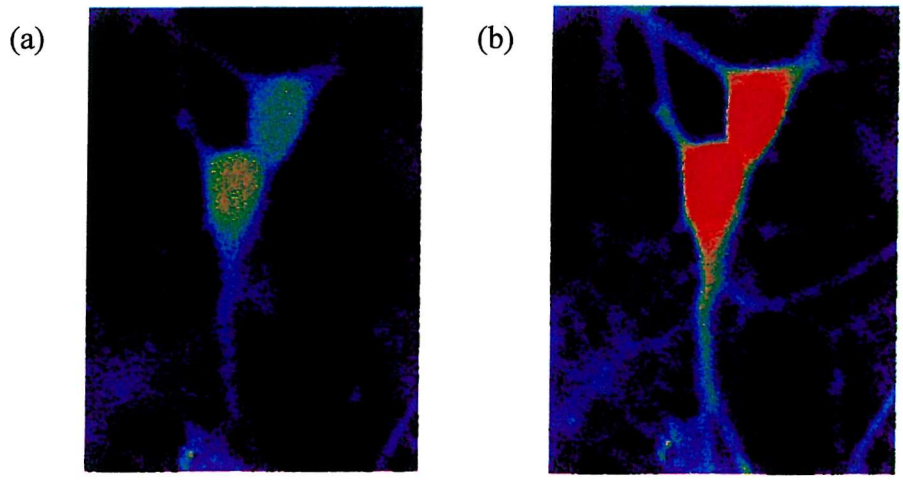

Fig. 4.31 Images selected from a time series of confocal images showing Fluo-3 fluorescence in hippocampal neurons before (a) and after (b) the addition of quisqualate. The increase in fluorescence is indicative of elevated $[Ca^{2+}]_c$ and probably mainly arises from calcium release from intracellular stores, with a smaller component originating from influx through both receptor operated- and voltage dependent Ca^{2+} channels.

4.3.3 MitoTracker Green staining in cultured hippocampal neurons

The distribution of mitochondria within cultured hippocampal neurons was investigated by staining with MitoTracker Green FM, a probe which preferentially stains mitochondria regardless of mitochondrial membrane potential. MitoTracker Green is nonfluorescent in aqueous solution, and only fluoresces once it accumulates in the lipid environment of mitochondria. Staining revealed the ubiquitous presence of mitochondria throughout the soma and dendrites of cultured hippocampal neurons (**Fig. 4.32**).

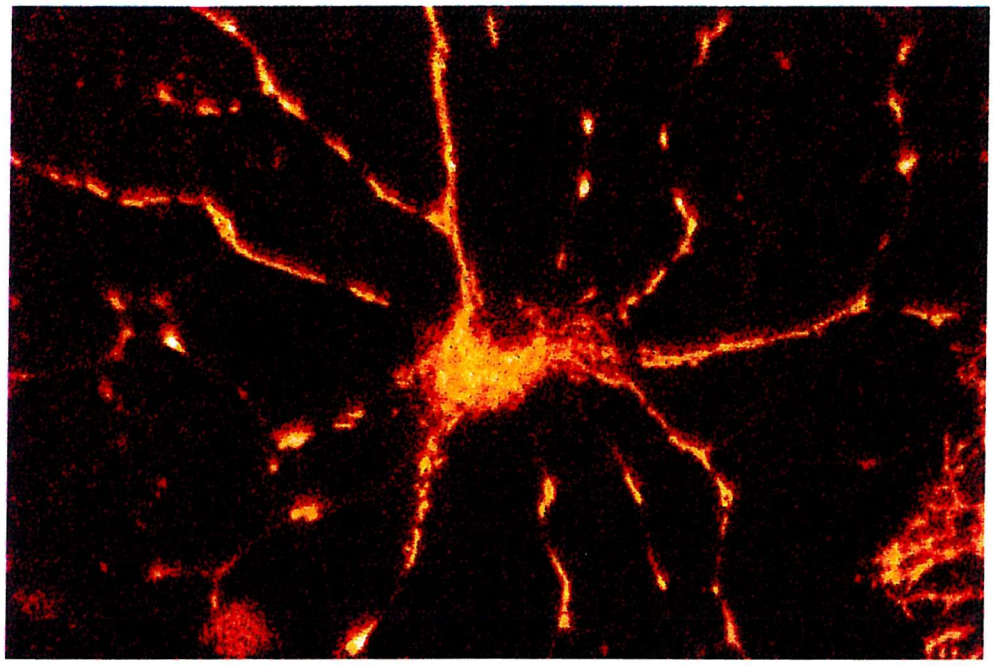

Fig 4.32 Mitochondria within a cultured hippocampal neuron. Hippocampal neurons cultured for at least 10 days in vitro were incubated with MitoTracker Green FM (Molecular Probes) which accumulates in mitochondria forming a stable conjugate. Cells were visualized by confocal microscopy. The image shows the abundant presence of thread-like mitochondria within the neuroites and occupying the cytoplasm surrounding the nucleus within the soma. Magnification: x 40

4.3.4 Changes in $\Delta\Psi m$ following neuronal challenge with excitatory amino acids

Mitochondria are known to buffer imposed cytosolic Ca^{2+} loads (Wang and Thayer, 1996; Svichar *et al*, 1997), and the uptake of calcium may cause mitochondrial depolarisation (White and Reynolds, 1996). With this in mind, we investigated the effect of different calcium loads on neuronal mitochondrial $\Delta\Psi$, using cultured hippocampal neurons loaded with TMRE and imaged with CLSM. The investigation of dose-response relationships in the first part of this study allowed doses of glutamate receptor agonist to be chosen which would impose a neuronal Ca^{2+} load of similar magnitude (seee Figure **4.49**).

The addition of 1μM FCCP, as expected, caused an immediate and irreversible mitochondrial depolarisation (see **Fig 4.33** and **4.34**), increasing TMRE fluorescence by a maximum of 3.35 ± 0.7 FU (increases normalised to resting fluorescence levels ± SEM). The addition of 2mM 4-AP also caused a significant mitochondrial depolarisation (see **Fig 4.35** and **4.36**), increasing the neuronal TMRE signal by 2.02 ± 0.37 FU.

Increases in neuronal Fluo-3 fluorescence elicited by the different glutamate receptor agonists and positive controls are summarised in **Fig. 4.49**, together with their effect on neuronal TMRE fluorescence. Despite the similar magnitude of neuronal Ca^{2+} load imposed by glutamate, kainate, 1S,3R-ACPD, NMDA AMPA and quisqualate, there was no correlation between the Ca^{2+} load imposed by these different glutamate receptor agonists and the extent of mitochondrial depolarisation (**Fig 4.50**). Exposure to 1mM glutamate caused mitochondrial depolarisation (see **Fig 4.37** and **4.38**), reflected in a maximal TMRE signal increase of 0.76 ± 0.12 FU relative to resting fluorescence levels. The addition of 500μM NMDA caused a large increase in TMRE fluorescence (3.02 ± 0.64 FU), reflecting a massive mitochondrial depolarisation (Figs **4.43** and **4.44**). Agonists at other glutamate receptor subtypes did not cause any significant mitochondrial depolarisation, whilst elevating $[Ca^{2+}]_c$ to the same extent as NMDA and

glutamate. **Figs 4.39** and **4.40b** show that kainate alone caused a negligable increase in TMRE signal (0.05 ± 0.02 FU) although the mitochondria could subsequently be fully depolarised with FCCP (**Fig 4.40c**). The addition of 1S,3R-ACPD caused virtually no change in TMRE signal (increase of 0.004 ± 0.002 FU) as shown in **Figs 4.41** and **4.42**. AMPA and quisqualate caused very small changes in TMRE fluorescence (increases of 0.1 ± 0.03 and 0.07 ± 0.01 FU respectively), as shown in **Figs 4.45**, **4.46**, **4.47** and **4.48**. The increases in TMRE fluorescence caused by glutamate and NMDA were very highly significantly greater than those caused by kainate, ACPD, AMPA or quisqualate.

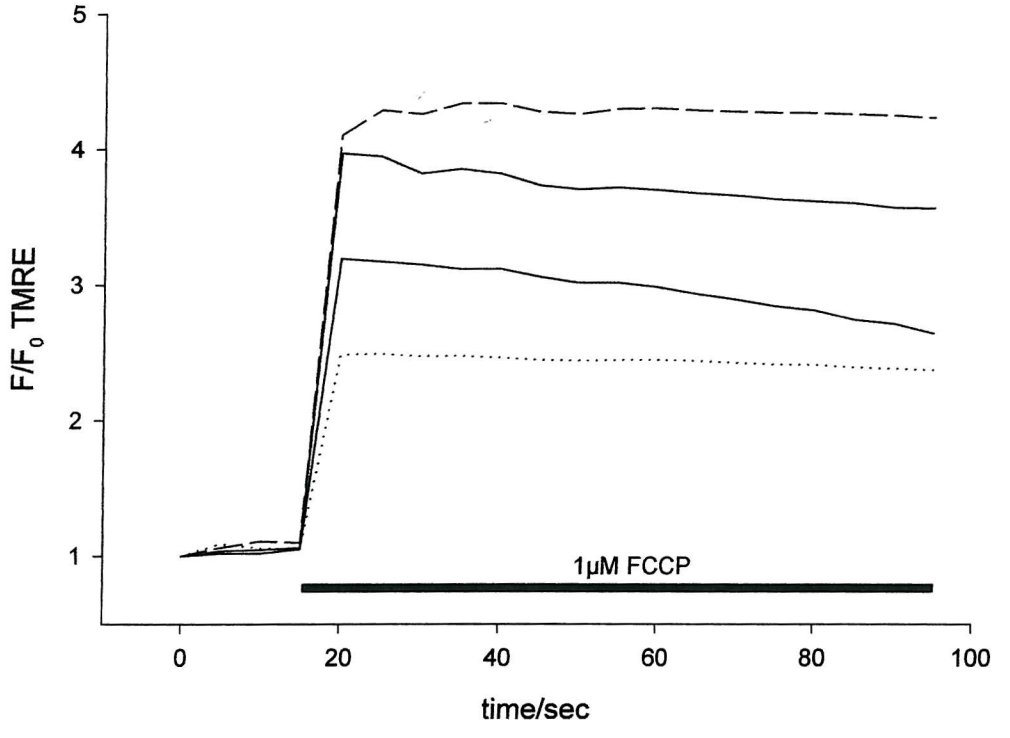

Fig. 4.33 Typical increase in TMRE fluorescence in response to 1μM FCCP. The trace shows the response of four neurons in a single cover slip, and is representative of twelve other separate experiments carried out on different cultures. Horizontal bar indicates time and duration of exposure to FCCP.

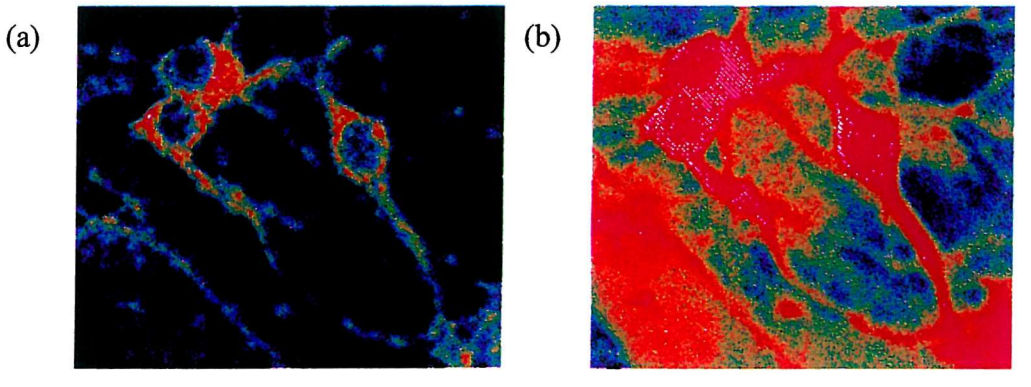

Fig. 4.34 Images selected from a time series of confocal images showing TMRE fluorescence in hippocampal neurons before (a) and after (b) the addition of FCCP. The sequestration of TMRE in mitochondria is driven by mitochondrial $\Delta\Psi$. Mitochondrial $\Delta\Psi$ may be reduced by the addition of FCCP, a protonophore which depolarizes mitochondria. The increase in fluorescence indicates reduced $m\Delta\Psi$. Notice the punctate pattern of staining in Fig. 4.36a, reflecting the accumulation of TMRE in polarised mitochondria.

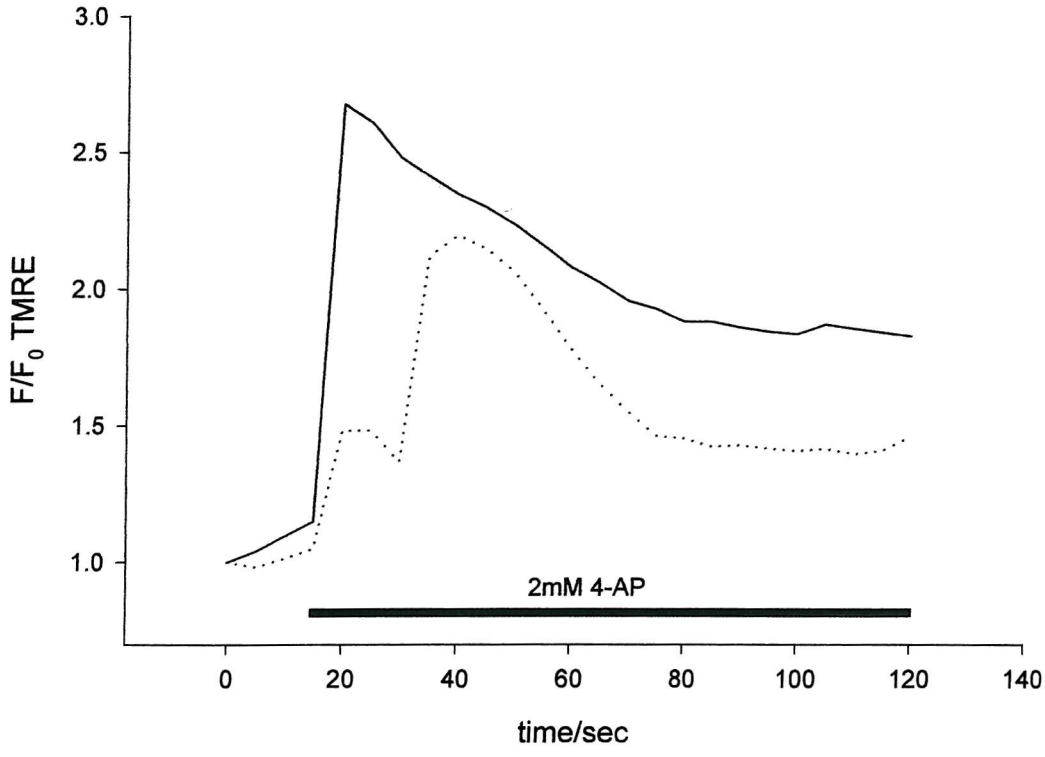

Fig. 4.35 Typical increase in neuronal TMRE fluorescence in response to 2mM 4-AP. The trace shows the response of two neurons, and is representative of the response of four neurons monitored in two separate experiments. Horizontal bar indicates time and duration of exposure to 4-AP.

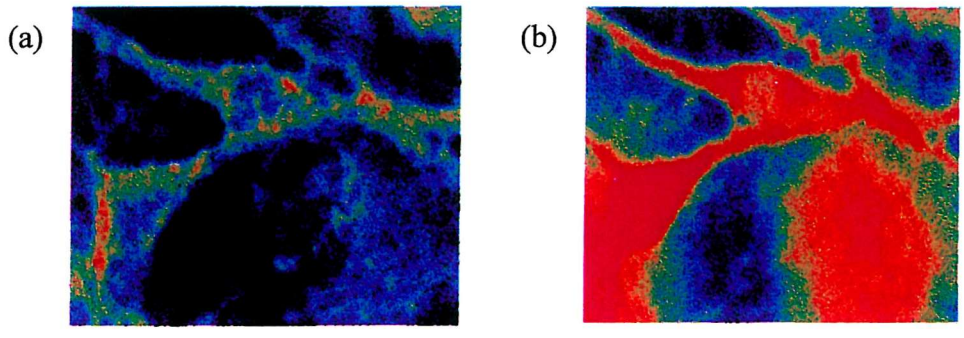

Fig. 4.36 Images selected from a time series of confocal images showing TMRE fluorescence in hippocampal neurons before (a) and after (b) the addition of 4-AP. The sequestration of TMRE in mitochondria is driven by mitochondrial $\Delta\Psi$. The increase in TMRE fluorescence indicates reduced mitochondrial $\Delta\Psi$. This could reflect mitochondrial buffering of the calcium load imposed by 4-AP, which persistently depolarises neurons and activates voltage-dependent calcium channels.

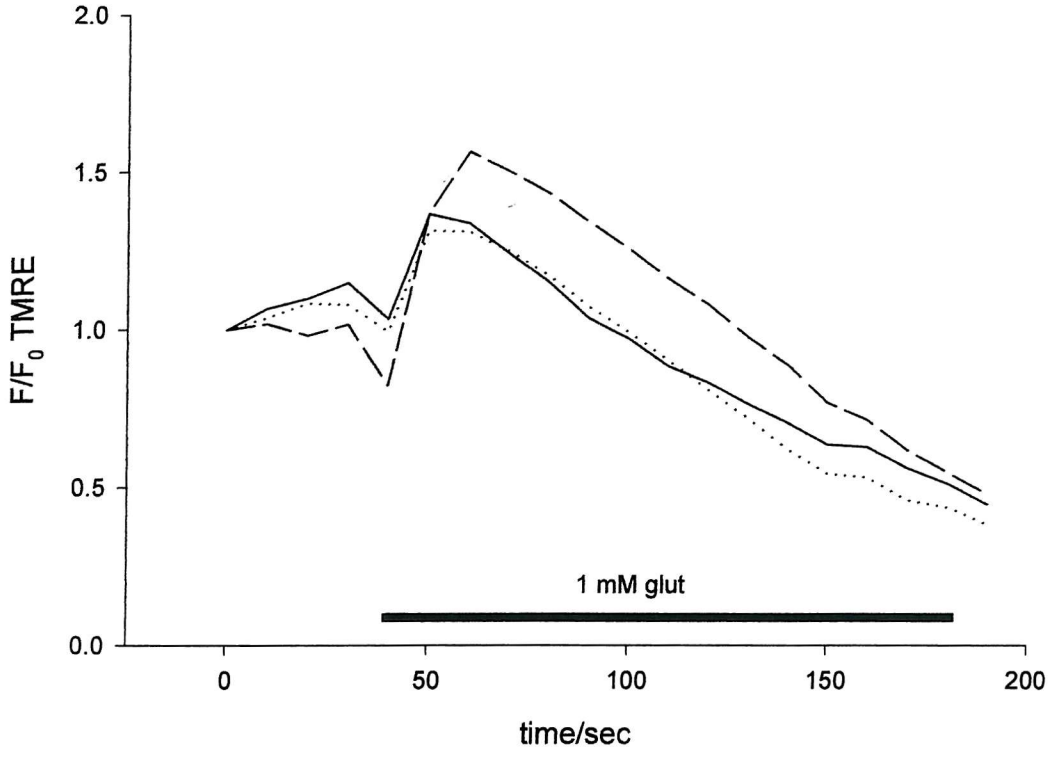

Fig. 4.37 Typical increase in neuronal TMRE fluorescence in response to 1mM glutamate. The trace shows the response of three neurons in a single coverslip, and is representative of eleven neurons monitored in five separate experiments. Horizontal bar indicates time and duration of exposure to glutamate

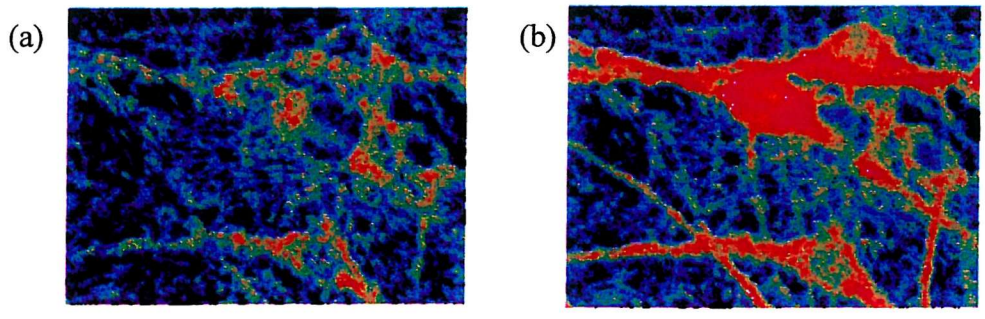

Fig. 4.48 Images selected from a time series of confocal images showing TMRE fluorescence in three hippocampal neurons before (a) and after (b) the addition of 1mM glutamate. The sequestration of TMRE in mitochondria is driven by mitochondrial $\Delta\Psi$. The increase in TMRE fluorescence suggests that glutamate causes mitochondrial depolarisation and redistribution of TMRE into the cytoplasm.

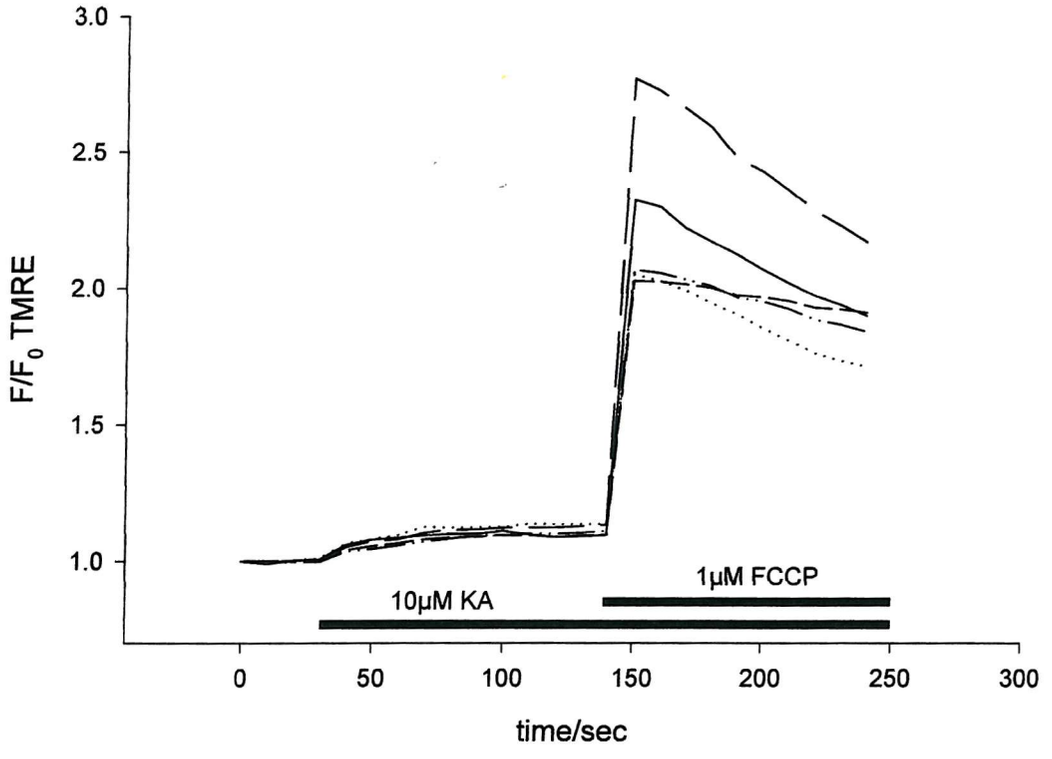

Fig. 4.39 Typical change in neuronal TMRE fluorescence in response to 10μM kainate. 1μM FCCP was added at the end of the recording as a positive control. The trace shows the response of five neurons in a single coverslip, and is representative of eleven neurons monitored in three separate experiments. Horizontal bars indicate time and duration of exposure to kainate.

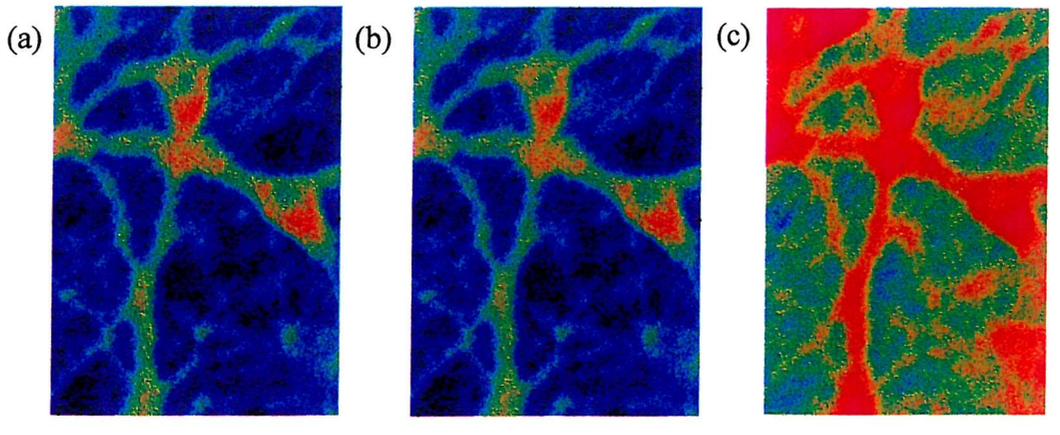

Fig. 4.40 Images selected from a time series of confocal images showing TMRE fluorescence in hippocampal neurons before (a) and following the addition of 10μM kainate (b) and after the addition of 1μM FCCP (c). TMRE fluorescence is unchanged by kainate, indicating that the calcium load imposed by kainate does not depolarise mitochondria. The mitochondrial uncoupler FCCP was added at the end of the experiment to completely dissipate $m\Delta\Psi$, reflected in an increase in TMRE signal (Xc).

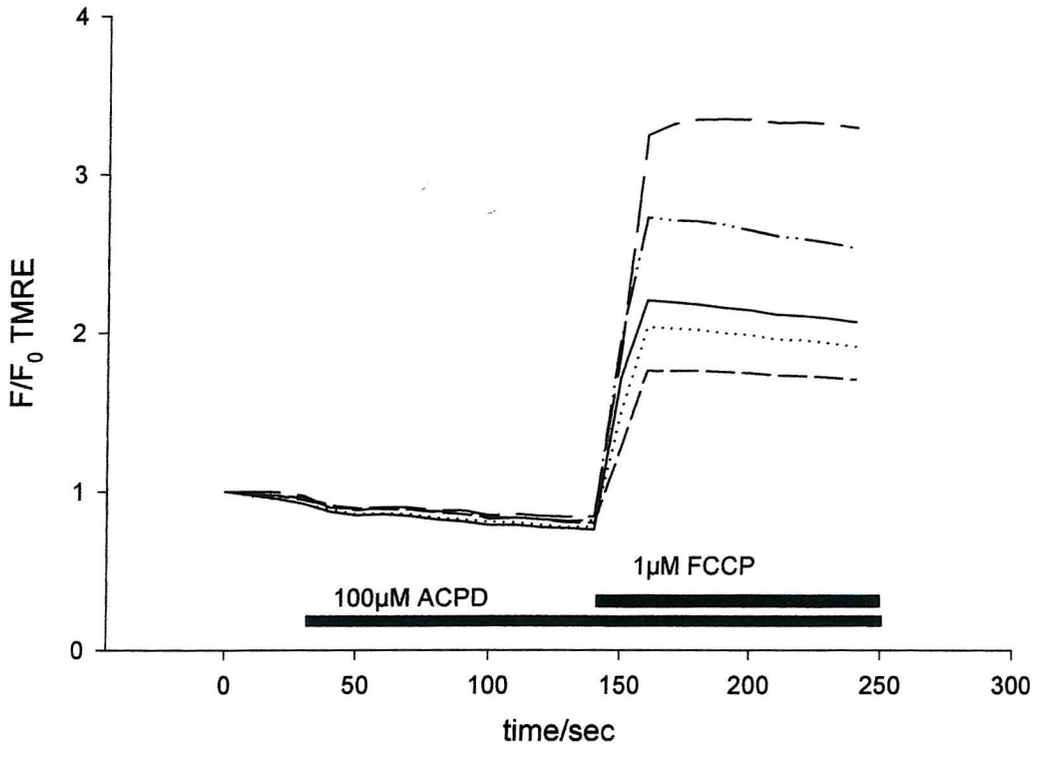

Fig. 4.41 Typical change in neuronal TMRE fluorescence in response to 100μM 1S,3R-ACPD. 1μM FCCP was added at the end of the recording as a positive control. The trace shows the response of five neurons in a single coverslip, and is representative of 24 cells monitored in three separate experiments. Horizontal bars indicate time and duration of exposure to 1S,3R-ACPD and FCCP.

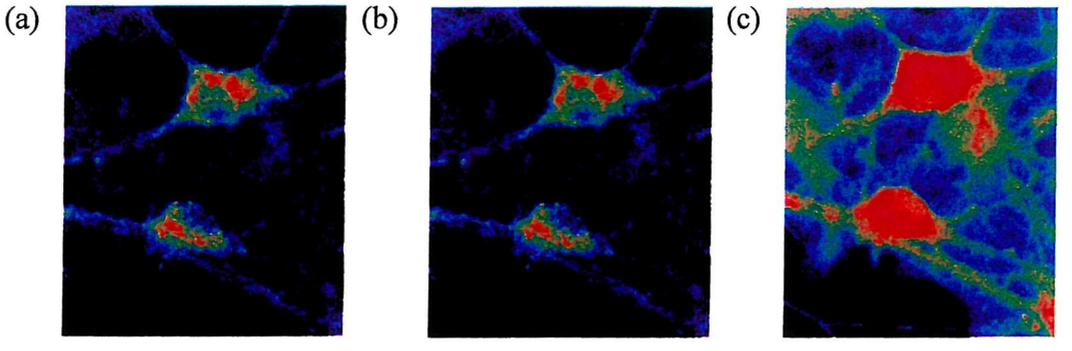

Fig. 4.42 Images selected from a time series of confocal images showing TMRE fluorescence in hippocampal neurons before (a) and after (b) the addition of 100μM 1S,3R-ACPD and after the addition of FCCP (c). The addition of ACPD did not change the TMRE signal, indicating that the calcium load imposed by ACPD did not depolarise mitochondria. The mitochondrial uncoupler FCCP was added at the end of the recording to completely dissipate $m\Delta\Psi$, which caused a large in crease in TMRE signal (c).

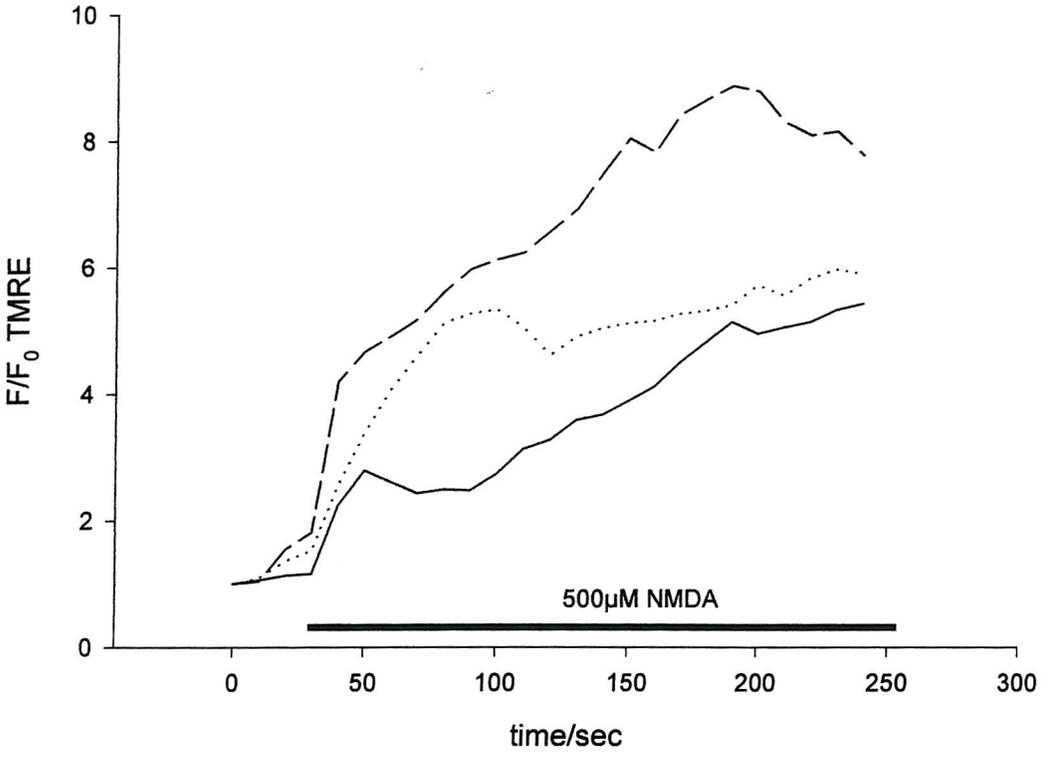

Fig. 4.43 Typical change in TMRE fluorescence in response to 500μM NMDA. The trace shows the response of three neurons in the same field of view, and is representative of sixteen other cells monitored in three separate experiments. Horizontal bar indicates time and duration of exposure to NMDA.

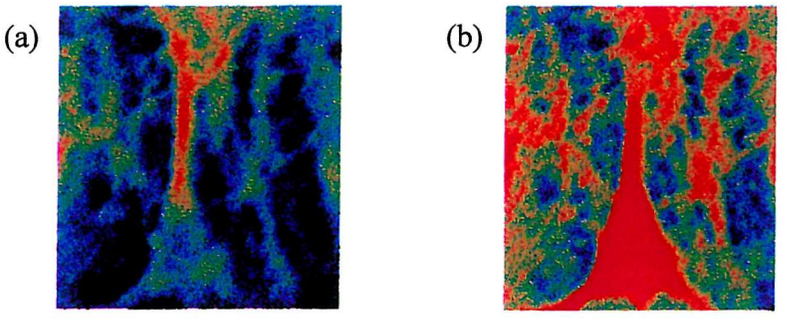

Fig. 4.44 Images selected from a time series of confocal images showing TMRE fluorescence in hippocampal neurons before (a) and following (b) the addition of 500μM NMDA. TMRE is sequestered by healthy mitochondria as a function of mitochondrial $\Delta\Psi$. The addition of NMDA increases TMRE fluorescence, indicating that NMDA causes mitochondrial depolarisation.

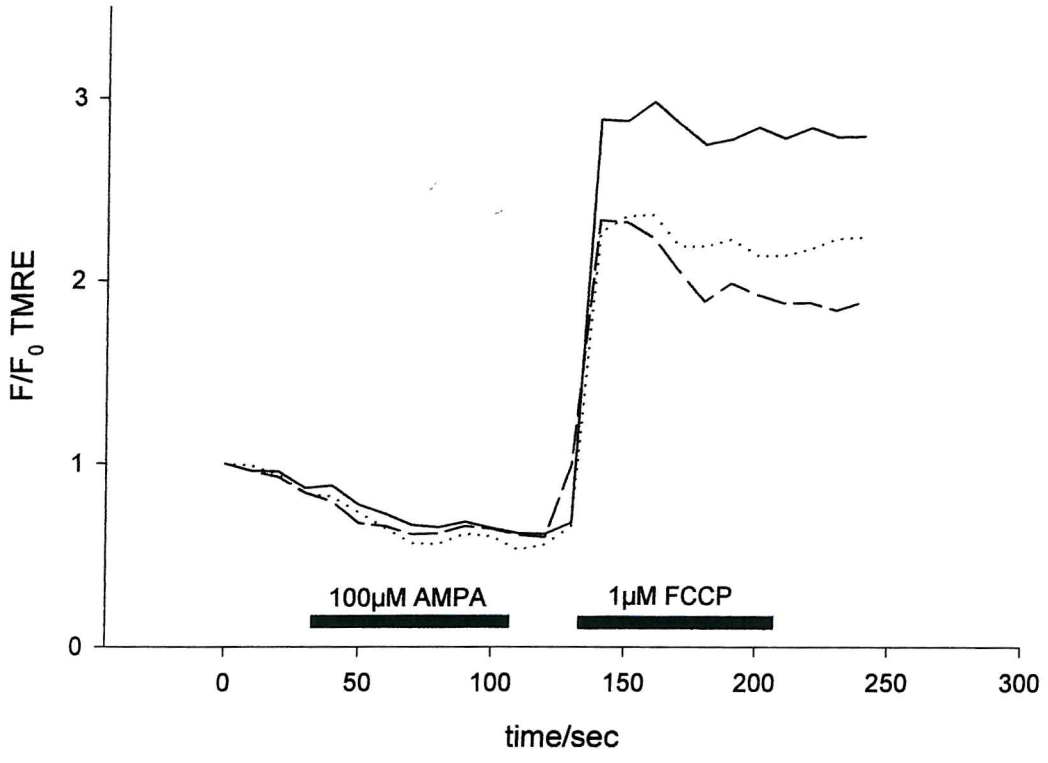

Fig. 4.45 Typical change in neuronal TMRE fluorescence in response to 100μM AMPA. 1μM FCCP was added at the end of the experiment as a positive control. The trace shows the response of three neurons on the same cover slip, and is representative of sixteen cells monitored in four separate experiments. Horizontal bars indicate time and duration of exposure to AMPA and FCCP.

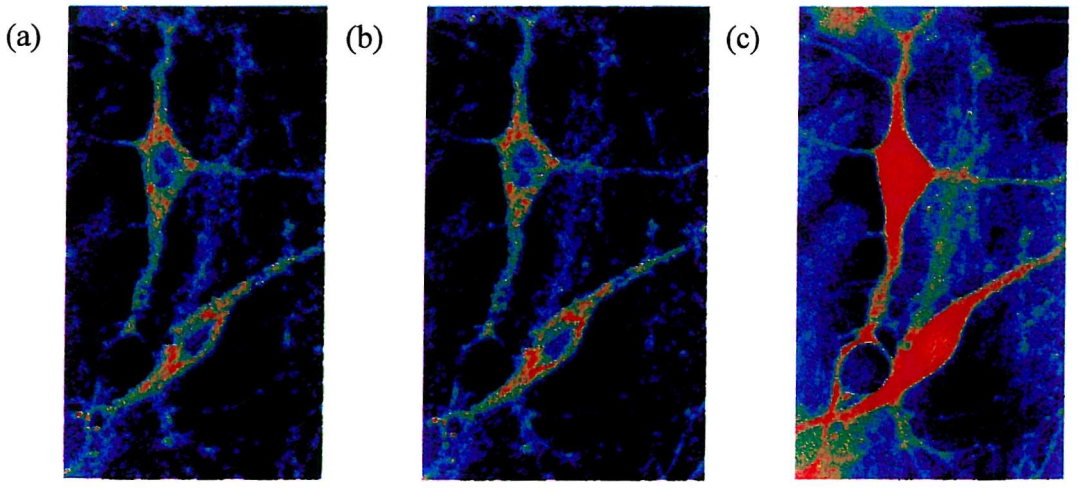

Fig. 4.46 Images selected from a time series of confocal images showing TMRE fluorescence in hippocampal neurons before (a) and after (b) the addition of 100μM AMPA. The addition of AMPA did not alter the TMRE signal, indicating that the Ca^{2+} load imposed by AMPA did not depolarise mitochondria. FCCP was added at the end of the recording to completely dissipate $m\Delta\Psi$, causing a large increase in TMRE signal (c).

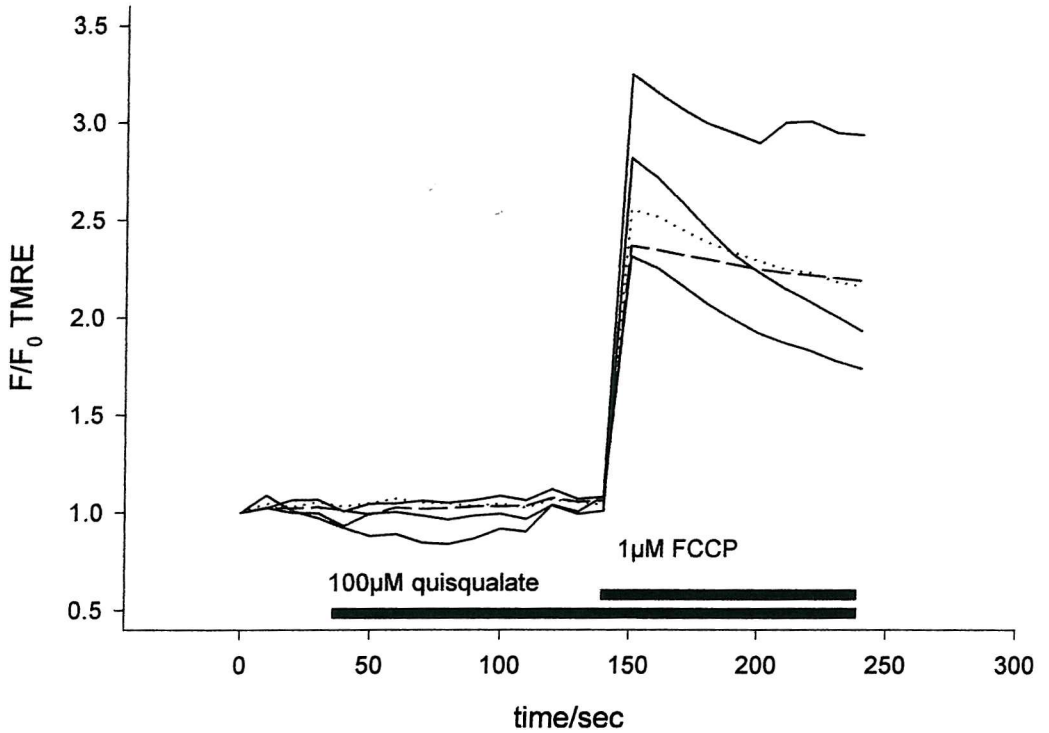

Fig. 4.47 Typical change in neuronal TMRE fluorescence in response to 100μM quisqualate. 1μM FCCP was added at the end of the experiment as a positive control. The trace shows the response of five neurons in a single coverslip, and is representative of fourteen other cells monitored in three separate experiments. Horizontal bars indicate time and duration of exposure to quisqualate and FCCP.

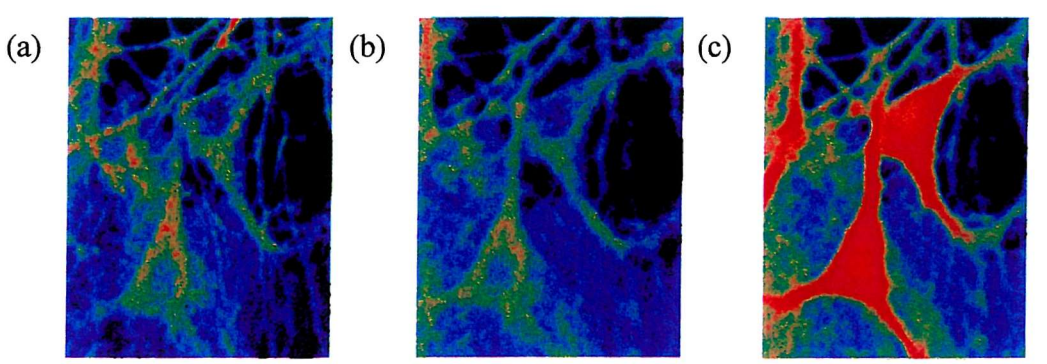

Fig. 4.48 Images selected from a time series of confocal images showing TMRE fluorescence in hippocampal neurons before (a) and after (b) the addition of 100μM quisqualate, and after the addition of 1μM FCCP (c). The addition of quisqualate did not alter the TMRE signal indicating that the Ca^{2+} load imposed by quisqualate did not cause mitochondrial depolarisation. FCCP was added at the end of the recording to completely dissipate $m\Delta\Psi$, indicated by a large increase in TMRE signal (c).

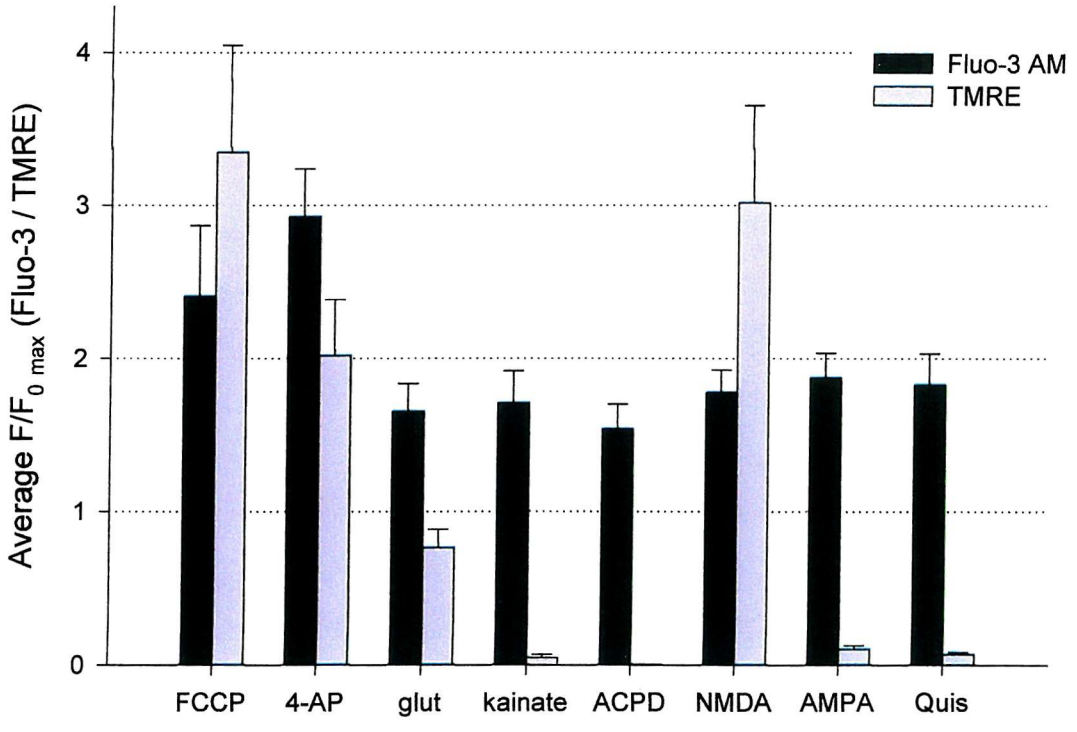

Fig. 4.49 Imposed calcium loads do not necessarily shift mitochondrial $\Delta\Psi$ in cultured hippocampal neurons. Summary of the average initial increases in neuronal Fluo-3 and TMRE fluorescence following exposure to glutamate receptor agonists and positive controls (FCCP, 4-AP). Doses of glutamate receptor agonist were chosen to elicit equivalent initial calcium responses. The initial increases in neuronal Fluo-3 fluorescence caused by each drug were deemed to be "equivalent" given that they were not significantly different when compared with the students t-test. No relationship was apparent between the magnitude of initial imposed Ca^{2+} and mitochondrial depolarisation, since glutamate and NMDA caused a large increase in TMRE fluorescence, indicative of a significant mitochondrial depolarisation, whereas kainate, AMPA, ACPD and quisqualate did not.

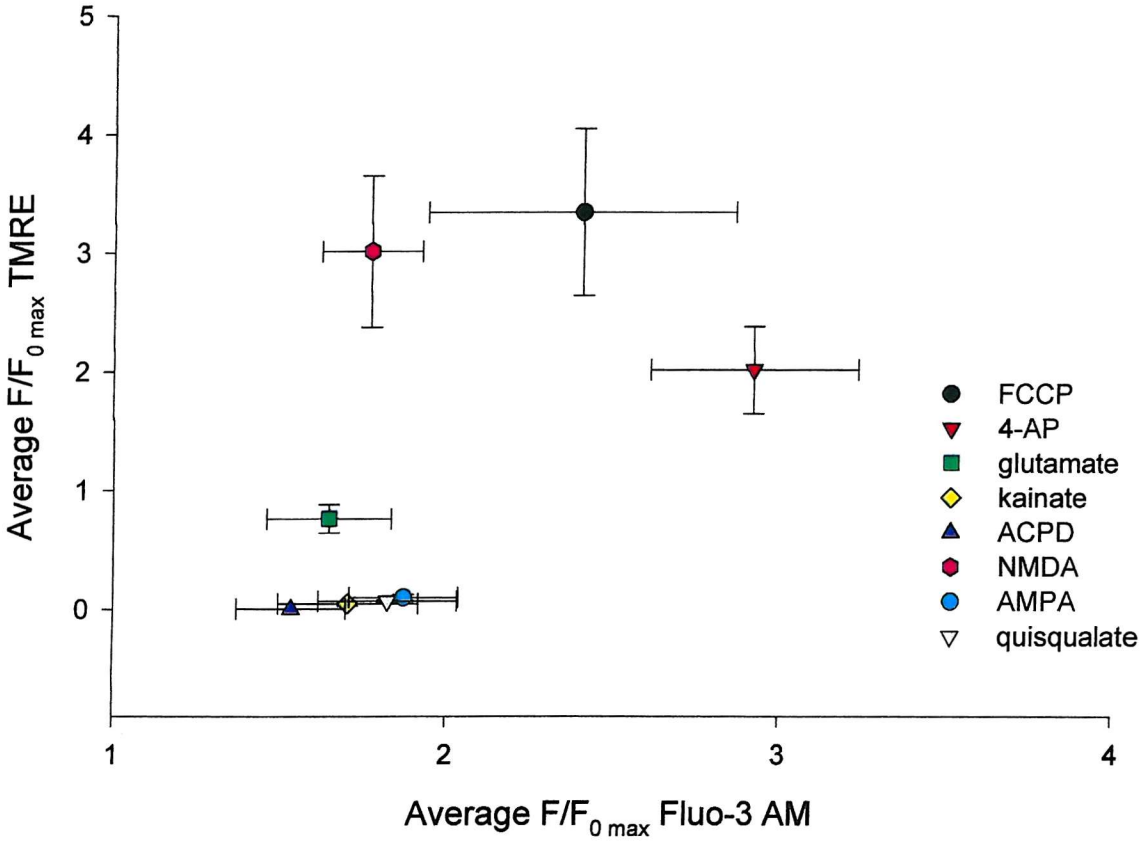

Fig. 4.50 Correlation between average shifts in TMRE and Fluo-3 fluorescence, reporting mitochondrial $\Delta\Psi$ and $[Ca^{2+}]_i$ respectively, elicited by glutamate receptor agonists and positive controls (FCCP and 4-AP), in cultured hippocampal neurons. The lack of correlation between these parameters suggests that the neurotoxicity of excitatory amino acids is not purely a function of the neuronal calcium load, as purported by the "calcium hypothesis" of neurotoxicity. Rather, different routes of calcium increase may have different pathological consequences for neurons.

4.3.5 Mechanism of the kainate-induced increase in neuronal $[Ca^{2+}]_i$

In section **4.3.2**, we made the observation that the addition of kainate to cultured hippocampal neurons caused a rapid and sustained initial increase in $[Ca^{2+}]_i$. The source of this Ca^{2+} is of particular interest, because data presented throughout this study suggests that the Ca^{2+} load imposed by kainate has different pathological consequences to the Ca^{2+} load imposed by NMDA. We investigated the contribution of VDCCs, ionotropic glutamate receptors, extracellular Ca^{2+}, ER Ca^{2+} stores and G-protein coupled mechanisms to the elevation in neuronal $[Ca^{2+}]_i$ caused by kainate. **Figure 4.51** shows the typical initial increase in $[Ca^{2+}]_i$, monitored by Fluo-3 AM, elicited by the addition of 10μM kainate to cultured hippocampal neurons. The magnitude of this initial Ca^{2+} response was monitored in neurons pretreated with antagonists of VDCCs (100μM Cd^{2+}) and ionotropic receptors (100μM D-AP5 and 100μM CNQX) to investigate the contribution of these channels to the kainate Ca^{2+} response. The initial elevation of $[Ca^{2+}]_i$ caused by 10μM kainate was not significantly changed by either the blockade of VDCCs (**Fig. 4.52**) or the blockade of ionotropic glutamate receptors (**Fig. 4.53**). The removal of extracellular Ca^{2+} and chelation of residual Ca^{2+} with 100μM EDTA did not significantly reduce the initial neuronal Ca^{2+} response (**Fig. 4.54**).

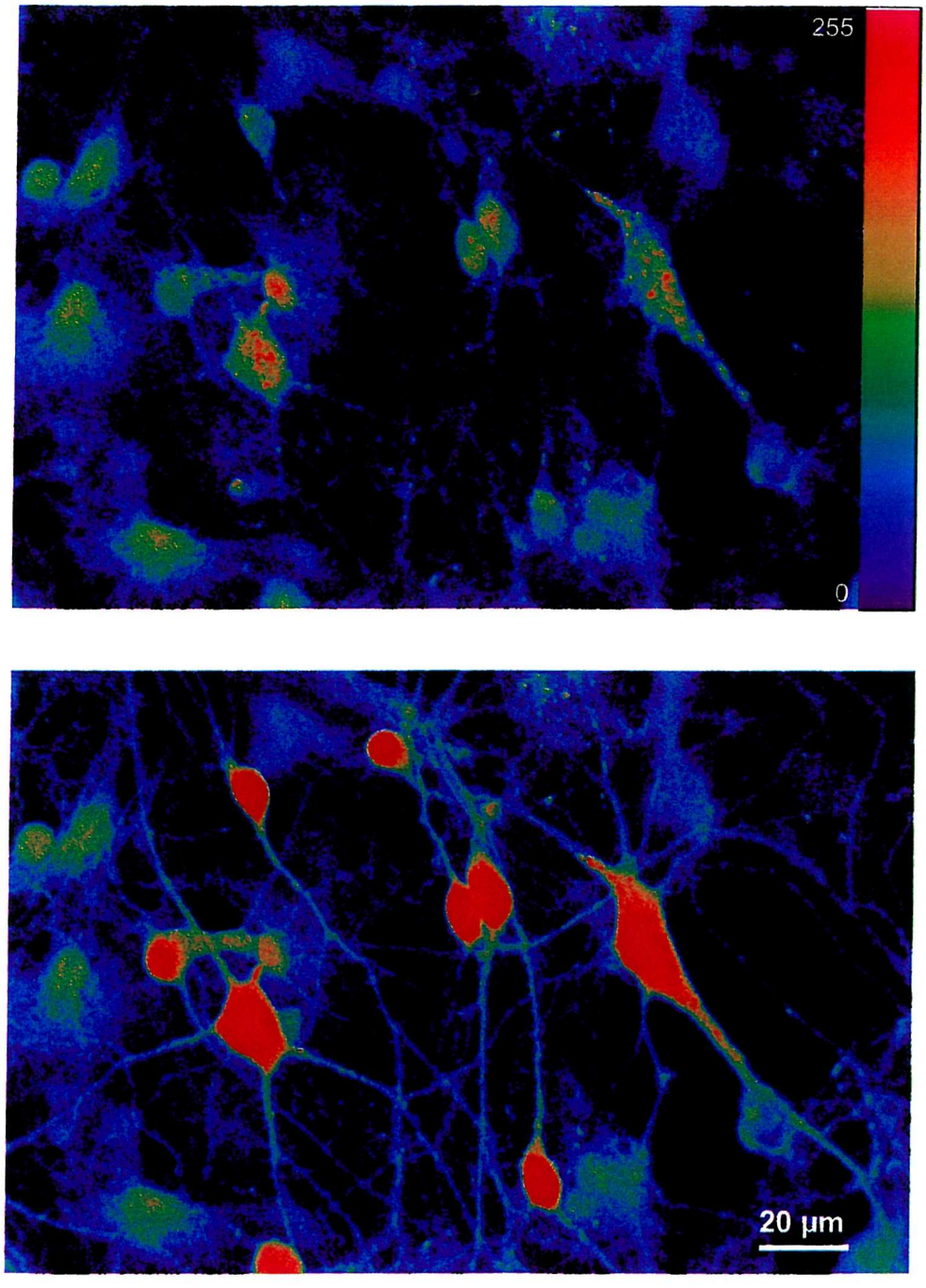

Figure 4.51 Confocal images showing Fluo-3 fluorescence in cultured hippocampal neurons before (top) and after (bottom) the addition of 10µM kainate. The image clearly illustrates the increase in $[Ca^{2+}]_i$ caused by kainate in different subtypes of hippocampal neuron including stellate, pyramidal and bipolar cells.

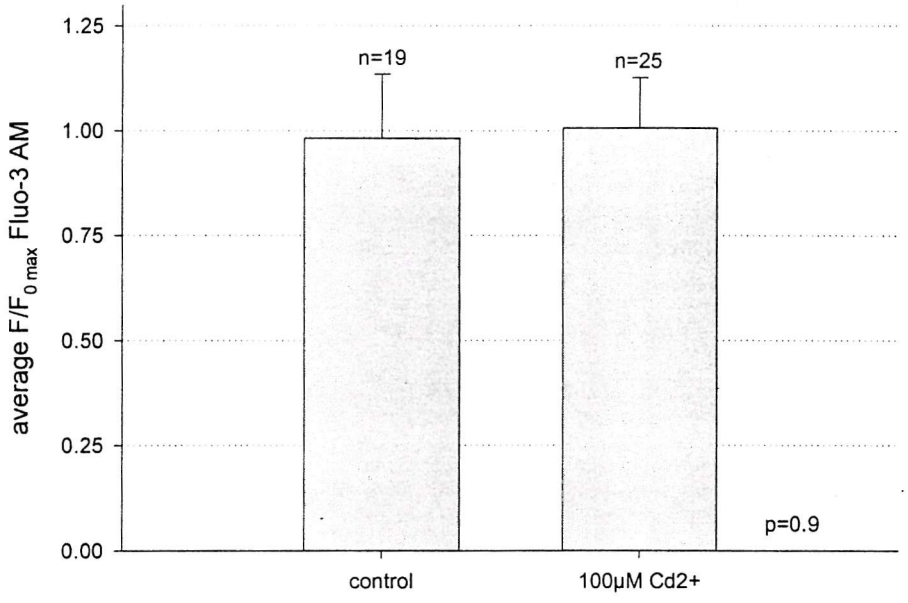

Figure 4.52 Average magnitude of initial increase in Fluo-3 fluorescence in untreated cells and cells pretreated with the VDCC blocker Cd^{2+}, following exposure to 10µm kainate. Neurons from age-matched cultures. Each bar represents the average of at least 3 culture plates from each treatment group.

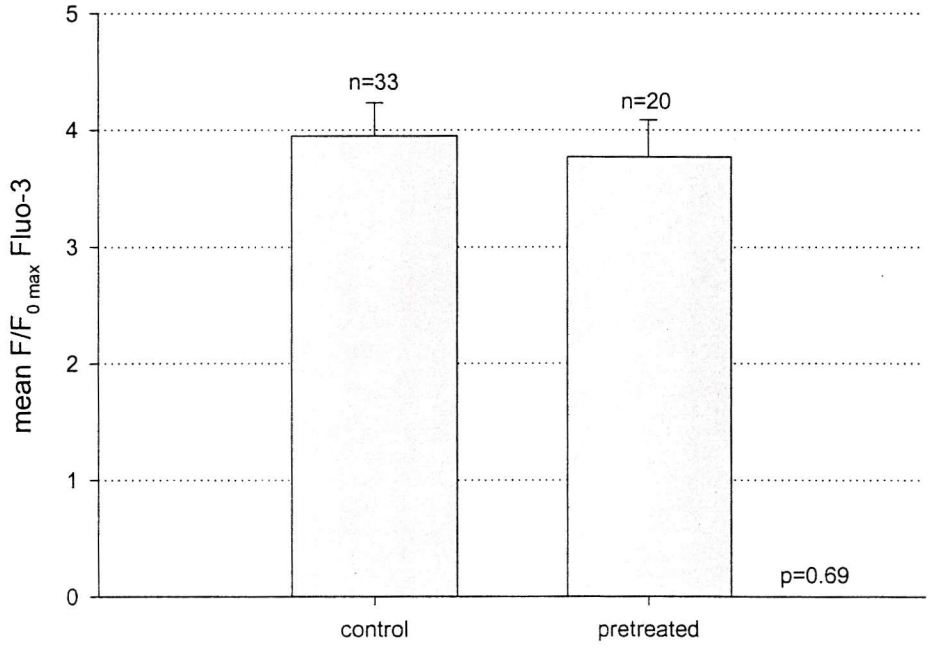

Figure 4.53 Average magnitude of initial increase in Fluo-3 fluorescence in untreated cells and in cells pretreated with a mixture of 100µM D-AP5 and 100µM CNQX, following the addition of 10µM kainate. Neurons from age matched cultures. Each bar represents the average of at least 3 culture plates from each treatment group.

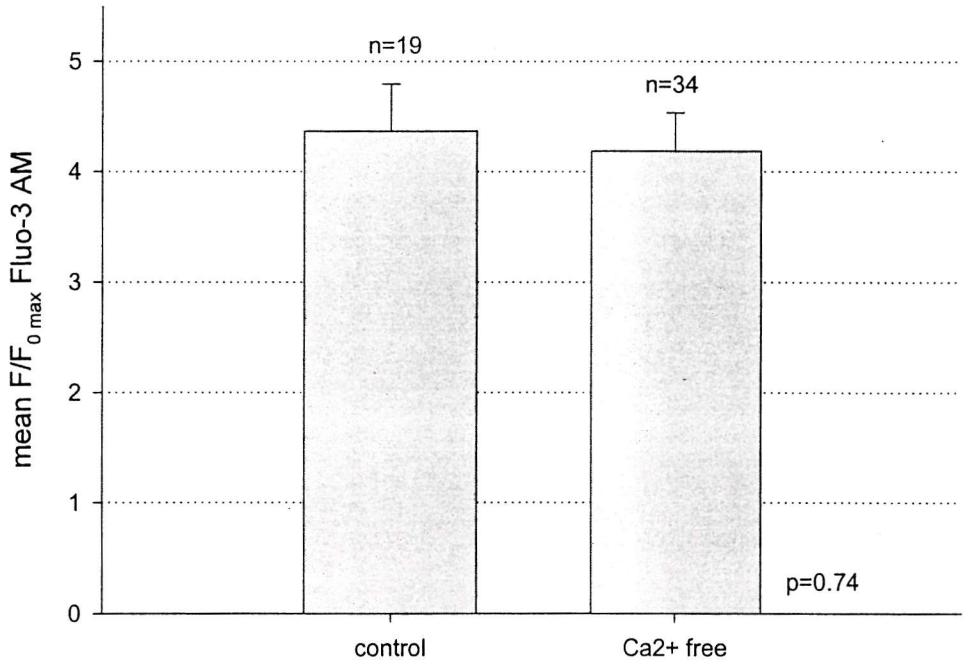

Figure 4.54 Average magnitude of initial increase in Fluo-3 fluorescence in control neurons and neurons in zero Ca^{2+} buffer with 100μM EDTA, following exposure to 10μm kainate. Neurons from age matched cultures. Each bar represents the average of at least 3 culture plates from each treatment group.

The contribution of intracellular Ca^{2+} stores to the kainate-induced initial increase in neuronal $[Ca^{2+}]_i$ was investigated by the pretreatment of neurons with thapsigargin. Thapsigargin inhibits the ER Ca^{2+}-ATPase, preventing the refilling of ER Ca^{2+} stores, which become depleted through the non-specific Ca^{2+}-leak pathway. Thapsigargin very significantly potentiated the initial neuronal Ca^{2+} response to kainate and also to glutamate (**Fig. 4.55**), and reduced the initial neuronal Ca^{2+} response to 1S,3R-ACPD. Dantrolene, which blocks Ca^{2+} release from the ER, had no significant effect on initial Ca^{2+} responses to glutamate, kainate or ACPD (**Fig. 4.55**).

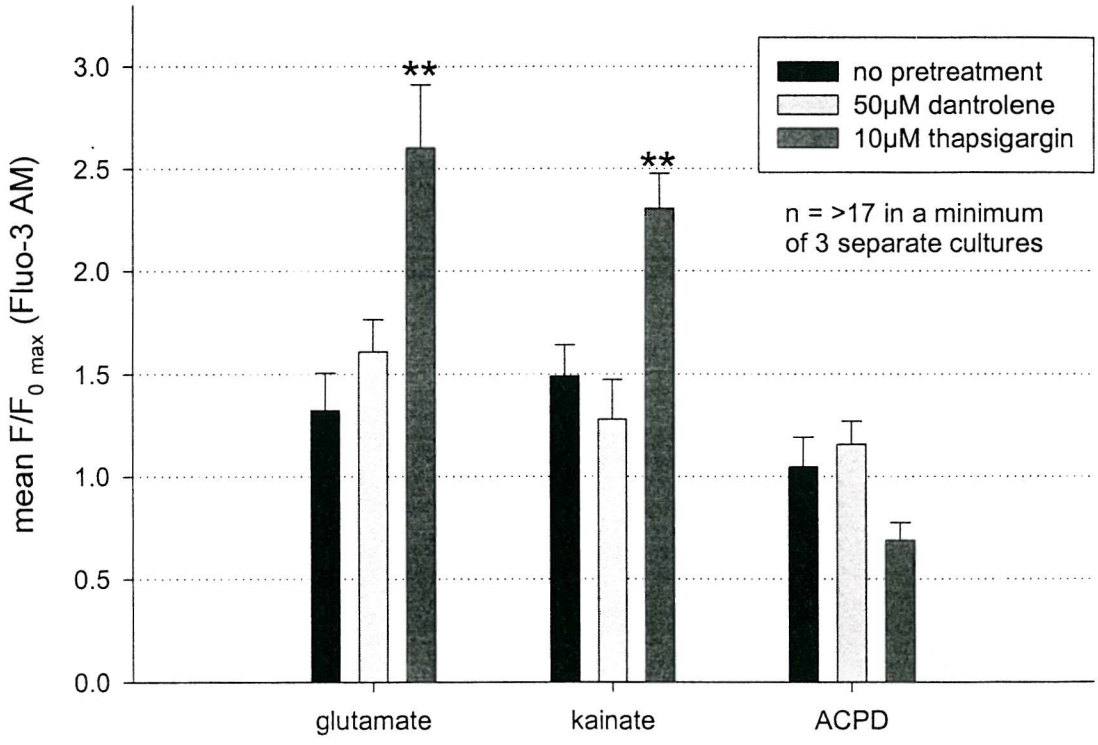

Figure 4.55 Average magnitude of initial increase in Fluo-3 fluorescence in control neurons, neurons treated with 10μM thapsigargin and neurons treated with 50μM dantrolene, following the addition of 10μM kainate. Each bar represents the average of at least 3 culture plates from each treatment group.

Neurons were treated overnight with 5μg/ml pertussis toxin (PTX) to investigate the involvement of G-proteins in the neuronal Ca^{2+} response to 10μM kainate. Pretreatment with PTX was found to significantly reduce the initial increase in neuronal Fluo-3 fluorescence after exposure to kainate (**Fig. 4.56**). **Fig. 4.57** (overleaf) shows Fluo-3 fluorescence in PTX-pretreated hippocampal neurons before and after the addition of 10μM kainate.

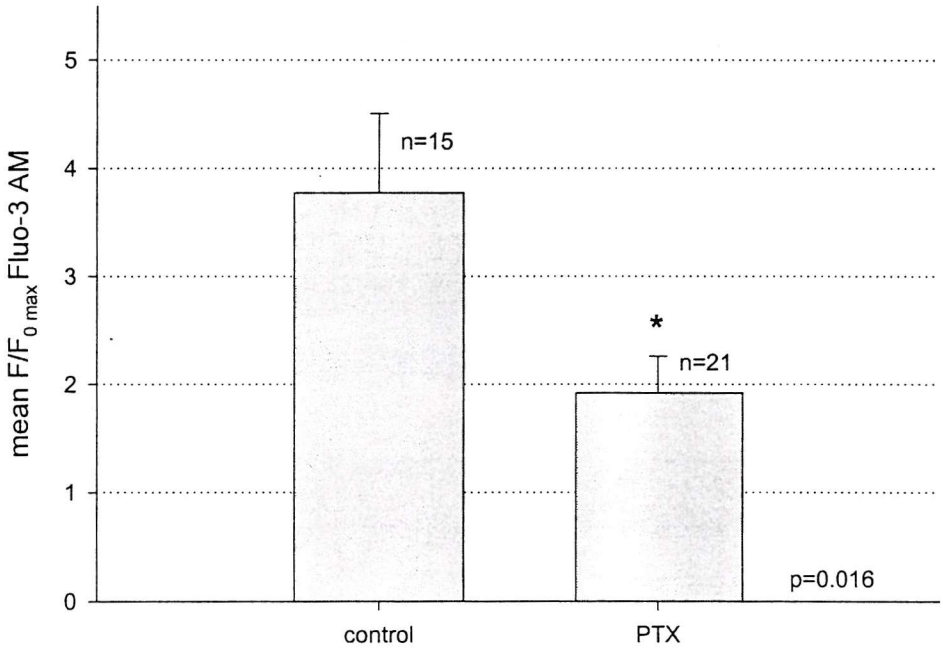

Figure 4.56 Average initial increase in Fluo-3 fluorescence in untreated neurons and neurons treated with 5μg/ml PTX, following the addition of 10μM kainate. Each bar represents the average of at least 3 culture plates from each treatment group.

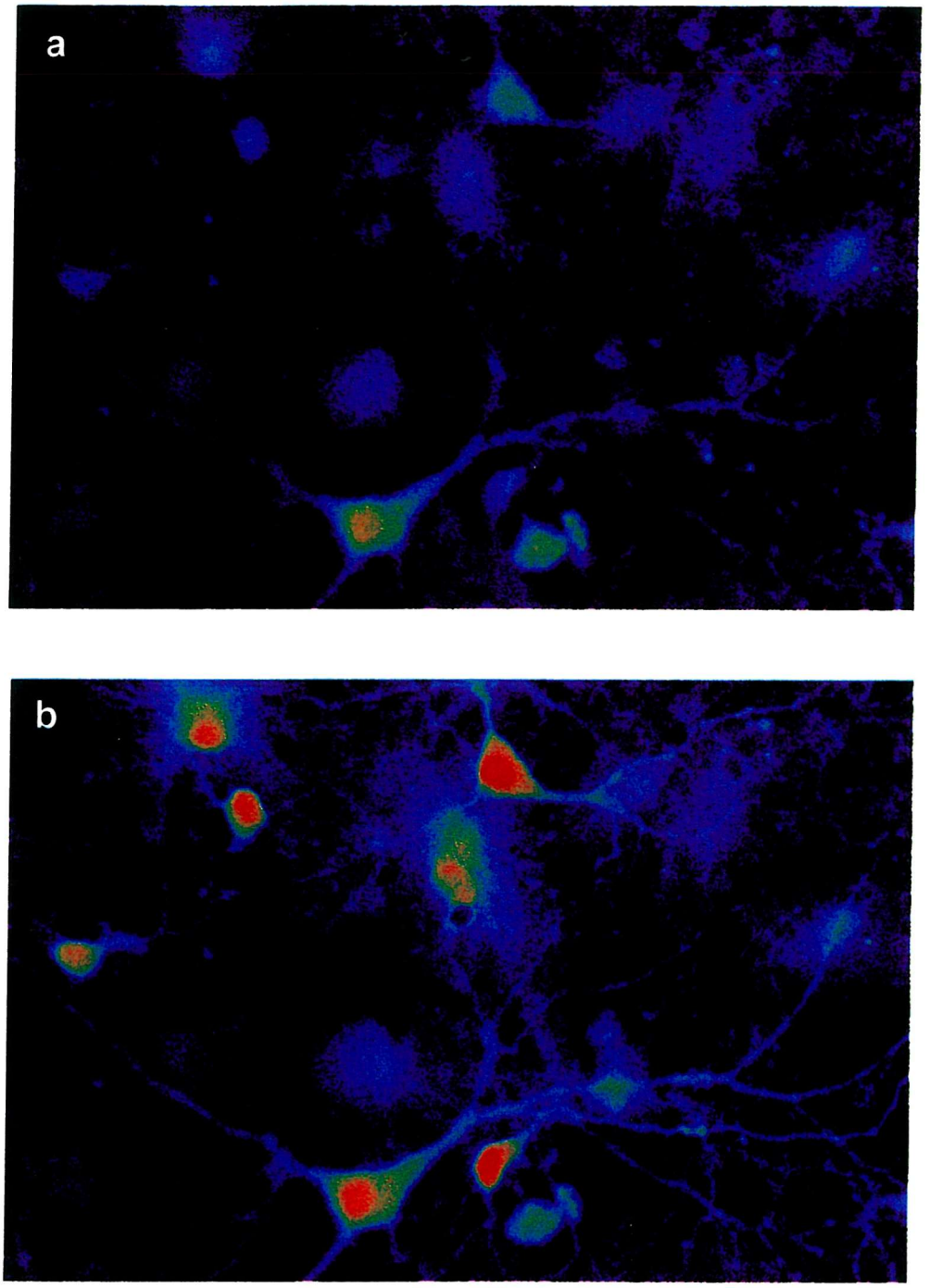

Fig. 4.57 Confocal images of PTX-pretreated hippocampal neurons, loaded with Fluo-3 AM. Images show neurons before (a) and after (b) stimulation with 10μM kainate.

4.3.6 Delayed Ca^{2+} deregulation revealed with Fluo 5N AM

Several recent studies have raised the possibility that high affinity Ca^{2+}-indicators such as Fluo-3 AM may underestimate increases in intracellular $[Ca^{2+}]$ associated with neurotoxic glutamate treatments, both in terms of magnitude and dynamics (Keelan *et al*, 1999; Hyrc *et al*, 1997; Stout and Reynolds, 1999). It was found that that kainate- and depolarization-induced $[Ca^{2+}]_i$ responses could be differentiated from glutamate responses only with low affinity indicators such as Mag-fura-2 (Stout and Reynolds, 1999). With this in mind, neuronal Ca^{2+} responses were monitored in cultured hippocampal neurons loaded with the low affinity Ca^{2+} indicator Fluo-5N AM (K_d for Ca^{2+} = 90μM) and exposed to kainate or NMDA. Figure **4.59** shows a typical timecourse of the change in neuronal Fluo-5N fluorescence caused by 500μM NMDA. Figure **4.58** (below) shows average neuronal Fluo-5N fluorescence at two timepoints following the addition of NMDA or kainate.

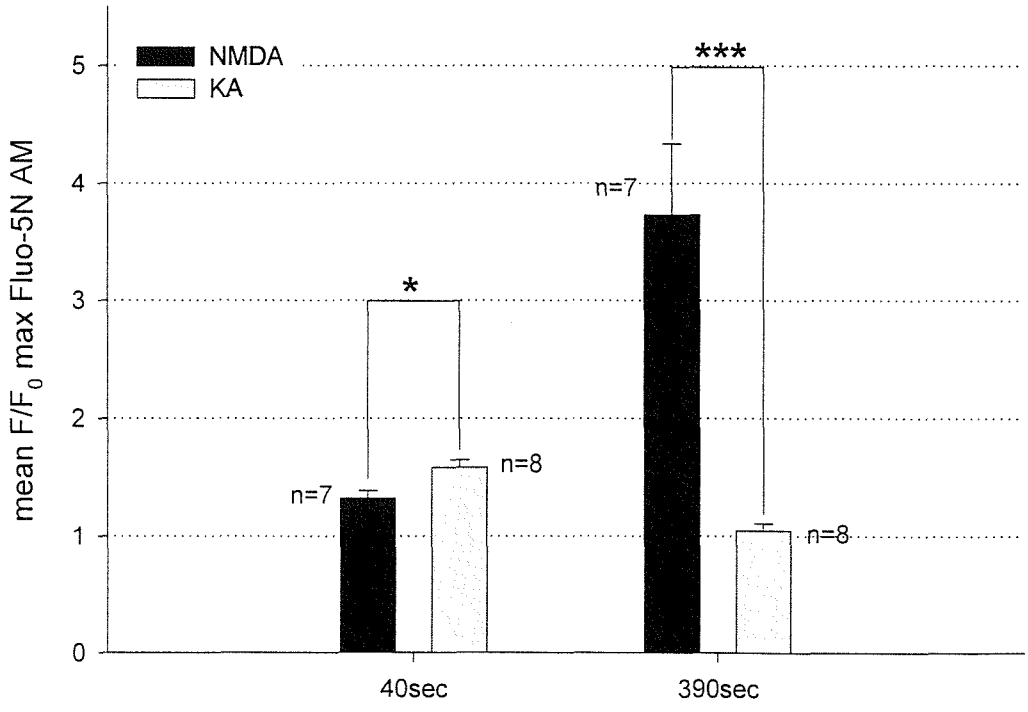

Figure 4.58 Average level of Fluo-5N fluorescence in cultured hippocampal neurons exposed to 500μM NMDA or 10μM kainate, at 40 seconds (initially following drug addition) and at 390 seconds (350 seconds after drug addition). Each bar represents the average of at least 3 culture plates from each treatment group.

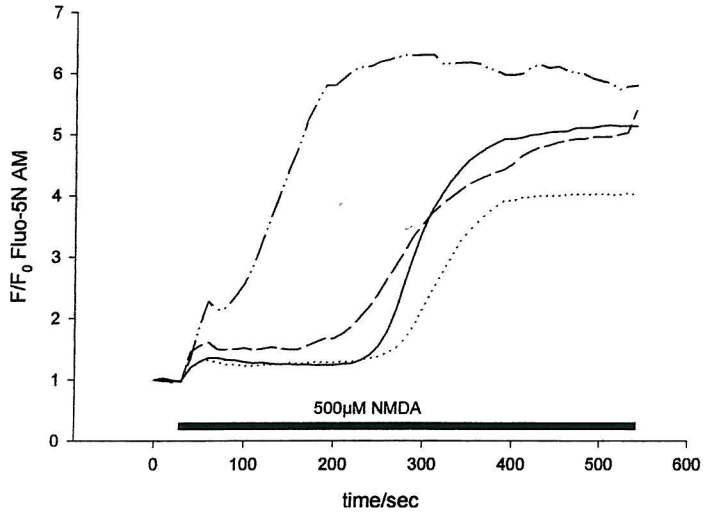

Fig. 4.59 Typical increase in neuronal Fluo-5N fluorescence in response to 500μM NMDA. The trace shows the response of four neurons on a single coverslip, and is representative of seven cells monitored in three separate experiments. Horizontal bar indicates time and duration of exposure to NMDA.

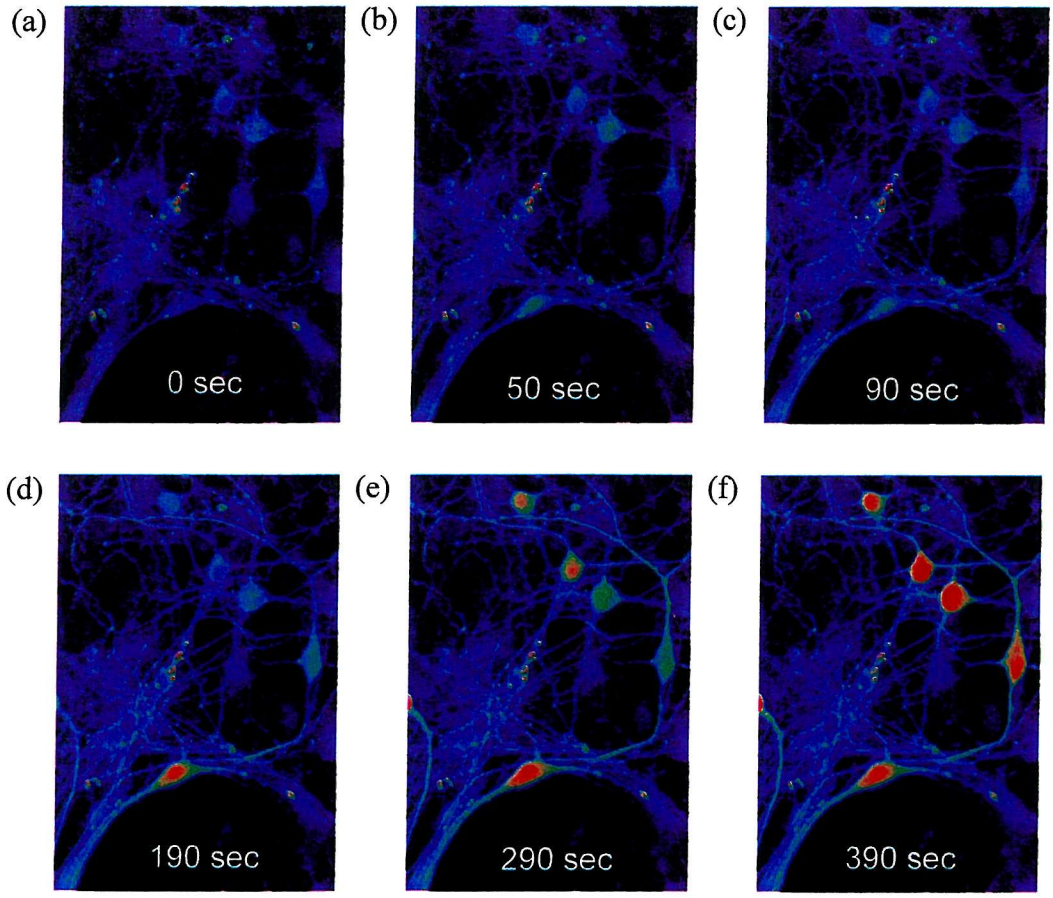

Fig. 4.60 Images selected from a time series of confocal images showing Fluo-5N fluorescence in hippocampal neurons before (a) and following (b-f) the addition of 500μM NMDA. The images correspond to time points of 0, 50, 90, 190, 290 and 390 seconds on the graph, respectively.

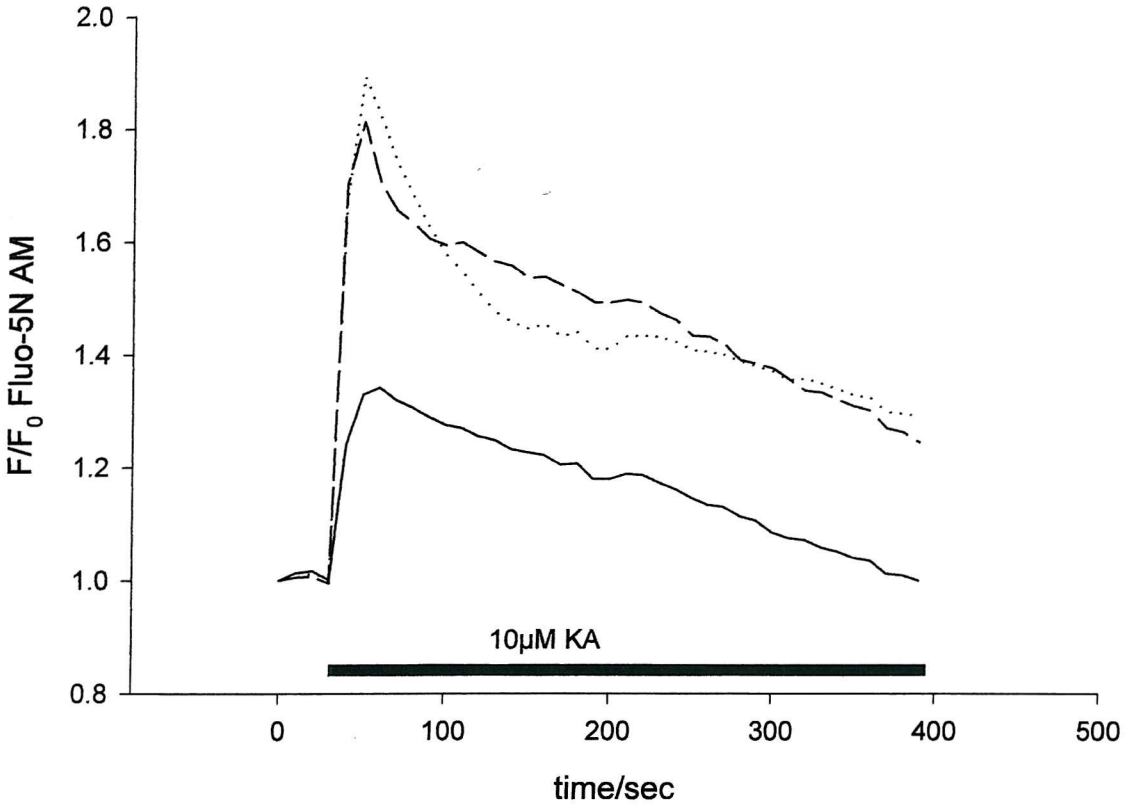

Fig. 4.61 Typical change in neuronal Fluo-5N fluorescence in response to 10μM kainate. The trace shows the response of three neurons on the same coverslip, and is representative of eleven cells monitored in three separate experiments. Horizontal bar indicates time and duration of exposure to kainate.

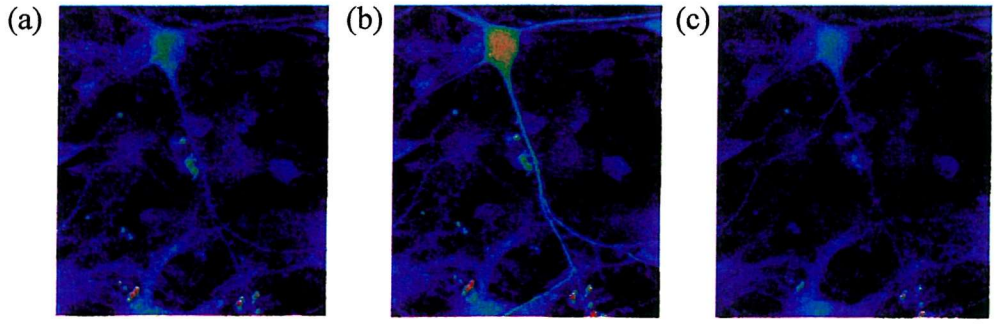

Fig. 4.62 Images selected from a time series of confocal images showing Fluo-5N fluorescence in a hippocampal neuron before (a) and following (b) and (c) the addition of 10μM kainate. The images correspond to timepoints of 0, 50 and 390 seconds on the graph, respectively.

Neurons showed an initial increase in fluorescence upon addition of NMDA or kainate. Figure **4.58** shows that the addition of kainate caused a significantly greater initial increase in Fluo-5N fluorescence at 40 seconds than that observed in neurons stimulated with NMDA. However, at 390 seconds, Fluo-5N fluorescence was very highly significantly greater in NMDA-stimulated neurons than in neurons exposed to kainate, where fluorescence had returned to resting levels. Fluo-5N revealed a delayed secondary increase in fluorescence starting at 160 sec after the addition of NMDA (earlier in one of the neurons monitored), indicating a delayed Ca^{2+} deregulation, a phenomenon that was never observed with the high affinity Ca^{2+} indicator, Fluo-3. Example images of neuronal Fluo-5N fluorescence before and throughout NMDA exposure are shown in Figure **4.60**. Figure **4.61** shows a typical timecourse of the change in neuronal Fluo-5N fluorescence caused by 10μM kainate. We observed no secondary rise in Fluo-5N fluorescence after the addition of kainate. Images of Fluo-5N fluorescence in neurons before and following the addition of kainate are shown in Figure **4.62**.

4.4 Discussion

4.4.1 Ca^{2+} responses and $\Delta\Psi m$ measured in acutely dissociated hippocampal neurons prior to being placed in culture

The aim of the initial part of this study was to examine the capabilities of acutely dissociated mouse hippocampal neurons in terms of neuronal Ca^{2+} handling and mitochondrial energetics, before the cells were placed in culture. Using CLSM and the calcium-sensitive probe Fluo-3, we investigated calcium responses in acutely dissociated adult mouse hippocampal neurons, following plasma membrane depolarisation with 40mM K^+. Neurons generally responded with an increase in the Fluo-3 fluorescent signal (**Figs. 4.2** and **4.4**), reflecting elevated neuronal [Ca^{2+}]. The source of this Ca^{2+} was likely to be influx through VDCCs that are activated following depolarisation of the plasma membrane. The increase in Fluo-3 signal was reversible, with fluorescence increases returning close to baseline levels following wash off (see **Figs. 4.1** and **4.3**). This would suggest that acutely dissociated hippocampal neurons are able to maintain adequate calcium homeostasis under experimental conditions.

Despite these reversible neuronal calcium responses following exposure to K^+, no changes in Fluo-3 signal were observed upon the addition of 1mM glutamate, 100μM ACPD or 100μM kainate. It is likely that dissociated hippocampal neurons undergo substantial damage to their cell surface receptors as a consequence of exposure to proteases and mechanical damage during the process of trituration and are therefore rendered unable to respond to certain agonists.

We examined mitochondrial energetics in acutely dissociated hippocampal neurons from adult and neonatal mice, using CLSM and the potentiometric dye, TMRE. The addition of the protonophore FCCP increased TMRE fluorescence in both isolated neurons (**Figs. 4.5** and **4.6**) and neuronal clumps (**Figs. 4.7** and **4.8**) prepared from both adult and neonatal mice. The observed increase in TMRE fluorescence reflects redistribution of the dye

from mitochondria to the cytoplasm, a consequence of the mitochondrial depolarisation induced by FCCP. These results suggest that acutely dissociated hippocampal neurons are energetically viable, maintaining polarised mitochondria. The neurons could either have fully functional mitochondria producing ATP, or could be drawing on cellular ATP reserves to sustain mitochondrial $\Delta\Psi$, but these differences were not investigated.

In summary, acutely dissociated hippocampal neurons were found to be viable in terms of mitochondrial energetics and their ability to undergo reversible calcium increases following stimulation. However, we decided to use cultured mouse hippocampal neurons as an experimental model for the purposes of this investigation, given their many advantages over acutely dissociated neurons. During the culture period, neurons are able to re-establish dendrites and cell surface receptors damaged during the isolation procedure, and become firmly adherent to the cover slip. This lack of movement is a crucial factor to successful imaging experiments.

4.4.2 Increased neuronal Ca^{2+} activity elicited by excitatory amino acids

Cultured neurons have been used extensively in studies employing imaging techniques to investigate neuronal Ca^{2+} responses and changes in mitochondrial function which follow glutamate receptor activation. In the first part of this study, we exposed cultured hippocampal neurons to the glutamate receptor agonists glutamate, kainate, 1S,3R-ACPD, NMDA, quisqualate and AMPA, and examined neuronal Ca^{2+} increases using CLSM and Fluo-3. In each instance, neurons responded with an initial increase in $[Ca^{2+}]_i$ (see Figures **4.11 – 4.31**), in good agreement with the literature, where it is well documented that exposure to EAAs causes elevated neuronal Ca^{2+} activity. Increased Ca^{2+} levels have been measured, using fluorescent Ca^{2+} indicators, in neurons exposed to glutamate (Adamec *et al*, 1998; Keelan *et al*, 1999), kainate (Hoyt *et al*, 1998; Yin *et al*, 1999), NMDA (Segal and Manor, 1992; Schinder *et al*, 1996; Savidge and Bristow, 1997), 1S,3R-ACPD (Phenna *et al*, 1995), quisqualate (Murphy and Miller, 1989) and AMPA (Brorson *et al*, 1994; Okada *et al*, 1999).

4.4.3 Effect of excitatory amino acids on mitochondrial membrane potential

Doses of each glutamate receptor agonist were chosen to elicit equivalent initial increases in neuronal $[Ca^{2+}]_i$. The initial increases in neuronal Fluo-3 fluorescence caused by each drug were deemed to be "equivalent" given that they were not significantly different when compared with the students t-test. In the second part of this study, we investigated the effect of these imposed Ca^{2+} loads on mitochondrial $\Delta\Psi$, using CLSM and the potentiometric dye TMRE. In agreement with the large volume of literature relating to this field (Schinder *et al*, 1996; White and Reynolds, 1996; Keelan *et al*, 1999; Khodorov *et al*, 1996; Stout *et al*, 1998; Isaev *et al*, 1996, Hoyt *et al*, 1997) the exposure of cultured hippocampal neurons to neurotoxic doses of either glutamate or NMDA caused an irreversible and highly reproducible mitochondrial depolarisation (see Fig. **4.38** and **4.44**). The addition of kainate caused a negligible change in TMRE signal (see Figs **4.39** and **4.40**), despite its well known neurotoxic properties (Berg *et al*, 1995). This correlates well with other studies which have found kainate to have no effect on mitochondrial membrane potential (Hoyt *et al*, 1998; Kiedrowski, 1998). The mGluR agonist 1S,3R-ACPD also did not have any effect on mitochondrial $\Delta\Psi$ (see Fig. **4.41**, **4.42**), although it has been shown to cause irreversible neuronal injury to striatal cells (Wang *et al*, 1997), and when infused into the rat hippocampus (Schoepp *et al*, 1995). It is surprising that ACPD, which causes the release of Ca^{2+} from intracellular stores, caused no apparent mitochondrial depolarisation, given that mitochondria have a well-established capacity to detect cytoplasmic Ca^{2+} signals resulting from the discharge of ER Ca^{2+} stores (Landolfi *et al*, 1998). IP_3-dependent Ca^{2+} responses have been observed to be accurately translated into elevations in mitochondrial Ca^{2+} levels, reflected in transient mitochondrial depolarisations (Simpson and Russell, 1998), but no change in mitochondrial polarisation was apparent in this study. No significant change in TMRE fluorescence was seen following neuronal exposure to AMPA (Fig. **4.45** and **4.46**), suggesting that the Ca^{2+} load imposed by AMPA caused a negligible mitochondrial depolarisation. In contrast, a recent flow-cytometric study using acutely

dissociated CGCs showed that AMPA caused a considerable reduction in mitochondrial membrane potential (Camins *et al*, 1998). This reduction in $\Delta\Psi m$ was potentiated by cyclothiazide, a blocker of AMPA receptor desensitization. In the same study, the observation was made that FCCP enhanced the AMPA induced Ca^{2+} increase, implying that the Ca^{2+} load imposed by AMPA is buffered by mitochondria (Camins *et al*, 1998). The exposure of cultured hippocampal neurons to quisqualate caused virtually no change in neuronal TMRE fluorescence (Figs **4.47** and **4.48**), showing that the neuronal Ca^{2+} load imposed by quisqualate did not cause mitochondrial depolarisation.

4.4.4 Imposed neuronal Ca^{2+} loads do not necessarily cause mitochondrial depolarisation

These data clearly show a lack of correlation between the magnitude of imposed neuronal Ca^{2+} load and mitochondrial depolarisation (**Fig 4.49 and 4.50**). This suggests that in pathological processes, the route of calcium increase in neurons may be more critical than absolute neuronal Ca^{2+} load, a proposal borne out by several recent studies. Notably, Ca^{2+} loading of cortical neurons via NMDA receptor channels was found to be highly toxic, whereas identical Ca^{2+} loads incurred through VDCCs were completely innocuous (Sattler *et al*, 1998). Our data suggests that Ca^{2+} entry through the NMDA receptor may be focussed onto a vulnerable excitotoxic locus within the cell, given that the Ca^{2+} load imposed by NMDA caused a large mitochondrial depolarisation, and equivalent Ca^{2+} loads caused by other EAAs did not. Two possible mechanisms may account for the particular neurotoxicity of Ca^{2+} entry through the NMDA receptor:

1) The polyamine spermine is released in certain brain regions by NMDA receptor activation (Fage *et al*, 1992), and stimulates the rapid mode of mitochondrial Ca^{2+} uptake (Sparagna *et al*, 1995). This could explain the large mitochondrial depolarisation that follows neuronal exposure to NMDA or glutamate, but not kainate or AMPA.

2) NMDA receptor activation could be coupled to the activation of damaging intracellular signalling processes by PSD-95 protein (Sattler *et al*,

1999). PSD-95 is a scaffolding protein which anchors various molecules such as NOS in close proximity to the intracellular face of the NMDA receptor channel. Such molecules are therefore ideally placed to be activated by incoming Ca^{2+}. Calcium entry through the NMDA receptor could trigger the production of NO, which in itself is not neurotoxic, but may combine with superoxide to produce peroxynitrite, a highly damaging free radical.

4.4.5 Mechanism of the kainate-induced increase in neuronal $[Ca^{2+}]$

The addition of 10μM kainate to cultured hippocampal neurons caused a robust initial increase in $[Ca^{2+}]_i$ (Fig. **4.51**). In this study, we investigated the source of this elevated $[Ca^{2+}]_i$. The blockade of VDCCs (Cd^{2+}) (Fig. **4.52**) and NMDA and AMPA receptors (D-AP5 and CNQX) (Fig. **4.53**) did not significantly reduce the magnitude of Ca^{2+} response following the addition of KA, suggesting that Ca^{2+} influx through Ca^{2+}-permeable kainate receptors (Ca-A/K receptors) may be the main route of Ca^{2+} increase. It is highly possible that dissociated hippocampal cultures express elevated numbers of Ca-A/K receptors, since the synthesis of GluR2 is selectively reduced by trauma such as transient global ischaemia (Pellegrini-Giampietro *et al*, 1992), a condition mimicked by the mechanical and enzymatic stress intrinsic to the dissociation procedure. There is recent experimental evidence for the existence of Ca^{2+}-permeable kainate receptors on the dendrites, but not soma, of hippocampal neurons (Yin *et al*, 1999). Ca-A/K receptors are thought to coexist with Ca^{2+} -impermeable AMPA/kainate receptors on neuronal membranes (Weiss and Sensi, 2000) and there is much evidence to support their involvement in neurotoxicity. In cortical cultures, the application of kainate elicited a rapid Ca^{2+} influx through Ca-A/K receptors, causing neuronal Ca^{2+} overload and mitochondrial ROS production (Carriedo *et al*, 1998). Synaptically released Zn^{2+} is able to gain access to neurons through Ca-A/K receptors, where it potently causes mitochondrial dysfunction (Sensi *et al*, 1999). There are no known neuronal clearance mechanisms for Zn^{2+}, which therefore has persistent and potentially very damaging effects. Ca-A/K receptor channels are ideally suited for contributing to neurotoxicity, since they lack the voltage-dependent Mg^{2+} block of NMDA receptors that limits

the entry of ions in the absence of neuronal depolarisation (Weiss and Sensi, 2000). However, in our experiments, the removal of extracellular Ca^{2+} did not significantly reduce the magnitude of Ca^{2+} response elicited by kainate, even in the presence of 100μM EDTA (Fig. **4.54**). Influx of Ca^{2+} across the plasma membrane may therefore not contribute significantly to the initial increase in cytoplasmic [Ca^{2+}] that follows the application of kainate. This would also explain the apparent lack of effect of antagonists of VDCCs and ionotropic glutamate receptors.

The inhibition of G-proteins with pertussis toxin significantly reduced the kainate Ca^{2+} response (Fig. **4.56**), pointing to the possible involvement of metabotropic kainate receptors coupled to PTX-sensitive G_i/G_0 proteins in this response. Experimental evidence is emerging for the existence of G protein-coupled kainate receptors in CA1 of the hippocampus (Melyan *et al*, 2002; Rodriguez-Moreno and Lerma, 1998; Cunha *et al*, 1999). It is not therefore inconceivable that G protein-coupled kainate receptors could cause Ca^{2+} release from intracellular Ca^{2+} stores, possibly through the activation of the PLC/phosphoinositide/Ca^{2+} cascade. Further characterization of the functional role of metabotropic kainate receptors is undoubtedly required. Confocal images of PTX-pretreated neurons (**Fig. 4.57**) show healthy looking neurons with extensive dendrites (compare to Figures **3.5** and **3.6** in Chapter 3, showing healthy cultured neurons and cultured neurons following lethal exposure to NMDA). It is unlikely, therefore, that PTX reduced the kainate-induced Ca^{2+} response purely by causing neuronal damage. The preincubation of neurons with thapsigargin, an inhibitor of SERCAs, was found to significantly potentiate the neuronal Ca^{2+} response to KA (Fig. **4.55**). This suggests that the neuronal Ca^{2+} increase caused by kainate (which may originate from an as-yet-unidentified intracellular Ca^{2+} store coupled to G-proteins) may usually be buffered by Ca^{2+} uptake into the ER or other Ca^{2+} stores through SERCA pumps.

4.4.6 Delayed Ca^{2+} deregulation revealed with Fluo 5N AM

Using the low affinity Ca^{2+} indicator Fluo-5N AM, we monitored the pattern of increased $[Ca^{2+}]_i$ in cultured hippocampal neurons exposed to NMDA (500μM) or kainate (10μM). The initial Ca^{2+} increase (measured at 40 seconds) was significantly greater in neurons exposed to kainate than in those neurons stimulated with NMDA (Figure **4.58**). However, by 390 seconds, Fluo-5N fluorescence was very highly significantly higher in neurons stimulated with NMDA than in those stimulated with kainate (Figure **4.58**). NMDA therefore caused a large, late increase in Fluo-5N fluorescence, indicating delayed Ca^{2+} deregulation. This phenomenon was not seen with kainate, where fluorescence returned to resting levels after the initial increase (Figure **4.58-4.62**). We therefore found no evidence of delayed Ca^{2+} deregulation in neurons stimulated with kainate. When fluorescence changes were monitored using the high affinity Ca^{2+} indicator Fluo-3 AM, NMDA and kainate caused an immediate increase in neuronal fluorescence which remained elevated at a plateau level (Figures **4. 24** and **4.18**) and decreased from this plateau level when measured at 390 seconds (data not shown), a very different pattern to that seen with Fluo-5N AM (Figures **4.59** and **4.61**). These data mirror the results of a recent study where a biphasic Ca^{2+} response to glutamate in cultured hippocampal neurons was observed with the low affinity Ca^{2+}-indicator fura-2FF, but not its high affinity counterpart fura-2 (Keelan *et al*, 1999). What then could account for the delayed calcium deregulation observed in our experimental model? It is unlikely that DCD could be attributed to opening of the mitochondrial PTP since this phenomenon would result in a profound mitochondrial depolarisation. In our model, mitochondrial depolarisation was an early phenomenon that did not coincide temporally with DCD. It is more probable that the DCD may have occurred as a combined result of (1) Ca^{2+}-triggered free radical attack on the neuronal membrane and cellular components such as Ca^{2+} extruding proteins, and (2) an energetic crisis caused by the run down of neuronal ATP reserves following early mitochondrial depolarisation.

More than a decade ago, the observation was made that a delayed Ca^{2+} increase in cultured neurons lethally challenged with glutamate was a reliable indicator of impending cell death (Manev *et al*, 1989). This has been confirmed by subsequent studies showing a secondary, irreversible Ca^{2+} increase in cultured spinal and hippocampal neurons exposed to neurotoxic levels of glutamate (Tymianski *et al*, 1993; Randall and Thayer, 1992). In some studies, the delayed Ca^{2+} overload was dependent on extracellular Ca^{2+} (Manev *et al*, 1989; Randall and Thayer, 1992), but other studies suggest that impaired Ca^{2+} extrusion by the plasma membrane Na^{+}/Ca^{2+} exchanger may be more important than Ca^{2+} influx in the delayed loss of Ca^{2+} homeostasis (Khodorov *et al*, 1993). Several theories have been put forward to account for the phenomenon of delayed Ca^{2+} deregulation (DCD). Evidence that mitochondrial dysfunction may be involved in DCD was provided by a study where the addition of the mitochondrial inhibitors antimycin and oligomycin to cerebellar granule cells exposed to a 1 minute glutamate pulse caused DCD, when Ca^{2+} levels would usually recover in the absence of these inhibitors (Khodorov *et al*, 1996). This suggested that mitochondria have a role in protecting neurons against glutamate induced Ca^{2+} loads. Subsequent experiments found there was a strong correlation between glutamate induced mitochondrial depolarisation and DCD (Khodorov *et al*, 1996). Loss of $\Delta\Psi$ could contribute to DCD in several ways: by reducing the neuronal Ca^{2+}-buffering capacity, or by reversal of the ATP synthase, causing hydrolysis of cytoplasmic ATP and reducing the activity of ATP-dependent Ca^{2+}-exchangers on the plasma membrane. Both routes would ultimately destabilize neuronal Ca^{2+} homeostasis. In many cases, there is evidence for a role for ATP depletion in DCD. The ATP/ADP ratio is known to fall in neurons that undergo DCD (Ankarkrona *et al*, 1995; Budd and Nicholls, 1996). However, there is evidence that mitochondria within glutamate-stimulated neurons continue to generate ATP in the latent period before DCD (Nicholls and Budd, 2000). It is likely that ATP depletion could be a late stage consequence of DCD rather than a causative factor. It has been proposed that the secondary irreversible Ca^{2+} increase seen in neurons lethally challenged with glutamate could correspond to opening of the mitochondrial PTP, following excessive mitochondrial Ca^{2+} uptake

Chapter 5

INVOLVEMENT OF REACTIVE OXYGEN SPECIES AND TRACE METALS IN EAA TOXICITY IN CULTURED HIPPOCAMPAL NEURONS

CHAPTER 5 INVOLVEMENT OF REACTIVE OXYGEN SPECIES AND TRACE METALS IN EAA TOXICITY

5.1 Introduction

The overactivation of glutamate receptors is thought to be responsible for excitotoxic neuronal death in many instances of brain injury, including trauma, epilepsy and cerebral ischaemia. In most experimental models, it has been shown that glutamate toxicity is mediated through the activation of Ca^{2+} permeable NMDA receptors (Tymianski *et al*, 1993). Reduction of Ca^{2+} influx by the selective antagonism of NMDA receptors (Choi, 1988) or intracellular Ca^{2+} chelation (Abdel-Hamid and Tymianski, 1997) has been shown to reduce neurotoxicity, suggesting that NMDA-receptor mediated neuronal death is a consequence of neuronal Ca^{2+} overload. It is unlikely that neurotoxicity is a direct consequence of the degree of neuronal Ca^{2+} loading, as previously discussed in Chapter **4** (Michaels and Rothman, 1990; Dubinsky and Rothman, 1991; Tymianski *et al*, 1993; Sattler *et al*, 1998). The relative importance of the diverse downstream effects triggered by neuronal Ca^{2+} overloading is still under investigation. Ca^{2+}-induced nitric oxide production (Dawson *et al*, 1991), activation of calpains (Brorson *et al*, 1994) and cytoskeletal modifications (Nicotera *et al*, 1992) are all likely to contribute to excitotoxic damage.

Mitochondria are known to take up large amounts of Ca^{2+} during glutamate exposure (White and Reynolds, 1996). Originally, this was thought to be a beneficial Ca^{2+} buffering mechanism that would protect neurons against Ca^{2+} overload (Nicholls, 1985), but recent research would support mitochondrial Ca^{2+} uptake as having an obligate role in NMDA-receptor mediated neuronal death (Stout *et al*, 1998). Mitochondrial Ca^{2+} loading could cause lethal neuronal damage by ATP depletion (Ankarkrona *et al*, 1995), release of pro-apoptotic factors (Kruman and Mattson, 1999) or increased generation of

reactive oxygen species (ROS) (Dugan *et al*, 1995). A number of recent studies have employed oxidation-sensitive fluorescent probes to show that neurons generate ROS, including superoxide, during the toxic activation of glutamate receptors (Dugan *et al*, 1995; Bindokas *et al*, 1996; Patel *et al*, 1996; Prehn, 1998; Carriedo *et al*, 2000; Ceccon *et al*, 2000; Luetjens *et al*, 2000). These ROS were found to be generated intracellularly, since SOD or catalase, which scavenge extracellular ROS, did not reduce their production (Dugan *et al*, 1995). Inhibitors of mitochondrial electron transport, such as rotenone or antimycin, abolished the generation of ROS, strongly implicating mitochondria as the source of these ROS (Dugan *et al*, 1995; Bindokas *et al*, 1996; Sengpiel *et al*, 1998; Carriedo *et al*, 2000). The glutamate receptor-induced generation of ROS was strongly dependent on $[Ca^{2+}]_e$, and could be abolished by EGTA (Dugan *et al*, 1995) or by the use of Ca^{2+}-free saline (Patel *et al*, 1996). However, the increase in ROS triggered by glutamate receptor activation could not be mimicked by the Ca^{2+}-ionophore A232187 (Bindokas *et al*, 1996), and was blocked by NMDA receptor antagonists (Reynolds and Hastings, 1995), suggesting ROS production is a specific consequence of glutamate receptor activation.

There is some controversy in the literature as to whether the production of ROS is particular to the activation of NMDA receptors, or whether other glutamate receptor subtypes may trigger an increase in ROS. In murine cultures, $[Ca^{2+}]_i$ was increased by the addition of NMDA, kainate, KCl, ACPD and ionomycin, but only NMDA caused a concurrent elevation in ROS (Dugan *et al*, 1995). Other studies have shown that kainate toxicity is not associated with the generation of O_2^- radicals (Lafoncazal *et al*, 1993; Reynolds and Hastings, 1995). In contrast, the addition of AMPA and/or kainate increased neuronal ROS in cultured hippocampal neurons (Bindokas *et al*, 1996; Prehn, 1998), in cultured spinal neurons (Carriedo *et al*, 2000), in cultured cerebellar granule cells (Ceccon *et al*, 2000) and in rat cortical cultures (Patel *et al*, 1996). Further evidence for the involvement of ROS in neurotoxicity comes in the finding that antioxidants are protective in models of acute neuronal damage, as detailed in section **1.3.4.1**.

There is much evidence to support the involvement of NO in neurotoxicity (see section **1.3.3.1**). NMDA receptor activation generates nitric oxide via the Ca^{2+} dependent activation of neuronal NO synthase (Aizenman *et al*, 1998). This NO may be damaging when produced in excess. Inhibitors of nitric oxide synthase are neuroprotective in many models of neuronal death (Almeida *et al*, 1999), and NO donors are directly toxic to cultured neurons (Brorson *et al*, 1999).

Trace metals are likely to exacerbate neuronal oxidative stress given their role as catalysts of the Fenton reaction, which generates highly damaging hydroxyl radicals. Recent research has highlighted the potential involvement of Zn^{2+} and other trace metals in neural injury (see section **1.3.5**). In particular, it has been observed that the toxicity of Zn^{2+} to cortical cultures was worsened by the addition of AMPA or kainate; conversely zinc has been shown to potentiate the toxicity of AMPA and kainate in cortical cultures (Yin and Weiss, 1995). Zn^{2+} is thought to gain access to neurons through Ca^{2+}-permeable AMPA/kainate receptors (Ca-A/K channels), where it causes mitochondrial dysfunction (Sensi *et al*, 1999). A recent study has demonstrated direct Zn^{2+} uptake into mitochondria in intact neurons, where it triggered a sustained loss of $\Delta\Psi$ and prolonged ROS production (Sensi *et al*, 2000).

With these findings in mind, we decided to investigate superoxide production in cultured hippocampal neurons in response to a range of glutamate receptor agonists. We then looked for a possible correlation between the neurotoxicity of different glutamate receptor agonists, as investigated in **Chapter 3**, and their effect on neuronal superoxide production. We monitored the effect of oxidants on mitochondrial membrane potential, and finally, we investigated the putative neuroprotection afforded by ROS scavengers, inhibitors of nitric oxide synthase and chelation of trace metals in a model of NMDA neurotoxicity.

5.2 Methods

Imaging neuronal superoxide production

Cultured hippocampal neurons were loaded with 10μM dihydroethidium for at least 30 minutes at 37°C, then rinsed in PIPES buffer. Neuronal fluorescence was imaged before and after drug addition using CLSM, as described in Section **2.5**.

Imaging mitochondrial membrane potential

Cultured hippocampal neurons were loaded with 5μM TMRE for 5-10 minutes at 37°C then rinsed in PIPES buffer. Neuronal fluorescence was imaged before and after drug addition using CLSM, as described in Section **2.5**.

Imaging neuronal $[Ca^{2+}]_i$

Cultured hippocampal neurons were loaded with 10μM Fluo-3 AM for 120 minutes at 37°C, then rinsed in PIPES buffer. Neuronal fluorescence was imaged before and after drug addition using CLSM, as described in Section **2.5**.

Assessment of neuronal damage following exposure to EAAs

Cultured hippocampal neurons were prepared as previously described (Section **2.4.2.**). Neurons were exposed to EAAs for controlled periods of time, then allowed a 24-hour recovery time in fresh culture medium. Neuronal damage was assessed by counting the number of viable neurons (defined as being phase bright with dendrites) in a defined field of view, using an inverted Nikon microscope. In the neuroprotection experiments, neurons were exposed to the protective agent for at least 30 minutes prior to insult, then left for a 24-hour recovery period post-insult in fresh culture medium containing the protective agent.

5.3 Results

5.3.1 Imaging neuronal superoxide production in response to the addition of glutamate receptor agonists

The production of superoxide ($O_2^{\cdot}$) was measured in cultured hippocampal neurons by monitoring the fluorescence of dihydroethidium (Het). Dihydroethidium is essentially non-fluorescent until oxidised by superoxide to the fluorescent product ethidium. Studies using rat hippocampal neurons have shown that Het is oxidised only by $O_2^{\cdot}$, not by •OH, NO, $^{\cdot}ONOO$, H_2O_2, hypochlorite or singlet O_2 (Bindokas *et al*, 1996). An increase in fluorescence in cells loaded with Het is therefore taken as a selective indication of superoxide production. To ensure that in our system Het accurately reported changes in neuronal superoxide levels, a positive control was conducted using the enzymatic production of superoxide by xanthine/xanthine oxidase. Figure **5.2** shows that neuronal Het fluorescence was stable upon the addition of 100μM xanthine, and increased with the addition of xanthine oxidase. An increase in Het fluorescence is therefore a useful indicator of neuronal levels of superoxide. Figure **5.1** shows images of Het fluorescence in cultured hippocampal neurons before and following the addition of 100μM xanthine and 100mU xanthine oxidase. The mitochondrial uncoupler FCCP increased neuronal Het fluorescence (see Figures **5.3** and **5.4**).

Different glutamate receptor subtypes were selectively activated in an attempt to dissect out which glutamate receptor subtypes may be coupled to an increase in neuronal superoxide production, given that previous studies have shown that glutamate triggers neuronal production of reactive oxygen species (Carriedo *et al*, 2000). Therefore, Het fluorescence was measured in cultured hippocampal neurons exposed to 1mM glutamate, 10μM kainate, 500μM NMDA, 100μM ACPD, 100μM AMPA and 100μM quisqualate. Figures **5.5** to **5.16** show example images and example time courses of increased Het fluorescence in neurons exposed to these glutamate receptor agonists.

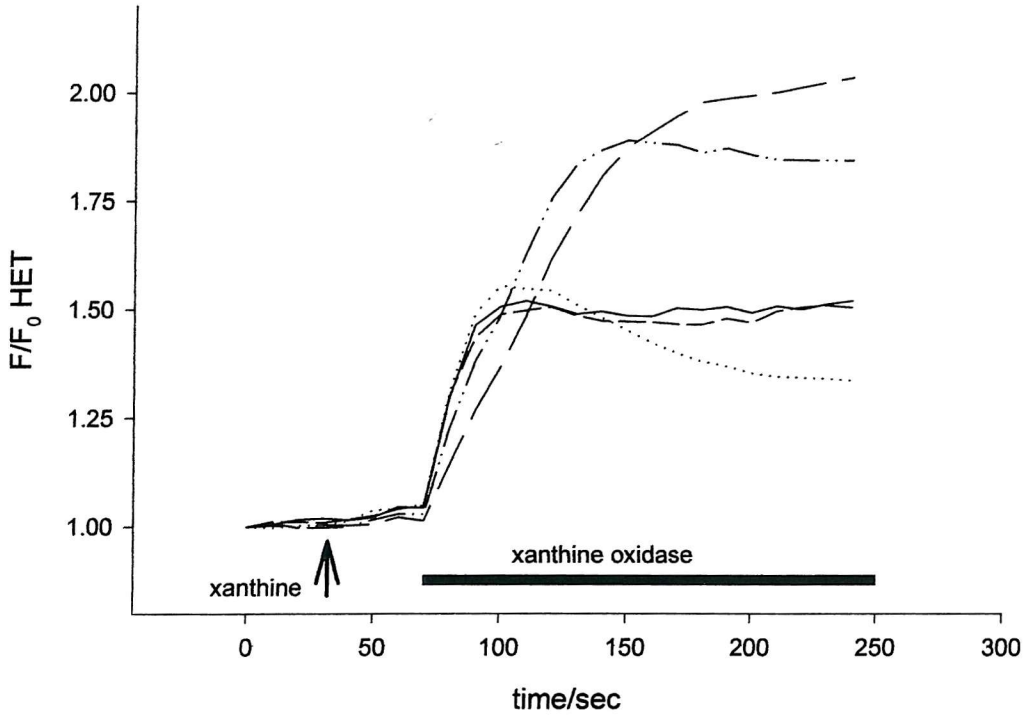

Figure 5.1 Typical change in neuronal Het fluorescence in response to the addition of 100μM xanthine and 100mU xanthine oxidase. Xanthine oxidase catalyses the oxidation of xanthine to uric acid with the concurrent production of superoxide. The trace shows the response of 5 neurons in a single cover slip, and is representative of 26 neurons monitored in 6 separate experiments. Horizontal bar indicates time and duration of exposure to XO.

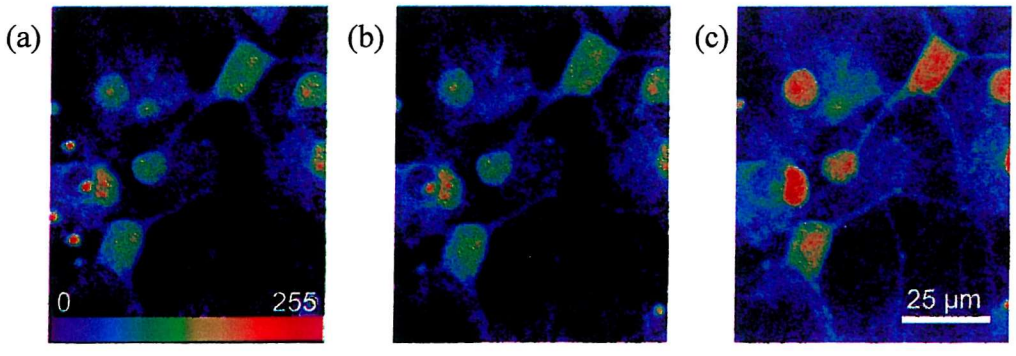

Figure 5.2 Images selected from a time series of confocal images showing Het fluorescence in hippocampal neurons before (a) and after (b) the addition of 100μM xanthine, and following the addition of 100mU xanthine oxidase (c). Het fluorescence was unchanged by xanthine, but increased upon the addition of xanthine oxidase. Het is therefore useful as an indicator of neuronal superoxide production.

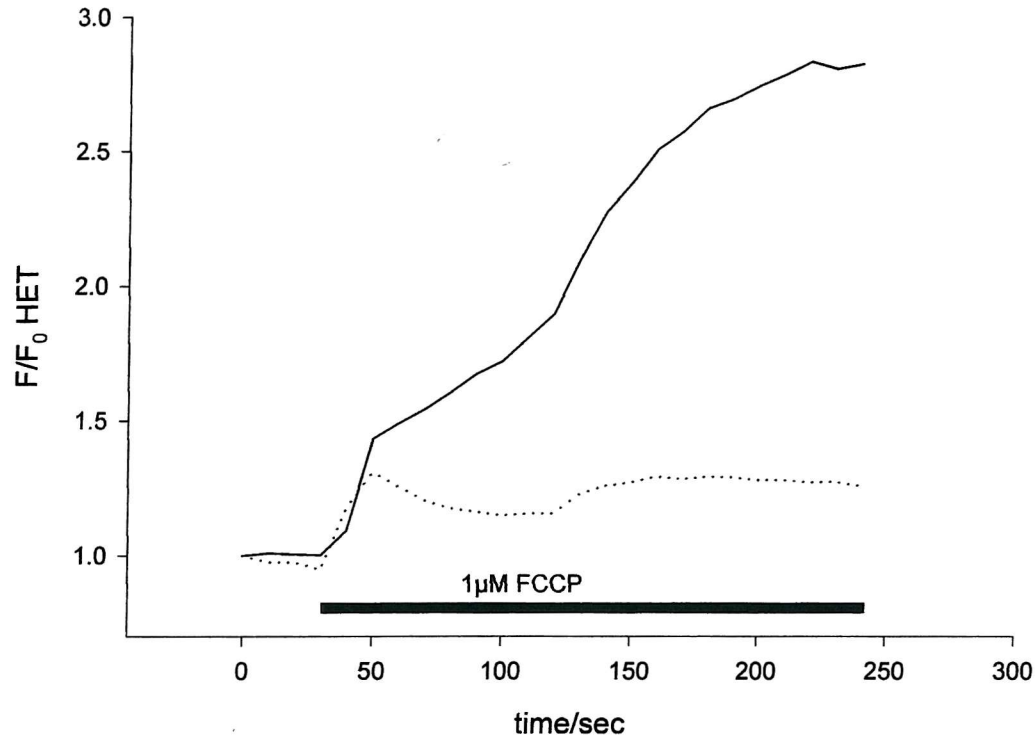

Figure 5.3 Typical increase in dihydroethidium fluorescence in response to 1μM FCCP. The trace shows the response of two neurons in a single cover slip, and is representative of twenty cells monitored in four separate experiments. Horizontal bar indicates time and duration of exposure to FCCP.

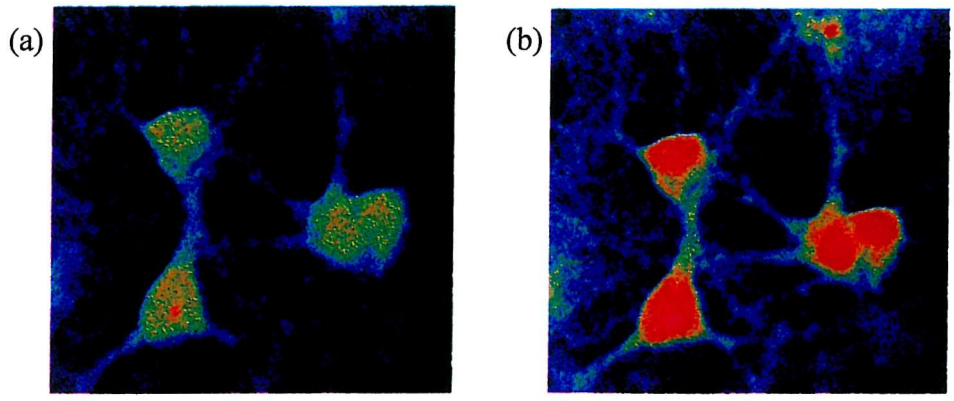

Figure 5.4 Images selected from a time series of confocal images showing dihydroethidium fluorescence in hippocampal neurons before (a) and after (b) the addition of 1μM FCCP. The increase in fluorescence may arise either from increased neuronal superoxide production following mitochondrial uncoupling, or from dequenching of mitochondrially sequestered dye.

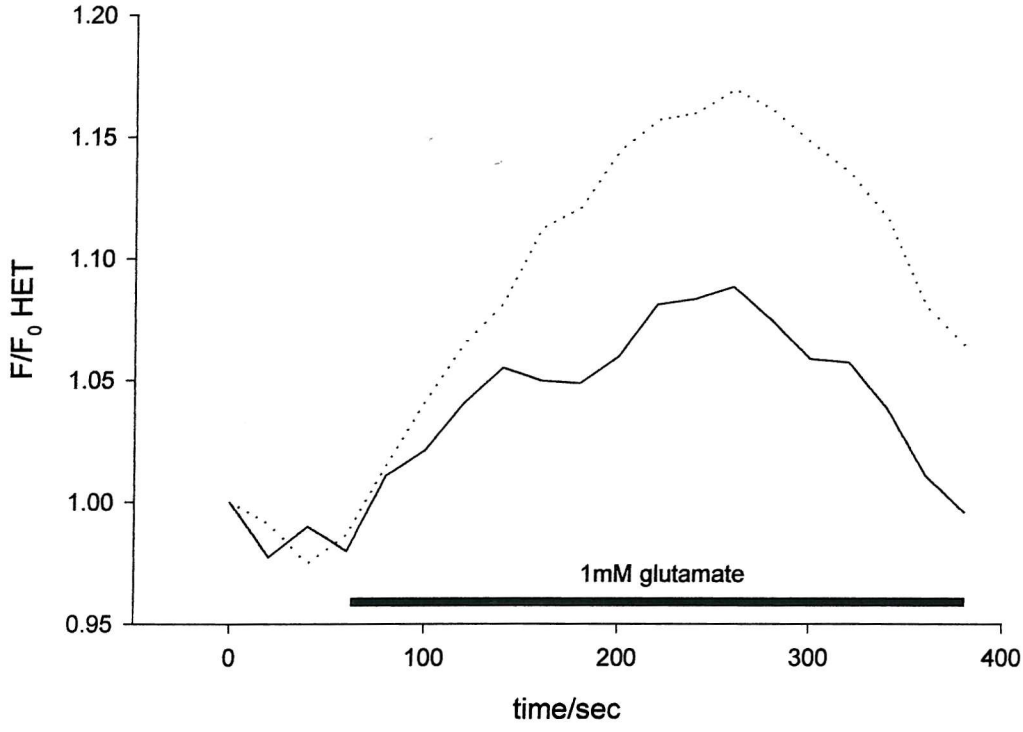

Figure 5.5 Typical increase in Het fluorescence in response to 1mM glutamate. The trace shows the response of two neurons in a single coverslip, and is representative of 24 cells monitored in 5 separate experiments. Horizontal bar indicates time and duration of exposure to glutamate.

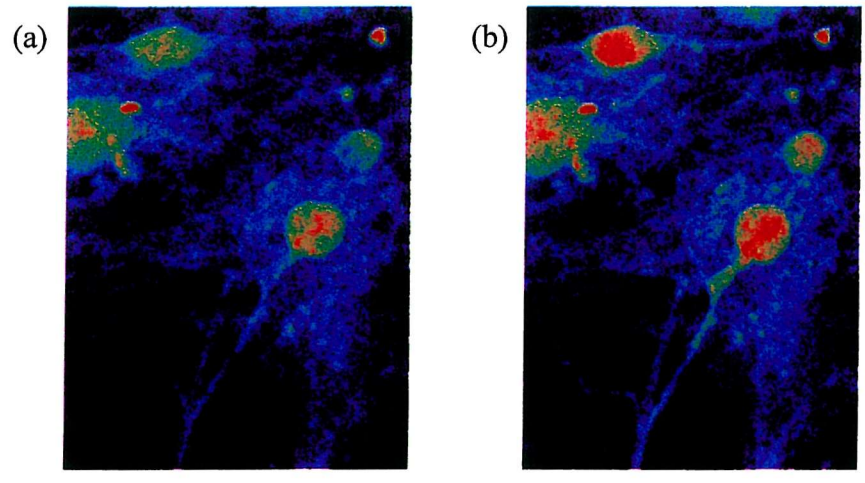

Figure 5.6 Images selected from a time series of confocal images showing Het fluorescence in hippocampal neurons before (a) and after (b) the addition of 1mM glutamate. The increase in Het fluorescence is indicative of neuronal superoxide production.

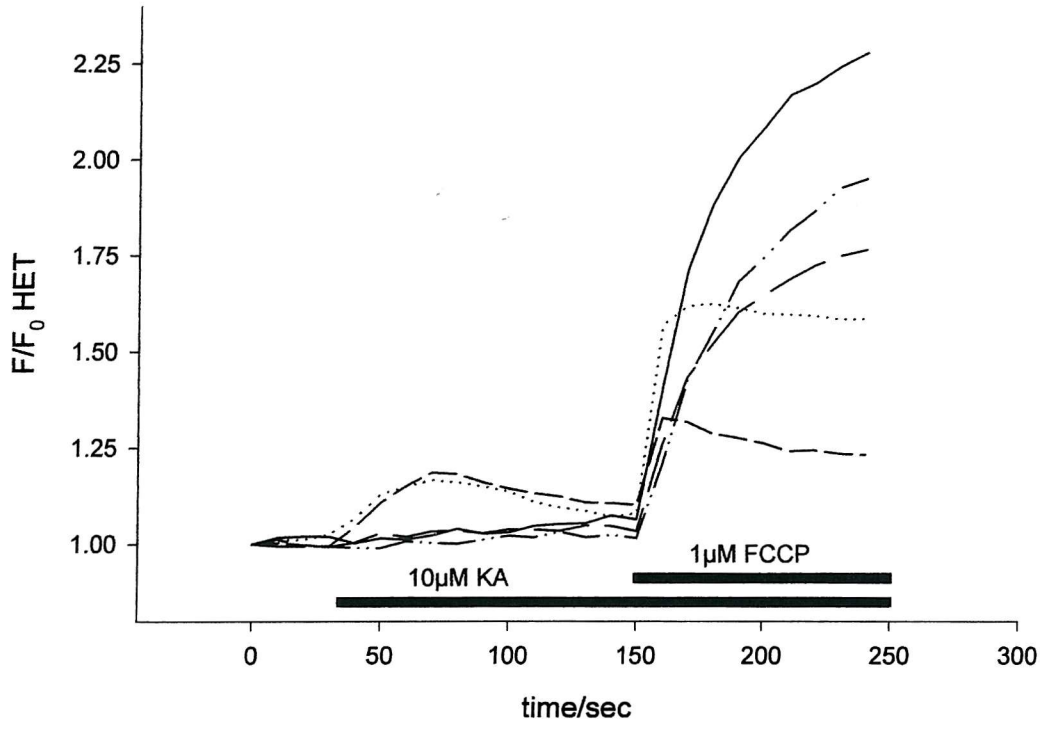

Figure 5.7 Typical change in neuronal HET fluorescence following exposure to 10μM kainate and 1μM FCCP. The trace shows the response of 5 neurons on the same coverslip, and is representative of 20 cells monitored in 4 separate experiments. Horizontal bars indicate time and duration of exposure to kainate and FCCP.

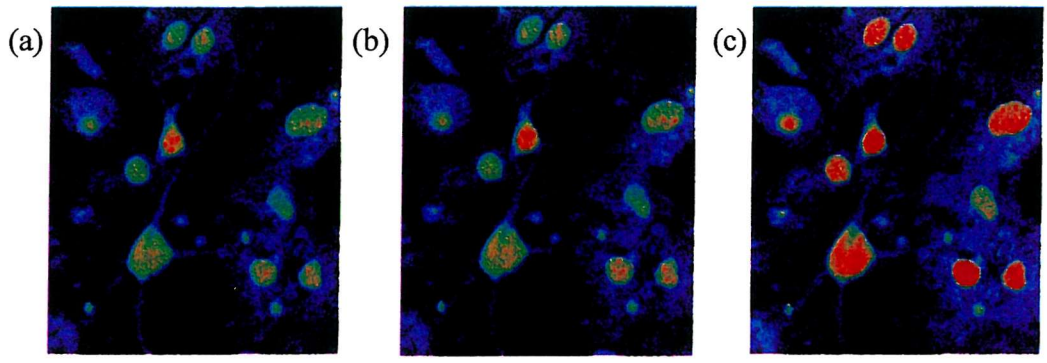

Figure 5.8 Images selected from a time series of confocal images showing dihydroethidium fluorescence in hippocampal neurons before (a) and after (b) the addition of 10μM kainate and (c) after the addition of 1μM FCCP. All neurons responded to FCCP with an increase in fluorescence, whereas only two neurons increased their fluorescence in response to kainate. Kainate may therefore cause an increase in superoxide production in only a subpopulation of neurons.

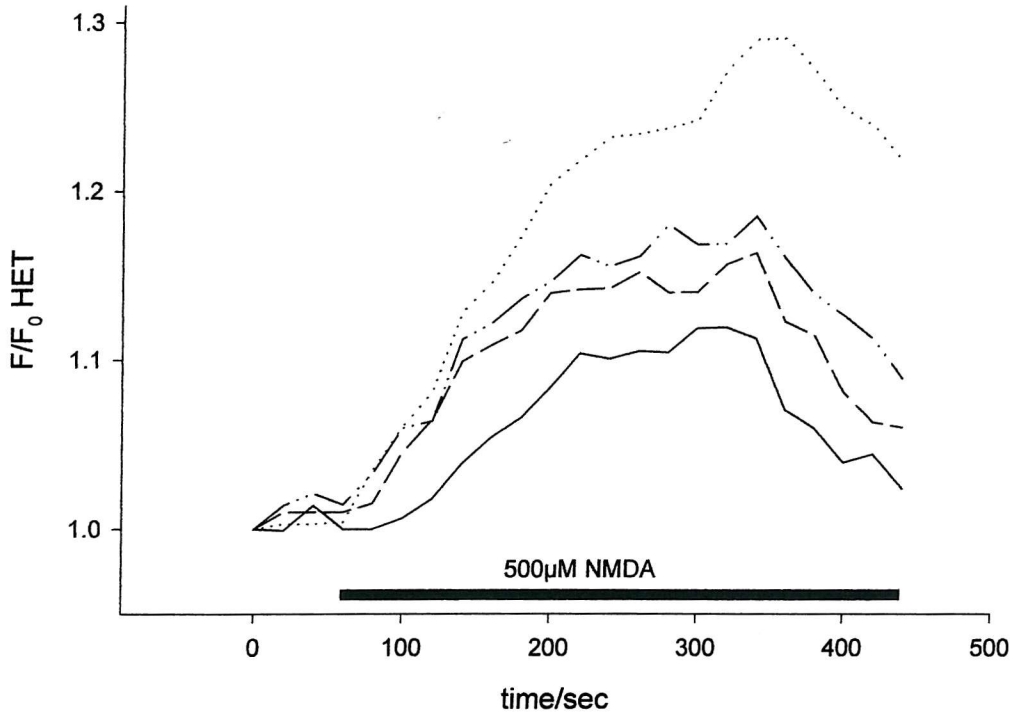

Figure 5.9 Typical increase in neuronal dihydroethidium fluorescence in response to 500μM NMDA. The trace shows the response of four neurons in a single cover slip, and is representative of twenty cells monitored in four separate experiments. Horizontal bar indicates time and duration of exposure to NMDA.

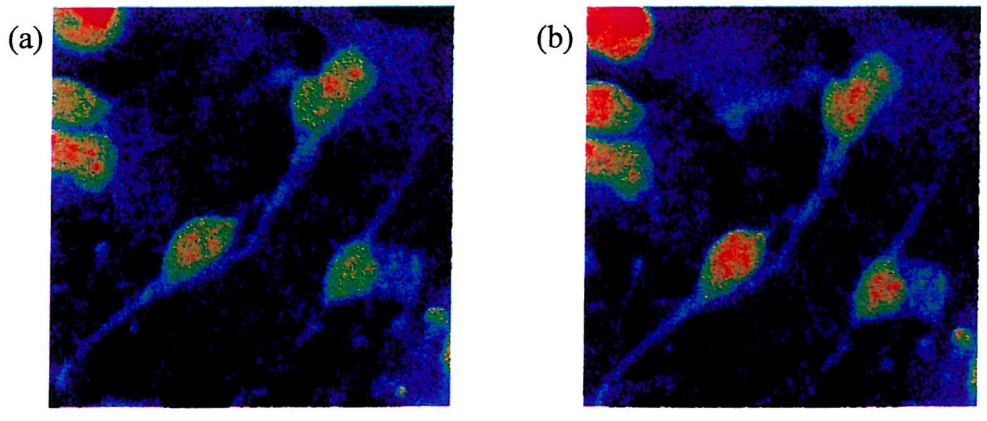

Figure 5.10 Images selected from a time series of confocal images showing dihydroethidium fluorescence in hippocampal neurons before (a) and after (b) the addition of 500μM NMDA. The increase in fluorescence is indicative of increased neuronal superoxide production.

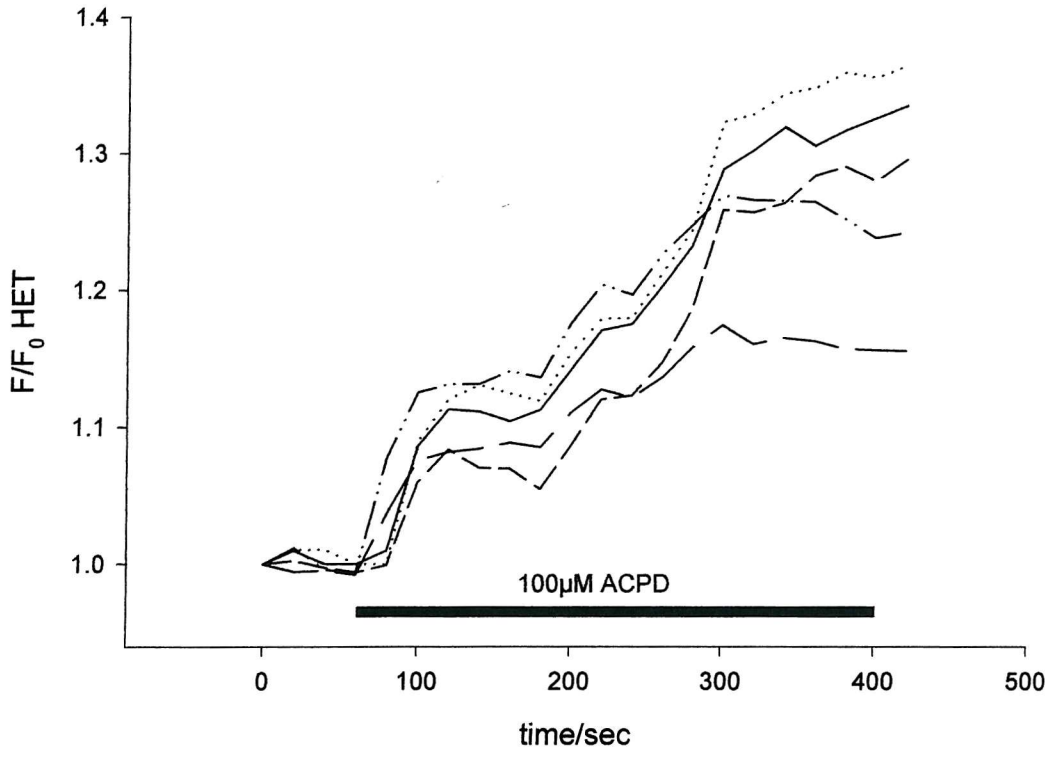

Figure 5.11 Typical change in neuronal HET fluorescence following exposure to 100μM ACPD. The trace shows the response of 5 neurons on the same coverslip, and is representative of 24 cells monitored in 4 separate experiments. Horizontal bars indicate time and duration of exposure to ACPD.

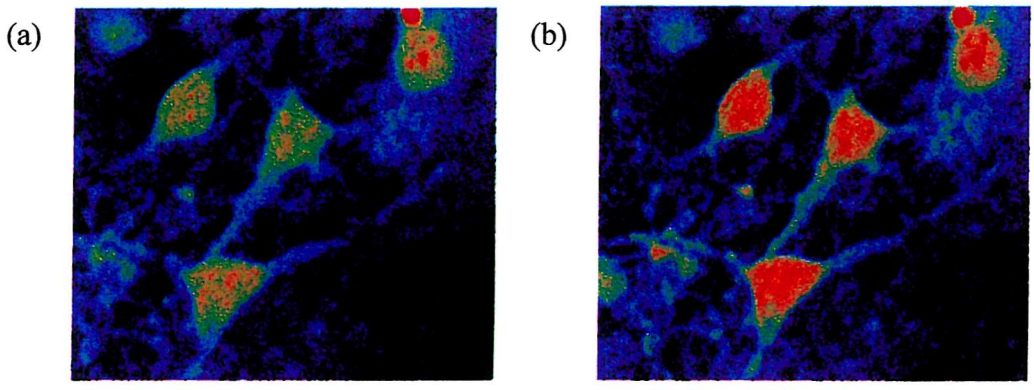

Figure 5.12 Images selected from a time series of confocal images showing dihydroethidium fluorescence in hippocampal neurons before (a) and after (b) the addition of 100μM ACPD. The increase in fluorescence is indicative of increased neuronal superoxide production.

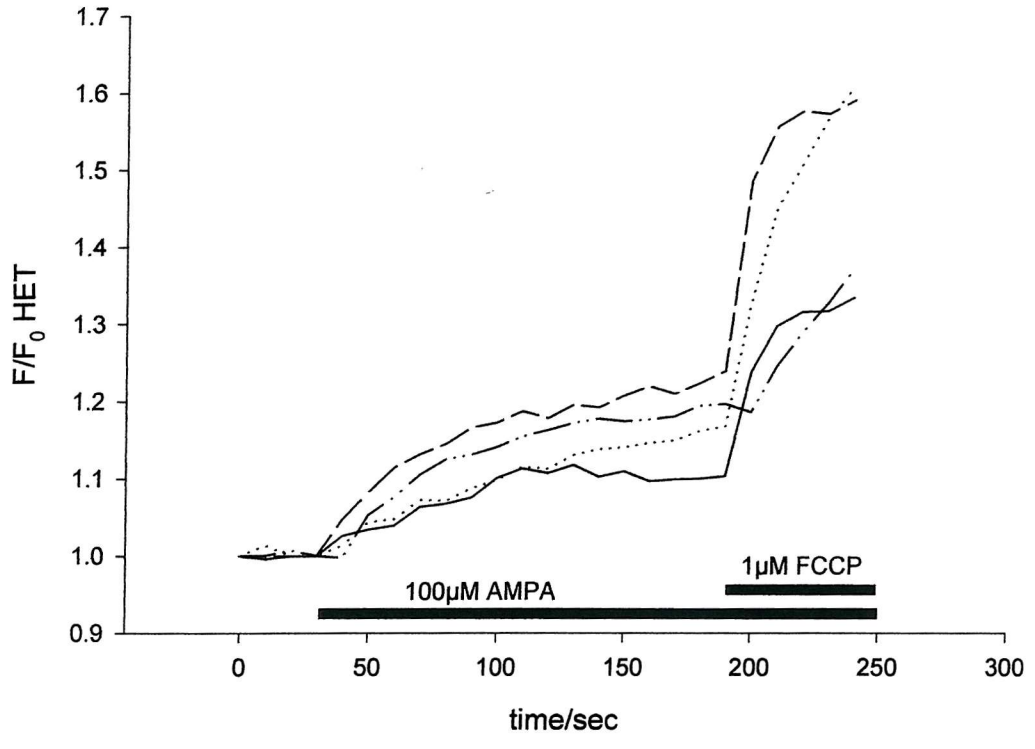

Figure 5.13 Typical change in neuronal HET fluorescence following exposure to 100μM AMPA and 1μM FCCP. The trace shows the response of 4 neurons on the same coverslip, and is representative of 20 cells monitored in 3 separate experiments. Horizontal bars indicate time and duration of exposure to AMPA and FCCP.

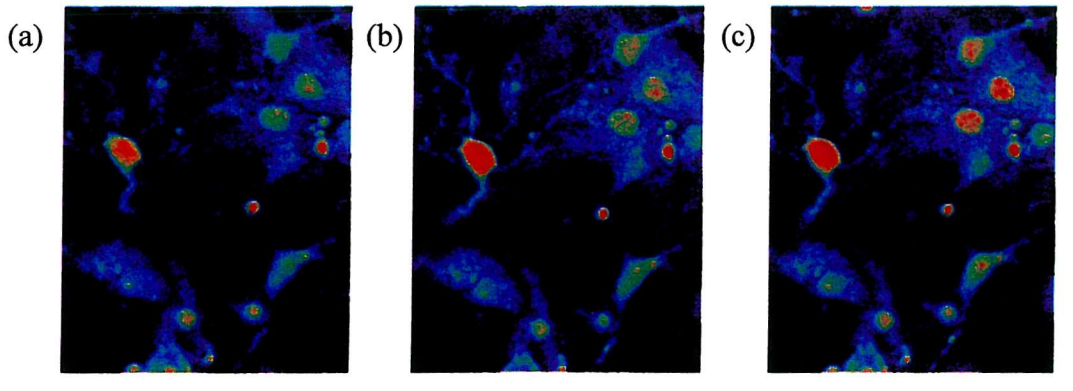

Figure 5.14 Images selected from a time series of confocal images showing dihydroethidium fluorescence in hippocampal neurons before (a) and after (b) the addition of 100μM AMPA and (c) after the addition of 1μM FCCP. The increase in fluorescence is indicative of increased neuronal superoxide production.

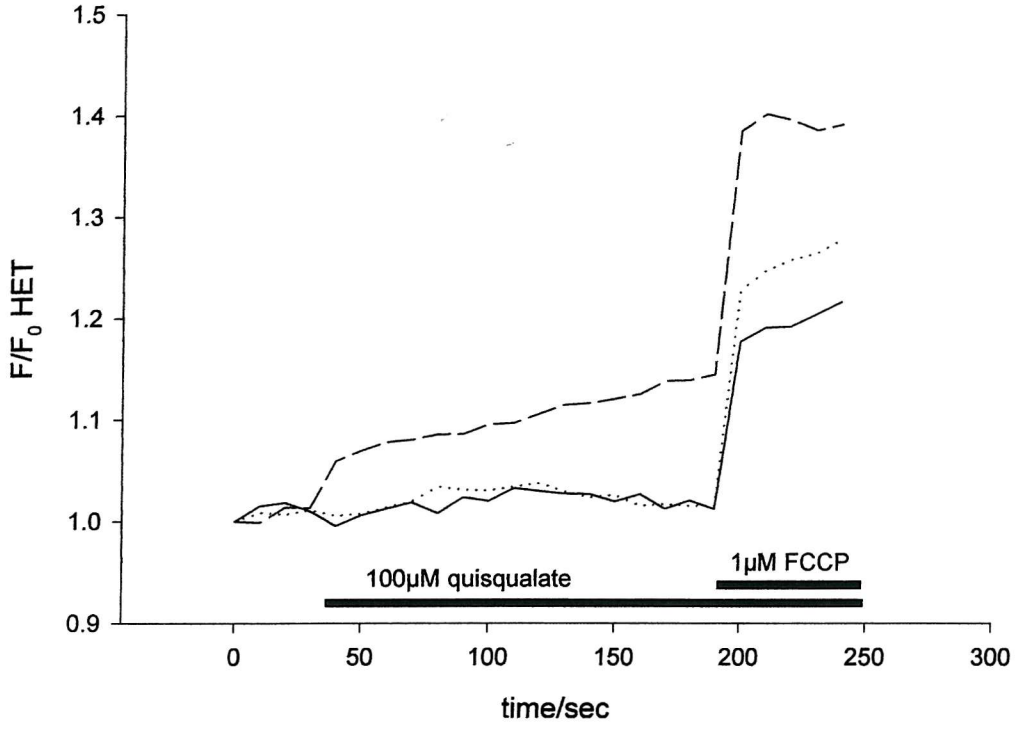

Figure 5.15 Typical change in neuronal HET fluorescence following exposure to 100μM quisqualate and 1μM FCCP. The trace shows the response of three neurons on the same coverslip, and is representative of five cells monitored in two separate experiments. Horizontal bars indicate time and duration of exposure to quisqualate and FCCP.

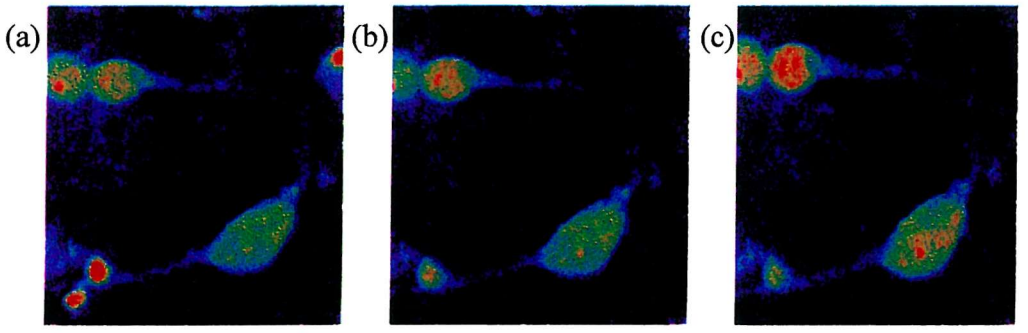

Figure 5.16 Images selected from a time series of confocal images showing dihydroethidium fluorescence in hippocampal neurons before (a) and after (b) the addition of 100μM quisqualate and (c) after the addition of 1μM FCCP. Both neurons responded to FCCP with an increase in fluorescence, whereas only the topmost neuron increased its fluorescence in response to quisqualate. Quisqualate may therefore cause an increase in superoxide production in only a subpopulation of neurons.

Neuronal Het fluorescence increased above control levels in many neurons following exposure to glutamate receptor agonists (Fig. **5.17**) but this response was variable. Het fluorescence did not increase in *all* neurons monitored in a single field of view. The number of neurons responding with an increase in Het fluorescence is indicated above each bar (Fig. **5.17**). Each bar shows the average increase in fluorescence in those neurons where Het fluorescence did increase above control levels. Neurons where Het fluorescence remained unchanged are not included in Figure **5.17**.

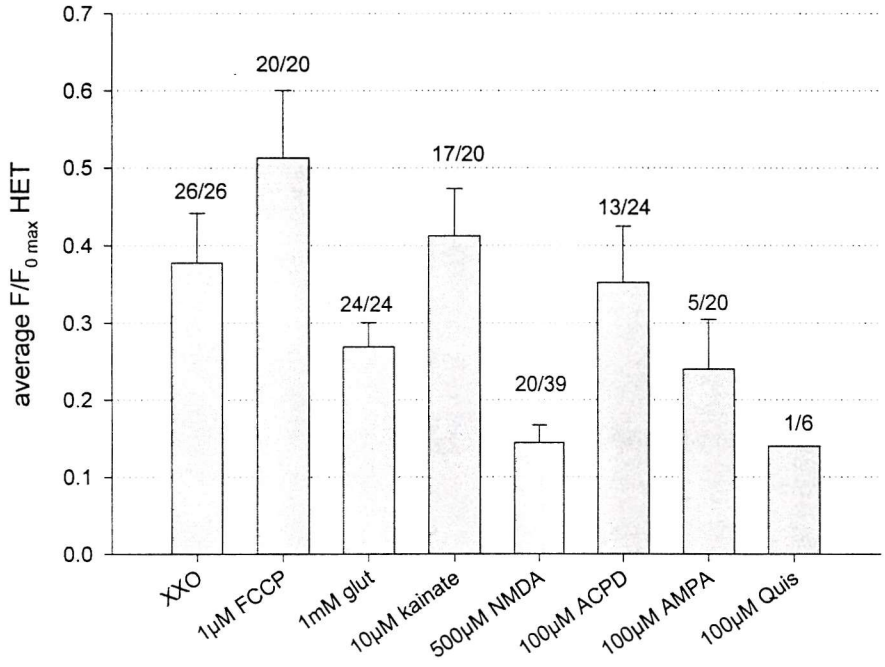

Figure 5.17: Average peak increases in neuronal dihydroethidium fluorescence caused by the addition of EAAs and positive controls to cultured hippocampal neurons Number of cells responding with an increase in Het fluorescence shown above bar. Each bar represents the average of at least 3 culture plates from each treatment group.

The percentage of neurons monitored which showed increased Het fluorescence in response to the addition of EAAs is shown in Fig. **5.18** (overleaf).

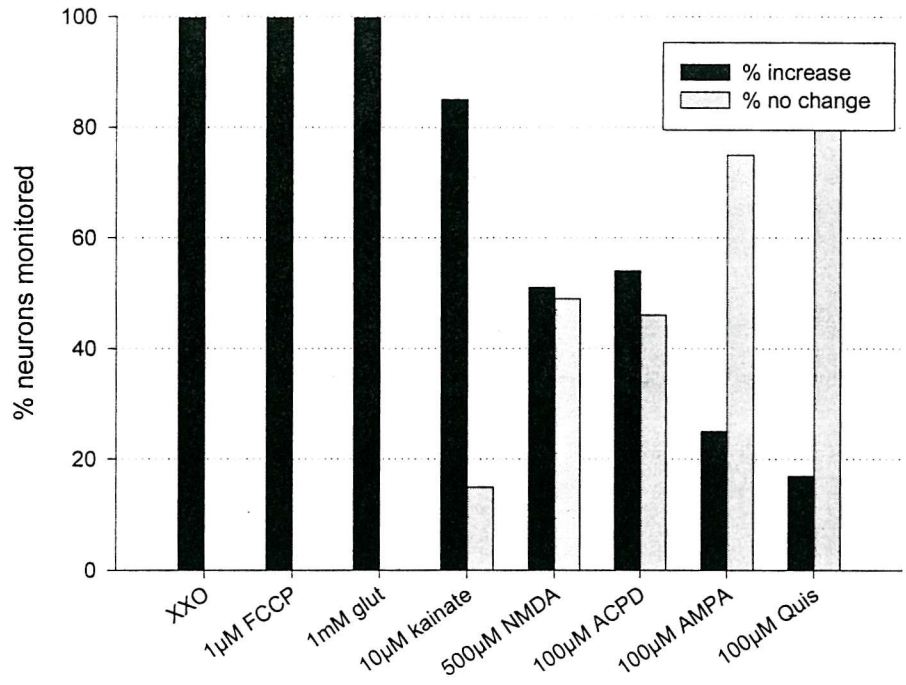

Figure 5.18 Variability of neuronal superoxide production in response to EAAs: percentage of neurons showing increased dihydroethidium fluorescence in response to EAAs and positive controls.

5.3.2 Effect of ROS on mitochondrial membrane potential

The effect of ROS on neuronal mitochondrial membrane potential was investigated by monitoring TMRE fluorescence in cultured hippocampal neurons exposed to hydrogen peroxide (H_2O_2). Figures **5.19** and **5.20** show that the addition of H_2O_2 caused a marked increase in neuronal TMRE fluorescence, indicative of mitochondrial depolarisation. Before the addition of H_2O_2, the pattern of TMRE staining in neurons was punctate, consistent with the accumulation of the probe in polarised mitochondria (Figure **5.20a**). The addition of H_2O_2 caused the redistribution of TMRE from mitochondria to the cytoplasm, resulting in increased fluorescence and a more diffuse pattern of staining (Figure **5.20b**).

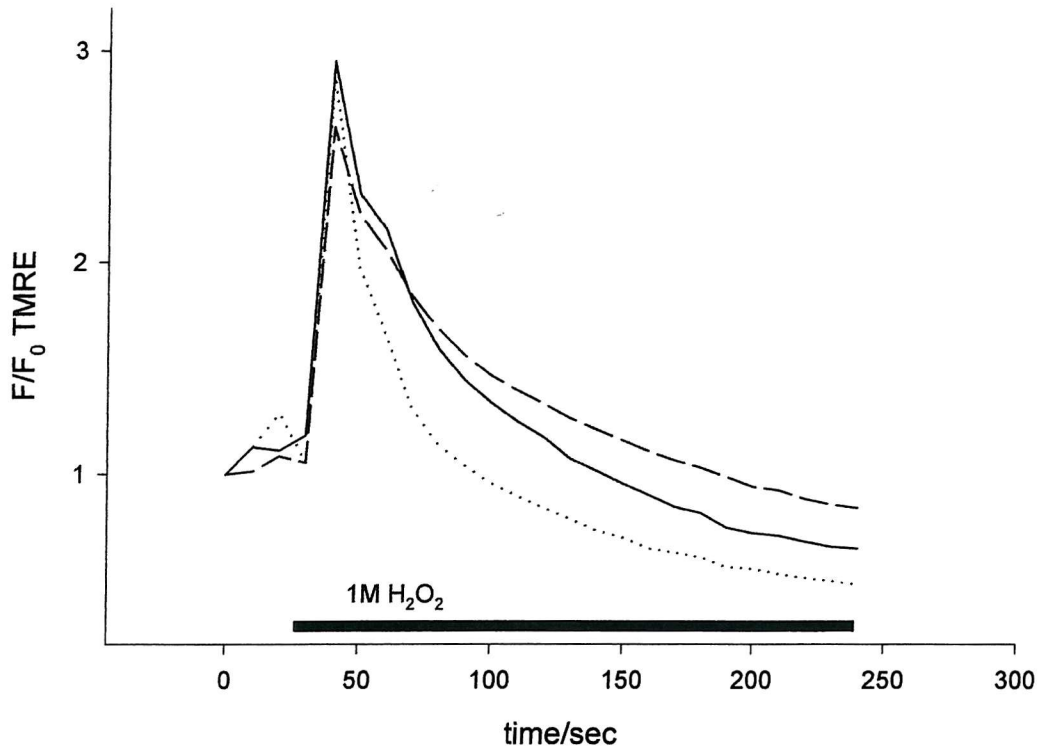

Fig. 5.19 Typical change in TMRE fluorescence in response to 1M H_2O_2. The trace shows the response of three neurons in the same field of view, and is representative of 12 other cells monitored in 4 separate experiments. Horizontal bar indicates time and duration of exposure to H_2O_2.

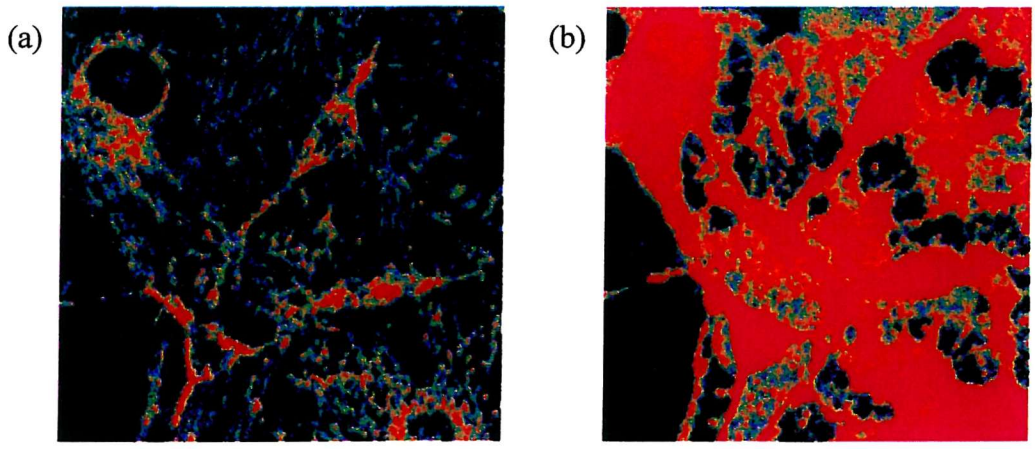

Fig. 5.20 Images selected from a time series of confocal images showing TMRE fluorescence in hippocampal neurons before (a) and following (b) the addition of 1M H_2O_2. TMRE is sequestered by healthy mitochondria as a function of mitochondrial $\Delta\Psi$. The addition of H_2O_2 increases TMRE fluorescence, indicating that H_2O_2 causes mitochondrial depolarisation.

5.3.3 *Involvement of ROS and NO in NMDA neurotoxicity*

To investigate the involvement of ROS in neurotoxicity, neuronal survival was measured in cultures exposed to 500μM NMDA for 15 minutes, and in cultures pretreated with L-NAME or a cocktail of antioxidants, and then treated with 15 minutes NMDA. The antioxidant cocktail contained 1mM ascorbate and 500μM Trolox, both potent antioxidants, 200μM TEMPO, a spin-trap for NO, and 250U/ml catalase, which catalyses the breakdown of H_2O_2 into water and O_2. Neuronal viability was reduced to 10% following treatment with NMDA. Pretreatment with 100μM L-NAME, a NOS inhibitor, increased neuronal survival very highly significantly, to 39%, and pretreatment with the antioxidant cocktail increased neuronal survival very highly significantly to 22% (Figure **5.21**). Pretreatment of neurons with the antioxidant cocktail had no significant effect on the peak increase in Het fluorescence caused by the enzymatic generation of superoxide with xanthine/xanthine oxidase (Figure **5.22**). The peak increase in neuronal $[Ca^{2+}]_i$ caused by 500μm NMDA was very significantly reduced by pretreatment with antioxidants (Figure **5.23**).

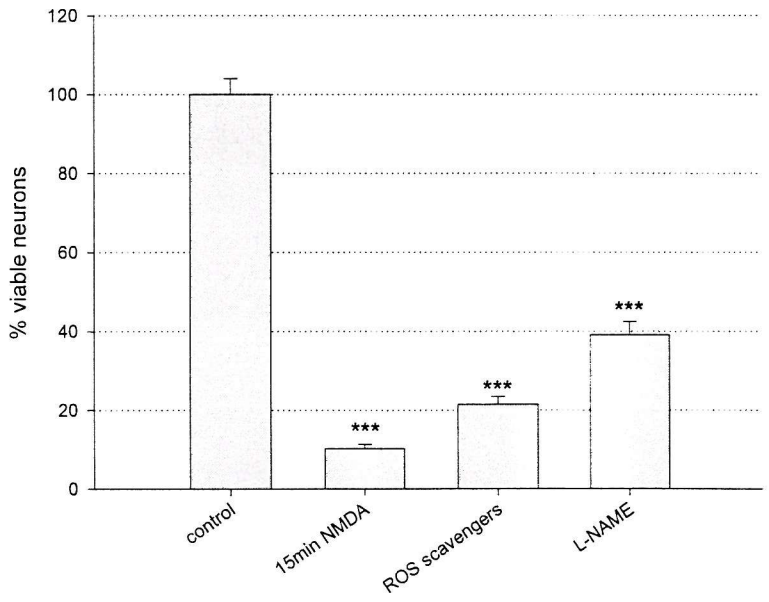

Figure 5.21 Percentage neuronal viability in control cultures, cultures exposed to 15 minutes NMDA (500μM), and cultures pretreated with L-NAME or a cocktail of ROS scavengers and then treated with 15 minutes NMDA. Each bar represents the average of at least 3 culture plates from each treatment group.

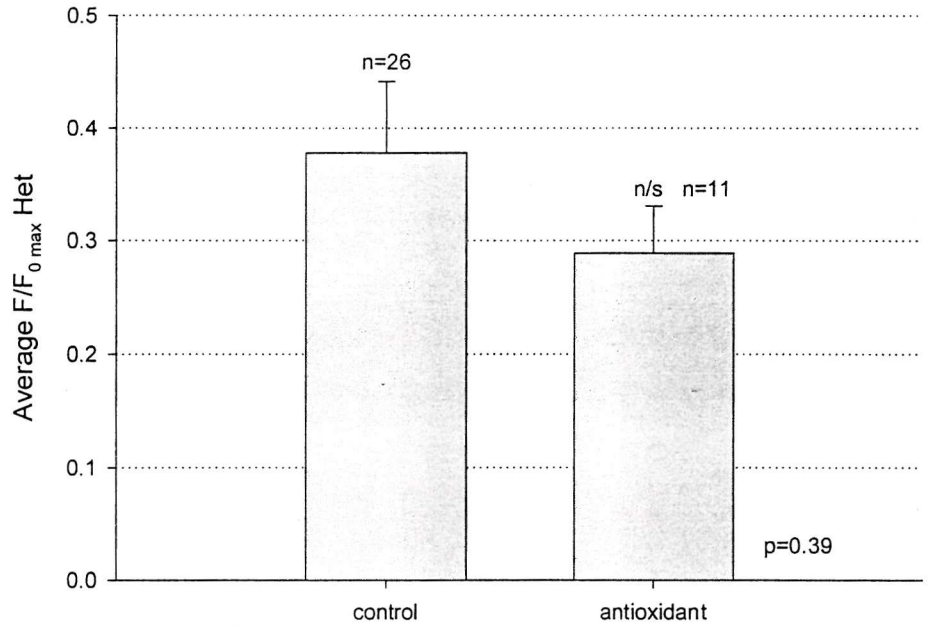

Figure 5.22 Average increase in neuronal Het fluorescence in control cultures and cultures pretreated with ROS scavengers, following the addition of 100μM xanthine and 100mU xanthine oxidase. Each bar represents the average of at least 3 culture plates from each treatment group.

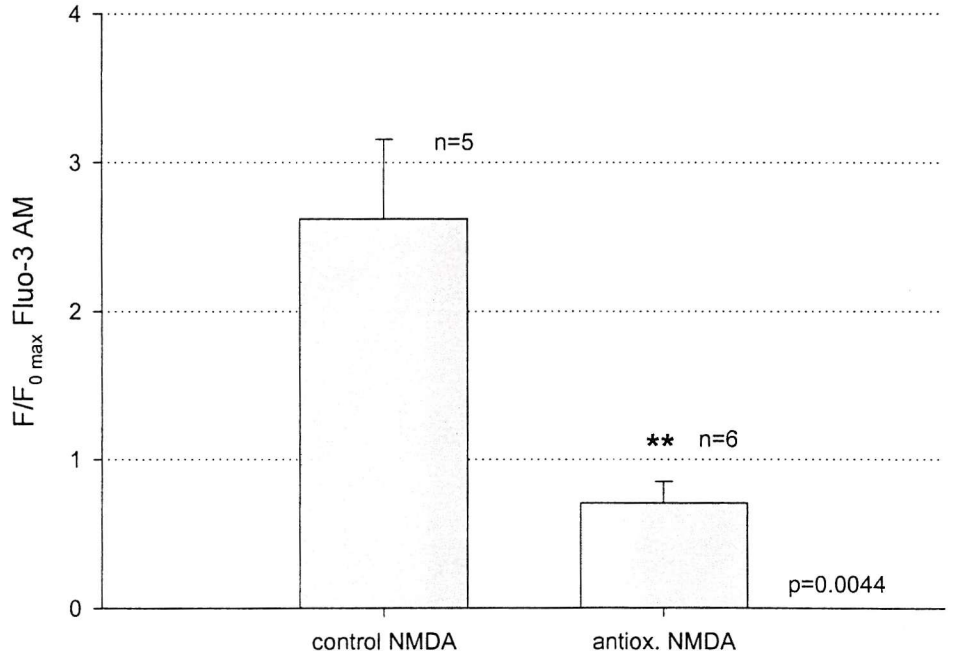

Figure 5.23 Average peak increase in neuronal Fluo-3 fluorescence elicited by 500μM NMDA, in control cultures and in cultures pretreated with ROS scavengers. Peak fluorescence changes measured within 200 seconds of drug addition. Each bar represents the average of at least 3 culture plates from each treatment group.

5.3.4 *Involvement of heavy metals in NMDA neurotoxicity*

To investigate the involvement of heavy metals in neurotoxicity, neuronal survival was measured in cultures exposed to 500μM NMDA for either 15 minutes or 1 hour, and in cultures pretreated with 100μM EDTA and then treated with NMDA (500μM) for 15 minutes or 1 hour. EDTA is a chelator of metal ions. Both durations of NMDA insult reduced neuronal viability to 10%. Pretreatment of neurons with EDTA increased neuronal survival very highly significantly, to 19% with 24 hour NMDA insult, and to 49% with 15 minute NMDA (Figure **5.24**).

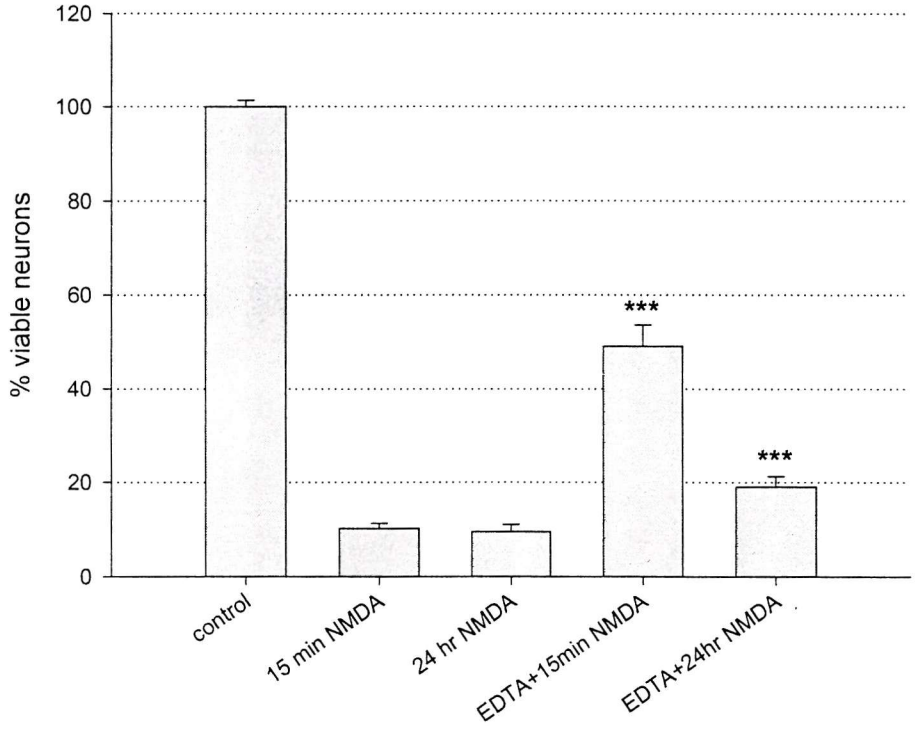

Figure 5.24 Percent neuronal viability in control cultures, cultures exposed to 15 minutes or 24 hours NMDA (500μM), and cultures pretreated with 100μM EDTA and then treated with 15 minutes or 24 hours NMDA (500μM). Each bar represents the average of at least 3 culture plates from each treatment group.

To ascertain whether the neuroprotective action of EDTA was exerted through a reduction in neuronal Ca^{2+} influx following NMDA receptor activation, peak Ca^{2+} increases were measured in control cultures exposed to 500 μM NMDA, and in cultures pretreated with 100μM EDTA then exposed to NMDA in the presence of 100μM EDTA. The peak increase in neuronal $[Ca^{2+}]_i$ caused by 500μM NMDA was not significantly reduced by pretreatment of neurons with EDTA (Figure **5.25**).

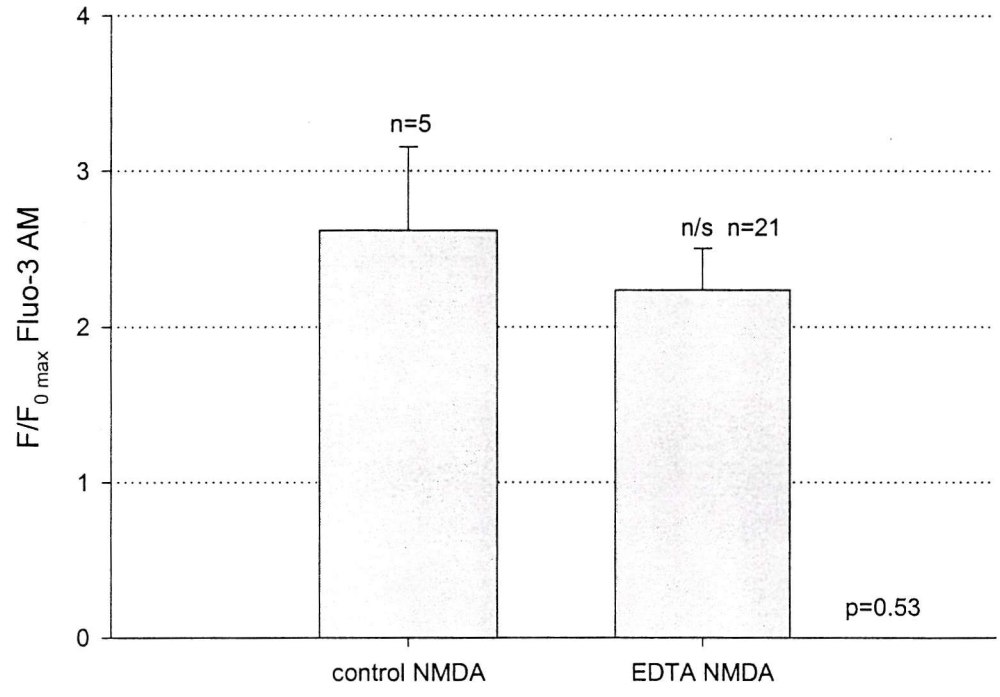

Figure 5.25 Average peak increase in neuronal Fluo-3 fluorescence elicited by 500μM NMDA, in control cultures and in cultures pretreated with 100μM EDTA. Each bar represents the average of at least 3 culture plates from each treatment group.

5.4 Discussion

5.4.1 Neuronal superoxide production in response to the addition of glutamate receptor agonists

In the first part of this study, we selectively activated different glutamate receptor subtypes to investigate which receptors may be coupled to increased neuronal superoxide levels in cultured hippocampal neurons, using CLSM and the oxidation sensitive probe dihydroethidium. We hypothesized that NMDA may impose greater oxidative stress on neurons than other glutamate receptor agonists, by causing excessive production of superoxide. However, no clear relationship was found between the neurotoxic potential of any glutamate receptor agonist (see Chapter 1) and the amount of neuronal superoxide production triggered by that agonist. The application of each glutamate receptor agonist caused increased superoxide production in some, but not necessarily all, neurons monitored in a field of view (**Figure 5.17**). This was in contrast to the changes in neuronal $[Ca^{2+}]_i$ or mitochondrial membrane potential measured in Chapter 4, where all neurons monitored in any one field of view responded uniformly. This variability in neuronal response could reflect differences in endogenous neuronal antioxidant defences such as GSH, which may be non-uniformly distributed between different neuronal subtypes. The increase in neuronal superoxide levels could be attributed to the initial neuronal Ca^{2+} increase caused by each glutamate receptor agonists (as measured in chapter 4). Elevated neuronal $[Ca^{2+}]_i$ is a trigger for many cellular processes culminating in increased ROS production, including the activation of neuronal NOS and the activation of PLA_2 (Leist and Nicotera, 1998). Furthermore, elevated neuronal $[Ca^{2+}]_i$ induces the release of ROS from mitochondria (Tymianski and Tator, 1996).

The average increase in neuronal Het fluorescence caused by ACPD was considerably greater than that elicited by NMDA (**Fig. 5.17**), despite the fact that in our system, NMDA was considerably more neurotoxic than ACPD (**Fig 3.4**). A possible explanation for this phenomenon lies in the extent of

mitochondrial polarisation during EAA exposure. Several studies have raised the possibility that mitochondrial depolarisation or uncoupling may limit superoxide production by this organelle (e.g. Votyakova *et al*, 2001). In cultured forebrain neurons, NMDA receptor-induced increases in superoxide were blocked by the protonophore FCCP (Reynolds and Hastings, 1995). Other studies suggest that mitochondria generate superoxide only under conditions of high $\Delta\Psi$ (Nicholls *et al*, 1999). If this premise held true, then it would be logical that in our system, NMDA and glutamate did not dramatically increase neuronal superoxide production. This is because we have previously shown in this study that neuronal exposure to NMDA or glutamate causes a prolonged mitochondrial depolarisation (**Fig 4.39, 4.30, 4.45,** and **4.46**), which could limit the generation of superoxide. This could also explain why agonists such as kainate and ACPD, which did not depolarise mitochondria (Chapter 4), caused larger increases in neuronal superoxide production than either glutamate or NMDA. On the other hand, several studies have monitored both mitochondrial polarisation and superoxide production in cultured neurons, and report that agonists which depolarise mitochondria also increase neuronal superoxide production (Prehn, 1998; Carriedo *et al*, 2000). It is possible that some of the superoxide that is generated following EAA exposure could evade detection by dihydroethidium by combining with NO to produce peroxynitrite, a highly damaging free radical. In addition to triggering superoxide production, calcium entry through the NMDA receptor could activate the NOS anchored to the intracellular face of the NMDA receptor, thereby increasing neuronal levels of NO. It would therefore have been interesting to repeat these experiments (imaging neuronal superoxide production subsequent to the addition of EAAs) in the presence of L-NAME. In our experiments, we monitored Het fluorescence for only the first 400 seconds or less following drug addition. Superoxide could have been produced after this time frame but not detected. In cerebellar granule cells, Het reported an increased rate of ROS generation in response to glutamate, but this was only seen 30-40 min after the addition of glutamate (Castilho *et al*, 1999).

The depolarisation of mitochondria with FCCP caused increased neuronal Het fluorescence **Figs 5.3, 5.4, 5.17**). It is difficult to account for this phenomenon, since there is some controversy over whether this increase arises through an increase in neuronal superoxide caused by the uncoupling of mitochondrial oxidative phosphorylation (Dugan *et al*, 1995; Sengpiel *et al*, 1998), or whether it is an artifact. It has been reported (Budd *et al*, 1997) that in cultured cerebellar neurons, Het accumulates in the mitochondrial matrix in response to mitochondrial $\Delta\Psi$. The depolarisation of mitochondria by FCCP then allows a rapid efflux of Het, which binds nuclear DNA with an extensive fluorescent enhancement, unrelated to superoxide production.

In this study, it is unlikely that the observed changes in neuronal Het fluorescence caused by different glutamate receptor agonists were artifactual, purely reflecting changes in mitochondrial polarisation. This is because several of the agonists had completely different effects on mitochondrial polarisation (as measured by TMRE) and neuronal superoxide levels (as measured by Het). For example, ACPD and AMPA caused increased neuronal Het fluoresence (Figures **5.11 – 5.14**) while causing no discernible change in neuronal TMRE fluorescence (Figures **4.41**, **4.42**, **4.45** and **4.46**).

The source of neuronal superoxide was not investigated in this study, but the general consensus in the literature is that superoxide is generated by mitochondria, possibly following mitochondrial Ca^{2+} accumulation, since the process is Ca^{2+}-dependent (Sengpiel *et al*, 1998; Dugan *et al*, 1995; Bindokas *et al*, 1996; Carriedo *et al*, 2000; Patel *et al*, 1996). Arachidonic acid (AA) may be another source of ROS, given that the inhibition of PLA_2 partially blocked the glutamate-induced production of ROS in cultured forebrain neurons (Reynolds and Hastings, 1995). However, in murine cultures, the NMDA-induced production of ROS was unaffected by inhibitors of NO or AA, but was abolished by inhibitors of mitochondrial electron transport (Dugan *et al*, 1995). New research has shown that neuronal superoxide production may be Zn^{2+} dependent. The influx of Zn^{2+} through Ca-A/K

channels caused a sharp increase in the rate of Het oxidation in cultured cortical neurons (Sensi *et al*, 1999).

Figure **5.17** shows that neuronal Het fluorescence was increased by glutamate, kainate, NMDA, ACPD, AMPA and quisqualate. These fluorescence increases were generally smaller than the increase caused by xanthine and xanthine oxidase. This suggests that neuronal superoxide production may be increased by the activation of both NMDA and non-NMDA ionotropic glutamate receptors, and also by the activation of mGluRs. This does not agree with earlier studies, which suggested that neuronal superoxide production was a specific consequence of NMDA receptor activation (Reynolds and Hastings, 1995; Dugan *et al*, 1995). This may be explained by the fluorescent probes used in these studies, DCF-H_2 and R123 respectively, which may not be as sensitive or reliable as dihydroethidium which is widely used today. Recent studies that have employed Het have reported increased neuronal Het fluorescence in response to AMPA and/or kainate (Bindokas *et al*, 1996; Prehn, 1998; Carriedo *et al*, 2000).

In this study, increased neuronal superoxide production was not a good indicator of impending neuronal death. The majority of studies find the production of ROS to correlate strongly with the subsequent degree of neuronal injury (Patel *et al*, 1996; Sengpiel *et al*, 1998; Prehn, 1998; Carriedo *et al*, 2000). Undoubtedly, oxidative stress increases the likelihood of neuronal injury or death, but oxidative stress may not always be manifested as an increase in the levels of neuronal superoxide. Experimentally, it is difficult to quantify neuronal antioxidant defences, yet reduced antioxidant defences could be just as damaging to neurons as elevated level of ROS. These issues have been partially addressed in recent studies that measure intraneuronal GSH levels. The exposure of cerebellar granule cells to 30 minutes kainate (500μM) reduced cell viability by 45%, and reduced GSH levels by 36% as measured by enzymatic assay (Ceccon *et al*, 2000). Intraneuronal levels of GSH may also be measured by imaging the fluorescent dye monochlorobimane (MCB), which is non-fluorescent until

irreversibly conjugated to GSH in a reaction catalyzed by glutathione-s-transferase. Toxic glutamate exposure causing mitochondrial depolarisation and cell death in cultured hippocampal neurons was associated with a significant decrease in cytoplasmic GSH (Keelan *et al*, 2000).

5.4.2 Effect of ROS on mitochondrial membrane potential

The addition of 1M H_2O_2 to TMRE-loaded hippocampal neurons caused a robust increase in fluorescence, indicative of mitochondrial depolarisation. The dose used (1M) was a high dose, but H_2O_2 is known to be stable, such that superoxide production is fairly low in the absence of catalysts such as trace metals. A similar effect was seen in cultured forebrain neurons exposed to H_2O_2, where mitochondrial $\Delta\Psi$ was monitored with JC-1 (Scanlon and Reynolds, 1998). Here, no recovery was seen after removal of the oxidant. In a patho-physiological situation, it is likely that oxidants increase the sensitivity to Ca^{2+} -induced mitochondrial depolarization after an excitotoxic stimulus. There are several mechanisms by which oxidants could enhance mitochondrial depolarization, including oxidation of the dithiol groups on PTP components, increasing the likelihood of PTP opening; oxidative impairment of enzymes involved in glycolysis and oxidative phosphorylation; and structural damage to mitochondria via lipid peroxidation of the inner mitochondrial membrane. Oxidative damage to the respiratory chain can be self-propagating, promoting additional ROS production through faulty electron transfer.

5.4.3 Involvement of ROS and NO in NMDA neurotoxicity

In the assay of neuronal viability, the treatment of neurons with a cocktail of antioxidants very highly significantly improved neuronal survival ($p < 0.001$) after a 15 minute NMDA insult (500μM), doubling neuronal survival from 10.2% to 21.5% (**Fig. 5.21**). The cocktail contained the free radical scavengers ascorbate and Trolox, known to inhibit lipid peroxidation, the NO spin trap TEMPO, and catalase, which catalyses the breakdown of H_2O_2 into

water and O_2^-. Neuronal treatment with L-NAME, a NOS inhibitor, was even more protective, very highly significantly increasing neuronal survival from 10.2% to 39.1%. These data strongly implicate reactive oxygen species and NO in NMDA neurotoxicity.

The peak increase in neuronal Het fluorescence caused by X/XO was not significantly reduced in cultures pretreated with the antioxidant cocktail (**Fig. 5.22**). The oxidative stress imposed by the dose of xanthine/xanthine oxidase used may well have overwhelmed the capacity of the free radical scavengers. It should be pointed out that the neuroprotective action of this antioxidant cocktail might be linked to a reduction in Ca^{2+} influx following NMDA receptor activation, rather than a reduction in oxidative stress, since NMDA receptors are known to be subject to redox regulation. NMDA receptor responses were reported to be potentiated after exposure to reducing agents (Aizenman *et al*, 1989). This modulation was found to occur via two cysteine residues in the NR1 subunit of the receptor, which are thought to constitute the molecular determinants of the redox modulatory site (Sullivan *et al*, 1994). Transient exposure of neurons to the disulphide reducing agent DTT has been observed to exacerbate NMDA receptor-mediated neurotoxicity (Levy *et al*, 1990). More recently, the NMDA receptor ion channel has been shown to be modulated by endogenous and exogenous nitric oxide, by way of s-nitrosylation of Cys 349 on the NR2A subunit (Choi *et al*, 2000). **Fig. 5.23** shows that the pretreatment of neurons with ROS scavengers very significantly reduced the peak increase of neuronal $[Ca^{2+}]_i$ caused by NMDA (peak increase in fluorescence measured within 200 seconds of drug addition). The reduction in Ca^{2+} influx following NMDA receptor activation caused by the antioxidant cocktail could account for its neuroprotective effect, given the well-known damaging sequelae of raised neuronal Ca^{2+} levels (see section **1.2**).

In the literature, there is a wealth of information supporting the involvement of ROS in excitotoxicity, yet little is known about the exact role of ROS in neuronal damage, or at which stage in the temporal sequence of neuronal damage they become involved. Two recent reports propose a late stage role

for ROS in excitotoxic damage. In cultured hippocampal neurons, different combinations of antioxidants were highly neuroprotective against a 10-minute glutamate insult, but did not prevent a disruption in Ca^{2+} homeostasis or collapse of mitochondrial $\Delta\Psi$ (Vergun *et al*, 2001), suggesting that oxidative damage occurs downstream of these events. The brief exposure of cultured hippocampal neurons to NMDA was observed to cause a biphasic increase in superoxide production, with a burst of superoxide occurring 4 hours after the initial insult and coinciding with mitochondrial depolarisation (Luetjens *et al*, 2000).

5.4.4 Involvement of heavy metals in NMDA neurotoxicity

The pretreatment of cultured hippocampal neurons with EDTA, a chelator of metal ions, was highly protective against a 15 minute NMDA insult (**Fig. 5.24**), improving neuronal viability very highly significantly, from 10.2% to 49.1% post insult. To investigate whether this neuroprotection was related to the chelation of extracellular Ca^{2+}, the neuronal Ca^{2+} response to 500μM NMDA was measured in control cultures and in cultures treated with EDTA (**Fig. 5.25**). EDTA did not significantly reduce the peak increase in $[Ca^{2+}]_i$ elicited by NMDA. This is not surprising, because the EDTA molecule has one binding site for Ca^{2+} and is therefore able to chelate equimolar Ca^{2+}, i.e. 100μM. Since under experimental imaging conditons, neurons were bathed in PIPES buffer (containing 1mM $CaCl_2$), clearly 90% of the extracellular Ca^{2+} would still be non-chelated and available to move into neurons upon the opening of ligand- or voltage-gated Ca^{2+} channel proteins. EDTA may therefore exert its neuroprotection through the chelation of other metal ions, such as Zn^{2+} and Fe^{2+}, implicating these trace metals in the neuronal death caused by NMDA. It is not certain how trace metals would be involved in NMDA toxicity in dissociated cultures. Brain zinc is selectively stored in presynaptic terminals of glutamatergic neurons. The translocation of Zn^{2+} from pre- to postsynaptic neurons is known to contribute to neuronal injury in *in vivo* models of cerebral ischaemia or epilepsy where the brain is intact (Koh, 1996; Suh *et al*, 2000), but it is not certain whether such synaptic

translocation could occur in dissociated neuronal cultures. Both the culture medium (Neurobasal) and experimental buffer (PIPES) were nominally free from trace metals. Undoubtedly, zinc is toxic to neurons, and is known to potentiate the toxicity of AMPA and kainate in cultured cortical neurons (Yin and Weiss, 1995), through mechanisms outlined in section **1.3.5**. Trace metals are likely to exacerbate neuronal oxidative stress given their role as catalysts of the Fenton reaction, which generates highly damaging hydroxyl radicals. However, in the absence of exogenously applied zinc, it is unclear how metal chelation by EDTA was neuroprotective in our model of NMDA toxicity.

In summary, increases in neuronal Het fluorescence were found to be a reliable indicator of neuronal superoxide production. We observed increased neuronal superoxide production following the application of glutamate. The selective activation of different glutamate receptor subtypes using kainate, NMDA, ACPD, AMPA and quisqualate showed that all these agonists increased neuronal superoxide production, although not uniformly in all the cells within one culture dish. Superoxide production is therefore probably not a critical component of NMDA neurotoxicity. Nitric oxide, ROS and trace metals were found to be involved in the neurotoxicity of NMDA.

Chapter 6

GENERAL DISCUSSION

GENERAL DISCUSSION

In this study, we have sought to investigate the mechanisms of glutamate neurotoxicity, a phenomenon that is likely to contribute to the pathogenesis of acute and chronic neurodegenerative diseases. Glutamate neurotoxicity is a multi-stage process with many contributing factors, and in the course of this investigation we have attempted to answer a number of questions.

Which glutamate receptor subtypes trigger glutamate toxicity?

Glutamate is known to act upon a number of subtypes of neuronal plasma membrane receptors, encompassing ionotropic and metabotropic receptors. The selective activation of these different receptor subtypes using a range of glutamate receptor agonists showed that the activation of NMDA receptors was particularly damaging to cultured hippocampal neurons, reducing neuronal viability very highly significantly, by over 80% when neurons were counted 24 hours following drug removal (Figure **3.7**). In contrast, the metabotropic glutamate receptor agonist 1S-3R ACPD did not significantly reduce neuronal viability (Figure **3.7**). Kainate and AMPA both reduced neuronal viability very highly significantly, by 14% and 73% respectively. The application of NMDA was therefore very damaging to neurons, compared to the application of agonists at other glutamate receptor subtypes. The blockade of NMDA receptors with MK801 increased neuronal survival very highly significantly, from 12% to 46% following NMDA application (Figure **3.9**), confirming that the activation of NMDA receptors was neurotoxic. Furthermore, MK801 was very highly significantly neuroprotective in our acute dissociate model of neuronal trauma and excitotoxicity (Figure **3.1**). However, MK801 was not fully neuroprotective in either instance, suggesting that other routes of neuronal damage were also relevant to neurotoxicity. In particular, the activation of voltage-dependent Ca^{2+} channels may contribute to neurotoxicity, given that Cd^{2+} (a non-specific blocker of VDCCs) and nimodipine (an L-type VDCC antagonist) were very highly significantly neuroprotective in the acute dissociate model of neuronal damage (Figure **3.1**).

What are the intracellular consequences of glutamate receptor activation?

(1) Elevated intracellular Ca^{2+}

There is general agreement in the literature that glutamate neurotoxicity is the consequence of increased neuronal $[Ca^{2+}]_i$ (Randall and Thayer, 1992; Eirmerl and Schramm, 1994; Lu *et al*, 1996; Hyrc *et al*, 1997). Elevated levels of Ca^{2+} trigger a number of damaging intracellular cascades. We therefore constructed dose –Ca^{2+} response curves, and selected doses of glutamate receptor agonists that elicited comparable initial increases in neuronal $[Ca^{2+}]_i$ as measured with the fluorescent Ca^{2+} indicator Fluo-3 AM. As shown in Figure **3.7**, these doses of glutamate receptor agonist did not cause equivalent neuronal damage. We therefore found no evidence that the neurotoxicity of EAAs was related to the magnitude of initial neuronal Ca^{2+} elevations caused by that EAA.

(2) Loss of mitochondrial $\Delta\Psi$

Since the initial neuronal Ca^{2+} elevation was not a reliable indicator of impending neuronal death, we monitored other cellular parameters that might be adversely affected in neurotoxicity. We investigated whether a loss of mitochondrial membrane potential was associated with the neurotoxicity of different EAAs. We applied doses of EAA known to cause comparable initial neuronal Ca^{2+} increases to cultured hippocampal neurons loaded with TMRE, a potentiometric indicator of mitochondrial $\Delta\Psi$ (section **4.3.4**). The application of glutamate caused a robust mitochondrial depolarisation (Figures **4.39** and **4.40**). The stimulation of neurons with selective agonists of different glutamate receptor subtypes revealed that mitochondrial depolarisation appeared to be a specific consequence of NMDA receptor activation (Figures **4.45** and **4.46**). Agonists at non-NMDA receptors, namely AMPA, kainate, ACPD and quisqualate did not cause mitochondrial depolarisation (Figure **4.51**). The uptake of cytosolic Ca^{2+} is thought to contribute to mitochondrial depolarisation, but our data suggest that imposed cytosolic Ca^{2+} loads of comparable magnitude do not equally cause mitochondrial depolariation (Figure **4.52**). It would appear that Ca^{2+} ions

might have different consequences for cell viability depending on their provenance. It should be mentioned that mitochondrial depolarisation was also caused by 4-AP (Figure **4.37** and **4.38**), which blocks K^+ channels, causing persistent neuronal depolarisation. This mitochondrial depolarisation could be due to Ca^{2+} influx through VDCCs, although the activation of VDCCs with K^+ did not cause mitochondrial depolarisation in cultured rat hippocampal neurons (Vergun *et al*, 1999). Alternatively, the 4-AP induced neuronal depolarization could cause the release of glutamate from presynaptic terminals and the consequent activation of NMDA receptors, an event known to cause mitochondrial depolarisation.

(3) Neuronal generation of ROS: superoxide and nitric oxide

We then decided to investigate the contribution of various Ca^{2+}-triggered events to the neurotoxicity of different EAAs. Firstly, we looked at the contribution of reactive oxygen species (ROS) and nitric oxide (NO). Neuronal production of ROS might be increased by mitochondrial dysfunction following excessive mitochondrial Ca^{2+} accumulation. The production of NO by neuronal NOS is Ca^{2+}-dependent. Treatment of neurons with an antioxidant cocktail very highly significantly improved neuronal survival after a 15 minute NMDA insult (Figure **5.21**). This implicated ROS in the pathogenesis of neuronal injury following NMDA exposure. However, the precise identity of the free radical(s) that contributes to neuronal injury is unknown. Neuronal production of superoxide was monitored in cells loaded with the oxidation-sensitive probe dihydroethidium and exposed to EAAs (Figure **5.17**). Neuronal superoxide production was not found to be a reliable indicator of impending cell death. However, the inhibition of nitric oxide synthase with L-NAME was even more neuroprotective than the antioxidant cocktail (Figure **5.21**). It is possible that superoxide could evade detection by combining with NO to form the highly damaging radical peroxynitrite (Radi *et al*, 1991). Alternatively, NO might be more destructive than superoxide in processes of neurotoxicity.

(4) Trace Metals

We investigated the possible involvement of trace metals in NMDA neurotoxicity, given recent experimental evidence that Zn^{2+} translocation is involved in cerebral ischaemic damage (Suh, 2000). The pretreatment of neurons with EDTA, a metal ion chelator, was very highly significantly protective against a 15-minute NMDA insult (Figure **5.24**). Trace metals may therefore be involved in processes of neurotoxicity, although the precise mechanism of this process is unclear. Brain zinc is selectively stored in presynaptic terminals of glutamatergic neurons, and the toxicity of zinc translocation from pre- to postsynaptic terminals is well documented in *in vivo* models of brain injury (Koh, 1996; Suh *et al*, 2000). In dissociated cultures, perhaps zinc is released from presynaptic terminals upon NMDA-induced neuronal firing. Both the culture medium (Neurobasal, Brewer *et al*, 1993) and experimental buffer (PIPES) were nominally free from trace metals.If present, trace metals could exacerbate neuronal oxidative stress by catalysing the Fenton reaction (section **1.3.4**).

(5) Delayed calcium deregulation

Monitoring neuronal Ca^{2+} levels using the low affinity Ca^{2+}-indicator Fluo-5N AM revealed that NMDA caused a delayed secondary increase in neuronal $[Ca^{2+}]_i$ (Figures **4.60**, **4.61**) that was not seen with kainate (Figures **4.62**, **4.63**). At 390 seconds, the Fluo-5N fluorescence in neurons stimulated with NMDA was very highly significantly greater than that in neurons stimulated with kainate (Figure **4.58**). It is generally accepted that large changes in $[Ca^{2+}]_i$ cannot be detected using high affinity Ca^{2+} indicators such as Fluo-3 AM since they become saturated at lower concentrations of Ca^{2+} than the new, lower affinity Ca^{2+} indicators (Stout and Reynolds, 1999). This delayed calcium deregulation could be the consequence of the toxic intracellular cascades triggered by NMDA receptor activation. Because the activation of non-NMDA receptors has different pathological consequences for neurons, perhaps the activation of damaging cascades that culminate in DCD is particular to NMDA receptor activation.

What is the temporal sequence of intracellular events following toxic NMDA receptor activation?

The data outlined above are in agreement with current opinions on the mechanism of glutamate neurotoxicity, and can be synthesised into a model of intracellular events following toxic NMDA receptor activation.

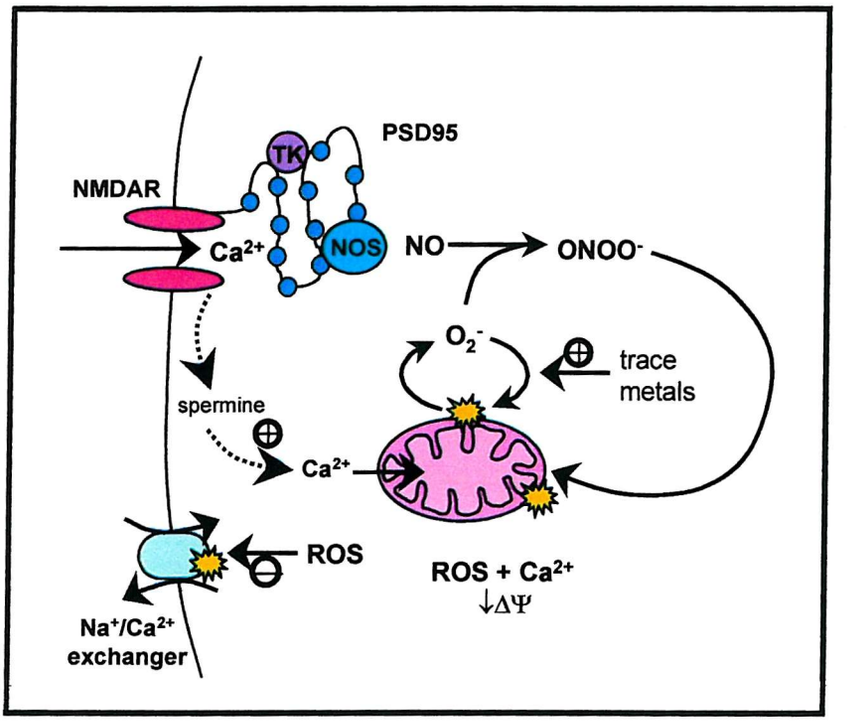

Figure 6.1 Model of intracellular events that follow toxic NMDA receptor activation

Early stage: Up to 200 seconds following NMDA application

Toxic NMDA receptor activation leads to removal of the Mg^{2+} block and a large initial influx of Ca^{2+} through the NMDA receptor channel. This initial Ca^{2+} influx is well placed to activate Ca^{2+}-dependent enzymes including tyrosine kinase and nitric oxide synthase which are anchored close to the intracellular face of the NMDA receptor by the PSD95 protein complex. Various cascades, including the production of NO are triggered. Ca^{2+} that has entered via the NMDA receptor has been reported to have privileged access to mitochondria (Peng and Greenamyre, 1998). One possible mechanism may be the release of spermine following NMDA receptor activation. Spermine diffuses to mitochondria and stimulates the rapid mode of mitochondrial Ca^{2+}

uptake. Mitochondria are able to accumulate large amounts of Ca^{2+} by virtue of the electrochemical gradient ($\Delta\Psi$) that exists across the inner membrane. Excessive Ca^{2+} uptake of the initial elevation in neuronal Ca^{2+}, however, may lead to damaging downstream sequelae.

Delayed stage: more than 300 seconds following drug addition

Excessive Ca^{2+} uptake by mitochondria may lead to the increased generation of ROS, mitochondrial depolarisation and eventual neuronal ATP depletion. Generated ROS may damage cellular components including Ca^{2+} extrusion mechanisms such as the Na^{+}/Ca^{2+} exchanger, and the mitochondrial membrane, increasing ROS production in a vicious cycle. Generated superoxide may combine with enzymatically generated NO to form peroxynitrite, a highly damaging free radical capable of inflicting lethal damage on cellular components. Under conditions of mitochondrial dysfunction and impaired Ca^{2+} extrusion mechanisms, neurons may undergo a secondary increase in $[Ca^{2+}]_i$, or delayed Ca^{2+} deregulation. In some instances, this DCD may correspond to opening of the mitochondrial megachannel (PTP) and dumping of Ca^{2+} contained within the mitochondrial matrix. This is unlikely to be the case in our experimental model, since mitochondrial depolarisation did not coincide temporally with DCD. In our model, DCD was seen to begin at 350 seconds following drug application, whereas DCD has been reported to be a much later phenomenon in other experimental models. DCD has been reported to occur 70 minutes after the addition of glutamate to cultured cerebellar granule cells (Nicholls and Budd, 1998), 15-20 minutes after the exposure of cultured striatal neurons to NMDA (Alano *et al*, 2002), 90 minutes after the exposure of cultured hippocampal neurons to glutamate (Randall and Thayer, 1992) and 30 minutes after the exposure of cultured spinal neurons to glutamate (Tymianski *et al*, 1993). In cultured hippocampal neurons, a secondary increase in neuronal $[Ca^{2+}]_i$ has been reported to occur approximately 180 seconds after glutamate addition (Keelan *et al*, 1999). The relatively early onset of DCD in our experimental model could be due to (i) the high dose of NMDA used (500μM) and (ii) the fact that hippocampal neurons are

exceptionally vulnerable to excitotoxic and traumatic damage. Certainly, CA1 hippocampal neurons are known to succumb to injury before neurons of other brain regions in experimental models of cerebral ischaemia (Abe *et al*, 1995).

What are the intracellular events following the activation of kainate receptors?

The events outlined above may account for the neurotoxicity of NMDA in cultured hippocampal neurons, but why was the application of kainate considerably less neurotoxic? One possibility is that kainate caused a smaller initial neuronal Ca^{2+} increase than NMDA. Using the high affinity Ca^{2+} indicator Fluo-3 AM, the initial Ca^{2+} increases caused by NMDA and kainate (Figure **4.51**) were not significantly different. In the light of concerns that high affinity Ca^{2+} indicators may underestimate Ca^{2+} increases caused by NMDA (Stout and Reynolds, 1999), we conducted the same measurements using the low affinity Ca^{2+} indicator Fluo-5N AM. Surprisingly, the data showed a significantly greater initial Ca^{2+} increase with kainate rather than NMDA (Figure **4.59**). This would add further weight to our hypothesis that the initial Ca^{2+} increase caused by glutamate receptor agonists is not a good indicator of impending neuronal death. Another possibility is that the kainate-induced Ca^{2+} increase was not coupled to damaging downstream events. Although kainate increased neuronal superoxide production (Figure **5.17**), it did not cause mitochondrial depolarisation (Figure **4.41**) nor did it result in DCD (Figure **4.62**). Our attempts to determine the origin of the Ca^{2+} increase caused by kainate were inconclusive. Contrary to the literature, our data argued against the transmembrane flux of Ca^{2+}(Figures **4.54-4.56**), and pointed to the G-protein coupled release of Ca^{2+}, probably from intracellular stores (Figure **4.58**). Perhaps Ca^{2+} released form intracellular stores does not have privileged access to mitochondria, and therefore has less damaging consequences for neurons. This could also explain why the Ca^{2+} increase caused by the mGluR agonist 1S-3R ACPD was relatively innocuous.

The data gathered in this study consolidate the prevailing view in the literature that the mitochondrion is a major player in neuronal life/death decisions, since the loss of mitochondrial $\Delta\Psi$ was the most reliable indicator of impending cell death following EAA exposure. However, it should be emphasised that in our model, mitochondrial depolarisation alone was insufficient to cause neuronal death. The exposure of neurons to 1μM FCCP caused a profound and reproducible mitochondrial depolarisation (Figures **4.33** and **4.34**), but reduced neuronal viability by less than 40%, whereas NMDA alone reduced neuronal viability by over 80% (Figure **3.7**). Mitochondrial function is a critical determinant of neuronal viability, not only in acute neurological insults but also in chronic neurological disorders, where the gradual accumulation of sub-clinical mitochondrial lesions can cause progressive neurodegeneration. It is an attractive proposition that excessive mitochondrial Ca^{2+} uptake causes a decrease in $\Delta\Psi$, but the causality of this event has not yet been proved. Damage caused by NO, ROS or trace metals could be equally important in mitochondrial dysfunction, particularly given the recent finding that mitochondrial Zn^{2+} uptake causes sustained mitochondrial depolarization (Sensi, 2000). The involvement of ROS in glutamate neurotoxicity needs further rationalisation, because two recent studies suggest a late-stage role for ROS in neurotoxicity (Vergun, 2001; Luetjens, 2000).

In summary, we found that of the measured responses to the activation of different glutamate receptors, mitochondrial depolarisation and delayed Ca^{2+} deregulation were predictive of neuronal death, whereas early Ca^{2+} elevation and superoxide production alone were not well correlated to neuronal death. However, reactive oxygen species are implicated in neuronal death by the neuroprotection observed with antioxidants, metal chelators and blockade of nitric oxide production.

REFERENCES

REFERENCES

Abdel-Hamid, K. M. and Tymianski, M. (1997). Mechanisms and Effects of Intracellular Calcium Buffering on Neuronal survival in Organotypic Hippocampal Cultures Exposed to Anoxia/Aglycaemia or to Excitotoxins. *Journal of Neuroscience.* **17**(10), 3538-3553.

Abe, K., Aoki, M., Kawagoe, J., Yoshida, T., Hattori, A., Kogure, K., and Itoyama, Y. (1995). Ischaemic Delayed Neuronal Death - A Mitochondrial Hypothesis. *Stroke.* **26**, 1478-1489.

Adamec, E., Didier, M., and Nixon, R. A. (1998). Developmental regulation of the recovery process following glutamate-induced rise in rodent primary neuronal cultures. *Developmental Brain Research.* **108**, 101-110.

Ahlijanian, M. K., Westenbroek, R. E., and Catterall, W. A. (1990). Subunit structure and localization of dihydropyridine-sensitive calcium channels in mammalian brain, spinal cord and retina. *Neuron.* **4**, 819-832.

Aizenman, E., Lipton, S. A., and Loring, R. H. (1989). Selective modulation of NMDA responses by reduction and oxidation. *Neuron.* **2**, 1257-1263.

Aizenman, E., Brimecombe, J. C., Potthoff, W. K., and Rosenberg, P. A. (1998). Why is the role of nitric oxide in NMDA receptor function and dysfunction so controversial? *Progress in Brain Research.* **118**, 53-71.

Alano, C. C., Beutner, G., Dirksen, R. T., Gross, R. A., and Sheu, S-S. (2002). Mitochondrial permeability transition and calcium dynamics in striatal neurons upon intense NMDA receptor activation. *Journal of Neurochemistry.* **80**, 531-538.

Almeida, A., Bolanos, J. P., and Medina, J. M. (1999). Nitric oxide mediates glutamate-induced mitochondrial depolarization in rat cortical neurons. *Brain Research.* **816**, 580-586.

Ambrosio, A. F., Silva, A. P., Malva, J. O., Mesquita, J. F., Carvalho, A. P., and Carvalho, C. M. (2000). Role of desensitization of AMPA receptors on the neuronal viability and on the $[Ca^{2+}]_i$ changes in cultured rat hippocampal neurons. *European Journal of Neuroscience.* **12**, 2021-2031.

Andreyev, A. Y., Fahy, B., and Fiskum, G. (1998). Cytochrome c release from brain mitochondria is independent of the mitochondrial permeability transition. *FEBS Letters.* **439**, 373-376.

Ankacrona, M., Dypbukt, J. M., Bonfoco, E., Zhivtovsky, B., Orrenius, S., Lipton, S. A., and Nicotera, P. (1995). Glutamate-Induced Neuronal Death: A Succession of Necrosis or Apoptosis Depending on Mitochondrial Function. *Neuron.* **15**, 961-973.

Ankacrona, M., Dypbukt, J. M., Orrenius, S., and Nicotera, P. (1996). Calcineurin and mitochondrial function in glutamate-induced neuronal cell death. *FEBS Letters.* **394**, 321-324.

Ankacrona, M. (1998). Glutamate induced cell death: Apoptosis or necrosis? *Progress in Brain Research.* **116**, 265-272.

Antonawich, F. J., Federoff, H. J., and Davis, J. N. (1999). Bcl-2 transduction,using a herpes simplex virus amplicon, protects hippocampal neurons from transient global ischaemia. *Experimental Neurology.* **156**, 130-137.

Antonsson, B. and Martinou, J-C. (2000). The Bcl-2 Protein Family. *Experimental Cell Research.* **256**, 50-57.

Armstrong, C., Leong, W., and Lees, G. J. (2001). Comparative effects of metal chelating agents on the neuronal cytotoxicity induced by copper (Cu^{2+}), iron (Fe^{3+}) and zinc in the hippocampus. *Brain Research.* **892**, 51-62.

Arnaiz, S. L., Coronel, M. F., and Boveris, A. (1999). Nitric Oxide, Superoxide, and Hydrogen Peroxide Production in Brain Mitochondria after Haloperidol Treatment. *Nitric Oxide: Biology and Chemistry.* **3**(3), 235-243.

Babcock, D. F., Herrington, J., Goodwin, P. C., Park, Y. B., and Hille, B. (1997). Mitochondrial participation in the intracellular Ca^{2+} network. *Journal of Cell Biology.* **136**(4), 833-844.

Barinaga, M. (1998). Death by Dozens of Cuts. *Science.* **280**, 32-34.

Bär, P. R. (1996). Apoptosis - the cell's silent exit. *Life Sciences.* **5-6**, 369-378.

Beal, M. F. (1992). Mechanisms of excitotoxicity in neurologic diseases. *FASEB Journal.* **6**, 3338-3344.

Beal, M. F., Hyman, B. T., and Koroshetz, W. (1993). Do defects in mitochondrial energy metabolism underlie the pathology of neurodegenerative diseases? *TINS.* **16**(4), 125-131.

Beal, M. F. (1995). Aging, energy, and oxidative stress in neurodegenerative diseases. *Annals of Neurology.* **38**, 357-366.

Beal, M. F. (2000). Energetics in the pathogenesis of neurodegenerative diseases. *TINS.* **23**(7), 298-304.

Bean, B. P. (1989). Classes of calcium channels in vertebrate cells. *Annual Review of Physiology.* **51**, 367-384.

Berg, J.M., Tymoczko, J.L.,and Stryer, L. (2002) *Biochemistry*, 5th Ed. W.H.Freeman & Co., New York

Berg, M., Bruhn, T., Frandsen, A., Schousboe, A., and Diemer, N. H. (1995). Kainic acid-induced seizures and brain damage in the rat: role of calcium homeostasis. *Journal of Neuroscience Research.* **40**, 641-646.

Berman, S. B., Watkins, S. C., and Hastings, T. G. (2000). Quantitative Biochemical and Ultrastructural Comparison of Mitochondrial Permeability Transition in Isolated Brain and Liver Mitochondria: Evidence for reduced Sensitivity of Brain Mitochondria. *Experimental Neurology.* **164**, 415-425.

Bernadi, P., Broekmeier, K. M., and Pfeiffer, D. R. (1994). Recent Progress on Regulation of the Mitochondrial Permeability Transition Pore; a Cyclosporin-Sensitive Pore in the Inner Mitochondrial Membrane. *Journal of Bioenergetics and Biomembrane.* **26**(5), 509-517.

Bernadi, P. and Petronilli, V. (1996). The Permeability Transition Pore as a Mitochondrial Calcium Release channel: A Critical Appraisal. *Journal of Bioenergetics and Biomembrane.* **28**(2), 131-138.

Bernadi, P. (1999). Mitochondrial Transport of Cations: Channels, Exchangers, and Permeability Transition. *Physiological Reviews.* **79**(4), 1127-1155.

Bernardi, P., Basso, E., Colanna, R., Costantini, P., Di Lisa, F., Ericsson, O., Fontaine, E., Forte, M., Ichas, F., Massari, S., Nicolli, A., Petronilli, V., and Scorrano, L. (1998). Perspectives on the mitochondrial permeability transition. *Biochimica et Biophysica Acta.* **1365**, 200-206.

Bernardi, P., Scorrano, L., Colonna, R., Petronilli, V., and Di Lisa, F. (1999). Mitochondria and cell death: Mechanistic aspects and methodological issues. *European Journal of Biochemistry.* **264**, 687-701.

Berridge, M. J. (1995). Capacitative calcium entry. *Biochemical Journal.* **312**, 1-11.

Berridge, M. J. (1998). Neuronal Calcium Signaling. *Neuron.* **21**, 13-26.

Berridge, M. J., Bootman, M. D., and Lipp, P. (1998). Calcium - a life and death signal. *Nature.* **395**, 645-648.

Bertolino, M. and Llinas, R. R. (1992). The Central Role of Voltage-Activated and Receptor-Operated Calcium Channels in Neuronal Cells. *Annual Review of Pharmacology and Toxicology.* **32**, 399-421.

Bindokas, V. P., Jordan, J., Lee, C. C., and Miller, R. J. (1996). Superoxide Production in Rat Hippocampal Neurons: Selective Imaging with Hydroethidine. *Journal of Neuroscience.* **16**(4), 1324-1336.

Blaabjerg, M., Kristensen, B. W., Bonde, C., and Zimmer, J. (2001). The metabotropic glutamate receptor agonist 1S,3R-ACPD stimulates and modulates NMDA receptor mediated excitotoxicity in organotypic hippocampal slice cultures. *Brain Research.* **898**, 91-104.

Blaustein, M. P. (1988). Calcium transport and buffering in neurons. *TINS.* **11**(10), 438-443.

Blaustein, M. P. and Golovina, V. (2001). Structural complexity and functional diversity of endoplasmic reticulum Ca^{2+} stores. *TINS.* **24**(10), 602-608.

Bleakman, D. and Lodge, D. (1998). Neuropharmacology of AMPA and kainate receptors. *Neuropharmacology.* **37**, 1187-1204.

Bogaert, L., O'Neill, M. J., Moonen, J., Sarre, S., Smolders, I., Ebinger, G., and Michotte, Y. (2001). The effects of LY393613, nimodipine and verapamil, in focal cerebral ischaemia. *European Journal of Pharmacology.* **411**(1-2), 71-83.

Bolanos, J. P., Almeida, A., Fernandez, E., Medina, J. M., Land, J. M., Clark, J. B., and Heales, S. J. R. (1997). Potential mechanisms for nitric oxide-mediated impairment of brain mitochondrial energy metabolism. *Biochemical Society Transactions.* **25**, 944-949.

Brenner, C., Marzo, I., and Kroemer, G. (1998). A revolution in apoptosis: from a nucleocentric to a mitochondriocentric perspective. *Experimental Gerontology.* **33**(6), 543-553.

Brewer, G. J., Torricelli, J. R., Evege, E. K., and Price, P. J. (1993). Optimized Survival of Hippocampal Neurons in B27-Supplemented Neurobasal™, a New Serum-free Medium Combination. *Journal of Neuroscience Research.* **35**, 567-576.

Brierley, E. J., Johnson, M. A., James, O. F. W, and Turnbull, D. M. (1996). Effects of physical activity and age on mitochondrial function. *Quarterly Journal of Medicine.* **89**, 251-258.

Bringold, U., Ghafourifar, P., and Richter, C. (2000). Peroxynitrite formed by mitochondrial NO synthase promotes mitochondrial Ca^{2+} release. *Free Radical Biology and Medicine.* **29**(3-4), 343-348.

Brorson, J. R., Manzolillo, P. A., and Miller, R. J. (1994). Calcium entry via AMPA/kainate receptors and excitotoxicity in cultured cerebellar Purkinje cells. *Journal of Neuroscience.* **14**, 187-197.

Brorson, J. R. and Zhang, H. (1997). Disrupted $[Ca^{2+}]_i$ Homeostasis Contributes to the Toxicity of Nitric Oxide in Cultured Hippocampal Neurons. *Journal of Neurochemistry.* **69**, 1882-1889.

Brorson, J. R., Sulit, R. A., and Zhang, H. (1997). Nitric Oxide Disrupts Ca^{2+} Homeostasis in Hippocampal Neurons. *Journal of Neurochemistry.* **68**, 95-105.

Brorson, J. R., Schumacker, P. T., and Zhang, H. (1999). Nitric Oxide Acutely Inhibits Neuronal Energy Production. *Journal of Neuroscience.* **19**(1), 147-158.

Brown, G. C. and Borutaite, V. (1999). Nitric oxide, cytochrome c and mitochondria. *Biochemistry Society Symposium.* **66**, 17-25.

Brustovetsky, N., Brustovetsky, K., Jemmerson, R., and Dubinsky, J. M. (2002). Calcium-induced cytochrome c release from CNS mitochondria is associated with the permeability transition and rupture of the outer membrane. *Journal of Neurochemistry.* **80**, 207-218.

Budd, S. L. and Nicholls, D. G. (1996). A reevaluation of the role of mitochondria in neuronal Ca^{2+} homeostasis. *Journal of Neurochemistry.* **66**, 403-411.

Budd, S. L. and Nicholls, D. G. (1996). Mitochondria, calcium regulation, and acute glutamate excitotoxicity in cultured cerebellar granule cells. *Journal of Neurochemistry.* **67**, 2282-2291.

Budd, S. L., Castilho, R. F., and Nicholls, D. (1997). Mitochondrial membrane potential and hydroethidine-monitored superoxide generation in cultured cerebellar granule cells. *FEBS Letters.* **415**, 21-24.

Buisson, A., Margaill, I., Callebert, J., Plotkine, M., and Boulu, R. G. (1993). Mechanisms involved in the neuroprotective activity of a nitric-oxide synthase inhibitor during focal cerebral ischemia. *Journal of Neurochemistry.* **61**(2), 690-696.

Cai, J., Yang, J., and Jones, D. P. (1998). Mitochondrial control of apoptosis: the role of cytochrome c. *Biochimica et Biophysica Acta.* **1366**, 139-149.

Cai, J. and Jones, D. P. (1999). Mitochondrial Redox Signaling during Apoptosis. *Journal of Bioenergetics and Biomembrane.* **31**, 327-334.

Camins, A., Gabriel, C., Aguirre, L., Sureda, F. X., Pallas, M, Escubedo, E., and Camarasa, J. (1998). Flow Cytometric Study of Mitochondrial Dysfunction After AMPA Receptor Activation. *Journal of Neuroscience Research.* **52**, 684-690.

Carafoli, E. (1987). Intracellular Calcium Homeostasis. *Annual Review of Biochemistry.* **56**, 395-433.

Carriedo, S. G., Sensi, S. L., Yin, H. Z., and Weiss, J. H. (2000). AMPA Exposures Induce Mitochondrial Ca^{2+} Overload and ROS Generation in Spinal Motor Neurons *In Vitro*. *Journal of Neuroscience.* **20**(1), 240-250.

Carriedo.S.G., Yin, H. Z., Sensi, S. L., and Weiss, J. H. (1998). Rapid Ca^{2+} Entry through Ca^{2+}-Permeable AMPA-Kainate Channels Triggers Marked Intracellular Ca^{2+} Rises and Consequent Oxygen Radical Production. *Journal of Neuroscience.* **18**(19), 7727-7738.

Cassarino, D. S. and Bennett, J. P. Jr. (1999). An evaluation of the role of mitochondria in neurodegenerative diseases: mitochondrial mutations and oxidative pathology, protective nuclear responses, and cell death in neurodegeneration. *Brain Research Reviews.* **29**, 1-25.

Castilho, R. F., Hansson, O., Ward, M. W., Budd, S. L., and Nicholls, D. G. (1998). Mitochondrial control of acute glutamate excitotoxicity in cultured cerebellar granule cells. *Journal of Neuroscience.* **18**(24), 10277-10286.

Castilho, R. F., Ward, M. W., and Nicholls, D. (1999). Oxidative stress, mitochondrial function, and acute glutamate excitotoxicity in cultured cerebellar granule cells. *Journal of Neurochemistry.* **72**, 1394-1401.

Castillo, J., Rama, R., and Davalos, A. (2000). Nitric Oxide-Related Brain Damage in Acute Ischemic Stroke. *Stroke.* **31**, 852-857.

Catteral, W. A. (2000). Structure and regulation of voltage-gated Ca^{2+} channels. *Annual Review of Cell and Developmental Biology.* **16**, 521-555.

Cazevieille, C., Muller, A., Meynier, F., and Bonne, C. (1993). Superoxide and nitric oxide cooperation in hypoxia/reoxygenation-induced neuron injury. *Free Radical Biology and Medicine.* **14**(4), 389-395.

Ceccon, M., Giusti, P., Facci, L., Borin, G., Imbesi, M., Floreani, M., and Skaper, S. D. (2000). Intracellular glutathione levels determine cerebellar granule neuron sensitivity to excitotoxic injury by kainic acid. *Brain Research.* **862**, 83-89.

Chabrier, P-E., Demerle-Pallardy, C., and Auguet, M. (1999). Nitric oxide synthases: targets for theraputic strategies in neurological diseases. *Cellular and Molecular Life Sciences.* **55**, 1029-1035.

Chan, P. H. (1996). Role of Oxidants in Ischemic Brain Damage. *Stroke.* **27**, 1124-1129.

Chittajallu, R., Braithwaite, S. P., Clarke, V. R. J., and Henley, J. M. (1999). Kainate receptors: subunits, synaptic localization and function. *TIPS.* **20**, 26-35.

Choi, D. W. (1985). Glutamate neurotoxicity in cortical cell culture is calcium dependent. *Neuroscience Letters.* **58**, 293-297.

Choi, D. W. (1987). Ionic dependence of glutamate neurotoxicity. *Journal of Neuroscience.* **7**, 369-379.

Choi, D. W. (1988). Calcium - mediated neurotoxicity: relationship to specific channel types and role in ischaemic damage. *TINS.* **11**(10), 465-469.

Choi, D. W. and Koh, J-Y. (1998). Zinc and Brain Injury. *Annual Review of Neuroscience.* **21**, 347-375.

Choi, Y-B, Tenneti, L., Le, D. A., Ortiz, J., Bai, G., Chen, H-S, and Lipton, S. A. (2000). Molecular basis of NMDA receptor-coupled ion channel modulation by *s*-nitrosylation. *Nature Neuroscience.* **3**(1), 15-21.

Ciani, E., Grineng, L., Voltattorni, M., Rolseth, V., Contestabile, A., and Paulsen, R. E. (1996). Inhibition of free radical production or free radical scavenging protects from the excitotoxic cell death mediated by glutamate in cultures of cerebellar granule neurons. *Brain Research.* **728**(1), 1-6.

Clark, R. S. B., Chen, J., Watkins, S. C., Kochanek, P. M., Chen, M. Z., Stetler, R. A., Loeffert, J. E., and Graham, S. H. (1997). Apoptosis-suppressor gene bcl-2 expression after traumatic brain injury in rats. *Journal of Neuroscience.* **17**(23), 9172-9182.

Clarke, F. J. and Leonard, J. K. (1989). Proposal for a standardised continuous pseudo-colour spectrum with optimum visual contrast and resolution. In *Third International Conference On Image Processing and its Applications*, **307**, 687-691. Institute of Electrical Engineers (IEE) Conference Publications, IEE, Stevenage, UK.

Cole, T. B. et al. (2000). Seizures and neuronal damage in mice lacking vescicular zinc. *Epilepsy Research.* **39**, 153-169.

Conn, P. J. and Pin, J-P. (1997). Pharmacology and functions of metabotropic glutamate receptors. *Annual Review of Pharmacology and Toxicology.* **37**, 205-237.

Coyle, J. T. and Puttfarcken, P. . (1993). Oxidative stress, glutamate, and neurodegenerative disorders. *Science.* **262**, 689-695.

Craig, A. M., Blackstone, C. D., Huganir, R. N., and Banker, G. (1993). The distribution of glutamate receptors in cultured rat hippocampal neurons: postsynaptic clustering of AMPA-selective subunits. *Neuron.* **10**, 1055-1068.

Crompton, M. (1999). The mitochondrial permeability transition pore and its role in cell death. *Biochemical Journal.* **341**, 233-249.

Crompton, M., Virji, S., Doyle, V., Johnson, N., and Ward, J. M. (2000). The mitochondrial permeability transition pore. *Biochemistry Society Symposium.* **66**, 167-179.

Crompton, M. (2000). Mitochondrial intermembrane junctional complexes and their role in cell death. *Journal of Physiology.* **529.1**, 11-21.

Cuajungco, M. P. and Lees, G. J. (1997). Zinc Metabolism in the Brain: Relevance to Human Neurodegenerative Disorders. *Neurobiology of Disease.* **4**, 137-169.

Cuajungco, M. P. and Lees, G. J. (1998). Diverse effects of metal chelating agents on the neuronal cytotoxicity of zinc in the hippocampus. *Brain Research.* **799**, 97-107.

Cunha, R. A., Malva, J. O., and Ribeiro, J. A. (1999). Kainate receptors coupled to G (i)/G(0) proteins in the rat hippocampus. *Molecular Pharmacology.* **56**(2), 429-433.

David, G. Barrett, J. N. and Barrett, E. F. (1998). Evidence that mitochondria buffer physiological Ca^{2+} loads in lizard motor nerve terminals. *Journal of Physiology.* **509.1**, 59-65.

Davies, A. M. (1995). The Bcl-2 family of proteins, and the regulation of neuronal survival. *TINS.* **18**, 355-358.

Davis, K. L., Martin, E., Turko, I. V., and Murad, F. (2001). Novel Effects of Nitric Oxide. *Annual Review of Pharmacology and Toxicology.* **41**, 203-236.

Dawson, T. M., Dawson, V. L., and Snyder, S. H. (1992). *Annals of Neurology.* **32**, 297.

Dawson, V. L., Dawson, T. M., London, E. D., Bredt, D. S., and Snyder, S. H. (1991). Nitric oxide mediates glutamate neurotoxicity in primary cortical cultures. *Proceedings of the National Academy of Sciences USA.* **88**, 6368-6371.

Dawson, V. L., Dawson, T. M., Bartley, D. A., Uhl, G. R., and Snyder, S. H. (1993). Mechanisms of nitric oxide-mediated neurotoxicity in primary brain cultures. *Journal of Neuroscience.* **13**, 2651-2661.

Dawson, V. L. and Dawson, T. M. (1996). Nitric oxide neurotoxicity. *Journal of Chemical Neuroanatomy.* **10**, 179-190.

De Keyser, J., Sulter, G., and Luiten, P. G. (1999). Clinical trials with neuroprotective drugs in acute ischaemic stroke: are we doing the right thing? *TINS.* **22**(12), 535-540.

Desagher, S., Glowinski, J., and Premont, J. (1997). Pyruvate Protects Neurons against Hydrogen Peroxide-Induced Toxicity. *Journal of Neuroscience.* **17**(23), 9060-9067.

Dingledene, R., Borges, K., Bowie, D., and Traynelis, S. F. (1999). The Glutamate Receptor Ion Channels. *Pharmacological Reviews.* **51**(1), 7-61.

Doble, A. (1999). The Role of excitotoxicity in Neurodegenerative Disease: Implications for Therapy. *Pharmacology and Theraputics.* **81**(3), 163-221.

Dubinsky, J. M. and Rothman, S. M. (1991). Intracellular Calcium Concentrations during "Chemical Hypoxia" and Excitotoxic Neuronal *Injury. Journal of Neuroscience.* **11**(8), 2545-2551.

Dubinsky, J. M., Kristal, B. S., and Elizondo-Fournier, M. (1995). On the probabilistic nature of excitotoxic neuronal death in hippocampal neurons. *Neuropharmacology.* **34**, 701-711.

Dubinsky, J. M. and Levi, Y. (1998). Calcium-Induced Activation of the Mitochondrial Permeability Transition in Hippocampal Neurons. *Journal of Neuroscience Research.* **53**, 728-741.

Dubinsky, J. M., Brustovetsky, N., Pinelis, V., Kristal, B. S., Herman, C., and Li, X. (1999). The mitochondrial permeability transition: the brain's point of view. *Biochemistry Society Symposium.* **66**, 75-84.

Duchen, M. (1998). Mitochondria in animal physiology - a whimsical perspective. *Physiological Society Magazine.* 19-20.

Duchen, M. R. (1999). Contributions of mitochondria to animal physiology: from homeostatic sensor to calcium signalling and cell death. *Journal of Physiology.* **516.1** , 1-17.

Duchen, M. R. (1992). Ca^{2+} -dependent changes in the mitochondrial energetics in single dissociated mouse sensory neurons. *Biochemical Journal.* **283**, 41-50.

Duchen, M. R. (2000). Mitochondria and calcium: from cell signalling to cell death. *Journal of Physiology.* **526.1**, 57-68.

Duffy, S., So, A., and Murphy, T. H. (1998). Activation of Endogenous Antioxidant Defenses in Neuronal Cells Prevents Free Radical-Mediated Damage. *Journal of Neurochemistry.* **71**, 69-77.

Dugan, L. L. and Choi, D. W. (1994). Excitotoxicity, Free Radicals, and Cell Membrane Changes. *Annals of Neurology.* **35**, S17-S21.

Dugan, L. L. Sensi, S. L., Canzoniero, L. M. T., Handran, S. D., Rothman, S. M., Lin, T.-S., Goldberg, M. P., and Choi, D. W. (1995). Mitochondrial production of reactive oxygen species in cortical neurons following exposure to N-methyl-D-Aspartate. *Journal of Neuroscience.* **15**(10), 6377-6388.

Dugan, L. L., Sensi, S. L., and Canzoniero, L. M. T. (2001). Mitochondrial Production of Reactive Oxygen Species in Cortical Neurons Following Exposure to NMDA.

Dypbukt, J. M., Thor, H., and Nicotera, P. (1990). Intracellular calcium chelators prevent DNA damage and protect hepatoma 1c1c7 cells from quinone-induced cell killing. *Free Radical Research Communications.* **8**, 347-354.

Eirmerl, S. and Schramm, M. (1994). The Quantity of Calcium that Appears to Induce Neuronal Death. *Journal of Neurochemistry.* **62**, 1223-1226.

Ellerby, H. M., Martin, S. J., Ellerby, L. M., Naiem, S. S., Rabizadeh, S., Salvese, G. S., Casiano, C. A., Cashman, N. R., Green, D. R., and Bredesen, D. E. (1997). Establishment of a cell-free system of neuronal apoptosis: comparison of premitochondrial, mitochondrial and postmitochondrial phases. *Journal of Neuroscience.* **17**, 6165-6178.

Ertel, E., Campbell, K. P., Harpold, M. M., Hofmann, F., Mori, Y., and et al. (2000). Nomenclature of voltage-gated calcium channels. *Neuron.* **25**, 533-535.

Faden, A. I., Demediuk, P., Panter, S. S., and Vink, R. (1989). The role of excitatory amino acids and NMDA receptors in traumatic brain injury. *Science.* **244**, 799-800.

Fage, D., Voltz, C., Scatton, B., and Carter, C. (1992). Selective release of spermine and spermidine from the rat striatum by *N*-methyl-D-aspartate receptor activation *in vivo*. *Journal of Neurochemistry.* **58**, 2170-2175.

Fagni, L. and Bockaert, J. (1996). Effects of nitric oxide on glutamate-gated channels and other ionic channels. *Journal of Chemical Neuroanatomy.* **10**, 231-240.

Fagni, L., Chavis, P., Ango, F., and Bockaert, J. (2000). Complex interactions between mGluRs, intracellular Ca^{2-} stores and ion channels in neurons. *TINS.* **23**(2), 80-88.

Fasolato, C., Zottini, M., and Clementi, E. (1991). Intracellular Ca^{2+} pools in PC12 cells - 3 intracellular pools are distinguished by their turnover and mechanisms of Ca^{2+} accumulation, storage and release. *Journal of Biological Chemistry.* **266**(30), 20159-20167.

Filippov, V. M., Pinchenko, V., Volkova, T. M., and Krishtal, O. A. (1999). Membrane responses to changes in the extracellular potassium concentration in isolated hippocampal pyramidal neurons. *Neurophysiology.* **30**(4-5), 259-263.

Finucane, D. M., Waterhouse, N. J., Amarente-Mendes, G. P., Cotter, T. G., and Green, D. R. (1999). Collapse of the Inner Mitochondrial Transmembrane Potential Is Not Required for Apoptosis of HL60 Cells. *Experimental Cell Research.* **251**, 166-174.

Fiskum, G. (2000). Mitochondrial Participation in Ischaemic and Traumatic Neural Cell Death. *Journal of Neurotrauma.* **17**(10), 843-855.

Floyd, R. A. (1999). Antioxidants, Oxidative Stress, and Degenerative Neurological Disorders. *Proceedings of the Society for Experimental Biology and Medicine.* **222**, 236-245.

Fontaine, E. and Bernardi, P. (1999). Progress on the Mitochondrial Permeability Transition Pore: Regulation by Complex I and Ubiquinone Analogs. *Journal of Bioenergetics and Biomembrane.* **31**(4), 335-345.

Frandsen, A., Drejer, J., and Schousboe, A. (1989). Direct evidence that excitotoxicity in cultured neurons is mediated via NMDA as well as non-NMDA receptors. *Journal of Neurochemistry.* **53**, 297-299.

Frandsen, A. and Schousboe, A. (1991). Dantrolene prevents glutamate cytotoxicity and Ca^{2-} release from intracellular stores in cultured cerebral cortical neurons. *Journal of Neurochemistry.* **56**, 1075-1078.

Frandsen, A. and Schousboe, A. (1992). Mobilization of dantrolene-sensitive intracellular calcium pools is involved in the cytotoxicity induced by quisqualate and N-methyl-D-aspartate but not by 2-amino-3-(3-hydroxy-5-methylisoxazol-4-yl)propionate and kainate in cultured cerebral cortical neurons. *Proceedings of the National Academy of Sciences USA.* **89**, 2590-2594.

Frandsen, A. and Schousboe, A. (1993). Excitatory Amino Acid-Mediated Cytotoxicity and Calcium Homeostasis in Cultured Neurons. *Journal of Neurochemistry.* **60**, 1202-1211.

Frederickson, C. J. et al. (1989). Translocation of zinc may contribute to seizure-induced death of neurons. *Brain Research.* **480**, 317-321.

Friberg, H., Ferrand-Drake, M., Bengtsson, F., Halestrap, A. P., and Wieloch, T. (1998). Cyclosporin A, but not FK506, Protects Mitochondria and Neurons against Hypoglycaemic Damage and Implicates the Mitochondrial Permeability Transition in Cell Death. *Journal of Neuroscience.* **18**(14), 5151-5159.

Fridovich, I. (1999). Fundamental Aspects of Reactive Oxygen Species, or What's the Matter with Oxygen? *Annals of the New York Academy of Sciences.* **893**, 13-18.

Friedman, J. and Hadda, G. G. (1993). Major differences in Ca^{2+}_i response to anoxia between neonatal and adult rat CA1 neurons: Role of Ca^{2+}_o and Na^{+}_o. *Journal of Neuroscience.* **13**(1), 63-72.

Gareri, P., Mattace, R., Nava, F., and de Sarro, G. (1995). Role of Calcium in Brain Aging. *General Pharmacology.* **26**(8), 1651-1657.

Garthwaite, G. and Garthwaite, J. (1986). Neurotoxicity of excitatory amino acid receptor agonists in rat cerebral slices: dependence on calcium concentration. *Neuroscience Letters.* **66**, 193-198.

Garthwaite, G. and Garthwaite, J. (1989). Differential dependence on Ca^{2+} of NMDA and quisqualate neurotoxicity in young rat hippocampal slices. *Neuroscience Letters.* **97**, 316-322.

Garthwaite, G. and Garthwaite, J. (1994). Nitric oxide does not mediate acute glutamate neurotoxicity, nor is it protective, in rat brain slices. *Neuropharmacology.* **33**(11), 1431-1438.

Garthwaite, J. and Boulton, C. L. (1995). Nitric oxide signaling in the central nervous system. *Annual Review of Physiology.* **57**, 683-706.

Ghafourifar, P., Schenk, U., Klein, S. D., and Richter, C. (1999). Mitochondrial Nitric-oxide Synthase Stimulation Causes Cytochrome c release from Isolated Mitochondria. *Journal of Biological Chemistry.* **274**(44), 31185-31188.

Goel, R. and Khanduja, K. L. (1998). Oxidative stress-induced apoptosis - An overview. *Current Science.* **75**(12), 1338-1343.

Greene, J. G. Greenamyre, J. T. (1996). Bioenergetics and glutamate excitotoxicity. *Progress in Neurobiology.* **48**, 613-634.

Greiner, C., Schmidinger, A., Hulsmann, S., Moskopp, D., Wolfer, J., Kohling, R., Speckmann, E. J., and Wassmann, H. (2000). Acute protective effect of nimodipine and dimethyl sulfoxide against hypoxic and ischemic damage in brain slices. *Brain Research.* **887**(2), 316-322.

Gunter, K. K. and Gunter, T. E. (1994). Transport of Calcium by Mitochondria. *Journal of Bioenergetics and Biomembrane.* **26**(5), 471-485.

Gunter, T. E and Pfeiffer, D. R. (1990). Mechanisms by which mitochondria transport calcium. *American Journal of Physiology.* **258**, C755-C786.

Gunter, T. E. Gunter, K. K., Sheu, S., and Gavin, C. E. (1994). Mitochondrial calcium transport: physiological and pathological relevance. *American Journal of Physiology.* **267**, C313-C339.

Gunter, T. E. (1994). Cation Transport by Mitochondria. *Journal of Bioenergetics and Biomembranes.* **26**(5), 465-469.

Gunter, T. E., Buntinas, L., Sparagna, G. C., and Gunter, K. K. (1998). The Ca^{2+} transport mechanisms of mitochondria and Ca^{2-} uptake from physiological-type Ca^{2+} transients. *Biochimica et Biophysica Acts.* **1366**, 5-15.

Hajnoczky, G. Robb-Gaspers, L. D., Seitz, M. B., and Thomas, A. P. (1995). Decoding of cytosolic calcium oscillations in the mitochondria. *Cell.* **82**, 415-424.

Halestrap, A. P. (1999). The mitochondrial permeability transition: its molecular mechanism and role in reperfusion injury. *Biochemistry Society Symposium.* **66**, 181-203.

Hall, E. D., Kupina, N. C., and Althaus, J. S. (1999). Peroxynitrite Scavengers for the Acute Treatment of Traumatic Brain Injury. *Annals of the New York Academy of Sciences.* **893**, 462-468.

Hansford, R. G. (1994). Physiological Role of Mitochondrial Ca^{2+} Transport. *Journal of Bioenergetics and Biomembranes.* **26**(5), 495-508.

Harman, A. W. and Maxwell, M. J. (1995). An evaluation of the role of calcium in cell injury. *Annual Review of Pharmacology and Toxicology.* **35**, 129-144.

Harman, D. (1994). Aging: Prospects for further increases in the functional lifespan. *Age.* **17**, 119-146.

Hartley, D. M., Kurth, M. C., Bjerkness, L., Weiss, J. H., and Choi, D. W. (1993). Glutamate Receptor-induced $^{45}Ca^{2+}$ Accumulation in Cortical Cell Culture Correlates with Subsequent Neuronal Degeneration. *Journal of Neuroscience.* **13**(5), 1993-2000.

Hasbani, M. J., Hyrc, K. L., Faddis, B. T., Romano, C., and Goldberg, M. P. (1998). Distinct roles for sodium, chloride and calcium in excitotoxic dendritic injury and recovery. *Experimental Neurology.* **154**, 241-258.

He, H. L., Lam, M., and McCormick, T. S. (1997). Maintenance of calcium homeostasis in the endoplasmic reticulum by bcl-2. *Journal of Cell Biology.* **138**(6), 1219-1228.

Heales, S. J. R., Barker, J. E., Stewart, V. C., Brand, M. P., Hargreaves, R. P., Foppa, P., Land, J. M., Clark, J. B., and Bolanos, J. P. (1997). Nitric oxide, energy metabolism and neurological disease. *Biochemical Society Transactions.* **25**, 939-943.

Heales, S. J. R., Bolanos, J. P., Stewart, V. C., Brookes, P. S., Land, J. M., and Clark, J. B. (1999). Nitric oxide, mitochondria and neurological disease. *Biochimica et Biophysica Acta.* **1410**, 215-228.

Herrington, J. Park, Y. B., Babcock, D. F., and Hille, B. (1996). Dominant role of mitochondria in clearance of large Ca^{2+} loads from rat adrenal chromaffin cells. *Neuron.* **16**, 219-228.

Hirsch, T., Marzo, I., and Kroemer, G. (1997). Role of the Mitochondrial Permeability Transition Pore in Apoptosis. *Bioscience Reports.* **17**(1), 67-76.

Hobbs, A. J., Higgs, A., and Moncada, S. (1999). Inhibition of nitric oxide synthase as a potential theraputic target. *Annual Review of Pharmacology and Toxicology.* **39**, 191-220.

Hollmann, M., Hartley, M., and Heinemann, S. (1991). Calcium permeability of kainate-AMPA gated glutamate receptor channels depends on subunit composition. *Science.* **252**, 851-853.

Hoth, M. and Penner, R. (1992). Depletion of intracellular calcium stores activates a calcium current in mast cells. *Nature.* **355**, 353-356.

Hoyt, K. R., Stout, A. K., Cardman, J. M., and Reynolds, I. J. (1998). The role of intracellular Na^{+} and mitochondria in buffering of kainate-induced intracellular free Ca^{2+} changes in rat forebrain neurones. *Journal of Physiology.* **509.1**, 103-116.

Huser, J., Rechenmacher, C. E., and Blatter, L. A. (1998). Imaging the permeability transition in single isolated mitochondria . *Biophysical Journal.* **74**, 2129-2137.

Hyrc, K., Handran, S. D., Rothman, S. M., and Goldberg, M. P. (1997). Ionized Intracellular Calcium Concentration Predicts Excitotoxic Neuronal Death: Observations with Low-Affinity Fluorescent Calcium Indicators. *Journal of Neuroscience.* **17**(17), 6669-6677.

Iadecola, C., Zhang, F, Casey, R, Nagayama, M., and Ross, E. M. (1997). Delayed reduction of ischaemic brain injury and neurological deficits in mice lacking the inducible nitric oxide synthase gene. *Journal of Neuroscience.* **17**(23), 9157-9164.

Ichas, F. Jouaville, L. S. and Mazat, J. P. (1997). Mitochondria are excitable organelles capable of generating and conveying electrical and calcium signals. *Cell.* **89**, 1145-1153.

Iihara, K., Joo, D. T., and Henderson, J. (2001). The influence of glutamate receptor 2 expression on excitotoxicity in GluR2 null mutant mice. *Journal of Neuroscience.* **21**(7), 2224-2239.

Isacson, O. (1993). On neuronal health. *TINS.* **16**(8), 306-308.

Isaev, N. K., Zorov, D. B., Stelmashook, E. V., Uzbekov, R. E., Kozhemyakin, M. B., and Victorov.I.V. (1996). Neurotoxic glutamate treatment of cultured cerebellar granule cells induces Ca^{2+}-dependent collapse of mitochondrial membrane potential and ultrastructural alterations of mitochondria. *FEBS Letters.* **392**, 143-147.

Ishikawa, Y., Satoh, T., Enokido, Y., Nishio, C., Ikeuchi, T., and Hatanaka, H. (1999). Generation of reactive oxygen species, release of L-glutamate and activation of caspases are required for oxygen-induced apoptosis of embryonic hippocampal neurons in culture. *Brain Research.* **824**, 71-80.

Israel, M. and Dunant, Y. (1998). Acetylcholine release and the cholinergic genomic locus. *Molecular Neurobiology.* **16**, 1-20.

Izumi, Y., Benz, A. M., Clifford, D. B., and Zorumski, C. F. (1992). Nitric-oxide inhibitors attenuate NMDA excitotoxicity in rat hippocampal slices. *Neuroscience Letters.* **135**(2), 227-230.

Jacewicz, M., Brint, S., Tanabe, J., and Pulsinelli, W. A. (1990). Continuous nimodipine treatment attenuates cortical infarction in rats subjected to 24 hours of focal cerebral ischaemia. *Journal of Cerebral Blood Flow and Metabolism.* **10**, 89-96.

Jacobsen, M. D. and Raff, M. C. (1995). Programmed cell death and Bcl-2 protection in very low oxygen. *Nature.* **374**, 814-816.

Jacotot, E., Costantini, P., Laboureau, E., Zamzami, N., Susin, S. A., and Kroemer, G. (1999). Mitochondrial Membrane Permeabilization during the Apoptotic Process. *Annals of the New York Academy of Sciences.* **893**, 18-30.

Jane, S. D. Phenna, S. and Chad, J. E. (1995). Confocal ratiometric measurements of intracellular calcium ion activity in acutely dissociated pyramidal neurones and their preparation from the rat hippocampus.

Jornot, L., Maechier, P., Wollheim, C. B., and Junod, A. F. (1999). Reactive oxygen metabolites increase mitochondrial calcium in endothelial cells: implication of the Ca^{2+}/Na^{+} exchanger. *Journal of Cell Science.* **112**, 1013-1022.

Jurgensmeier, J. M., Xie, Z., Deverzux, Q., Ellerby, L., Bredesen, D. E., and Reed, J. C. (1998). Bax directly induces release of cytochrome c from isolated mitochondria. *Proceedings of the National Academy of Sciences USA.* **95**, 4997-5002.

Kader, A., Frazzini, V. I., Soloman, R. A., and Triffiletti, R. R. (1993). Nitric oxide production during focal cerebral ischemia in rats. *Stroke.* **24**(11), 1709-1716.

Kalous, M. and Drahota, Z. (1996). The role of mitochondria in aging. *Physiological Research.* **45**, 351-359.

Kashii, S., Mandai, M., Kikuchi, M., Honda, Y., Tamura, Y., Kaneda, K., and Akaike, A. (1996). Dual actions of nitric oxide in NMDA receptor-mediated neurotoxicity in cultured retinal neurons. *Brain Research.* **711**, 93-101.

Keelan, J., Vergun, O., and Duchen, M. (1999). Excitotoxic mitochondrial depolarisation requires both calcium and nitric oxide in rat hippocampal neurons. *Journal of Physiology.* **520.3**, 797-813.

Keelan, J., Allen, N. J., and Duchen, M. (2000). Glutathione, oxidative stress and glutamate excitotoxicity in hippocampal cultures. *Society for Neuroscience Abstract.* **378.12**.

Keller, J. N., Kindy, M. S., Holtsberg, F. W., St Clair, D. K., Yen, H-C., Germyer, A., Steiner, S. M., Bruce-Keller, A. J., Hutchins, J. B., and Mattson, M. (1998). Mitochondrial Manganese Superoxide Dismutase Prevents Neural Apoptosis and reduces Ischemic Brain Injury: Suppression of Peroxynitrite Production, Lipid Peroxidation, and Mitochondrial Dysfunction. *Journal of Neuroscience.* **18**(2), 687-697.

Kennedy, M. B. (1989). Regulation of Neuronal Function by Calcium. *TINS.* **12**(11), 417-420.

Khodorov, B., Pinelis, V., Golovina, V., Fajuk, D., Andreeva, N., Uvarova, T., Khaspekov, L., and Victorov, I. (1993). On the origin of a sustained increase in cytosolic Ca^{2+} concentration after a toxic glutamate treatment of the nerve cell culture. *FEBS Letters.* **324**(3), 271-273.

Khodorov, B., Pinelis, V., Vergun, O., Storozhevykh, T., and Vinskaya, N. (1996). Mitochondrial deenergization underlies neuronal calcium overload following a prolonged glutamate challenge. *FEBS Letters.* **397**, 230-234.

Khodorov, B., Pinelis, V., Storozhevykh, T., Vergun, O., and Vinskaya, N. (1996). Dominant role of mitochondria in protection against a delayed neuronal Ca^{2+} overload induced by endogenous excitatory amino acids following a glutamate pulse. *FEBS Letters.* **393**, 135-138.

Khodorov, B., Pinelis, V., Storozhevykh, T., Yuravichus, A., and Khaspekhov, L. (1999). Blockade of mitochondrial Ca^{2+} uptake by mitochondrial inhibitors amplifies the glutamate-induced calcium response in cultured cerebellar granule cells. *FEBS Letters.* **458**, 162-166.

Khodorov, B. and Borodin, A. (2001). Inter-relationships between mitochondrial potential and cytoplasmic calcium in nerve cells caused by prolonged glutamate exposure: computer simulation. *Journal of Physiology (in press).*

Kiedrowski, L. (1998). The difference between mechanisms of kainate and glutamate excitotoxicity *in vitro*: osmotic lesion versus mitochondrial depolarization. *Restorative Neurology and Neuroscience.* **12**, 71-79.

Kim, E. Y., Koh, J-Y., Kim, Y-H., Sohn, S., Joe, E., and Gwag, B. J. (1999). Zn^{2+} entry produces oxidative neuronal necrosis in cortical cell cultures. *European Journal of Neuroscience.* **11**, 327-334.

Kim, Y-H., Kim, E. Y., Gwag, B. J., Sohn, S., and Koh, J-Y. (1999). Zinc-induced cortical neuronal death with features of apoptosis and necrosis: mediation by free radicals. *Neuroscience.* **89**(1), 175-182.

Knowles, R. G. (1997). Nitric oxide biochemistry. *Biochemical Society Transactions.* **25**, 895-901.

Koh, D. S., Geiger, J. R. P., Jonas, P., and Sakmann, B. (1995). Ca^{2+}-permeable AMPA and NMDA receptor channels in basket cells of rat hippocampal dentate gyrus. *Journal of Physiology.* **485**(2), 383-402.

Koh, J. Y. (1996). The role of zinc in selective neuronal death after transient global ischemia. *Science.* **272**, 1013-1016.

Korenkov, A. I., Pahnke, J., Frei, K., Warzok, R., Schroeder, H. W. S., Muljana, L., Piek, J., Yonekawa, Y., and Gaab, M. R. (2000). Treatment with nimodipine or mannitol reduces programmed cell death amd infarct size following focal cerebral ischemia. *Neurosurgical Review.* **23**(3), 145-150.

Korge, P. and weiss, J. N. (1999). Thapsigargin directly induces the mitochondrial permeability transition. *European Journal of Biochemistry.* **265**, 273-280.

Korkotian, E. and Segal, M. (1997). Calcium-containing organelles display unique reactivity to chemical stimulation in cultured hippocampal neurons. *Journal of Neuroscience.* **17**, 1670-1682.

Kristal, B. S. Dubinsky, J. M. (1997). Mitochondrial permeability transition in the central nervous system: induction by calcium cycling-dependent and -independent pathways. *Journal of Neurochemistry.* **69**, 524-538.

Kristian, T. and Siesjo, B. K. (1998). Calcium in Ischemic Cell Death. *Stroke.* **29**, 705-718.

Kroemer, G., Petit, P. X., Zamzami, N., Vayssiere, J-L., and Mignotte, B. (1995). The biochemistry of apoptosis. *FASEB Journal.* **9**, 1277-1287.

Kroemer, G., Dallaporta, B., and Resche-Rigon, M. (1998). The mitochondrial death/life regulator in apoptosis and necrosis. *Annual Review of Physiology.* **60**, 619-642.

Kroemer, G. (1999). Mitochondrial control of apoptosis: an overview. *Biochemistry Society Symposium.* **66**, 1-15.

Kroemer, G. and Reed, J. C. (2000). Mitochondrial control of cell death. *Nature Medicine.* **6**(5), 513-519.

Krohn, A. J., Wahlbrink, T., and Prehn, J. H. M. (1999). Mitochondrial Depolarization Is Not Required for Neuronal Apoptosis. *Journal of Neuroscience.* **19**(17), 7394-7404.

Kruman, I. I. and Mattson, M. (1999). Pivotal Role of Mitochondrial Calcium Uptake in Neural Cell Apoptosis and Necrosis. *Journal of Neurochemistry.* **72**, 529-540.

Kudo, Y., Takeda, K., and Yamazaki, K. (1990). Quin2 protects against neuronal cell death due to Ca^{2+} overload. *Brain Research.* **528**, 48-54.

Lafoncazal, M., Culcasi, M., and Gaven, F. (1993). Nitric oxide, superoxide and peroxynitrite - putative mediators of NMDA-induced cell death in cerebellar granule cells. *Neuropharmacology.* **32**(11), 1259-1266.

Landolfi, B., Curci, S., and Debellis, L. (1998). Ca^{2+} homeostasis in the agonist-sensitive internal store: Functional interactions between mitochondria and the ER measured in situ in intact cells. *Journal of Cell Biology.* **142**(5), 1235-1243.

Lee, K. S., Frank, S., Vanderklish, P., Arai, A., and Lynch, G. (1991). Inhibition of proteolysis protects hippocampal neurons from ischaemia. *Proceedings of the National Academy of Sciences, USA.* **88**, 7233-7237.

Lees, G. J., Cuajungco, M. P., and Leong, W. (1998). Effect of metal chelating agents on the direct and seizure-related neuronal death induced by zinc and kainic acid. *Brain Research.* **799**, 108-117.

Leist, M., Single, B., Castoldi, A. F., Kuhnle, S., and Nicotera, P. (1997). Intracellular adenosine triphosphate (ATP) concentration: a switch in the decision between apoptosis and necrosis. *Journal of Experimental Medicine.* **185**(8), 1481-1486.

Leist, M. and Nicotera, P. (1998). Calcium and neuronal death . *Reviews of Physiology, Biochemistry and Pharmacology.* **132**, 79-125.

Leist, M. and Nicotera, P. (1998). Apoptosis, Excitotoxicity, and Neuropathology. *Experimental Cell Research.* **239**, 183-201.

Leist, M., Single, B., Naumann, H., Fava, E., Simon, B., Kuhnle, S., and Nicotera, P. (1999). Nitric Oxide Inhibits Execution of Apoptosis at Two Distinct ATP-Dependent Steps Upstream and Downstream of Mitochondrial Cytochrome c Release. *Biochemical and Biophysical Research Communications.* **258**, 215-221.

Leist, M., Single, B., Naumann, H., Fava, E., Simon, B., Kuhnle, S., and Nicotera, P. (1999). Inhibition of Mitochondrial ATP Generation by Nitric Oxide Switches Apoptosis to Necrosis. *Experimental Cell Research.* **249**, 396-403.

Lemasters, J., Nieminen, A-L., Qian, T., Trost, L. C., Elmore, S. P., Nishimura, Y., Crowe, R. A., Cascio, W. E., Bradham, C. A., Brenner, D. A., and Herman, B. (1998). The mitochondrial permeability transition in cell death: a common mechanism in necrosis, apoptosis and autophagy. *Biochimica et Biophysica Acta.* **1366**, 177-196.

Lemasters, J., Qian, T., Bradham, C. A., Brenner, D. A., Cascio, W. E., Trost, L. C., Nishimura, Y., Nieminen, A-L., and Herman, B. (1999). Mitochondrial Dysfunction in the Pathogenesis of Necrotic and Apoptotic Cell Death. *Journal of Bioenergetics and Biomembrane.* **31**(4), 305-319.

Lemasters, J., Qian, T., Trost, L. C., Herman, B., Cascio, W. E., Bradham, C. A., Brenner, D. A., and Nieminen, A-L. (1999). Confocal microscopy of the mitochondrial permeaility transition in necrotic and apoptotic cell death. *Biochemistry Society Symposium.* **66**, 205-222.

Lenaz, G. (1998). Role of mitochondria in oxidative stress and ageing. *Biochimica et Biophysica Acta.* **1366**, 53-67.

Lerma, J., Paternain, A. V., Rodriguez-Moreno, A., and Lopez-Garcia, J. C. (2001). Molecular Physiology of Kainate Receptors. *Physiological Reviews.* **81**(3), 971-998.

Lernernatoli, M., Ronduin, G., Debock, F., and Bockaert, J. (1992). Chronic NO synthase inhibition fails to protect hippocampal neurons against NMDA toxicity. *NeuroReport.* **3**(12), 1109-1112.

Letts, V. A., Felix, R., Biddlecome, G. H., Arikkath, J., and Mahaffey, C. L. (1998). The mouse *stargazer* gene encodes a neuronal Ca^{2+} channel γ subunit. *Nature Genetics.* **19**, 340-347.

Levy, D. I., Sucher, N. J., and Lipton, S. A. (1990). Redox modulation of NMDA receptor-mediated toxicity in mammalian central neurons. *Neuroscience Letters.* **110**, 291-296.

Lipton, S. A. and Nicotera, P. (1998). Calcium, free radicals and excitotoxins in neuronal apoptosis. *Cell Calcium.* **23**(2-3), 165-171.

Liu, H., De Waard, M., Scott, V. E. S., Gurnett, C. A., and Lennon, V. A. (1996). Identification of three subunits of the high affinity ω-conotoxin MVIIC-sensitive calcium channel. *Journal of Biological Chemistry.* **271**, 13804-13810.

Liu, J. and Mori, A. (1999). Stress, Aging, and brain Oxidative Damage. *Neurochemical Research.* **24**(11), 1479-1497.

Liu, S-S. (1997). Generating, Partitioning, Targeting and Functioning of Superoxide in Mitochondria. *Bioscience Reports.* **17**(3), 259-272.

Liu, X., Kim, C. N., Yang, J., Jemmerson, R., and Wang, X. (1996). Induction of apoptosis programme in cell-free extracts: requirement for dATP and cytochrome c. *Cell.* **86**, 147-157.

Llinas, R. R. and Yarom, Y. (1981). Electrophysiology of mammalian inferior olivary neurones in vitro. Different types of voltage-dependent ionic conductances. *Journal of Physiology.* **315**, 569-584.

Lu, Y. M., Yin, H. Z., Chiang, J., and Weiss, J. H. (1996). Ca^{2+} -Permeable AMPA/Kainate and NMDA Channels: High Rate of Ca^{2+} Influx Underlies Potent Induction of Injury. *Journal of Neuroscience.* **16**(17), 5457-5465.

Luetjens, C. M., Bui, N. T., Sengpiel, B., Munstermann, G., Poppe, M., Krohn, A. J., Bauerbach, E., Krieglstein, J., and Prehn, J. H. M. (2000). Delayed Mitochondrial Dysfunction in Excitotoxic Neuron Death: Cytochrome c Release and a Secondary Increase in Superoxide Production. *Journal of Neuroscience.* **20**(15), 5715-5723.

Lui, P. Y., Kong, S. K., Kwok, T. T., and Lee, C. Y. (1998). The nucleus of HeLa cell contains tubular structures for Ca^{2+} signalling. *Biochemical and Biophysical Research Communications.* **247**, 88-93.

Luo, X., Budihardjo, I., Zou, H., Slaughter, C., and Wang, X. (1998). Bid, a Bcl2 Interacting Protein, Mediates Cytochrome c Release from Mitochondria in Response to Activation of Cell Surface Death Receptors. *Cell.* **94**, 481-490.

Macho, A, Castedo, M, Marchetti, P., Aguilar, J. J., Decaudin, D., Zamzami, N., Girad, P. M., and Kroemer, G. (1995). Mitochondrial dysfunctions in circulating T lymphocytes from Human Immunodeficiency Virus-1 carriers. *Blood.* **86**(7), 2481-2487.

Maher, P. and Schubert, D. (2000). Signaling by reactive oxygen species in the nervous system. *Cellular and Molecular Life Sciences.* **57**, 1287-1305.

Malen, P. L. and Chapman, P. F. (1997). Nitric Oxide Facilitates Long-Term Potentiation, But Not Long-Term Depression. *Journal of Neuroscience.* **17**(7), 2645-2651.

Malviya, A. N. and Rogue, P. J. (1998). "Tell Me Where Is Calcium Bred": Clarifying the Roles of Nuclear Calcium. *Cell.* **92**, 17-23.

Manev, H., Favaron, M., Guidotti, A., and Costa, E. (1989). Delayed Increase of Ca^{2+} Influx Elicited by Glutamate: Role in Neuronal Death. *Molecular Pharmacology.* **36**, 106-112.

Marchetti, P., Castedo, M, Susin, S. A., Zamzami, N., Hirsch, T., Macho, A, Haeffner, A., Hirsch, F., Geuskens, M., and Kroemer, G. (1996). Mitochondrial Permeability Transition is a Central Coordinating Event of Apoptosis. *Journal of Experimental Medicine.* **184**, 1155-1160.

Markram, H., Helm, P. J., and Sakmann, B. (1995). Dendritic calcium transients evoked by single back-propagating action-potentials in rat neocortical pyramidal neurons. *Journal of Physiology.* **485**, 1-20.

Martin-Moutot, N., Leveque, C., Sato, K., Kato, R., and Takahashi, M. (1995). Properties of omega conotoxin MVIIC receptors associated with α_{1A} calcium channel subunits in rat brain. *FEBS Letters.* **366**, 21-25.

Martinez-Serrano, A. and Satrustegui, J. (1992). Regulation of cytosolic free calcium-concentration by intrasynaptic mitochondria. *Molecular Biology of the Cell.* **3**(2), 235-248.

Marzo, I., Susin, S. A., Petit, P. X., Ravagnan, L., Brenner, C., Larochette, N., Zamzami, N., and Kroemer, G. (1998). Caspases disrupt mitochondrial membrane barrier function. *FEBS Letters.* **427**, 198-202.

Matsumoto, S., Friberg, H., Ferrand-Drake, M., and Wieloch, T. (1999). Blockade of the Mitochondrial Permability Transition Pore Diminishes Infarct Size in the Rat After Transient Middle Cerebral Artery Occlusion. *Journal of Cerebral Blood Flow and Metabolism.* **19**, 736-741.

Matyja, E. (1997). Intracellular calcium overload in a model of quinolic acid neurotoxicity in organotypic culture of rat hippocampus; inhibited by nimodipine. *Folia Neuropathologica.* **35**(1), 8-17.

McBain, C. J. and Mayer, M. L. (1994). *N*-Methyl-D-Aspartic Acid Receptor Structure and Function. *Physiological Reviews.* **74**(3), 723-760.

McBurney, R. N. and Neering, I. R. (1987). Neuronal calcium homeostasis. *TINS.* **10**(4), 164-169.

McCleskey, E. W., Fox, A. P., Feldman, D. H., Cruz, L. J., and Olivera, B. M. (1987). ω-Conotoxin: direct and persisitent blockade of specific types of calcium channels in neurons but not muscle. *Proceedings of the National Academy of Sciences USA.* **84**, 4327-4231.

McConkey, D. J. and Orrenius, S. (1997). The Role of Calcium in the Regulation of Apoptosis. *Biochemical and Biophysical Research Communications.* **239**, 357-366.

McConkey, D. J. (1998). Biochemical determinants of apoptosis and necrosis. *Toxicology Letters.* **99**, 157-168.

McCormack, J. G. Halestrap, A. P. and Denton, R. M. (1990). Role of calcium ions in regulation of mammalian intramitochondrial metabolism. *Physiological Reviews.* **70**(2), 391-425.

McEnery, M. W., Snowman, A. M., Sharp, A. H., Adams, M. E., and Snyder, S. H. (1991). Purified ω-conotoxin GVIA receptor of rat brain resembles a dihydropyridine-sensitive L-type calcium channel. *Proceedings of the National Academy of Sciences USA.* **88**, 11095-11099.

McIntosh, T. K. (1994). Neurochemical sequelae of traumatic brain injury: theraputic implications. *Cerebrovascular and Brain Metabolism Reviews.* **6**, 109-162.

McIntosh, T. K., Juhler, M., and Wieloch, T. (1998). Novel pharmacologic strategies in the treatment of experimental brain injury: 1998. *Journal of Neurotrauma.* **15**(10), 731-769.

Mecocci, P. MacGarvey, U., Kaufman, A., Koontz, D., Shoffner, J. M, Wallace, D. C., and Beal, M. F. (1993). Oxidative damage to mitochondrial DNA shows marked age-dependent increases in human brain. *Annals of Neurology.* **34**, 609-616.

Melamed-Book, N. Rahamimoff, R. (1998). The revival of the role of the mitochondrion in regulation of transmitter release. *Journal of Physiology.* **509.1**, 2.

Melov, S. (1999). Mitochondrial Oxidative Stress. *Annals of the New York Academy of Sciences.* **893**, 219-225.

Melyan, Z., Wheal, H. V., and Lancaster, B. (2002). Metabotropic-mediated kainate receptor regulation of I_{sAHP} and axcitability in pyramidal cells. *Neuron.* **34**, 1-20.

Michaelis, E. K. (1997). Molecular biology of glutamate receptors in the central nervous system and their role in excitotoxicity, oxidative stress and aging. *Progress in Neurobiology.* **54**, 369-415.

Michaels, R. L. and Rothman, S. M. (1990). Glutamate Neurotoxicity in vitro: Antagonist Pharmacology and Intracellular Calcium Concentrations. *Journal of Neuroscience.* **10**(1), 283-292.

Mignotte, B. and Vayssiere, J-L. (1998). Mitochondria and apoptosis. *European Journal of Biochemistry.* **252**, 1-15.

Miller, R. J. (1988). Calcium signalling in neurons. *TINS.* **11**(10), 415-425.

Miller, R. J. (1991). The Control of Neuronal Ca^{2+} Homeostasis. *Progress in Neurobiology.* **37**, 255-285.

Miller, R. J. (1998). Mitochondria - the Kraken wakes! *TINS.* **21**(3), 95-97.

Minimikawa, T., Sriratana, A., Williams, D. A., Bowser, D. N., and Nagley, P. (1999). Chloromethyl-X-rosamine (MitoTracker Red) photosensitizes mitochondria and induces apoptosis in intact human cells. *Journal of Cell Science.* **112**(14), 2419-2430.

Minimikawa, T., Williams, D. A., Bowser, D. N., and Nagley, P. (1999). Mitochondrial Permeability Transition and Swelling Can Occur Reversibly without Inducing Cell Death in Intact Human Cells. *Experimental Cell Research.* **246**, 26-37.

Mintz, I. M., Adams, M. E., and Bean, B. P. (1992). P-type calcium channels in rat central and peripheral neurons. *Neuron.* **9**, 85-95.

Miura, S., Fukumura, D., Shiozaki, H., Suzuki, M., Kurose, I., Suematsu, M., Tsuchiya, M., and Ishii, H. (1995). Bile acid induced depolarization of mitochondrial membrane potential preceding cell injury in cultured gastric mucosal cells. *Journal of Gastroenterology and Hepatology.* **10**, 621-626.

Mody, I. and MacDonald, J. F. (1995). NMDA receptor-dependent excitotoxicity: the role of intracellular Ca^{2+} release. *TIPS.* **16**, 356-359.

Monaghan, D. T., Bridges, R. J., and Cotman, C. W. (1989). The Excitatory Amino Acid Receptors: Their Classes, Pharmacology, and Distinct Properties in the Function of the Central Nervous System. *Annual Review of Pharmacology and Toxicology.* **29** , 365-402.

Monje, M. L., Chatten-Brown, J., Hye, S. E., and Raley-Susman, K. M. (2000). Free radicals are involved in the damage to protein synthesis after anoxia/aglycaemia and NMDA exposure. *Brain Research.* **857**, 172-182.

Monks, T. J., Ghersi-Egea, J-F., Philbert, M., Cooper, A. J. L., and Lock, E. A. (1999). The Role of Glutathione in Neuroprotection and Neurotoxicity. *Toxicological Sciences.* **51**, 161-177.

Montal, M. (1998). Mitochondria, glutamate neurotoxicity and the death cascade. *Biochimica et Biophysica Acta.* **1366**, 113-126.

Morrison, R. S., Kinoshita, Y., Hong, X., Johnson, M. D., Kuntz, C., Ghatan, S., Ho, J. T., and Schwartzkroin, P. A. (1998). Mechanisms of Neuronal Cell Death. *Mental Retardation and Developmental Disabilities Research Reviews.* **4**, 157-170.

Motyl, T. (1999). Regulation of apoptosis: involvement of Bcl-2-related proteins. *Reproductive Nutrition and Development.* **39**, 49-59.

Mukhin, A., Fan, L., and Faden, A. I. (1996). Activation of metabotropic glutamate receptors subtype mGluR1 contributes to post-traumatic neuronal injury. *Journal of Neuroscience.* **16**, 6012-6020.

Murata, T., Omata, N., Fujibayashi, Y., Waki, A., Sadato, N., Yoshimoto, M., Wada, Y., and Yonekura, Y. (2000). Posthypoxic Reoxygenation-Induced Neurotoxicity Prevented by Free Radical Scavenger and NMDA/non-NMDA Antagonist in Tandem as Revealed by Dynamic Changes in Glucose Metabolism with Positron Autoradiography. *Experimental Neurology.* **164**, 269-279.

Murphy, A. N., Bredesen, D. E., Cortopassi, G., Wang, E., and Fiskum, G. (1996). Bcl-2 potentiates the maximal calcium uptake capacity of neural cell mitochondria. *Proceedings of the National Academy of Sciences, USA.* **93**, 9893-9898.

Murphy, A. N. (1999). Potential Mechanisms of Mitochondrial Cytochrome-c Release During Apoptosis. *Drug Development Research.* **46**, 18-25.

Murphy, A. N., Fiskum, G., and Beal, M. F. (1999). Mitochondria in Neurodegeneration:Bioenergetic Function in Cell Life and Death. *Journal of Cerebral Blood Flow and Metabolism.* **19**, 231-245.

Murphy, A. N. and Fiskum, G. (2000). Bcl-2 and Ca^{2+}-mediated mitochondrial dysfunction in neural cell death. *Biochemistry Society Symposia.* **66**, 33-41.

Murphy, S. N. and Miller, R. J. (1989). Two distinct quisqualate receptors regulate Ca^{2+} homeostasis in hippocampal neurons *in vitro*. *Molecular Pharmacology.* **35**, 671-680.

Mynlieff, M. (1997). Dissociation of postnatal hippocampal neurons for short term culture. *Journal of Neuroscience Research.* **73**, 35-44.

Nath, R., Probert, A., McGinnis, K. M., and Wang, K. (1998). Evidence for Activation of Caspase-3-like Protease in Excitotoxin- and Hypoxia/Hypglycaemia-Injured Neurons. *Journal of Neurochemistry.* **71**, 186-195.

Newell, D. W., Barth, A., Papermaster, V., and Malouf, A. T. (1995). Glutamate and non-glutamate receptor mediated toxicity caused by oxygen and glucose deprivation in organotypic hippocampal cultures. *Journal of Neuroscience.* **15**(11), 7702-7711.

Nicholls, D. and Scott, I. D. , I. D. (1980). The regulation of brain mitochondrial calcium ion transport. *Biochemical Journal.* **186**, 833-839.

Nicholls, D. (1985). A role for the mitochondrion in the protection of cells against calcium overload? *Progress in Brain Research.* **63**, 97-106.

Nicholls, D., Budd, S. L., Castilho, R. F., and Ward, M. W. (1999). Glutamate excitotoxicity and neuronal energy metabolism. *Annals of the New York Academy of Sciences.* **893**, 1-12.

Nicholls, D. G. and Ward, M. W. (2000). Mitochondrial membrane potential and neuronal glutamate excitotoxicity: mortality and millivolts. *TINS.* **23**, 166-174.

Nicholls, D. G. and Budd, S. L. (2000). Mitochondria and Neuronal Survival. *Physiological Reviews.* **80**, 315-360.

Nicholls, D. G., and Ferguson, S. J. (2002). *Bioenergetics 3*, Academic Press.

Nicholson, C., Bruggencate, G. C., Steinberg, R., and Stockle, H. (1977). Calcium modulation in brain extracellular microenvironment demonstrated with ion-selective micropipette. *Proceedings of the National Academy of Sciences USA.* **74**, 1287-1290.

Nicotera, P., Bellomo, G, and Orrenius, S. (1992). Calcium-mediated mechanisms in chemically induced cell death. *Annual Review of Pharmacology and Toxicology.* **32**, 449-470.

Nicotera, P. and Lipton, S. A. (1999). Excitotoxins in Neuronal Apoptosis and Necrosis. *Journal of Cerebral Blood Flow and Metabolism.* **19**, 583-591.

Nicotera, P., Leist, M., and Ferrando-May, E. (2000). Apoptosis and necrosis: different execution of the same death. *Biochemistry Society Symposia.* **66**, 69-73.

Nieminen, A-L., Petrie, T. G., Lemasters, J., and Selman, W. R. (1996). Cyclosporin A delays mitochondrial depolarization induced by NMDA in cortical neurons: evidence of the mitochondrial permeability transition. *Neuroscience.* **75**(4), 993-997.

Nowicky, A. V. Duchen, M. R. (1998). Changes in $[Ca^{2+}]_i$ and membrane currents during impaired mitochondrial metabolism in dissociated rat hippocampal neurons. *Journal of Physiology.* **507.1**, 131-145.

Nowycky, M. C., Fox, A. P., and Tsien, R. W. (1985). Three types of neuronal calcium channel with different calcium agonist sensitivity. *Nature.* **316**, 440-443.

Ogura, A., Miyamoto, M., and Kudo, Y. (1988). Neuronal death in vitro: parallelism between survivability of hippocampal neurones and sustained elevation of cytosolic Ca^{2+} after exposure to glutamate receptor agonist. *Experimental Brain Research.* **73**, 447-458.

Ohkuma, S., Katsura, M., Higo, A., Shirotani, K., Hara, A., Tarumi, C., and Ohgi, T. (2001). Peroxynitrite affects Ca^{2+} influx through voltage-dependent calcium channels. *Journal of Neurochemistry.* **76**, 341-350.

Okada, T., Schultz, K., Geurtz, W., Hatt, H., and Weiler, R. (1999). AMPA-preferring receptors with high Ca^{2+} permeability mediate dendritic plasticity of retinal horizontal cells. *European Journal of Neuroscience.* **11**, 1085-1095.

Olanow, C. W. (1993). A radical hypothesis for neurodegeneration. *TINS.* **16**, 439-444.

Olney, J. W. (1978). Neurotoxicity of excitatory amino acids. In: Kainic Acid as a Tool in Neurobiology, pp 95-112, McGeer, E.G., Olney, J.W. and McGeer, P.L. (eds.) Raven Press, New York.

Olney, J. W., Price, M., Salles, S., Labruyere, J., and Frierdich, G. (1987). MK-801 pwerfully protects against N-methyl aspartate neurotoxicity. *European Journal of Pharmacology.* **141**, 357-361.

Orrenius, S., Burkitt, M. J., Kass, G. E. N., Dypbukt, J. M., and Nicotera, P. (1992). Calcium Ions and Oxidative Cell Injury. *Annals of Neurology.* **32**, S33-S42.

Orrenius, S. and Nicotera, P. (1994). The calcium ion and cell death. *Journal of Neural Transmissions.* **[Suppl] 43**, 1-11.

Otterson, O. P. and Landsend, A. S. (1997). Organization of Glutamate Receptors at the Synapse. *European Journal of Neuroscience.* **9**, 2219-2224.

Ozawa, S., Kamiya, H., and Tsuzuki, K. (1998). Glutamate receptors in the mammalian central nervous system. *Progress in Neurobiology.* **54**, 581-618.

Ozawa, T. (1999). Mitochondrial Genome Mutation in Cell death and Aging. *Journal of Bioenergetics and Biomembrane.* **31**(4), 377-390.

Packer, M. A., Scarlett, J. L., Martin, S. W., and Murphy, M. P. (1997). Induction of the mitochondrial permeability transition by peroxynitrite. *Biochemical Society Transactions.* **25**, 909-914.

Palmer, A. M., Marion, D. W., Botscheller, M. L., Bowen, D. M., and Dekosky, S. T. (1994). Increased transmitter amino acid concentration in human ventricular CSF after brain trauma. *NeuroReport.* **6**, 153-156.

Parekh, A. B. and Penner, R. (1997). Store Depletion and Calcium Influx. *Physiological Reviews.* **77**(4), 901-930.

Paschen, W. (1996). Disturbances of calcium homeostasis within the endoplasmic reticulum may contribute to the development of ischemic cell damage. *Medical Hypotheses.* **47**(4), 283-288.

Paschen, W. and Doutheil, J. (1998). Disturbances of the Functioning of Endoplasmic Reticulum: A Key Mechanism Underlying Neuronal Cell Injury? *Journal of Cerebral Blood Flow and Metabolism.* **19**, 1-18.

Paschen, W. and Frandsen, A. (2001). Endoplasmic reticulum dysfunction - a common denominator for cell injury in acute and degenerative diseases of the brain? *Journal of Neurochemistry.* **79**, 719-725.

Patel, M., Day, B. J., Crapo, J. D., Fridovich, I., and McNamara, J. O. (1996). Requirement for Superoxide in Excitotoxic Cell Death. *Neuron.* **16**, 345-355.

Pauwels, P. J. and Leysen, J. E. (1992). Blockade of nitric oxide formation does not prevent glutamate-induced neurotoxicity in neuronal cultures from rat hippocampus. *Neuroscience Letters.* **143**(1-2), 27-30.

Pellegrini-Giampietro, D. E. et al. (1992). Switch in glutamate receptor subunit gene expression in CA1 subfield of hippocampus following global ischemia in rats. *Proceedings of the National Academy of Sciences, USA.* **89**, 10499-10503.

Pellegrini-Giampietro, D. E., Gorter, J. A., Bennett, M. V. L., and Zukin, R. S. (1997). The GluR2 (GluR-B) hypothesis: Ca^{2+}-permeable AMPA receptors in neurological disorders. *TINS.* **20**, 464-470.

Peng, T-I, Jou, M-J., Sheu.S-S., and Greenamyre, J. T. (1998). Visualization of NMDA Receptor-Induced Mitochondrial Calcium Accumulation in Striatal Neurons. *Experimental Neurology.* **149**, 1-12.

Peng, T. and Greenamyre, J. T. (1998). Privileged access to mitochondria of calcium influx through NMDA Receptors. *Molecular Pharmacology.* **53**, 974-980.

Perez-Pinzon, M. A., Xu, G. P., Born, J., Lorenzo, J., Busto, R., Rosenthal, M., and Sick, T. J. (1999). Cytochrome c is released from mitochondria into the cytosol after cerebral anoxia or ischaemia. *Journal of Cerebral Blood Flow and Metabolism.* **19**(1), 39-43.

Perez Velazquez, J. L. (1997). In Vitro Ischaemia Promotes Glutamate-Mediated Free Radical Generation and Intracellular Calcium Accumulation in Hippocampal Pyramidal Neurons. *Journal of Neuroscience.* **17**(23), 9085-9094.

Perez Velazquez, J. L., Frantseva, M. V., Huzar, D., Guezurian, C., and Carlen, P. L. (1999). Mitochondrial Porin, a Novel target to Prevent Ischemia-Induced Neurodegeneration? *Annals of the New York Academy of Sciences.* **893**, 369-371.

Perez Velazquez, J. L., Frantseva, M. V., Huzar, D. V., and Carlen, P. L. (2000). Mitochondrial porin required for ischaemia-induced mitochondrial dysfunction and neuronal damage. *Neuroscience.* **97**(2), 363-369.

Petersen, A., Castilho, R. F., Hansson, O., Wieloch, T., and Brundin, P. (2000). Oxidative stress, mitochondrial permeability transition and activation of caspases in calcium ionophore A23187-induced death of cultured striatal neurons. *Brain Research.* **857**, 20-29.

Petit, P. X., Goubern, M., Diolez, P., Susin, S. A., Zamzami, N., and Kroemer, G. (1998). Disruption of the outer mitochondrial membrane as a result of large amplitude swelling: The impact of irreversible permeability transition. *FEBS Letters.* **426**, 111-116.

Phenna, S. Jane, S. D. and Chad, J. E. (1995). Increased perinuclear Ca^{2+} activity evoked by metabotropic glutamate receptor activation in rat hippocampal neurones. *Journal of Physiology.* **486.1**, 149-161.

Pizzi, M., Consolandi, O., Memo, M., and Spano, P. (1996). Activation of multiple metabotropic glutamate receptor subtypes prevents NMDA-induced excitotoxicity in rat hippocampal slices. *European Journal of Neuroscience.* **8**, 1516-1521.

Prehn, J. H. M., Lippert, K., and Krieglstein, J. (1995). Are NMDA or AMPA/kainate receptor antagonists more efficacious in the delayed treatment of excitotoxic neuronal injury? *European Journal of Pharmacology.* **292**, 179-189.

Prehn, J. H. M., Jordan, J., and Ghadge, G. (1997). Ca^{2+} and reactive oxygen species in staurosporin-induced neuronal apoptosis. *Journal of Neurochemistry.* **68**, 1679-1685.

Prehn, J. H. M. (1998). Mitochondrial transmembrane potential and free radical production in excitotoxic neurodegeneration. *Naunyn-Schmiedeberg's Archives of Pharmacology.* **357**, 316-322.

Pringle, A. K. Benham, C., Sim, L., Kennedy, J., Iannotti, F., and Sundstrom, L. (1996). Selective N-type calcium channel antagonist omega conotoxin MVIIA is neuroprotective against hypoxic neurodegeneration in organotypic hippocampal slice cultures. *Stroke.* **11**, 2124-2130.

Pringle, A. K., Iannotti, F, Wilde, G. J. C., Chad, J. E., Seely, P. J., and Sundstrom, L. E. (1997). Neuroprotection by both NMDA and non-NMDA receptor antagonists in in vitro ischaemia. *Brain Research.* **755**, 36-46.

Racay, P., Kaplan, P, and Lehotsky, J. (1996). Control of Ca^{2+} homeostasis in Neuronal Cells. *General Physiology and Biophysics.* **15**, 193-210.

Radi, R., Beckman, J. S., Bush, K. M., and Freeman, B. A. (1991). Peroxynitrite-induced membrane lipid peroxidation: The cytotoxic potential of superoxide and nitric oxide. *Archives of Biochemistry and Biophysics.* **288**, 481-487.

Raff, M. C., Barres, B. A., Burne, J. F., Coles, H. S., Ishizaki, Y., and Jacobsen, M. D. (1993). Programmed Cell Death and the Control of Cell Survival: Lessons from the Nervous System. *Science.* **262**, 695-700.

Randall, A. and Tsien, R. W. (1995). Pharmacological dissection of multiple types of calcium channel currents in rat cerebellar granule neurons. *Journal of Neuroscience.* **15**, 2995-3012.

Randall, R. D. and Thayer, S. A. (1992). Glutamate-induced Calcium Transient Triggers Delayed Calcium Overload and Neurotoxicity in Rat Hippocampal Neurons. *Journal of Neuroscience.* **12**(5), 1882-1895.

Reed, J. C. (1997). Cytochrome c: Can't live with it - can't live without it. *Cell.* **91**, 559-562.

Reed, J. C., Jurgenmeier, J. M., and Matsuyama, S. (1998). Bcl-2 family proteins and mitochondria. *Biochimica et Biophysica Acta.* **1366**, 127-137.

Reichman, N. Porteous, C. and Murphy, M. (1994). Cyclosporin A blocks 6-hydroxydopamine-induced efflux of calcium from mitochondria without inactivating the mitochondrial inner-membrane pore. *Biochemical Journal.* **297**, 151-155.

Reuter, H. (1983). Calcium channel modulation by neurotransmitters, enzymes and drugs. *Nature.* **301**, 569-574.

Reynolds, I. J and Hastings, T. G. (1995). Glutamate induces the production of reactive oxygen species in cultured forebrain neurons following NMDA receptor activation. *Journal of Neuroscience.* **15**(5), 3318-3327.

Reynolds, I. J. (1999). Mitochondrial Membrane Potential and the Permeability Transition in Excitotoxicity. *Annals of the New York Academy of Sciences.* **893**, 33-41.

Richter, C. and Kass, G. E. N. (1991). Oxidative stress in mitochondria: its relationship to cellular Ca^{2+} homeostasis, cell death, proliferation, and differentiation. *Chemical and Biological Interactions.* **77**, 1-23.

Richter, C., Gogvadze, V., Laffranchi, R., Schlapbach, R., Schweizer, M., Suter, M., Walter, P., and Yaffee, M. (1995). Oxidants in mitochondria: from physiology to diseases. *Biochimica et Biophysica Acta.* **1271**, 67-74.

Richter, C., Ghafourifar, P., Schweizer, M., and Laffranchi, R. (1997). Nitric oxide and mitochondrial Ca^{2+}. *Biochemical Society Transactions.* **25**, 914-918.

Richter, C. and Ghafourifar, P. (2000). Ceramide induces cytochrome c release from isolated mitochondria. *Biochemistry Society Symposia.* **66**, 27-31.

Rizzuto, R. Brini, M., Murgia, M., and Pozzan, T. (1993). Microdomains with high Ca^{2+} close to IP_3-sensitive channels that are sensed by neighbouring mitochondria. *Science.* **262**, 744-747.

Rizzuto, R. Pinton, P., Carrington, W., Fay, F. S., Fogarty, K. E., Lifshitz, L. M., Tuft, R. A., and Pozzan, T. (1998). Close contacts with the endoplasmic reticulum as determinants of mitochondrial Ca^{2+} responses. *Science.* **280**, 1763-1766.

Rodriguez-Moreno, A. and Lerma, J. (1998). Kainate receptor modulation of GABA release involves a metabotropic function. *Neuron.* **20**(6), 1211-1218.

Rosemund, C., Stern-Bach, Y., and Stevens, C. (1998). The tetrameric structure of a glutamate receptor channel. *Science.* **280**, 1596-1599.

Rosenbaum, D. M., Kalberg, J., and Kessler, J. A. (1994). Superoxide Dismutase Ameliorates Neuronal Death From Hypoxia in Culture. *Stroke.* **25**, 857-863.

Rosenmund, C. and Westbrook, G. L. (1993). Calcium-induced actin depolymerization reduces NMDA channel activity. *Neuron.* **10**, 805-814.

Rothman, S. (1984). Synaptic release of excitatory amino acid neurotransmitter mediates anoxic neuronal death. *Journal of Neuroscience.* **4**, 1884-1891.

Rothman, S. M. (1985). The neurotoxicity of excitatory amino acids is produced by passive chloride influx. *Journal of Neuroscience.* **5**, 1483-1489.

Roy, M. and Sapolsky, R. (1999). Neuronal apoptosis in acute necrotic insults: why is this subject such a mess? *TINS.* **22**(10), 419-422.

Rutter, G. A., Fasolato, C., and Rizzuto, R. (1998). Calcium and Organelles: A Two-Sided Story. *Biochemical and Biophysical Research Communications.* **253**, 549-557.

Saatman, K. E., Murai, H., Bartus, R. T., Hayward, N. J., Perri, B. R., and McIntosh, T. K. (1996). Calpain inhibitor AK295 attenuates motor and cognitive deficits following experimental brain injury in the rat. *Proceedings of the National Academy of Sciences USA.* **93**, 3428-3433.

Sadoul, R. (1998). Bcl-2 family members in the development and degenerative pathologies of the nervous system. *Cell Death and Differentiation.* **5**, 805-815.

Sagara, Y. Schubert, D. (1998). The activation of metabotropic glutamate receptors protects nerve cells from oxidative stress. *Journal of Neuroscience.* **18**(17), 6662-6671.

Samdani, A. F., Dawson, T. M., and Dawson, V. L. (1997). Nitric Oxide Synthase in Models of Focal Ischemia. *Stroke.* **28**, 1283-1288.

Sapolsky, R. (2001). Cellular defenses against excitotoxic insults. *Journal of Neurochemistry.* **76**, 1601-1611.

Sastry, P. S. and Subba Rao, K. (2000). Apoptosis and the Nervous System. *Journal of Neurochemistry.* **74**, 1-20.

Sattler, R., Charlton, M. P., Hafner, M., and Tymianski, M. (1998). Distinct influx pathways, not calcium load, determine neuronal vulnerability to calcium neurotoxicity. *Journal of Neurochemistry.* **71**, 2349-2364.

Sattler, R., Xiong, X., Lu, W-Y., Hafner, M., MacDonald, J. F., and Tymianski, M. (1999). Specific Coupling of NMDA Receptor Activation to Nitric Oxide Neurotoxicity by PSD-95 Protein. *Science.* **284**, 1845-1848.

Sattler, R., Xiong, Z., Lu, W-Y., MacDonald, J. F., and Tymianski, M. (2000). Distinct roles of synaptic and extrasynaptic NMDA receptors in excitotoxicity. *Journal of Neuroscience.* **20**(1), 22-33.

Sattler, R., Joo, D. T., Henderson, J., Taverna, F. A., Lourensen, S., Orser, B. A., Roder, J. C., and Tymianski, M. (2001). The influence of Glutamate Receptor 2 Expression on Excitotoxicity in GluR2 Null Mutant Mice. *Journal of Neuroscience.* **21**(7), 2224-2239.

Savidge, J. R. and Bristow, D. R. (1997). Routes of NMDA- and K^+-stimulated calcium entry in rat cerebellar granule cells. *Neuroscience Letters.* **229**, 109-112.

Scaduto, R. C. and Grotyohann, L. W. (1999). Measurement of mitochondrial membrane potential using fluorescent rhodamine derivatives. *Biophysical Journal.* **76**, 469-477.

Scanlon, J. M. and Reynolds, I. J. (1998). Effects of oxidants and glutamate receptor activation on mitochondrial membrane potential in rat forebrain neurons. *Journal of Neurochemistry.* **71**, 2392-2400.

Schanne, F. A. X., Kane, A. B., Young, E. E., and Farber, J. L. (1979). Calcium Dependence of Toxic Cell Death: A Final Common Pathway. *Science.* **206**, 700-702.

Schapira, A. H. V. (1998). Mitochondrial dysfunction in neurodegenerative disorders. *Biochimica et Biophysica Acta.* **1366**, 225-233.

Scheff, S. W. and Sullivan, P. G. (1999). Cyclosporin A Significantly ameliorates Cortical Damage Following Experimental Traumatic Brain Injury in Rodents. *Journal of Neurotrauma.* **16**(9), 783-792.

Schendel, S. L., Montal, M., and Reed, J. C. (1998). Bcl-2 family proteins as ion-channels. *Cell Death and Differentiation.* **5**, 372-380.

Schinder, A. F. Olsen, E. C., Spitzer, N. C., and Montal, M. (1996). Mitochondrial dysfunction is a primary event in glutamate neurotoxicity. *Journal of Neuroscience.* **16**(19), 6125-6133.

Schoepp, D. D., Tizzano, J. P., Wright, R. A., and Fix, A. S. (1995). Reversible and Irreversible Neuronal Injury Induced by Intrahippocampal Infusion of the mGluR Agonist 1S,3R-ACPD in the Rat. *Neurodegeneration.* **4**, 71-80.

Schulz, J. B., Matthews, R. T., Klockgether, T., Dichgans, J., and Beal, M. F. (1997). The role of mitochondrial dysfunction and neuronal nitric oxide in animal models of neurodegenerative diseases. *Molecular and Cellular Biochemistry.* **174**, 193-197.

Scorrano, L., Petronilli, V., Colanna, R., Di Lisa, F., and Bernardi, P. (1999). Chloromethyltetramethylrosamine (MitoTracker Orange) induces the mitochondrial permeability transition and inhibits respiratory complex I. Implications for the mechanism of cytochrome c release. *Journal of Biological Chemistry.* **274**(35), 24657-24663.

Segal, M. and Manor, D. (1992). Confocal microscopic imaging of $[Ca^{2+}]_i$ in cultured rat hippocampal neurons following exposure to N-methyl-D-aspartate. *Journal of Physiology.* **448**, 655-676.

Sengpiel, B. Preis, E., Kriegstein, J., and Prehn, J. H. M. (1998). NMDA-induced superoxide production and neurotoxicity in cultured rat hippocampal neurons: role of mitochondria. *European Journal of Neuroscience.* **10**, 1903-1910.

Sensi, S. L., Yin, H. Z., Carriedo.S.G., Rao, S. S., and Weiss, J. H. (1999). Preferential Zn^{2+} influx through Ca^{2+}-permeable AMPA/kainate channels triggers prolonged mitochondrial superoxide production. *Proceedings of the National Academy of Sciences, USA.* **96**, 2414-2419.

Sensi, S. L., Yin, H. Z., and Weiss, J. H. (2000). AMPA/kainate receptor-triggered Zn^{2+} entry into cortical neurons induces mitochondrial Zn^{2+} uptake and persisitent mitochondrial dysfunction. *European Journal of Neuroscience.* **12**, 3813-3818.

Sharp, A. H., McPherson, P. S., Dawson, T. M., Aoki, C., Campbell, K. P., and Snyder, S. H. (1993). Differential immunohistochemical localization of inositol 1,4,5-triphosphate- and ryanodine-sensitive Ca^{2+} release channels in rat brain. *Journal of Neuroscience.* **13**, 3051-3063.

Sheline, C. T., Behrens, M. M., and Choi, D. W. (2000). Zinc-Induced Cortical Neuronal Death: Contribution of Energy Failure Attributable to Loss of NAD^+ and Inhibition of Glycolysis. *Journal of Neuroscience.* **20**(9), 3139-3146.

Shimizu, S., Eguchi, Y., Kamiike, W., Funahashi, Y., Mignon, A., Lacronique, V., Matsuda, H., and Tsujimoto, Y. (1998). Bcl-2 prevents apoptotic mitochondrial dysfunction by regulating proton flux. *Proceedings of the National Academy of Sciences USA.* **95**, 1455-1459.

Shimizu, S., Narita, M., and Tsujimoto, Y. (1999). Bcl-2 family proteins regulate the release of apoptogenic cytochrome c by the mitochondrial channel VDAC. *Nature.* **399**, 483-487.

Simbula, G., Glascott, P. A., Akita, S., Hoek, J. B., and Farber, J. L. (1997). Two mechanisms by which ATP depletion potentiates induction of the mitochondrial permeabilty transition. *American Journal of Physiology.* **273**(Cell Physiol. 42), c479-c488.

Simpson, P. B., Challiss, R. A. J., and Nahorski, S. R. (1995). Neuronal Ca^{2+} stores: activation and function. *TINS.* **18**(7), 299-306.

Simpson, P. B., Nahorski, S. R., and Challiss, R. A. J. (1996). Agonist-evoked Ca^{2+} mobilization from stores expressing inositol 1,4,-triphosphate receptors and ryanodine receptors in cerebellar granule neurons. *Journal of Neurochemistry.* **67**(1), 364-373.

Simpson, P. B. and Russell, J. T. , J. T. (1998). Role of mitochondrial Ca^{2+} regulation in neuronal and glial cell signalling. *Brain Research Reviews.* **26**, 72-81.

Smaili, S. S., Hsu, Y-T., Youle, R. J., and Russel, J. T. (2000). Mitochondria in Ca^{2+} Signaling and Apoptosis. *Journal of Bioenergetics and Biomembrane.* **32**(1), 35-46.

Small, D. L., Monette, R., Buchan, A. M., and Morley, P. (1997). Identification of calcium channels involved in neuronal injury in rat hippocampal slices subjected to oxygen and glucose deprivation. *Brain Research.* **753**, 209-218.

Soong, N. W. Hinton, D. R., Cortopassi, G., and Arnheim, N. (1992). Mosaicism for a specific somatic mitochondrial DNA mutation in adult human brain. *Nature Genetics.* **2**, 318-323.

Sparagna, G. C., Gunter, K. K., Sheu, S-S., and Gunter, T. E. (1995). Mitochondrial calcium uptake from physiological-type pulses of calcium. *Journal of Biological Chemistry.* **270**, 27510-27515.

Stout, A. K. Raphael, H. M., Kanterewicz, B. I., Klann, E., and Reynolds, I. J. (1998). Glutamate-induced neuron death requires mitochondrial calcium uptake. *Nature Neuroscience.* **1**(5), 366-373.

Stout, A. K. and Reynolds, I. J. (1999). High-affinity calcium indicators underestimate increases in intracellular calcium concentrations associated with excitotoxic glutamate stimulations. *Neuroscience.* **89**, 91-100.

Sugiyama, H., Ito, I., and Hirono, C. (1987). A new type of glutamate receptor linked to inositol phospholipid metabolism. *Nature.* **325**, 531-533.

Suh, S. W. et al. (2000). Evidence that synaptically-released zinc contributes to neuronal injury after traumatic brain injury. *Brain Research.* **852**, 268-273.

Sullivan, J. M., Traynelis, S. F., Chen, H-S, Escobar, W., Heinemann, S. F., and Lipton, S. A. (1994). Identification of two cysteine residues that are required for redox modulation of the NMDA subtype of glutamate receptor. *Neuron.* **13**, 929-936.

Sullivan, P. G., Thompson, M. B., and Scheff, S. W. (1999). Cyclosporin A Attenuates Acute Mitochondrial Dysfunction Following Traumatic Brain Injury. *Experimental Neurology.* **160**, 226-234.

Susin, S. A., Zamzami, N., Castedo, M, Hirsch, F., Marchetti, P., Macho, A, Daugas, E., Geuskens, M., and Kroemer, G. (1996). Bcl-2 inhibits the mitochondrial release of an apoptogenic protease. *Journal of Experimental Medicine.* **184**, 1331-1341.

Susin, S. A., Zamzami, N., and Kroemer, G. (1998). Mitochondria as regulators of apoptosis: doubt no more. *Biochimica et Biophysica Acta.* **1366**, 151-165.

Svichar, N., Kostyuk, P., and Verkhratsky, A. (1997). Mitochondrial calcium store shapes depolarization-induced but not caffeine-induced $[Ca^{2+}]_i$ transients in mouse DRG neurons. *Journal of Physiology.* **504P**, P184-P185.

Szalai, G., Krishnamurthy, R., and Hajnoczky, G. (1999). Apoptosis driven by IP_3-linked mitochondrial calcium signals. *EMBO.* **18**(22), 6349-6361.

Szatkowski, M. and Atwell, D. , D. (1995). Triggering and execution of neuronal death in brain ischaemia: two phases of glutamate release by different mechanisms. *TINS.* **17**, 359-365.

Takahashi, M., Seagar, M. J., Jones, J. F., Reber, B. F., and Catterall, W. A. (1987). Subunit structure of dihydropyridine-sensitive calcium channels from skeletal muscle. *Proceedings of the National Academy of Sciences USA.* **84**, 5478-5482.

Takei, N. and Endo, Y. (1994). Ca^{2+} ionophore-induced apoptosis on cultured embryonic rat cortical neurons. *Brain Research.* **652**, 65-70.

Tan, S., Wood, M., and Maher, P. (1998). Oxidative Stress Induces a Form of Programmed Cell Death with Characteristics of Both Apoptosis and Necrosis in Neuronal Cells. *Journal of Neurochemistry.* **71**, 95-105.

Tan, S., Sagara, Y., Liu, Y., Maher, P., and Schubert, D. (1998). The regulation of reactive oxygen species production during programmed cell death. *Journal of Cell Biology.* **141**(6), 1423-1432.

Tang, Y and Zucker, R. S. (1997). Mitochondrial involvement in post-tetanic potentiation of synaptic transmission. *Neuron.* **18**, 483-491.

Tatton, W. G. and Olanow, C. W. (1999). Apotosis in neurodegenerative diseases: the role of mitochondria. *Biochimica et Biophysica Acta.* **1410**, 195-213.

Taylor, D. L., Edwards, A. D., and Mehmet, H. (1999). Oxidative Metabolism, Apoptosis and Perinatal Brain Injury. *Brain Pathology.* **9**, 93-117.

Teismann, P. and Ferger, B. (2000). Comparison of the novel drug Ensaculin with MK-801 on the reduction of hydroxyl radical production in rat striatum after local application of glutamate. *Brain Research.* **857**, 165-171.

Tenneti, L., D'Emilia, D. M., Troy, C. M., and Lipton, S. A. (1998). Role of caspases in N-methyl-D-aspartate-induced apoptosis in cerebrocortical neurons. *Journal of Neurochemistry.* **71**(3), 946-959.

Thayer, S. A. and Miller, R. J. (1990). Regulation of the intracellular free calcium-concentration in single-rat dorsal-root ganglion neurons *in vitro*. *Journal of Physiology.* **425**, 85-115.

Thress, K., Kornbluth, S., and Smith, J. J. (1999). Mitochondria at the crossroad of Apoptotic Cell Death. *Journal of Bioenergetics and Biomembrane.* **31**(4), 321-326.

Timmerman, L. A., Clipstone, N. A., Ho, S. N., Northrop, J. P., and Crabtree, G. R. (1996). Rapid shuttling of NF-AT in discrimination of calcium signals and immunosuppression. *Nature.* **383**, 837-840.

Toescu, E. C. (1998). Apoptosis and cell death in neuronal cells: where does Ca^{2+} fit in? *Cell Calcium.* **24**(5-6), 387-403.

Tsien, R. W. and Tsien, R. Y. (1990). Calcium Channels, Stores and Oscillations. *Annual Review of Cell Biology.* **6**, 715-760.

Tsujimoto, Y. (1997). Apoptosis and Necrosis: Intracellular ATP level as a determinant for cell death modes. *Cell Death and Differentiation.* **4**, 429-434.

Tsujimoto, Y. (1998). Role of Bcl-2 family proteins in apoptosis: apoptosomes or mitochondria? *Genes to Cells.* **3**, 697-707.

Tsujimoto, Y. and Shimizu, S. (2000). Bcl-2 family: Life-or-death switch. *FEBS Letters.* **466**, 6-10.

Tymianski, M. Charlton, M., Carlen, P., and Tator, C. (1993). Secondary calcium overload indicates early neuronal injury which preceeds staining with viability indicators. *Brain Research.* **607**, 319-323.

Tymianski, M., Charlton, M. P., Carlen, P. L., and Tator, C. H. (1993). Source specificity of early calcium neurotoxicity in cultured embryonic spinal neurons. *Journal of Neuroscience.* **13**(5), 2085-2104.

Tymianski, M., Charlton, M., and Carlen, P. (1994). Properties of neuroprotective cell-permeant Ca^{2+} chelators - effects on $[Ca^{2+}]_i$ and glutamate neurotoxicity *in vitro*. *Journal of Neurophysiology.* **72**(4), 1973-1992.

Tymianski, M. and Tator, C. (1996). Normal and abnormal calcium homeostasis in neurons: a basis for the pathophysiology of traumatic and ischemic central nervous system injury. *Neurosurgery.* **38**(6), 1176-1195.

Uchino, H. Elmer, E., Uchino, K., Lindvall, O., and Seisjo, B. (1995). Cyclosporin A dramatically ameliorates CA1 hippocampal damage following transient forebrain ischaemia in the rat. *Acta Physiologica Scandinavica.* **155**, 469-471.

Vander Heiden, M. G., Chandel, N. S., Williamson, E. K., Schumacker, P. T., and Thompson, C. B. (1997). Bcl-x_l Regulates the Membrane Potential and Volume Homeostasis of Mitochondria. *Cell.* **91**, 627-637.

Vander Heiden, M. G. and Thompson, C. B. (1999). Bcl-2 proteins: regulators of apoptosis or of mitochondrial homeostasis? *Nature Cell Biology.* **1**, 209-216.

Vergun, O., Keelan, J., Khodorov, B., and Duchen, M. (1999). Glutamate-induced mitochondrial depolarisation and perturbation of calcium homeostasis in cultured rat hippocampal neurons. *Journal of Physiology.* **519.2**, 451-466.

Vergun, O., Sobolevsky, A. I., Yelshansky, M. V., Keelan, J., Khodorov, B., and Duchen, M. (2001). Exploration of the role of reactive oxygen species in glutamate neurotoxicity in rat hippocampal neurones in culture. *Journal of Physiology.* **531.1**, 147-163.

Verweij, B. Muizelaar, J., Vinas, F., Peterson, P., Xiong, Y., and Lee, C. (1997). Mitochondrial dysfunction after experimental and human brain injury and its possible reversal with a selective N-type calcium channel antagonist (SNX-111). *Neurological Research.* **19**, 334-339.

Voet, D., and Voet, J.G. (1995). *Biochemistry*, 2nd Ed. John Wiley & Sons Inc.

Vogt, K. et al. (2000). The actions of synaptically released zinc at hippocampal mossy fibre synapses. *Neuron.* **26**, 187-196.

Votyakova, T. V. and Reynolds, I. J. (2001). $\Delta\Psi_m$-dependent and -independent production of reactive oxygen species by rat brain mitochondria. *Journal of Neurochemistry.* **79**, 266-277.

Wadia, J. S., Chalmers-Redman, R. M. E., and Ju, W. J. H. (1998). Mitochondrial membrane potential and nuclear changes in apoptosis caused by serum and nerve growth factor withdrawal: Time course and modification by (-)-deprenyl. *Journal of Neuroscience.* **18**(3), 932-947.

Wallace, D. C. (1999). Mitochondrial Diseases in Man and Mouse. *Science.* **283**, 1482-1488.

Wang, G. J and Thayer, S. A. (1996). Sequestration of glutamate-induced Ca^{2+} loads by mitochondria in cultured rat hippocampal neurons. *Journal of Neurophysiology.* **76**(3), 1611-1621.

Wang, G. J., Randall, R. D., and Thayer, S. A. (1994). Glutamate-induced intracellular acidification of cultured hippocampal neurons demonstrates altered energy metabolism resulting from Ca^{2+} loads. *Journal of Neurophysiology.* **72**(6), 2563-2569.

Wang, Y., Qin, Z. H., Nakai, M., and Chase, T. N. (1997). Glutamate metabotropic receptor agonist 1S,3R-ACPD induces internucleosomal DNA fragmentation and cell death in rat striatum. *Brain Research.* **772**(1-2), 45-56.

Ward, M. W., Rego, C., Frenguelli, B. G., and Nicholls, D. G. (2000). Mitochondrial membrane potential and glutamate excitotoxicity in cultured cerebellar granule cells. *Journal of Neuroscience.* **20**(19), 7208-7219.

Weiss, J. H., Hartley, D. M., Koh, J., and Choi, D. W. (1990). The calcium blocker nifedipine attenuates slow excitatory amino acid neurotoxicity. *Science.* **247**, 1474-1477.

Weiss, J. H. and Sensi, S. L. (2000). Ca^{2+}-Zn^{2+} permeable AMPA or kainate receptors: possible key factors in selective neurodegeneration. *TINS.* **23**, 365-371.

Weiss, J. H., Sensi, S. L., and Koh, J. (2000). Zn^{2+}: a novel ionic mediator of neural injury in brain disease. *TIPS.* **21**, 395-401.

Westenbroek, R. E., Bausch, S. B., Lin, R. C. S., Franck, J. E., Noebels, J. L., and Catterall, W. A. (1998). Upregulation of L-type Ca^{2+} channels in reactive astrocytes after brain injury, hypomyelination and ischaemia. *Journal of Neuroscience.* **18**(7), 2321-2334.

White, A. R., Multhaup, G., Maher, F., Camakaris, J., Bellingham, S., Zheng, H., Bush, A. I., Beyreuther, K., Masters, C. L., and Cappai, R. (1999). The Alzheimer's Disease Amyloid Precursor Protein Modulates Copper-Induced Toxicity and Oxidative Stress in Primary Neuronal Cultures. *Journal of Neuroscience.* **19**(21), 9170-9179.

White, R. J. and Reynolds, I. J. (1996). Mitochondrial depolarization in glutamate-stimulated neurons: an early signal specific to excitotoxin exposure. *Journal of Neuroscience.* **16**(18), 5688-5697.

Wingrove, D.E., and Gunter, T.E. (1986).Kinetics of mitochondrial calcium transport. I. Characteristics of the sodium-independent calcium efflux mechanism of liver mitochondria. *Journal of Biological Chemistry*, **261**, 15159 – 15165.

Wood, J. and Garthwaite, J. (1994). Models of the diffusional spread of nitric oxide: implications for neuronal nitric oxide signalling and its pharmacological properties. *Neuropharmacology.* **33**, 1235-1244.

Yamakura, T. and Shimoji, K. (1999). Subunit- and site-specific pharmacology of the NMDA receptor channel. *Progress in Neurobiology.* **59**, 279-298.

Yin, H. Z. and Weiss, J. H. (1995). Zn^{2+} permeates Ca^{2+} permeable AMPA/kainate channels and triggers selective neural injury. *NeuroReport.* **6**, 2553-2556.

Yin, H. Z., Ha, D. H., Carriedo, S. G., and Weiss, J. H. (1998). Kainate-stimulated Zn^{2+} uptake labels cortical neurons with Ca^{2+}-permeable AMPA/kainate channels. *Brain Research.* **781**, 45-56.

Yin, H. Z., Sensi, S. L., Carriedo.S.G., and Weiss, J. H. (1999). Dendritic Localization of Ca^{2+}-Permeable AMPA/Kainate Channels in Hippocampal Pyramidal Neurons-. *Journal of Comparative Neurology.* **409**, 250-260.

Yin, H. Z., Sensi, S. L., Ogoshi, F., and Weiss, J. H. (2002). Blockade of Ca^{2+}-permeable AMPA/kainate channels decreases oxygen-glucose deprivation-induced Zn^{2+} accumulation and neuronal loss in hippocampal pyramidal neurons. *Journal of Neuroscience.* **22**(4), 1273-1279.

Yoon, Y. H., Jeong, K. H., Shim, M. J., and Koh, J-Y. (1999). High vulnerability of GABA-immunoreactive neurons to kainate in rat retinal cultures: correlation with the kainate-stimulated cobalt uptake. *Brain Research.* **823**, 33-41.

Zamzami, N., Susin, S. A., Marchetti, P., Hirsch, T., Gomez-Monterrey, I., Castedo, M, and Kroemer, G. (1996). Mitochondrial Control of Nuclear Apoptosis. *Journal of Experimental Medicine.* **183**, 1533-1544.

Zamzami, N., Hirsch, T., Dallaporta, B., Petit, P. X., and Kroemer, G. (1997). Mitochondrial implication in accidental and programmed cell death: Apoptosis and Necrosis. *Journal of Bioenergetics and Biomembranes.* **29**(2), 185-193.

Zeevalk, G. D. Nicklas, W. J. (1991). Mechanisms underlying initiation of excitotoxicity associated with metabolic inhibition. *Journal of Pharmacology and Experimental Theraputics.* **257**, 870-878.

Zhu, L., Ling, S., Yu, X-D., Venkatesh, L. K., Subramanian, T., Chinnadurai, G., and Kuo, T. H. (1999). Modulation of Mitochondrial Ca^{2+} Homeostasis by Bcl-2. *Journal of Biological Chemistry.* **274**(47), 33267-33273.

Zoratti, M. and Szabo, I. (1995). The mitochondrial permeability transition. *Biochimica et Biophysica Acta.* **1241**, 139-176.